COMPARISONS OF NORMAL MODE THEORY, RAY THEORY, AND MODIFIED RAY THEORY FOR ARBITRARY SOUND VELOCITY PROFILES RESULTING IN CONVERGENCE ZONES

Ira M. Blatstein

Naval Ordnance Laboratory
White Oak, Maryland

29 August 1974

UNCLASSIFIED

SECURITY CLASSIFICATION OF THIS PAGE *(When Data Entered)*

AD787629

REPORT DOCUMENTATION PAGE

READ INSTRUCTIONS BEFORE COMPLETING FORM

1. REPORT NUMBER: NOLTR 74-95	2. GOVT ACCESSION NO.
3. RECIPIENT'S CATALOG NUMBER	
4. TITLE *(and Subtitle)*: COMPARISONS OF NORMAL MODE THEORY, RAY THEORY, AND MODIFIED RAY THEORY FOR ARBITRARY SOUND VELOCITY PROFILES RESULTING IN CONVERGENCE ZONES	5. TYPE OF REPORT & PERIOD COVERED: Interim
	6. PERFORMING ORG. REPORT NUMBER
7. AUTHOR(s): Ira M. Blatstein	8. CONTRACT OR GRANT NUMBER(s)
9. PERFORMING ORGANIZATION NAME AND ADDRESS: Naval Ordnance Laboratory (Code 243), White Oak, Silver Spring, Maryland 20910	10. PROGRAM ELEMENT, PROJECT, TASK AREA & WORK UNIT NUMBERS: Subtask V99QAXNA003-04
11. CONTROLLING OFFICE NAME AND ADDRESS	12. REPORT DATE: 29 August 1974
	13. NUMBER OF PAGES: ~~188~~ 197
14. MONITORING AGENCY NAME & ADDRESS *(if different from Controlling Office)*	15. SECURITY CLASS. *(of this report)*: UNCLASSIFIED
	15a. DECLASSIFICATION/DOWNGRADING SCHEDULE

16. DISTRIBUTION STATEMENT *(of this Report)*

Approved for public release; distribution unlimited.

17. DISTRIBUTION STATEMENT *(of the abstract entered in Block 20, if different from Report)*

18. SUPPLEMENTARY NOTES

This research was sponsored in part by the Defense Nuclear Agency under Subtask V99QAXNA003-04.

19. KEY WORDS *(Continue on reverse side if necessary and identify by block number)*

Underwater Explosions	Caustics	Ray Theory
Nuclear Explosions	Shock Wave	Modified Ray Theory
Explosions	Convergence Zone Caustics	
Refraction	Normal Mode Theory	

20. ABSTRACT *(Continue on reverse side if necessary and identify by block number)*

Normal mode theory, ray theory, and modified ray theory are compared for several arbitrary velocity profiles. The normal mode theory program uses a finite difference approach to solve for the spectrum of discrete modes once an arbitrary sound velocity profile and a constant velocity fluid bottom are specified. A ray tracing program is used to find the coherent sum of rays at points of interest. Modified ray theory leading to an Airy function solution is used to correct ray theory at caustics and in adjacent shadow zones.

DD FORM 1 JAN 73 1473 EDITION OF 1 NOV 65 IS OBSOLETE S/N 0102-014-6601

197

UNCLASSIFIED

SECURITY CLASSIFICATION OF THIS PAGE *(When Data Entered)*

We first treat two arbitrary velocity profiles leading to convergence zones with what we characterize as vertical caustics. The agreement in the comparisons is quite good. The fall off in intensity in caustic shadow zones predicted by modified ray theory agrees with normal mode theory. Ray theory combined with modified ray theory contributions in caustic regions and caustic shadow zones agrees with most major features of the normal mode calculation. Interference between rays and shadow zone contributions from adjacent caustics causes many of the oscillations present in convergence zone propagation loss vs range curves.

For a bilinear velocity profile leading to convergence zones with more nearly horizontal caustics, the agreement is only fair. Caustic locations are verified, but the particular modified ray theory being used does not predict an intensity fall off into caustic shadow zones that is in agreement with normal mode calculations. Reasons for this are discussed.

COMPARISONS OF NORMAL MODE THEORY, RAY THEORY, AND MODIFIED RAY THEORY FOR ARBITRARY SOUND VELOCITY PROFILES RESULTING IN CONVERGENCE ZONES

By:
Ira M. Blatstein

ABSTRACT: Normal mode theory, ray theory, and modified ray theory are compared for several arbitrary velocity profiles. The normal mode theory program uses a finite difference approach to solve for the spectrum of discrete modes once an arbitrary sound velocity profile and a constant velocity fluid bottom are specified. A ray tracing program is used to find the coherent sum of rays at points of interest. Modified ray theory leading to an Airy function solution is used to correct ray theory at caustics and in adjacent shadow zones.

We first treat two arbitrary velocity profiles leading to convergence zones with what we characterize as vertical caustics. The agreement in the comparisons is quite good. The fall off in intensity in caustic shadow zones predicted by modified ray theory agrees with normal mode theory. Ray theory combined with modified ray theory contributions in caustic regions and caustic shadow zones agrees with most major features of the normal mode calculation. Interference between rays and shadow zone contributions from adjacent caustics causes many of the oscillations present in convergence zone propagation loss vs range curves.

For a bilinear velocity profile leading to convergence zones with more nearly horizontal caustics, the agreement is only fair. Caustic locations are verified, but the particular modified ray theory being used does not predict an intensity fall off into caustic shadow zones that is in agreement with normal mode calculations. Reasons for this are discussed.

EXPLOSIONS RESEARCH DEPARTMENT
UNDERWATER EXPLOSIONS DIVISION
NAVAL ORDNANCE LABORATORY
WHITE OAK, SILVER SPRING, MARYLAND

NOLTR 74-95 29 August 1974

This report is part of a continuing study of the refractive effects of oceanic sound velocity gradients upon the propagation of shock waves from underwater nuclear weapons. The work reported here was carried out in partial fulfillment of the degree of Doctor of Philosophy in Physics at the Catholic University of America. The study leading to the publication was supported in part by DNA (Subtask V99QAXNA003-04); however, preparation of the thesis and its publication for submission to the University was not so funded.

The author thanks Dr. Herbert Uberall for serving as his advisor during preparation of this thesis and for his guidance and many helpful suggestions. The author also thanks Robert M. Barash, his supervisor at the Naval Ordnance Laboratory, for his constant encouragement and patience. Jean Goertner and Robert Thrun of NOL contributed a great deal of time and effort to the modification of the CONGRATS ray tracing program. Dr. Thomas Eisler and Dr. Frank Andrews served as readers of this thesis. Alfred V. Newman of the Naval Research Laboratory contributed much to the author's understanding of normal mode theory in general and his normal mode program in particular. Helpful discussions with Dr. David Sachs of Cambridge Acoustical Associates, Dr. Frank Ingenito of the Naval Research Laboratory, and Dr. Henry Weinberg of the Naval Underwater Systems Center, New London are also acknowledged.

ROBERT WILLIAMSON II
Captain, USN
Commander

I. Kabik
I. KABIK
By direction

Table of Contents

List of Tables

List of Figures

List of Appendices

List of Symbols

$Ai(\rho)$	Airy function, Ai(o) = .36
$c(z)$	Sound velocity
c_i	Sound velocity in m^{th} finite difference layer
c_h	Sound velocity at receiver depth
c_s	Sound velocity at source depth
c_v	Sound velocity at turning point depth
f	Frequency, Hz
g_o, g_1, g_2	Parameters in equation for sound velocity layer
H	Water depth
$I_1(r,z)$	Coherent sum of rays (dB re 1 yd)
$I_r(r,z)$	Coherent sum of rays and caustic contributions
$k = \omega/c(z_o)$	Wave number
$L_j(r,z)$	Propagation loss for j^{th} ray at (r,z)
$M_n[r, z_c]$	Propagation loss of n^{th} caustic point at depth z_c, range r
$n(z)=c(z_o)/c(z)$	Index of refraction
$N(r,z)=10 \text{ Log } I_o/I$	Net propagation loss at (r,z)
p	Pressure
P_o	Pressure amplitude at source
r	Range
r_c	Range to caustic at depth z_c
$R = \rho_1/\rho_2$	
$\Delta r = r-r_c$	Horizontal distance from caustic point to point of interest
$T_j(r,z)$	Travel time to j^{th} ray to point (r,z)

$T\left[r_c(n)\right]$	Travel time of ray to n^{th} caustic point at depth z_c and range $r_c(n)$
$u_n(\eta_o)$	Amplitude of n^{th} normal mode at source depth, $\eta_o = z_o/H$
$u_n(\eta)$	Amplitude of n^{th} normal mode at receiver depth, η
v_o	Parameter in equation for sound velocity layer
$W(\xi, r, z) = \xi r + \phi(z_o) + \phi(z)$	Phase function along ray
z	Depth
z_o	Depth at top of CONGRATS velocity layer
$Z_n(1),(2)$	Unnormalized wave function (1) in water (2) in bottom fluid
z_τ	Turning point depth for particular ray
ϵ	Parameter which wave function should be less than at surface

$$\gamma = \left(\frac{1}{2}\left|\frac{\partial^3 W(\xi, r_c, z_c)}{\partial \xi^3}\right|_{\xi=\xi_c}\right)^{-1/3}$$

$\eta = z/H$	Normalized depth in normal mode calculation
θ_o	Angle of ray with vertical at source
$\xi = \sin\theta_o$	
$\xi_c = \sin(\theta_o)_c$	Source angle of ray having caustic point at (z_c, r_c)
$\rho = k^{2/3}\gamma r$	Argument of Airy function
ρ_1	Density in water
ρ'	Density in fluid bottom

$\phi(z) = \int_{z_T}^{z} \left[n^2(z) - \xi^2\right]^{1/2} dz$, in ray theory

$\Phi(r,z)$ Velocity potential in normal mode theory

$\phi(n)$ Additional phase shift of n^{th} caustic ray passing through (r, z)

$\phi_j(r,z)$ Additional phase shift of j^{th} ray passing through (r, z)

1. Introduction

Ray theory, modified ray theory, and normal mode theory are three different approaches for calculating accustic intensity at a given point in the ocean once the source location and prevailing sound velocity profile have been specified. Each has its own limitations and regions of intended use. Ray theory (1-4) has traditionally been the most widely used approach for propagation loss calculations for both cw (5-7) and explosive sources (8-11). Its popularity rests on both its relative ease of calculation and its intuitively appealing description of the channeling of energy along ray paths and within ray tubes of varying cross-section. More recently, modified ray theory (12-17) has seen increased use as a means of enhancing ray theory results by yielding predictions on caustics and in the adjacent caustic-related shadow zones, regions in which ray theory is invalid. Normal mode theory (18-23), actually the mos general of the three, has suffered until recently from a lack of the large, high speed computers needed for the solution of many realistic propagation problems. It has also suffered from, and continues to suffer from, the absence of a clear, intuitive description of the normal modes that could compete with ray diagrams (Figure 1.1) in explaining how energy gets from source to receiver. With the advent of larger computers, however, normal mode theory has seen development along several lines of approach, and it is fast becoming a widely used technique with as much of a following as ray theory.

As this continuing development has progressed, more effort has gone into comparisons of normal mode theory with ray theory, modified ray theory, and completely different approaches (24). The object has been to determine the conditions under which each theory is the appropriate choice for intensity calculations. From relatively small scale efforts at comparing two theories with each other (25-27), efforts have progressed to complete detailed comparisons of mode, ray, and modified ray theories for an analytic sound velocity profile (16). In this recent article, Pedersen and Gordon demonstrated how normal mode theory could be used to determine the validity of ray theory and modified ray theory in the region where all three overlap, near a caustic. They did this comparison for an analytic, monotonically decreasing sound velocity profile yielding a close-in caustic, and they suggested that it would be useful to do the same comparison for a deep ocean profile yielding a convergence zone caustic.

For some time, this author has been involved in studies of convergence zone caustics and their effect on propagating shock waves from underwater explosions (8, 28-30). To predict the effect of refraction on these transients at caustics, we have combined a frequency dependent modified ray derivation that accounts for refraction (13) with a Fourier series representation of the shock wave as an exponential decay from a peak pressure (29). With this approach, we have successfully matched experimental pressure records measured in a convergence zone during an at-sea test involving underwater explosions (8). However, one successful comparison does not validate a method. And the modified ray solution used to account for refraction

effects has not been extensively validated. Therefore, it was felt that a comparison with a more general approach was necessary to justify our continuing use of modified ray results. Normal mode theory seemed a logical choice for our standard of comparison since it is more general than, and lacks the drawbacks of, ray and modified ray theories.

However, combining results from a normal mode program that accepts an arbitrary sound velocity profile with a transient source representation is a difficult, time consuming task that, to this author's knowledge, has not yet been successfully accomplished. Furthermore, if ray and modified ray results are adequate for underwater explosion shock wave predictions near caustics - and if this can be verified without complete comparisons with normal mode results - such full scale comparisons may be unnecessary. In order to accomplish this partial validation, we decided to compare modified ray theory with normal mode theory for the lower frequencies in the shock wave (on the order of 50-100 Hz). At these low frequencies we would expect discrepancies between normal mode theory and modified ray theory - a "high frequency" approximation - to be most apparent. If, on the other hand, they agreed fairly well in this low frequency domain, we could expect them to agree at least as well at the higher frequencies in the shock wave. We could then have confidence in the use of modified ray theory on all parts of the shock wave spectrum without resorting to total pulse reconstruction involving normal mode theory. We decided to do these comparisons for a relatively arbitrary sound velocity profile so that we would be testing the theories for realistic and often encountered propagation conditions.

These comparisons led to several expected, and unexpected, chores. The finite difference normal mode program (22) required modification in order that it work properly for the deep-water profiles under consideration. A mode summing program had to be written. The ray program (6, 31) being used had to be made compatible with modified ray results previously derived (13). And a ray sorting program had to be written that could incorporate the effects of one or more caustics into the intensity calculation.

At one point the normal mode program was yielding incorrect results for propagation loss versus range. We found ourselves using ray theory and modified ray theory as the standards of comparison, with normal mode theory the sample requiring validation - a complete reversal of their intended roles. We will discuss this problem in order to point out some of the difficulties associated with finite difference calculations and to stress the need for validation of any model. It is not a revelation to state that any propagation model (any program, for that matter) can print out apparently reasonable propagation loss versus range curves while doing an incorrect calculation.

In the following sections we will first discuss the common roots of all three theories. We will then describe the specific ray, modified ray, and normal mode calculations used in these comparisons. After checking normal mode results for a shallow water model, we will examine a deep ocean profile, concerning ourselves only with the first caustic in the convergence zone and frequencies of 50 Hz and 100 Hz. Then for a slightly shallower profile, we will consider the various

caustics present in a typical convergence zone. Finally we will look at a profile yielding several more nearly horizontal caustics. This will turn out to be the most difficult to treat with the horizontal expansion form of modified ray theory that we are using, and here we will discuss a useful alternative derivation (14).

It is hoped that all of these comparisons will give a better feel for the strengths and weaknesses of the various theories as well as indicate where each one can be used to best advantage. They also should help explain what propagation paths and interference mechanisms are causing the complex propagation loss curves predicted by normal mode theory in convergence zones. Finally the comparisons will demonstrate that modified ray theory is valid - and often quite useful - in predicting pressures on and near caustics. For a realistic deep ocean profile, a combination of ray theory and modified ray theory results often yields a satisfactory prediction of pressures in the convergence zone when compared to a more general normal mode calculation. The fact that the modified ray theory has an explicit frequency dependence means one can locate the caustic once, calculate a few parameters, and then find the intensity for any frequency rapidly. This is as opposed to normal mode theory, where one has to calculate intensity at a given point independently for each frequency. Thus, modified ray theory is valid for the treatment of the various frequencies in the shock waves from underwater explosions near caustics, as well as being an inherently easier, more rapid calculation to make.

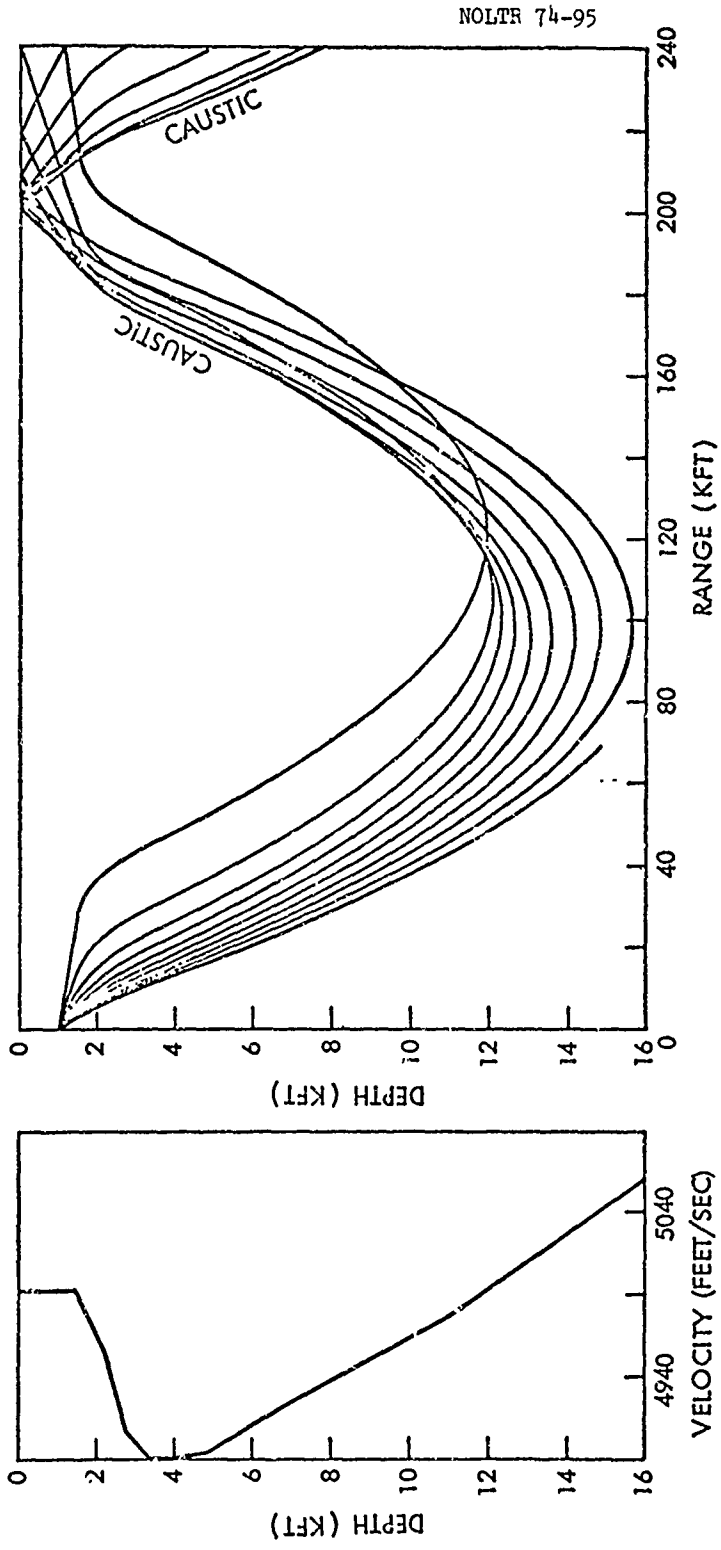

Figure 1.1 Sound Velocity Profile and Ray Diagram Showing Convergence Zone

2. Wave Equation Roots of Ray Theory, Modified Ray Theory and Normal Mode Theory

As we have said, there are many alternative solutions to the wave equation. More than one approach leads to ray theory type results, normal mode results, or any other category of solutions. Each approach emphasizes a particular aspect of propagation phenomena. In this section we will summarize the two basic derivations that have served as the basis for our work in modified ray theory and normal mode theory. We will first go through the details of the Sachs and Silbiger derivation (13) that arrives at a ray theory solution, shows what assumptions cause it to break down at caustics, and finally arrives at a modified ray theory solution by making the appropriate changes in the derivation. The main thrust of this derivation is to show how modified ray theory springs logically from ray theory's failure at caustics (ray theory itself can probably be better understood by examination of other derivations (1)). Then we will start again with the wave equation, but this time we will go through the details of Newman and Ingenito's (22) finite difference normal mode solution. So this section will summarize the basic equations from previous efforts that are modified, evaluated, and compared in the following sections.

We start with the reduced wave equation for pressure and an assumed $e^{-i\omega t}$ time dependence:

$$\nabla^2 p + k^2 n^2(z) = -P_0 \delta(x)\delta(y)\delta(z) \tag{2.1}$$

$$\text{where } n(z) = c(z_0)/c(z) \tag{2.2}$$

$$k = \omega / c(z_0) \tag{2.3}$$

Using cylindrical symmetry, Sachs and Silbiger (13) rewrite this as:

$$\frac{\partial^2 p}{\partial r^2} + \frac{1}{r}\frac{\partial p}{\partial r} + \frac{\partial^2 p}{\partial z^2} + k^2 n^2(z)\, p = -P_0 \frac{\delta(r)\delta(z)}{2\pi r} \qquad (2.4)$$

This equation is then multiplied by $J_0(k\xi r)$, and integrated from 0 to ∞ to obtain:

$$\frac{\partial^2 f}{\partial z^2} + k^2 [n^2(z) - \xi^2] f = -\frac{P_0}{2\pi}\delta(z) \qquad (2.5)$$

Where $$f(\xi, z) = \int_0^\infty p(r,z)\, J_0(k\xi r)\, r\, dr \qquad (2.6)$$

and $$p(r,z) = \int_0^\infty f(\xi,z)\, J_0(k\xi r)\, k^2 \xi\, d\xi \qquad (2.7)$$

$$= \tfrac{1}{2}\int_{-\infty}^{\infty} f(\xi,z)\, H_0^{(1)}(k\xi r)\, k^2 \xi\, d\xi \qquad (2.8)$$

Equation (2.5) is then solved using a WKB approximation to arrive at:

$$f_r(\xi, z) = \frac{P_0\, e^{ik[\phi(z_0) + \phi(z)]}}{4\pi k (n^2 - \xi^2)^{1/4} (1 - \xi^2)^{1/4}} \qquad (2.9)$$

where $$\phi(z) = \int_{z_T}^{z} [n^2(z) - \xi^2]^{1/2} dz \; ; \; z_T \text{ is the turning point depth.} \qquad (2.10)$$

These are the pertinent equations for rays beyond their turning points. Equation (2.8) for pressure is evaluated using Equation (2.9) and the asymptotic form of the Hankel function for large arguments:

$$p(r,z) = \frac{P_0}{4\pi}\int_{-\infty}^{\infty} \left[\frac{k\xi}{2\pi r (n^2 - \xi^2)^{1/2} (1 - \xi^2)^{1/2}}\right]^{1/2} e^{ikW(\xi,r,z) - i\frac{\pi}{4}} d\xi \qquad (2.11)$$

$$W(\xi, r, z) = \xi r + \phi(z_0) + \phi(z) \qquad (2.12)$$

To use a stationary phase approach, and with ray theory in mind, Sachs and Silbiger look for zeros $\xi = \xi_j$ of $\frac{\partial W}{\partial \xi}$ in the range $\xi < 1, n(z)$. They then assume that the main contributions to the integral are in the vicinity of these zeros. This corresponds to ray theory in that ξ_j will turn out to be $\sin\theta_0$, where θ_0 is the initial angle of a ray. As long as we move along this ray path, the value of the integral will be significant and energy will propagate.

The phase term $W(\xi)$ is then expanded around these zeros (13):

$$W(\xi) = W(\xi_j) + \tfrac{1}{2}(\xi-\xi_j)W''(\xi_j) + \tfrac{1}{6}(\xi-\xi_j)^3 W'''(\xi_j) \cdots \quad (2.13)$$

$$\text{where } W''(\xi_j) = \frac{\partial^2 W(\xi)}{\partial \xi^2}\Big|_{\xi=\xi_j} \quad (2.14)$$

$$\text{and } W'(\xi_j) = 0 \text{ by definition on a ray.} \quad (2.15)$$

Thus Equation (2.11) becomes:

$$p(r,z) = \frac{p_0}{4\pi} \sum_{-\infty}^{\infty} \left\{ \left[\frac{k\xi}{2\pi r (n^2-\xi^2)^{1/2}(1-\xi^2)^{1/2}} \right]^{1/2} \cdot \exp\left[-\frac{i\pi}{4} + ik\left(W(\xi_j) + \frac{(\xi-\xi_j)^2}{2} W''(\xi_j) + \frac{(\xi-\xi_j)^3}{6} W'''(\xi_j) \right) \right] \right\} d\xi \quad (2.16)$$

Assuming the integral in Equation (2.16) is slowly varying when ξ is near ξ_j and dropping higher order terms than $W''(\xi_j)$ yields:

$$p_r(r,z) = \frac{p_0}{4\pi} \sum_j \left\{ \frac{\xi_j}{r(1-\xi_j^2)^{1/2}(n^2-\xi_j^2)^{1/2}[\phi''(z_0)+\phi''(z)]} \right\}^{1/2} \cdot \exp\left\{ ik\left[\xi_j r + \phi(z_0) + \phi(z) \right] \right\} \quad (2.17)$$

This is a ray type solution for the refracted wave (beyond the ray turning point), where each term in the sum corresponds to a ray leaving the source at angle $(\theta_0)_j = \sin^{-1}\xi_j$ with the vertical.

We note that the amplitude of each ray is determined in part by:

$$\left[W''(\xi_j)\right]^{-1/2} = \left[\phi''(z_0) + \phi''(z)\right]^{-1/2} \qquad (2.18)$$

where $W''(\xi_j)$ was the only derivative of the Taylor series expansion (Equation 2.13) assumed to contribute to the integral (Equation 2.16).

A caustic can be defined in several ways: One alternative is to look at rays at a constant depth and plot range, r, versus $\xi_j = \sin\theta_0$ (Figure 2.1). We see that the caustic point at depth z is a range minimum point (it could also be a range maximum point). Thus for the caustic point:

$$\frac{\partial r}{\partial \xi}\Big|_{\xi=\xi_c} = \frac{\partial^2 W}{\partial \xi^2}\Big|_{\xi=\xi_c} = 0 \qquad (2.19)$$

The quantity $W''(\xi_j)$ that we assumed was larger than all higher derivatives turns out to be zero on the caustic. Then Equation (2.18) becomes infinite, and the pressure (Equation 2.17) becomes infinite. This then is the way ray theory breaks down at the caustic.

It is a natural step to now include the third derivative in the integral for pressure. However Sachs and Silbiger go through several steps in inserting the derivative that are mathematically correct, but not at all obvious. So we will explain this part of the derivation (32) in detail. If we are on a caustic at (z_c, r_c), the ray through the caustic point is given by $\xi_j = \xi_c$. Then

$$W'(\xi_c, r_c, z_c) = 0 \qquad (2.20)$$

This is just the criterion for being on a ray (Equation 2.15), applied to a particular caustic ray. By definition on the caustic, we also know

$$W''(\xi_c, z_c) = 0 \tag{2.21}$$

We note that W'' is independent of range, r, since r vanishes from Equation (2.12) upon taking two derivatives with respect to ξ. Thus if we are at depth z_c, but at a range r not equal to r_c, we can be on a ray, but not at the caustic:

$$W'(\xi_j, r, z_c) = 0 \qquad W''(\xi_j, z_c) \neq 0 \tag{2.22}$$
$$\tag{2.23}$$

However if we replace ξ_j by ξ_c in these two equations, we are not on a ray (the ray ξ_c passes through r_c at z_c), so:

$$W'(\xi_c, r, z_c) \neq 0 \tag{2.24}$$

But since there is a caustic at depth z_c, and the next derivative is independent of r (r_c or r makes no difference):

$$W''(\xi_c, z_c) = 0 \tag{2.25}$$

So if $W(\xi, r, z)$ is expanded around ξ_c for points off, as well as on, the caustic, then W'' will be zero for all r, not just r_c, therefore:

$$W(\xi_c, r, z_c) = W(\xi_c, r_c, z_c) + W'(\xi_c, r, z_c)(\xi - \xi_c) + \frac{1}{6} W'''(\xi_c, r, z_c)(\xi - \xi_c)^3 \tag{2.26}$$

We note that $W'(\xi_c, r, z_c)$ is non zero for $r \neq r_c$. Also from Equation (2.12):

$$W'(\xi_c, r, z_c) - W'(\xi_c, r_c, z_c) = \left[r + \phi'(z_c) + \phi'(z)\right] - \left[r_c + \phi'(z_c) + \phi(z)\right] \tag{2.27}$$

Since $W'(\xi_c, r_c, z_c) = 0$ (the caustic ray satisfies the ray criteria)

$$W'(\xi_c, r, z_c) = r - r_c = \Delta r \tag{2.28}$$

If we now also expand the amplitude factors in Equation (2.17) around ξ_c, drop higher than first order terms as leading to higher frequency terms after integration, and put in the other derivative information obtained above, we get Sachs and Silbiger's(33)integral expression for pressure on and near the caustic:

$$p(r z_c) = \frac{P_0}{4\pi}\left[\frac{K\xi_c}{2\pi r (n^2-\xi^2)^{1/2}(1-\xi^2)^{1/2}}\right]^{1/2} \exp\left[ikW_c - i\frac{\pi}{4}\right]\int_{-\infty}^{\infty}\exp\left\{i\left[\rho s + \frac{s^3}{3}\right]\right\} ds \tag{2.29}$$

$$s = \Delta\xi\left[\pm k^{1/3}\left|\frac{W_c'''}{2}\right|^{1/3}\right], \quad \rho = k^{2/3}\gamma\,\Delta r, \quad \gamma = \left(\frac{1}{2}\left|W'''\right|\right)^{-1/3} \tag{2.30}$$

and $(\pm)$ in s is used depending on the sign of W_c'''. The integral is then expressed in terms of the Airy function (Figure 2.2), yielding:

$$p(r, z_c) = \frac{P_0}{4\pi} k^{1/6}\gamma\left[\frac{2\pi\xi_c}{r_c(n^2-\xi_c^2)^{1/2}(1-\xi_c^2)^{1/2}}\right]^{1/2} Ai(\pm\rho)\exp\left(ikW_c - i\frac{\pi}{4}\right). \tag{2.31}$$

where $(\pm)$ in the Airy function is determined by $(W_c''' \gtrless 0)$. Equation (2.31) is valid on both sides of the caustic, as well as on the caustic at $\Delta r = 0$. We will go into considerable detail in later sections as to this equation's applicability under various circumstances. In general, it will turn out to

be quite useful in predicting pressures on the caustic itself as well as in the adjacent shadow zone and caustic region. And the Airy function will be important in understanding how pressure near the caustic varies with frequency and distance from the caustic, Δr .

We now start again with the wave equation - this time for velocity potential - and summarize the Newman and Ingenito derivation (22) resulting in a finite difference normal mode solution. They start off with the Helmholtz equation in both a water and a fluid bottom layer (Figure 2.3):

$$\nabla^2 \Phi_1(r,z) + \frac{\omega^2}{c_1^2(z)} \Phi_1(r,z) = -\frac{1}{2\pi r} \delta(r)\, \delta(z-z_0) \qquad (2.32)$$

for the region $0 \le z \le H$

and

$$\nabla^2 \Phi_2(r,z) + \frac{\omega^2}{c_2^2} \Phi_2(r,z) = 0 \qquad (2.33)$$

for the region $H \le z \le \infty$

The boundary conditions are

$$\Phi_1(r,0) = 0 \qquad (2.34)$$

$$\rho_1 \Phi_1(r,H) = \rho_2 \Phi_2(r,H) \qquad (2.35)$$

$$\frac{\partial \Phi_1(r,z)}{\partial z}\bigg|_{z=H} = \frac{\partial \Phi_2(r,z)}{\partial z}\bigg|_{z=H} \qquad (2.36)$$

the conventional pressure release surface, and continuity of impedance and normal particle velocity at the bottom boundary. Equation (2.32) leads to a solution for Φ_1 as a sum of discrete and continuous modes. Discrete modes dominate at ranges

beyond a few water depths, so these are all that are considered. (When we examine the mode sum in the normal mode section, it will be clear why contributions from modes in the continuum die out with range.) Separating variables, and normalizing the depth variable $\eta = z/H$, we are left with the η dependent wave equations to solve (34):

$$\frac{d^2 Z_n^{(1)}(\eta)}{d\eta^2} + H^2\left[\frac{\omega^2}{c_1^2(\eta)} - k_n^2\right] Z_n^{(1)}(\eta) = 0 \qquad (2.37)$$

$$0 \le \eta \le 1$$

$$\frac{d^2 Z_n^{(2)}(\eta)}{d\eta^2} + H^2\left[\frac{\omega^2}{c_2^2} - k_n^2\right] Z_n^{(2)}(\eta) = 0 \qquad (2.38)$$

$$1 \le \eta \le \infty$$

where k_n is the eigenvalue for the n^{th} eigenfunction. Newman and Ingenito divide the water layer into m equal finite difference layers, each with velocity $c_1(\eta)$ (Figure 2.4). This is accomplished by defining m layer depths, $1/m, 2/m, \cdots \eta \cdots 1$, and linearly interpo- ting between the input sound velocity points to find e velocity at each of these points. Then into Equation (2.37) in the water layer, they substitute a first central difference for the second derivative:

$$\frac{d^2 Z_{n,i}}{d\eta^2} = \frac{Z_{n,i+1} - 2Z_{n,i} + Z_{n,i-1}}{h^2} \qquad (2.39)$$

where h is the incremental layer depth H/m

Now the differential equation is in finite difference form:

$$Z^{(1)}_{n,i+1} = \left\{2 - H^2h^2\left[\frac{\omega^2}{(c_1^2)_i} - k_n^2\right]\right\} Z^{(1)}_{n,i} - Z^{(1)}_{n,i-1} \qquad (2.40)$$

Thus we now have an expression relating the wave function amplitude for the n^{th} mode at the i+1 depth point to the amplitude at the i^{th} and i-1 points, the velocity at the i^{th} point and the wave number k_n. We will discuss in Section (5) how this is used to find the individual modes, and how they are then summed to find the propagation loss.

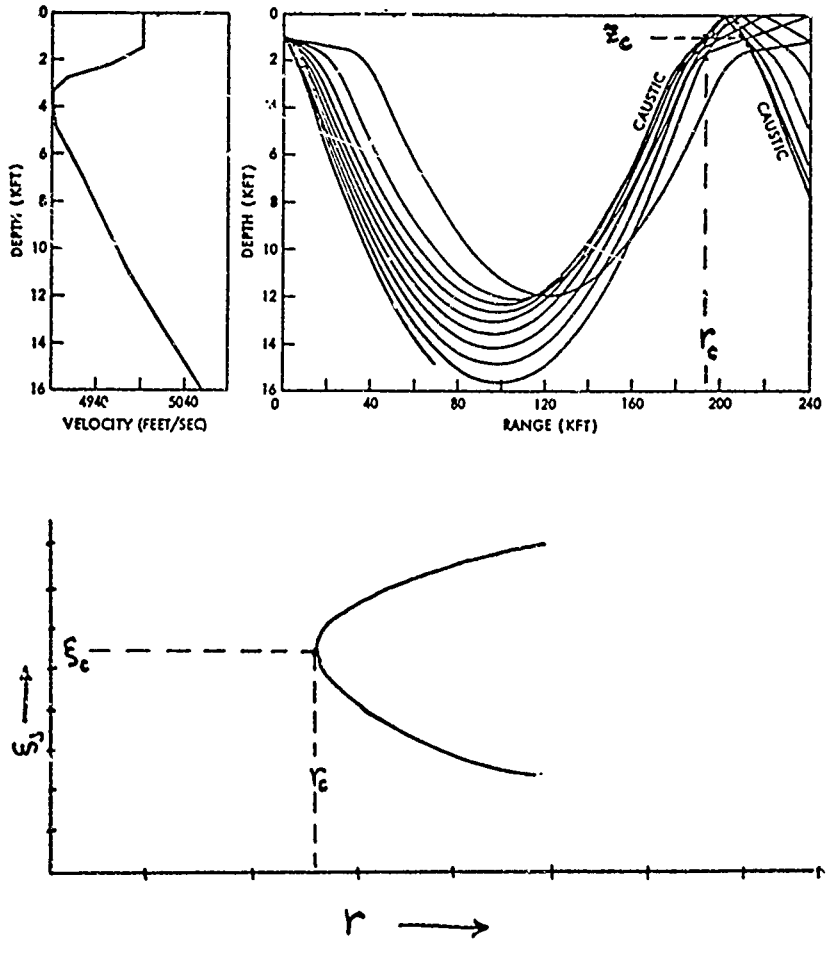

Figure 2.1 Range versus ξ_j ($\xi_j = \sin(\theta_0)_j$; $z_c = 1000$ ft)

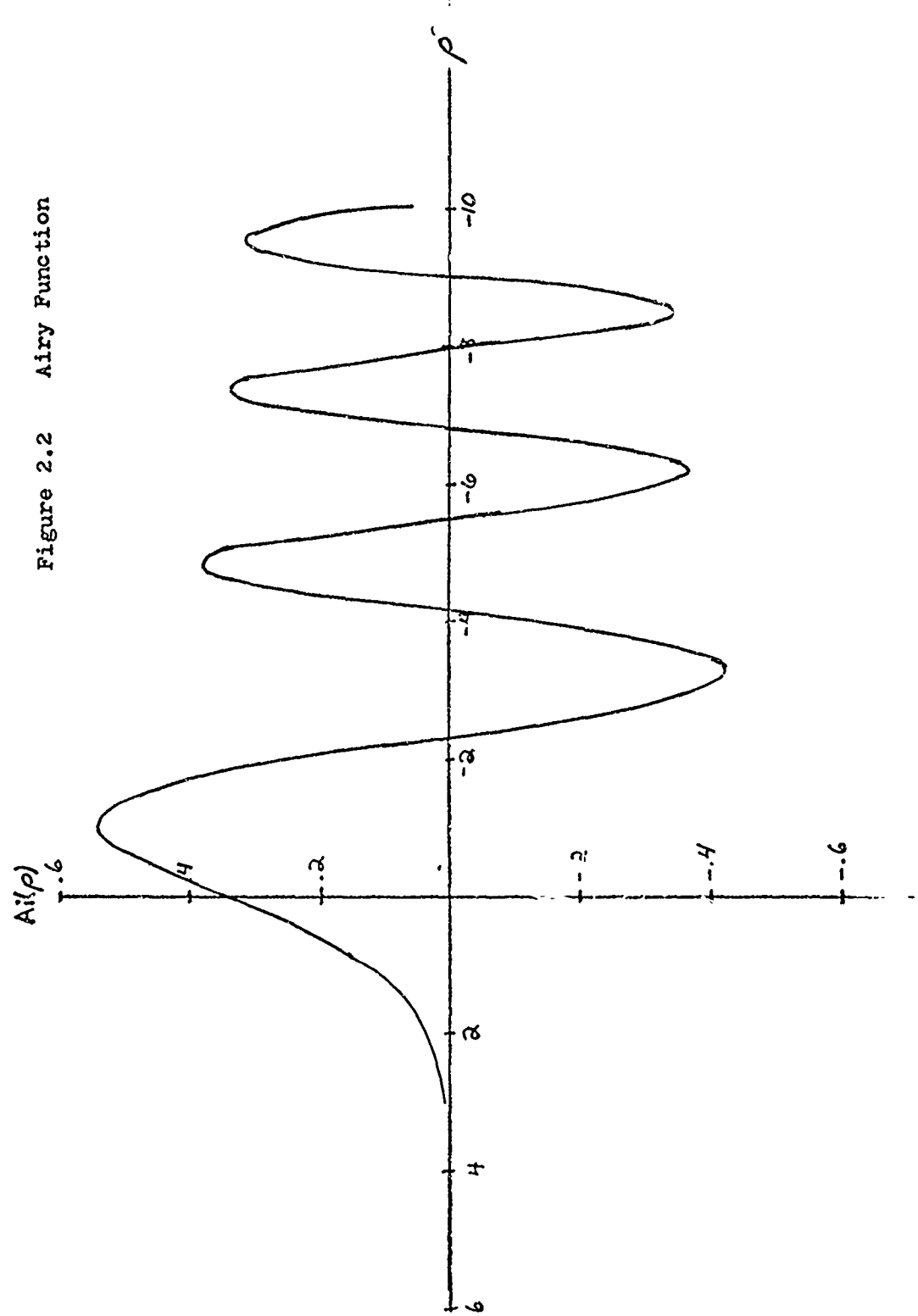

Figure 2.2 Airy Function

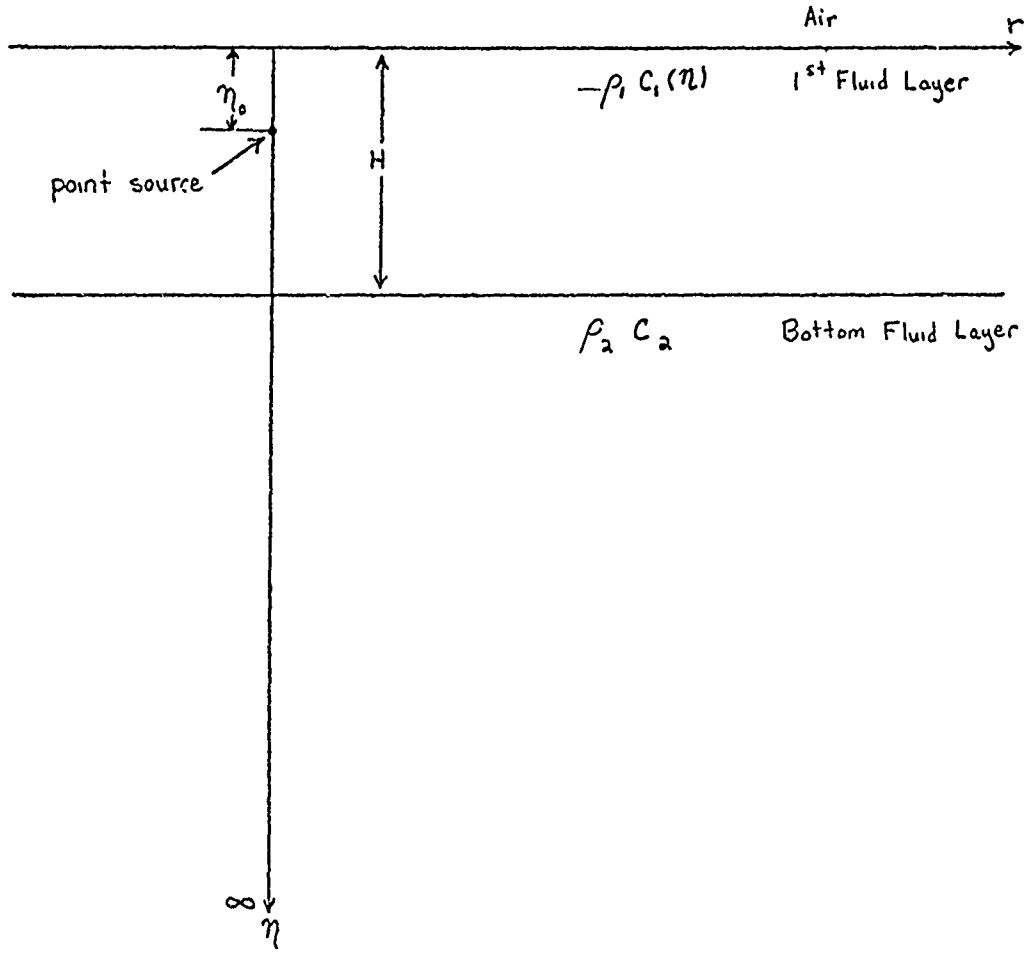

Figure 2.3 Two Fluid Half-Space Model

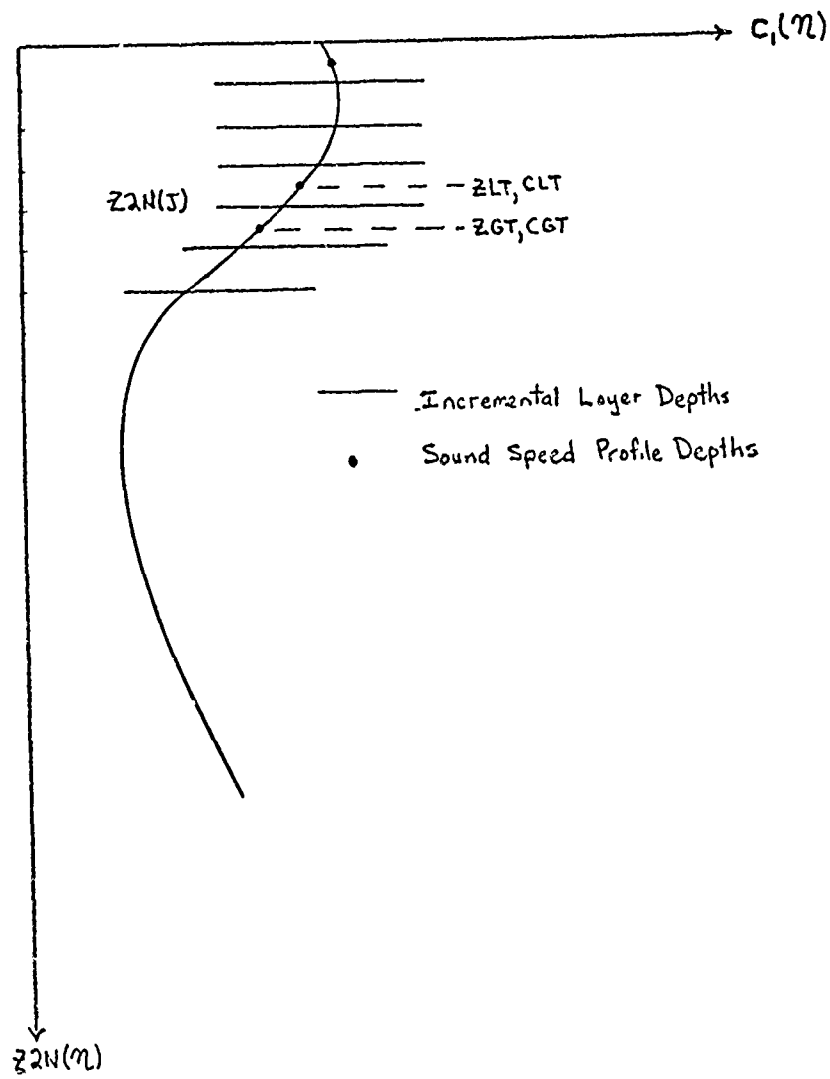

Figure 2.4 Sound Speed Profile Interpolation
(From Newman and Ingenito(22))

3. Ray Theory

It was felt that rather than add one more ray tracing program to the already infinite number in existence, we could modify one already existing to suit our purposes. We wanted first of all to be able to find all the ray paths to a given point in space and add the arrivals coherently in order to calculate the net intensity at that point. Then we wanted to be able to modify the program to calculate the actual pressure on the caustic using modified ray theory (Equation (2.31)). Finally, we wanted to be able to add in shadow zone contributions at a point of interest, when that point is in the shadow zone of one or more caustics.

We chose to use and modify CONGRATS (Continuous Gradient Ray Tracing System), a program written by Weinberg and Cohen at NUSC (31). CONGRATS fits the velocity profile data points with layers of the following depth dependence:

$$c(z) = \left\{ v_0 + (z - z_0) \cdot \frac{g_0 + (z - z_0) g_1}{\left[1 + (z - z_0) g_2\right]^2} \right\}^{-1/2} \qquad (3.1)$$

By the appropriate choices of the four arbitrary parameters v_0, g_0, g_1, g_2 (z_0 is the depth at the top of the layer), one can either describe the profile as a series of straight line segments each with the appropriate gradient (Figure 3.1A), or as a series of curves defined so that both the velocity and

gradient are continuous at each layer interface (Figure 3.1B).* Once the profile is specified, travel time, range, and amplitude along a ray can be easily obtained since the integrals for these quantities are readily evaluated in terms of elementary functions (31).

CONGRATS can be used to plot ray diagrams in order to qualitatively examine the sound field for a specific profile (Figure 1.1). But it can also be used to quantitatively evaluate the intensity at specific points in the sound field. This is accomplished in the following way. One specifies the velocity profile and defines the appropriate profile layers. Then the source depth is defined, as are the particular range-depth target points of interest. Finally, one specifies a grid of rays (by source angle) of fine enough spacing and sufficient angular width in order to ensonify the target range-depth points with each significant type of ray arrival (It is no small task to pick the ray spacing and grid, and skill at this ray selection increases with practice). CONGRATS then traces one ray at a time to each target depth of interest. When CONGRATS finds two consecutive rays that bracket a target range at the target depth (Figure 3.2), it assumes that a ray between those two (called an eigenray) would reach the target point. So the program then interpolates between

*The continuous layers can eliminate many of the false caustics caused when rays turn at layer interfaces and the gradients are discontinuous (35). In the cases we treated this was not a problem, however, and constant gradient layers were adequate.

the two rays in order to find the travel time, amplitude, etc., for that particular eigenray. It then was written to add all the eigenrays at each target range-depth point coherently or incoherently. By doing a series of range points at a fixed depth, one could then generate a typical propagation loss versus range curve (Figure 3.3).

As originally written, CONGRATS' sorting programs for adding the eigenrays coherently were not compatible with the CDC 6400 computer. Furthermore, it could not calculate actual intensity on the caustic when a ray passed through a caustic. And when points of interest were in the shadow zones of one or more caustics, it could not add in these shadow zone contributions to those from "real" rays passing through these points. These are the changes made at the Naval Ordnance Laboratory by the author with the help of Jean Goertner and Robert Thrun.

In this section, we will discuss the coherent sorting program written for a CDC 6400 computer. This program calculates the resultant intensity at each target point of interest. It also can add in shadow zone contributions at each point for any number of caustics, and eliminate bottom bounce arrivals if this is desired. In the modified ray section, we will discuss how CONGRATS has been modified to calculate intensity on the caustic using a modified ray calculation (13).

As we have said, CONGRATS finds the eigenrays that pass through each target point by interpolating between each pair

of rays that bracket each point. If we specify enough rays of different type (direct, surface reflected, etc.), to ensonify the region, we have at each point a complete set of eigenrays that account for all significant energy paths between source and receiver. CONGRATS then writes on tape or permanent file several blocks of data. Each case - defined as the set of input data cards up to the next process card - results first in the writing of a data block containing all of the input data in CONGRATS internal units: kyds, kyds/sec, seconds and radian. The second, and if necessary, succeeding blocks of output data are groups of 100 arrivals, each an eigenray. At this point they are sorted by increasing source angle with range-depth points all intermixed.

Appendix (I) is a listing of the program written at NOL to sort these arrivals and add them coherently. Each eigenray of source angle θ_j that passes through a target point (r, z) has a travel time T_j (r, z) seconds, propagation loss L_j (r, z) dB, and additional phase shift (from surface reflections, caustics, etc.) of ϕ_j (r, z). Ignoring shadow zones and caustics for the moment, one can then find the net propagation loss at a given point (r, z) and a specific frequency ω by:

$$N(r,z) = 20 \log p_0/|p_1(r,z)| \quad \text{dB} \tag{3.2}$$

p_0 is the source pressure at 1 yd

$$\text{and } p_1(r,z) = p_0 \sum_j 10^{(-L_j(r,z)/20)} \exp\left(i\left[\omega T_j(r,z) + \phi(r,z)\right]\right) \tag{3.3}$$

P_1 (r, z) is the net pressure at point (r,z). It is obtained by the coherent sum of real rays. This summation is what the main body of the program accomplishes. In the program listing in Appendix (I), lines 15-30 read the

input data block. Lines 34-90 read in the blocks of eigenrays into a doubly subscripted array Buffer (I, J) and convert from CONGRATS units (kyds, kyds/sec, etc.) to original input units (meters, meters/sec, etc.), (feet, feet/sec, etc.) or any other of the many combinations allowed in CONGRATS. The portion of the program from line (133) to the end first sorts the arrivals by increasing target depth and then by increasing target range for each depth. Then all the arrivals at a given target point (r, z) are added in phase according to Equation (3.3). Appendix (I), pages (149-155) show first the output data block containing all the original data, page (149), then the sorted collection of arrivals, pages (150-153), and finally the resultant intensity and phase at each target depth-range point, pages (154-155).

For some studies it is necessary to eliminate all rays that reflect off the bottom (or surface). For example, our normal mode calculations have been done (for simplicity) with a bottom fluid whose impedence is matched to the water column ($c_2 = c_1$ ($z = H$), $\rho_2 = \rho_1 = 1$). So we would not expect first order bottom reflections to be present in the normal mode calculation. And we would not want the ray calculations to include bottom reflections either. The easiest way to eliminate bottom reflections is to not include rays beyond the grazing ray in the calculation. But sometimes this is not advisable,*

*For example, CONGRATS needs at least one ray at each depth range point in order to store the point for coherent sorting. Sometimes when we are in the shadow zone, there are no real direct rays - only bottom reflected rays. We need these rays to "save" the points of interest so that we can add in the shadow zone arrivals at these points using the summing program.

and another way of eliminating bottom reflections must be used. CONGRATS has the capability for including bottom (or surface) loss as a function of incident angle. So if we want to drop out bottom (or surface) reflections, we set the loss for all angles of reflection to be 9000 dB. Then in the sorting program, Appendix (I), page (147), lines (173-184), we check to see if the propagation loss for any arrival is greater than 9000 dB (i.e. it has reflected off the bottom at least once). All of these arrivals are then eliminated from the calculation.

As we have said, the sorting program must also be able to add in shadow zone arrivals whenever the target point is in the shadow zone of a caustic. We have chosen to work with a modified ray expression that yields results at various ranges on either side of the caustic (as well as on it) at the fixed depth the caustic occurs at. A ray of source angle θ_0 may have a caustic at range r_c and depth z_c. Then the contribution from this caustic at any range r at the caustic depth z_c is given by:

$$p(r, z_c) = \frac{P_0}{4\pi} k^{1/2} \gamma \left[\frac{2\pi \xi_c}{r_c (n^2 - \xi_c^2)^{1/2} (1 - \xi_c^2)^{1/2}} \right]^{1/2} A_i(\pm\rho) \exp\left(ikW_c - i\frac{\pi}{4}\right) \quad (3.4)$$

$$(\pm : W_c''' \gtrless 0)$$

where all quantities of interest were defined in Section (2), Equations (2.30-2.31). The pressure expression, and its region of validity, are further discussed in the modified ray section. For negative ρ and $|\rho| > 1$ we are in the double arrival region associated with the caustic. In Section (4), we will discuss the use of the caustic solution in this region as opposed to the actual two arrivals as calculated from ray theory.

However, in the shadow zone there is no problem. Ray theory yields no shadow zone contribution, and the modified ray theory contribution is necessary for completeness. We need to evaluate both the amplitude and the phase of these arrivals, so that we may incorporate them into the coherent sum (Equation (3.2)). When a ray passes through a caustic, CONGRATS prints out the amplitude on the caustic. This is Equation (3.4) with $\Delta r = 0$, so $\rho = 0$. This is essentially:

$$p(r_c, z_c) = B\,Ai(0) \tag{3.5}$$

since the remainder of the amplitude expression is the same on and off the caustic. Off the caustic at arbitrary r, the pressure is then

$$p(r, z_c) = B\,Ai\left[k^{2/3}\delta(r - r_c)\right] = B\,Ai\left[k^{2/3}\delta\,\Delta r\right] \tag{3.6}$$

So the pressure off the caustic, in terms of the pressure on the caustic calculated by CONGRATS is:

$$p(r, z_c) = p(r_c, z_c)\,|Ai(\rho)|\,/\,Ai(0) \tag{3.7}$$

And the propagation loss at distance Δr off the caustic is

$$20\,Log\left[p(r, z_c)\right] = -20\,Log\left[p(r_c, z_c)\,|Ai(\rho)|\,/\,Ai(0)\right] \tag{3.8}$$

or

$$20\,Log\left[p(r, z_c)\right] = M(r, z_c) = AMPDB - 20\,Log\left[|Ai(\rho)|\,/.36\right] \tag{3.9}$$

where AMPDB is the propagation loss on the caustic calculated by CONGRATS. We also need the total phase of the arrival. We note that

$$W_c(r) = \xi_c r + \phi(z_0) + \phi(z_t) \tag{3.10}$$

It is defined in such a way (Equation (2.10)) that $\phi(z_o)$ and $\phi(z_c)$ must be integrated analytically or numerically. But we would like to use quantities already calculated by CONGRATS where possible to avoid unnecessary calculations. We can follow in reverse a derivation by Officer (36) in order to arrive at a relationship between $W_c(r_c)$ and $T(r_c)$, the travel time to the caustic already calculated in CONGRATS. We take $W_c(r_c)$.

$$W_c(r_c) = \xi_c r_c + \int_{z_T}^{z_o} [n^2(z) - \xi^2]^{1/2} dz + \int_{z_T}^{z_c} [n^2(z) - \xi^2]^{1/2} dz \tag{3.11}$$

$$= \xi_c r_c + \int_{z_o}^{z_c} [n^2(z) - \xi^2]^{1/2} dz \tag{3.12}$$

$$\text{where} \quad \xi_c = \sin(\theta_o)_c = \frac{c(z_o)\sin\theta}{c(z)} \tag{3.13}$$

$$= c(z_o)\xi_c' r_c + c(z_o)\int_{z_o}^{z_c} [\alpha^2(z) - (\xi_c')^2]^{1/2} dz \tag{3.14}$$

$$\text{where} \quad \alpha(z) = \frac{1}{c(z)} \qquad \xi' = \frac{\sin(\theta)}{c(z)} \tag{3.15}$$

Therefore:

$$\frac{W_c(r_c)}{c(z_o)} = \xi' r_c + \int_{z_o}^{z_c} [\alpha^2(z) - (\xi_c')^2]^{1/2} dz \tag{3.16}$$

But for a ray:

$$\frac{\partial W_c(r)}{\partial \xi} = 0 = r + \frac{\partial \phi(z_o)}{\partial \xi} + \frac{\partial \phi(z)}{\partial \xi} \tag{3.17}$$

Then: $$r = -\frac{\partial \phi(z_0)}{\partial \xi} - \frac{\partial \phi(z)}{\partial \xi} \qquad (3.18)$$

or taking the derivative of Equation (3.12),

$$r = \xi' \int_{z_0}^{z_c} \left[\alpha^2(z) - (\xi')^2\right]^{-1/2} dz \qquad (3.19)$$

Substituting this into Equation (3.16) for $r=r_c$ and combining terms:

$$\frac{W_c(r_c)}{C(z_0)} = \int_{z_0}^{z_c} \left[\frac{(\xi_c')^2}{\left[\alpha^2(z)-(\xi_c')^2\right]^{1/2}} + \left[\alpha^2(z)-(\xi_c')^2\right]^{1/2} \right] dz \qquad (3.20)$$

$$= \int_{z_0}^{z_c} \left[\frac{\alpha^2(z)}{\left[\alpha^2(z) - (\xi_c')^2\right]^{1/2}} \right] dz \qquad (3.21)$$

$$= \int_{z_0}^{z_c} \frac{dz}{C(z)\left[1 - (\xi_c')^2 C^2(z)\right]^{1/2}} \qquad (3.22)$$

$$\text{but} \quad \xi_c' = \frac{\sin\theta_c}{C(z)} \Rightarrow \cos\theta_c = \left[1 - (\xi_c')^2 C^2(z)\right]^{1/2} \qquad (3.23)$$

$$\text{Therefore} \quad \frac{W_c(r_c)}{C(z_0)} = \int_{z_0}^{z_c} \frac{dz}{C(z)\cos\theta_c} = \int_{z_0}^{z_c} \frac{ds}{C(z)} = T(r_c) \qquad (3.24)$$

So if we have travel time to the caustic from CONGRATS, $T(r_c)$, we can immediately evaluate $W(r_c)$ by:

$$W_c(r_c) = c(z_o)\,T(r_c) \tag{3.25}$$

Or for arbitrary r, off the caustic in either direction,

$$W_c(r) = \xi_c r + \phi(z_o) + \phi(z_c) \tag{3.26}$$

$$= \xi_c(r - r_c) + \phi(z_o) + \phi(z_c) + \xi_c r_c \tag{3.27}$$

$$= \xi_c(r - r_c) + W_c(r_c) \tag{3.28}$$

$$= \xi_c \Delta r + c(z_o)\,T(r_c) \tag{3.29}$$

$$\text{Then} \quad kW_c(r) = \frac{\omega\,\xi_c(\Delta r)}{c(z_o)} + \omega T(r_c) \tag{3.30}$$

Thus the main phase term in Equation (3.14) is readily calculated from constants (ξ_c, ω, $c(z_o)$, Δr) and the travel time to the caustic point $T(r_c)$ calculated by CONGRATS. To complete the phase we must also add $-\pi/4$ and any extra phase shift $\phi(n)$ associated with extra caustics, surface reflections, etc. the ray may have undergone. We can then add to the arrivals given by Equation (3.3) shadow zone arrivals for the caustics occurring at the depth of interest (z_c) and various ranges $r_c(1)$, $r_c(2)$ ... $r_c(n)$:

$$I_T(r, z_c) = I_1 + \sum_n 10^{-\left(M_n[r, z_c]/20\right)} \exp i\left[\frac{\omega(\xi_c)_n(\Delta r)_n}{c(z_o)} + \omega T[r_c(n)] - \frac{\pi}{4} + \phi(n)\right] \tag{3.31}$$

P_T is the coherent sum of all rays, including caustic shadow zone contributions. This is done in the sorting program, Appendix (I), lines (93-130). We only add an arrival from the n^{th} caustic as long as we are in the shadow zone of that particular caustic ($\pm\rho > o$). For a typical range minimum convergence zone caustic, W_c'''

is negative, so we use $Ai(-\rho)$. Thus Δr must be negative in order for $-\rho$ to be positive, and r must be less than r_c. So we are to the left of the caustic, nearer the source.

This then describes CONGRATS and the sorting program we have written to accompany it. The sorting program adds the regular ray arrivals coherently. It adds in shadow zone arrivals coherently when the target point is in the shadow zone of one or more caustics. And bottom reflections can be eliminated when this is desired.

Figure 3.1A Constant Gradient Fit to Profile Data Points

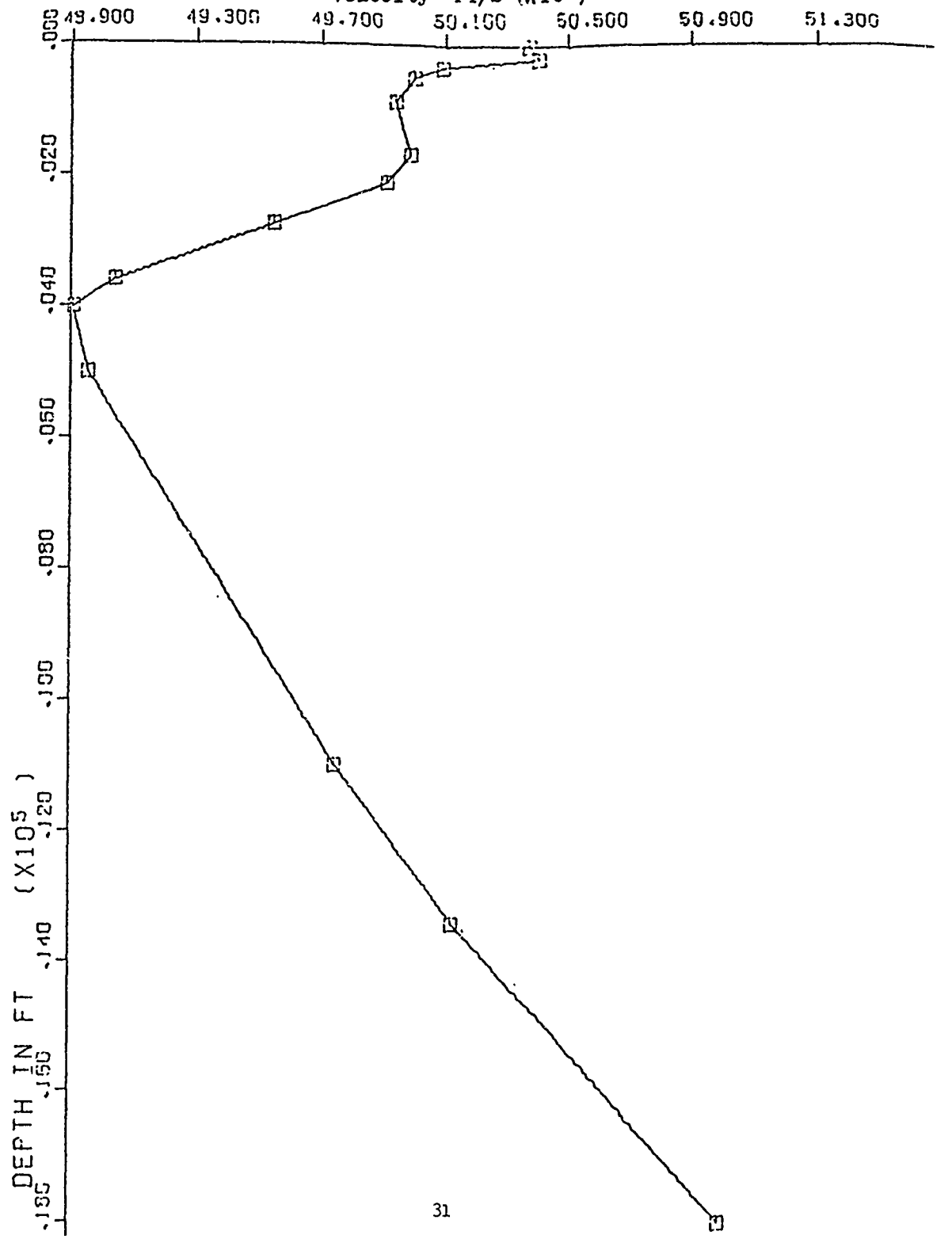

Figure 3.1B Continuous Gradient Fit to Profile Data Points

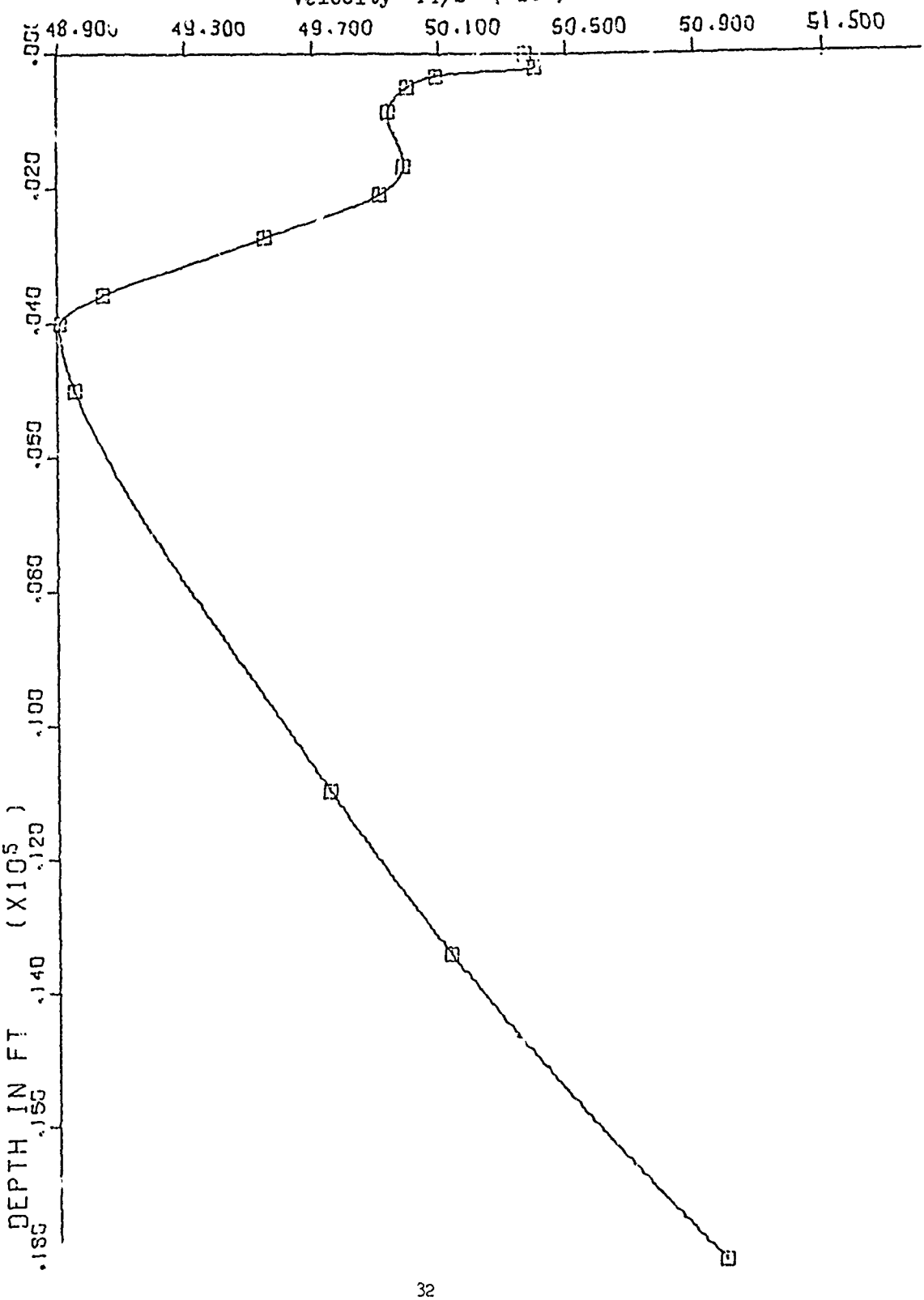

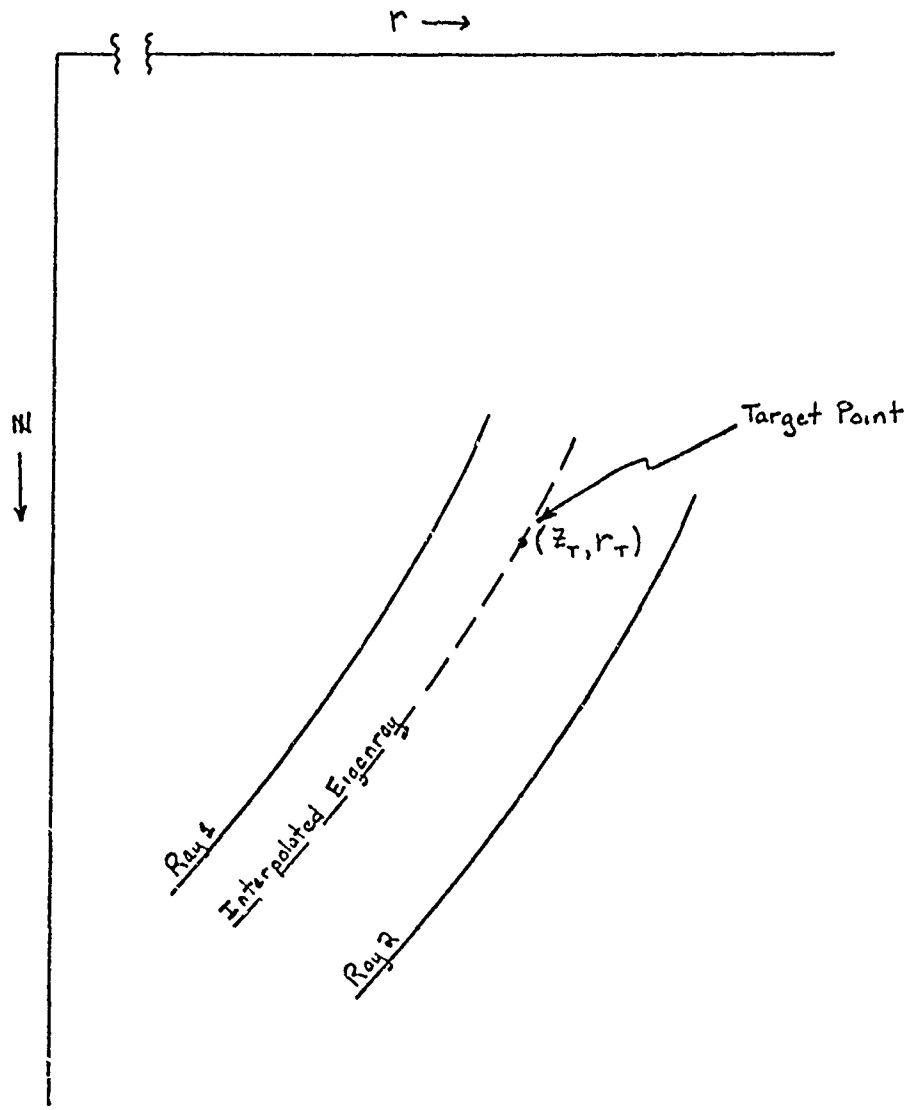

Figure 3.2 Search for Eigenray

Figure 3.3 Typical Propagation Loss vs. Range Plot

4. Modified Ray Theory

While ray theory is used extensively for propagation loss calculation, its failure near caustics is well documented. The predictions of infinite peak pressure on the caustic and zero pressure in the adjacent shadow zone are two unrealistic and unacceptable conditions. This failure occurs because of the "high frequency" approximation inherent in the eikonal equation (37). It yields a picture in which all energy within a ray tube of a given cross section at the source remains within that ray tube as the cross section goes to zero at the caustic (defined as the locus of points where infinitesimally close rays cross). So the finite amount of energy, contained in a zero cross section ray tube, yields infinite peak pressure. If we are interested in pressure on the caustic, or in the adjacent shadow zone, another solution must be used.

To this end, several authors (12-14) have solved the wave equation for expressions that remain valid on the caustic. Sachs and Silbiger (13) and Brekhovskikh (12) obtained an expression that yields pressure on the caustic, as well as off the caustic horizontally in either direction (Figure 4.1A). Ludwig's derivation (14) yields pressure on the caustic, and off the caustic in either direction normal to it (Figure 4.1B). Ludwig's solution has both a uniform and non-uniform result. The uniform asymptotic theory is exact in the ray double arrival region, while the non-uniform solution is only approximately correct there. Ludwig's non-uniform result is very similar to Sachs and Silbiger's result (13). The similarities and

differences between the various solutions will be discussed in more detail later on in this section. The horizontal expansions in particular have been used to predict pressure histories from underwater explosions in convergence zones (8) and in flooded quarries (8,9). They also have been compared with ray theory and normal mode theory for a monotomically decreasing sound velocity profile (6).

In our earlier work (8), we used a constant gradient profile for which the modified ray solution could be obtained analytically. We will start out by summarizing this derivation for pressure on and near a caustic. Then we will discuss the evaluation of the various quantities necessary to actually calculate pressure. And finally we will relate these expressions to the appropriate quantities in CONGRATS that were being, or are now being, calculated.

As we have pointed out in Section (2), one can solve the wave equation using a WKB approximation and arrive at a ray solution (Section 2, Equation 2.17). This equation breaks down at a caustic. A further derivation results in a new integral (2.29) for pressure on and near a caustic. When the integral is evaluated, Sachs and Silbiger (13) arrive at an expression valid at caustics (2.31):

$$p(r, z_c) = \frac{P_0}{4\pi} k^{1/6} \left[\frac{2\pi \xi_c}{r_c (n^2 - \xi_c^2)^{1/2} (1 - \xi_c^2)^{1/2}} \right]^{1/2} Ai(\pm\rho) \exp\left(ikW_c - i\frac{\pi}{4}\right) \quad (4.1)$$

$$(\pm : W_c''' \gtrless 0)$$

where $\xi_c = \sin(\theta_0)_c$, $(\theta_0)_c$ is the source angle passing through a caustic at (r_c, z_c) and the remaining quantities are defined in Equation (2.30).

For a typical convergence zone caustic (Figure 4.2), $W_c'''(r_c)$ is negative; hence we use $A_i(-\rho)$. Then for $r > r_c$, to the right of the caustic at $\rho = 0$, the Airy function, and so the pressure, first rises as we move through the caustic region (Figure 2.2). Further to the right ($|\rho| > 1$), we see oscillations in the Airy function that are typical of the well known ray double arrival region adjacent to the caustic. To the left of the caustic, for positive arguments of the Airy function, the pressure decays exponentially with distance off the caustic as well as frequency to the two thirds power. For a caustic with $W_c'''(r_c)$ positive, the picture is completely reversed with the shadow zone to the right of the caustic, etc.

Several quantities must be evaluated in order to calculate pressure on or near a caustic using Equation (4.1). First we have to know when a particular ray goes through a caustic. As has been pointed out, a caustic is a range minimum or maximum point at constant depth. So at a caustic

$$\frac{\partial r}{\partial \xi} = -\frac{c(z_0)}{\xi^2}\left(\frac{\partial r}{\partial c_v}\right) = 0 \qquad (4.2)$$

where $\sin\theta_0 = \xi = \frac{c(z_0)}{c_v}$

and C_v is the sound velocity at the vertex of the ray. CONGRATS determines this by evaluating $\frac{\partial r}{\partial c_v}$ along a ray, and checking for changes in sign of this quantity, indicating it has passed through zero. This is equivalent to the check on $\frac{\partial^2 W}{\partial \xi^2}$ we have used in previous work (38). So for a given source angle (θ_0) we can move along the ray until $\frac{\partial r}{\partial c_v}$

approaches zero. At this point (r_c, z_c) we are on the caustic. By tracing a number of rays of different source angles, we can generate one or more caustic curves in r, z space and find the caustics at a particular depth of interest (Figure 4.3). Then r_c, z_c, Δr (to the point of interest), $n^2(z_c)$, ξ_c, k, and $W_c(r)$ (Section 2, Equations 2.10 and 2.12) are fixed for each caustic.

Thus we need only to evaluate δ (Equation 2.30) in order to find the pressure on the caustic. We have an expression for δ in Sachs and Silbiger notation, but we first need the proper derivation in CONGRATS notation. In CONGRATS, the range increment in a layer is defined as:

$$|r| = \Delta R = \left| \int_{z_1}^{z_2} \frac{C(z)\,dz}{\sqrt{C_v^2 - C^2(z)}} \right| \qquad (4.3)$$

Because C(z) is defined analytically as a function of z (Equation 3.1), this integral can be evaluated in terms of elementary functions (39). Its first derivative, $\partial r/\partial C_v$, which is needed for ray amplitude calculation and caustic location, was also evaluated analytically. But we need the second derivative, $\partial^2 r/\partial C_v^2$, for caustic amplitude calculation. This derivative was obtained, and it is summarized in Appendix (IV). It was then inserted into CONGRATS. In order to use this derivative, we must relate it to $\frac{\partial^3 W_c(r_c)}{\partial \xi^3}$, the derivative in our modified ray notation (Equation 2.30).

We start off with:

$$W_c(r) = \xi_c r + \phi(z_0) + \phi(z_c) \tag{4.4}$$

$$\frac{\partial W_c(r)}{\partial \xi} = r + \frac{\partial \phi(z_0)}{\partial \xi} + \frac{\partial \phi(z_c)}{\partial \xi} \tag{4.5}$$

On a ray $$\frac{\partial W}{\partial \xi} = 0 \Rightarrow r_c = -\frac{\partial \phi(z_0)}{\partial \xi}\Big|_{\xi=\xi_c} - \frac{\partial \phi(z_c)}{\partial \xi}\Big|_{\xi=\xi_c} \tag{4.6}$$

From Equation(4.5), $$\frac{\partial^2 W}{\partial \xi^2} = \frac{\partial}{\partial \xi}\left[\frac{\partial \phi(z_0)}{\partial \xi} + \frac{\partial \phi(z_c)}{\partial \xi}\right] \tag{4.7}$$

But from Equation(4.6) $\frac{\partial^2 W}{\partial \xi^2} = -\frac{\partial r}{\partial \xi}$ as long as we are on a ray.

Then $$\frac{\partial^3 W}{\partial \xi^3} = -\frac{\partial^2 r}{\partial \xi^2} \tag{4.8}$$

where r is the analytic range expression in CONGRATS.

Since $$\frac{\partial r}{\partial \xi} = \frac{\partial r}{\partial c_v} \cdot \frac{\partial c_v}{\partial \xi} \tag{4.9}$$

$$\frac{\partial^3 W_c}{\partial \xi^3} = -\frac{\partial^2 r}{\partial \xi^2} = -\frac{\partial}{\partial \xi}\left[\frac{\partial r}{\partial c_v} \cdot \frac{\partial c_v}{\partial \xi}\right] \tag{4.10}$$

$$= -\frac{\partial}{\partial \xi}\left(\frac{\partial r}{\partial c_v}\right) - \frac{\partial r}{\partial c_v}\frac{\partial^2 c_v}{\partial \xi^2} \tag{4.11}$$

But $\frac{\partial r}{\partial c_v} = 0$ on a caustic, so

$$\frac{\partial^3 W_c}{\partial \xi^3} = -\frac{\partial}{\partial c_v}\frac{\partial c_v}{\partial \xi}\left(\frac{\partial r}{\partial c_v}\right) = -\frac{\partial c_v}{\partial \xi}\left[\frac{\partial^2 r}{\partial c_v^2}\right] \tag{4.12}$$

$$= \frac{c(z_0)}{\xi^2}\left[\frac{\partial^2 r}{\partial c_v^2}\right] \tag{4.13}$$

So with the second range derivative (Appendix IV) we have added to the program, and the appropriate constants, we can calculate $\partial^3 W_4(r_1)/\partial\xi^3$ and so γ. This then is the final quantity necessary to calculate pressure on the caustic by Equation (4.1), and evaluate modified ray theory arrivals in Equation (3.31).

Now that we have shown how to calculate the pressure on and near a caustic, we would like to discuss the validity of its use at various locations near the caustic and its relationship to other methods of caustic calculation. Looking at Equation (4.1), we can picture the pressure as a constant times the Airy function (Figure 2.2). For Ai(0), we are on the caustic and the expression is valid for most single, well-behaved caustics. For Ai($-\rho$), the pressure at first grows in what we call the caustic region ($0 \leq |\rho| \leq 1.5$). Here we expect the caustic solution to be better than the ray solution which is diverging (Figure 4.4). We note that $\rho = k^{2/3}\gamma\Delta r$. The quantity γ is roughly the focusing factor, indicating the strength of the caustic. It is also related to the slope of the caustic. For typical convergence zone caustics we characterize as vertical (Figure 4.2) (depth to range slope: 1:10), γ is on the order of .002. Therefore the source frequency and width of the caustic region (where ray theory is invalid) are related by:

$$\Delta r \approx 750/k^{2/3} \qquad (4.14)$$

Thus a 100 Hz source will have a caustic region about 2500 meters wide. The lower the frequency, the wider tne caustic region where ray theory is not valid.

For larger negative arguments (to the right or left of the caustic depending on whether $W_c'''(r_c)$ is negative or positive), we are in the ray double arrival region, where ray theory is valid. The caustic solution (with an asymptotic form of the Airy function) does yield two arrivals (40):

$$p(r, z_c) = \frac{P_0}{4\pi}\left[\frac{\xi_c \delta^{3/2}}{2r_c (1-\xi_c^2)^{1/2} (n^2-\xi_c^2)^{1/2} (\Delta r)^{1/2}}\right] \cdot \left\{\exp\left(ik\left[W_c - \left(\frac{2}{3}\delta \Delta r\right)^{3/2}\right]\right) + \exp\left(ik\left[W_c + \left(\frac{2}{3}\delta \Delta r\right)^{3/2}\right] - \frac{i\pi}{2}\right)\right\} \tag{4.15}$$

However, they are of equal amplitude, a condition that we only expect to be true very near the caustic.

Since this expression is only an approximation derived from the value on the caustic, we shall see that from case to case the oscillation pattern agrees more or less with the actual pressure as calculated by ray theory or normal mode theory. This agreement and disagreement can be understood by considering Figure (4.5). Consider a caustic at point (A) (Figure 4.5A). We then extend the caustic solution horizontally into the double arrival region to point (B). This extension will only be valid when the rays actually passing through point (B) have essentially the same history near the caustic as the ray passing through the caustic at point (A). Only this way can the ray going through (A) "know" what rays at (B) should look like.

For the simple circular caustic, this is easiest to see (Figure 4.5A). As long as the radius of curvature is roughly the same, rays at (B) (having passed through C) are roughly the same as the ray passing through a caustic at (A). Then an extrapolation to (B) based on (A) is roughly correct. This is easiest to see at Point (E) when ray (1) is at a distance from the caustic equal to AB. The ray pattern looks similar to that at (B). But if the curvature changes (Figure 4.5B) then the rays at (B) (having passed through C) do not have the same history as the ray passing through (A). Again look at (E), when ray (1) is the appropriate distance from the caustic. The ray pattern at (E) is different than at (B), while the expansion assumes the pattern is the same at both points. For more complicated caustics, it is not as easy to see. But the same rule of thumb applies. As long as the radius of curvature, or slope, of the caustic does not change much along the caustic, say from (C) to (A), we can extend the caustic solution horizontally to a point near (A) through which rays from (C) pass.

In the shadow zone, we have no real rays from that caustic to compare modified ray theory to. The shadow zone arrival is the only one. But from the Airy function (Figure 2.2), the pressure falls as the two thirds power of frequency at a given distance Δr, or linearly with horizontal distance from the caustic for a fixed frequency. We can only verify this behavior by comparison with normal mode theory, since ray theory predicts zero pressure in the shadow zone.

For more nearly horizontal caustics (Figure 4.6) that have depth to range slopes of approximately 1:100, δ is less than .001. In this case the width of the caustic region is roughly two to five times wider than in the vertical case (Equation 4.16). Intuitively we would expect the peak amplitude to be lower, as the energy is spread over a broader caustic region. This is generally the case. The horizontal caustics tend to have significantly lower peak amplitude, with the pressure falling off much more slowly into the shadow zone than in the vertical case.

The same arguments hold for extensions into the double arrival region from smooth horizontal caustics that hold for vertical caustics. Reasonable predictions depend on the caustic having the same radius of curvature throughout the region of interest. However for horizontal caustics (Figure 4.6) the rays must travel considerably farther to reach an arbitrary point (B), distance AB from the caustic. So the caustic must maintain the same local slope, or radius of curvature, for a much longer distance. This makes it more difficult for the horizontal expansion to work, and it is this case where a normal expansion is more reasonable. In Figure (6), FB is much shorter than AB. Thus a prediction for (B) based on (F) is more likely to work than one from (A) extended to (B). Furthermore, there may not be a caustic at the proper depth, line (D). In this case, a horizontal expansion into the shadow zone is not possible.

4.1A: Horizontal

4.1B: Normal

Figure 4.1 Horizontal and Normal Expansion off a Caustic

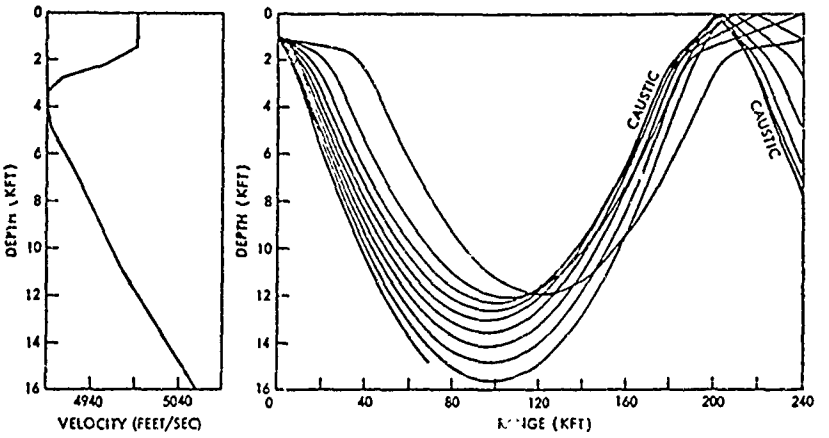

Figure 4.2 Typical Convergence Zone Caustic

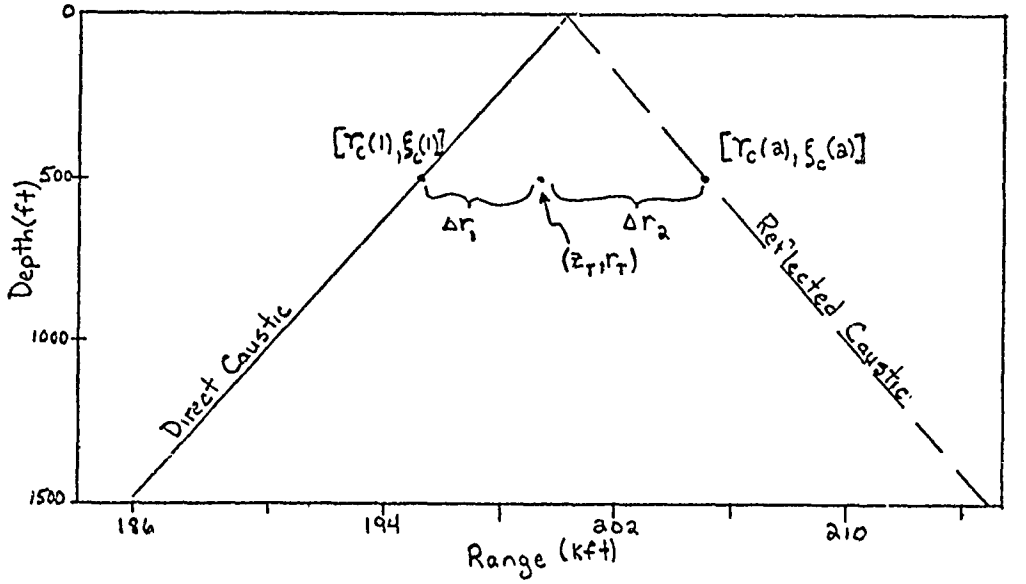

Figure 4.3 Caustic Curves for Profile in Figure (4.2)
(Shallow Portion, Caustics at Target Depth z_t)

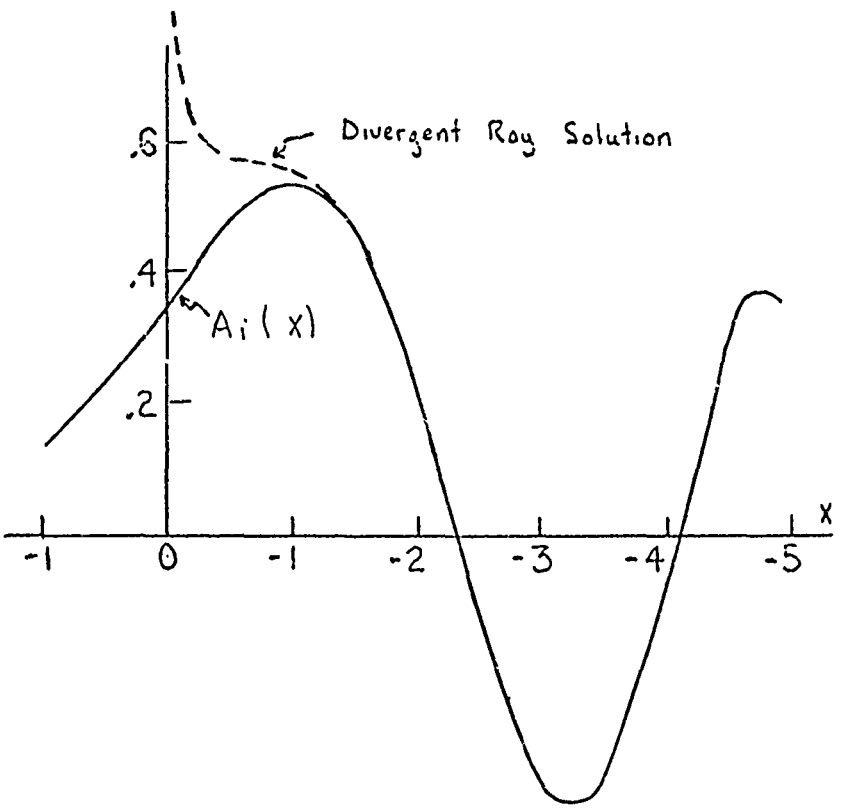

Figure 4.4 Airy Function and Divergent Ray Solution

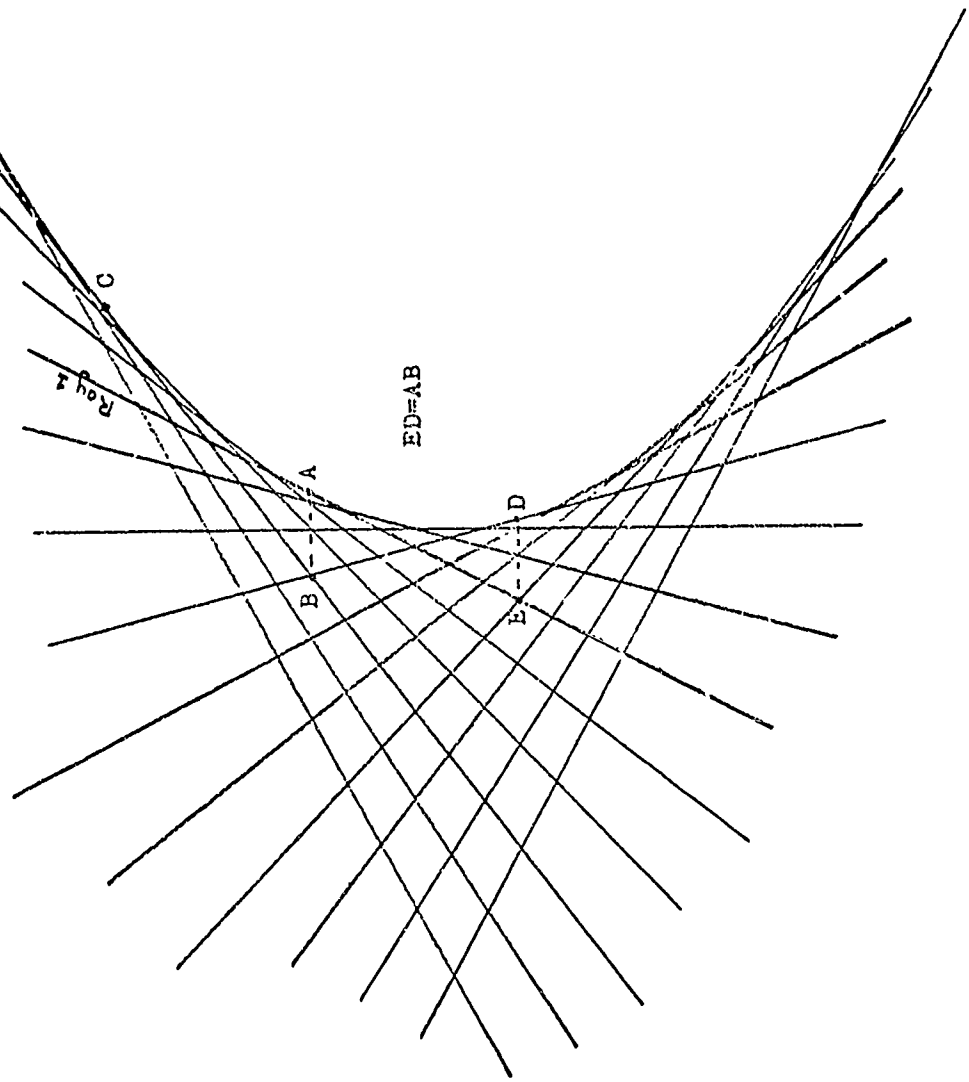

Figure 4.5A Constant Caustic Curvature

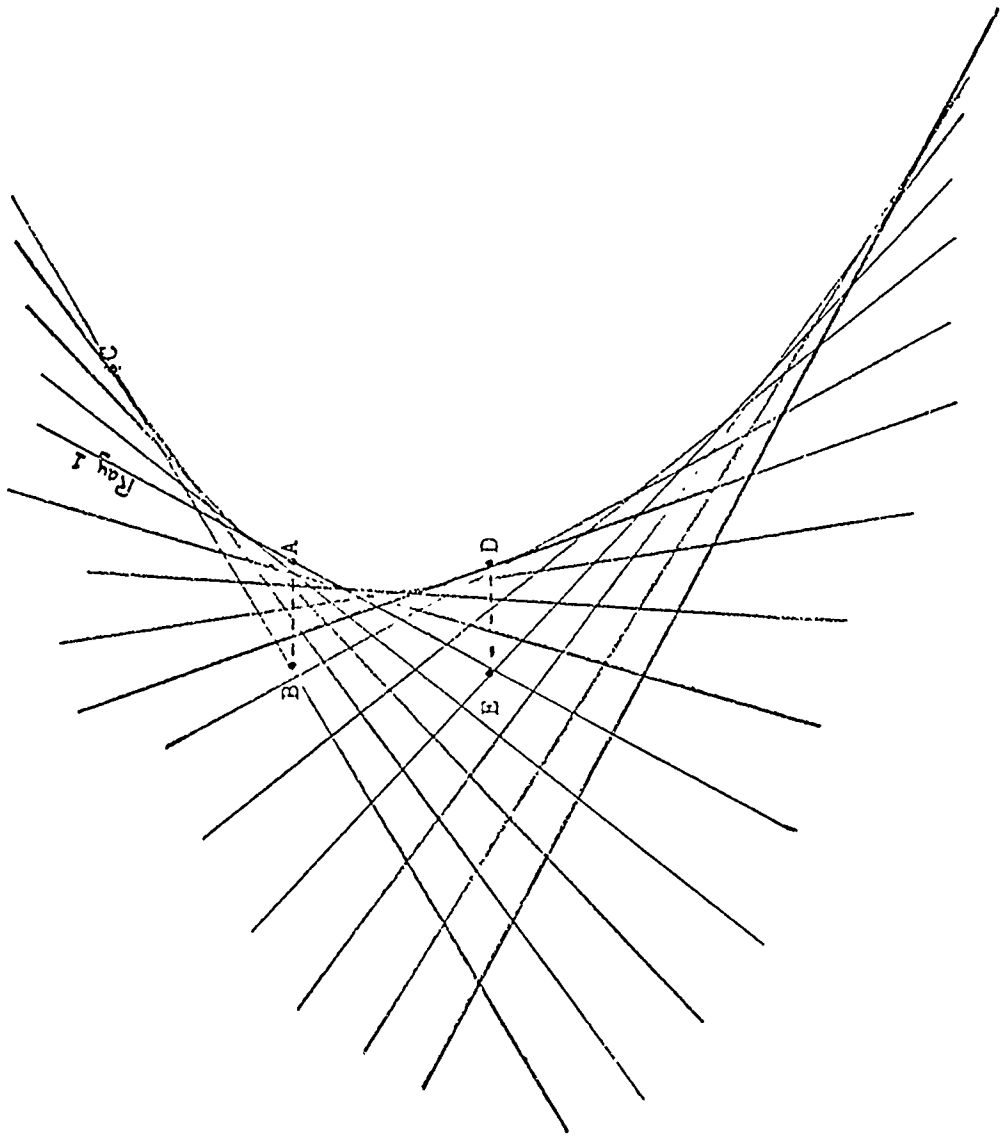

Figure 4.5B Changing Caustic Curvature

Figure 4.6 Typical Horizontal Caustic

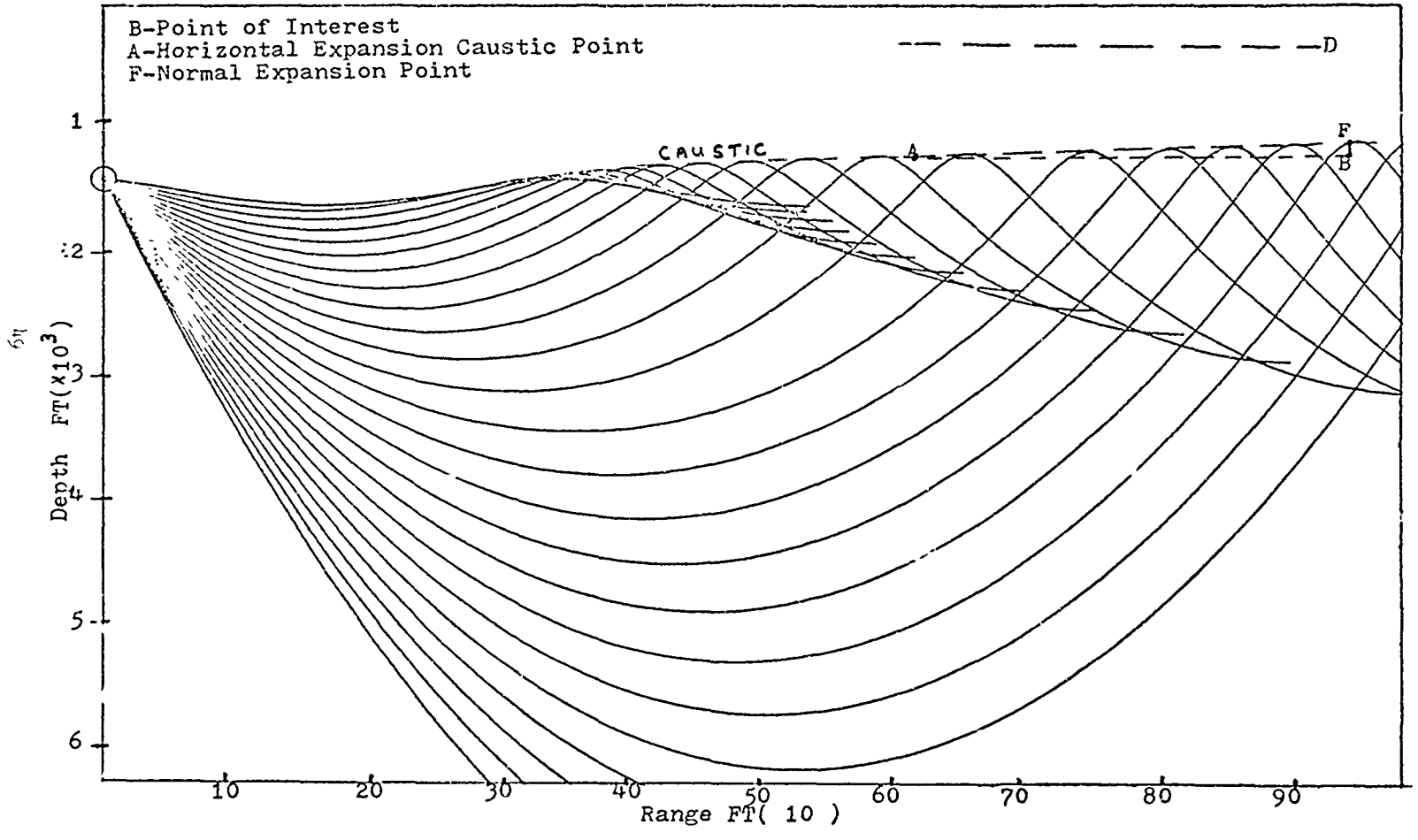

5. Normal Mode Theory and Program Validation

Normal mode theory is the most general of the three solutions to the wave equation that we have examined. By solving the wave equation directly, rather than the ray equation approximation, we avoid the problems inherent in ray theory and modified ray theory. Normal mode theory does not break down at caustics. It yields finite non-zero pressure in the shadow zone, accounting for energy diffracted from the caustic. And it yields the resultant intensity at a given point directly. No ray theory type addition of various ray energy paths - and the worry of missing one - need be done.

This is not to say that normal mode theory is flawless. In solving for the net intensity, it eliminates one of the nice things about ray theory - the very physical picture the ray diagram (Figure 4.2) gives about the paths that energy is taking between source and receiver. There have been attempts (41) to relate various portions of the mode spectrum to specific types of rays. However, we are more comfortable understanding the intensity in terms of the ray and modified ray arrivals interfering with each other, and then comparing this to the normal mode theory result in order to understand the significance of the various intensity variations in the propagation loss curve. Other faults of normal mode theory will be discussed during the remainder of this section. But in general, for deep ocean profiles it becomes a case of solving for many modes (which at some point becomes too many), and doing it completely over each time a different source frequency is specified. The

frequency dependence is not like ray or modified ray theory, where geometry is considered first as ray paths are calculated, and then frequency is accounted for only during the coherent addition of arrivals. In normal mode theory each frequency results in a completely different set of modes, and so a completely new calculation must be done from start to finish.

So as with anything else, each theory has its appropriate use. Normal mode theory is suitable for shallow water (few modes) profiles and for some deep water (moderate number of modes) profiles. It serves as an excellent standard of comparison with each to check out ray and modified ray theory results. Ray theory is especially useful for many deep water profiles, and modified ray theory extends its usefulness by adding the capability for intensity calculations on and near caustics.

Once one decides that a normal mode solution is desired, there are several alternative routes for doing the calculation. As discussed in Section (2), we have chosen to use a finite difference approach, enabling us to deal with an arbitrary velocity profile. We have taken a program originally written for the shallow water case, and we have made the appropriate modifications so that it could handle the deep water case. In the process we have learned quite a bit not only about normal mode calculations in general, but also about the peculiarities of finite difference calculations in particular.

First we will briefly describe the use of the equations obtained by Newman and Ingenito (22) to calculate the normal modes for a given profile. Then we will discuss the summing program written to calculate the propagation loss once the

normal modes have been obtained. Finally we will discuss the changes made in the normal mode computer program so that it could treat the deep water case.

As discussed in Section (2), Newman and Ingenito arrived at a finite difference expression for the unnormalized wave function at the i + 1 point in terms of the sound velocity in the i^{th} layer, the trial mode wave number k_n, and the value of the wave function at the i - 1 and i^{th} point:

$$Z^{(1)}_{n,i+1} = \left\{ 2 - H^2 h^2 \left[\frac{\omega^2}{(c_1^2)_i} - k_n^2 \right] \right\} Z^{(1)}_{n,i} - Z^{(1)}_{n,i-1} \qquad (5.1)$$

The velocity profile has been split up into m equal depth layers of depth h, and the velocity $(c_1)_i$ specified in each layer. If we had two points to start off Equation (5.1), $Z^{(1)}_{n,1}$ and $Z^{(1)}_{n,2}$, and a k_n, we could generate the mode shape. Then if the mode shape satisfied all the boundary conditions and had the correct shape (the n^{th} mode has n-1 zero crossings), we would know that we had the correct value of k_n, as well as the proper mode shape. Using the two boundary conditions at the water-bottom interface, Newman and Ingenito (42) arrive at expressions for the first two wave function values, at the water-bottom interface and one layer up:

$$Z^{(1)}_{n,1} = \rho_2/\rho_1 = R \qquad \text{for } z = H \text{ or } \eta = 1 \qquad (5.2)$$

$$Z^{(1)}_{n,2} = R \left\{ 1 + \frac{h}{R} A^{1/2} - \frac{h^2}{3} D - \frac{h^2}{6} W - h^3 \frac{A^{1/2} D}{6R} \cdots \right\} \qquad (5.3)$$

$$\text{for } \eta = 1 - h$$

where $$A = H^2\left[k_n^2 - \frac{\omega^2}{c_2^2}\right]$$

$$D = H^2\left[\frac{\omega^2}{c_1^2(\eta)} - k_n^2\right] \qquad (5.4)$$

$$W = H^2\left[\frac{\omega^2}{c_1^2(\eta-h)} - k_n^2\right]$$

(There are several typographical errors in this part of their report and this part of the program listing as well.)

The program then takes these two points, the trial k_n, Equation (5.1), and the velocity profile; it follows the wave function up to the surface. k_n is iterated on until we have the proper number of zero crossings, and the wave function is within some small epsilon of zero at the surface. This last requirement satisfies the last boundary condition of the surface as a pressure release boundary.

The iteration on k_n should be started in a way that minimizes the number of trial solutions tested before the proper k_n is obtained. For the first mode, a maximum mode wave number $k_n(\max)$, and a minimum mode wave number $k_n(\min)$ are defined by:

$$k_n(\max) = \frac{\omega}{\left[c(\eta)\right]_{\min}} \qquad (5.5)$$

$$k_n(\min) = \frac{\omega}{c_2} \qquad (5.6)$$

where $\left[c(\eta)\right]_{\min}$ is the minimum sound velocity in the water and c_2 is the velocity in the bottom. Several trial k_n between $k_n(\max)$ and $k_n(\min)$ are tried until a mode shape with no zero crossing is obtained*. Then this k_n and $k_n(\max)$ are used as the bracketing values which the final iteration

*The first mode just reaches zero amplitude at the surface.

process starts off with. For the n^{th} mode, k_{n-1} is used as a lower limit instead of $k_n(max)$, and the upper limit is adjusted down from $k_n(min)$ until n-1 zero crossings are obtained. Otherwise the iteration process is the same.

The normalization constant is found by numerical integration of the wave function in the water layer and analytical integration of it in the bottom layer. After each normalized mode $U_n(\eta)$ is calculated, the wave number, k_n, and other necessary information about the mode is written on a permanent file when our revised version is used. Also written on this file is the particular mode amplitude at one source depth $U_n(\eta_0)$ and up to five receiver depths $U_n(\eta)$ (Main program, lines 190-230). The file then serves as input for the summing program listed in Appendix (III).

In this summing program, we calculate the pressure at a given point in space by relating pressure to velocity potential:

$$p(r,z) = \rho \frac{\partial \Phi(r,z)}{\partial t} \tag{5.7}$$

Using the suppressed $e^{-i\omega t}$ time dependence and the velocity potential (43):

$$\Phi(r,z) = -i \left(\frac{1}{8\pi r}\right)^{1/2} \frac{\rho_1}{H} \sum_n \frac{U_n(\eta_0)\, U_n(\eta)}{k_n^{1/2}} e^{ik_n r - i\frac{\pi}{4}} \tag{5.8}$$

We obtain from (5.7)

$$p(r,z) = \frac{\omega \rho_1^2}{H} \left(\frac{1}{8\pi r}\right)^{1/2} \sum_n \frac{U_n(\eta_0)\, U_n(\eta)}{k_n^{1/2}} e^{ik_n r - i\frac{\pi}{4}} \tag{5.9}$$

The continuous portion of the mode spectrum consists of modes for which $|k_n| < \omega/c_2$. Solutions of Equations (2.37) and (2.38) lead to imaginary values of k_n and so an $\exp(-k_n r)$ in Equation (5.9). So these modes are damped out for ranges greater than a few water depths.

We then assume spherical spreading close in, so that the reference pressure at unit distance is (44):

$$P_0(r,z) = -\frac{i\omega\rho_1}{4\pi}\frac{e^{ikR}}{R} \tag{5.10}$$

which at 1 meter yields:

$$\frac{\omega\rho_1}{4\pi} \; nm^2 \tag{5.11}$$

Therefore the propagation loss is:

$$P.L. = 20\,Log\,\frac{P_0}{P} = -20\,Log\,\frac{\rho_1}{H}\frac{\sqrt{2\pi}}{\sqrt{r}}\sum_n \frac{u_n(z_0)\,u_n(z)}{k_n^{1/2}} \tag{5.12}$$

Thus given the mode wave numbers, other constants such as density and water depth, H, and mode amplitudes at the source and receiver depths for each mode, we can calculate the propagation loss. This is then what the summing program, Appendix (III), does. Since there is nothing special in Equation (5.12) about source and receiver depth, we have written the program so that any depth specified in the normal mode program can be used as the source depth in the summing program. The program reads in information from the normal mode program (Appendix II), checks what source and receiver depths are required, calculates propagation loss according to Equation (5.12), and plots or prints propagation loss versus range.

When Pedersen and Gordon (6) compared normal mode theory to ray theory, they pointed out that this interchangeability of source and receiver is not true with ray theory, only normal mode theory. They then proceeded to show that the ray theory

result should be modified by the ratio of source to receiver sound velocity to make it equivalent to and comparable to normal mode theory:

$$H_{nm} = H_r + 10 \text{ Log } (c_s/c_h) \qquad (5.13)$$

While the correction makes ray theory more "exact," it is not significant for many realistic profiles. For example, in our profile, Figure (4.2), the worst case would be source at the velocity minimum, receiver on the bottom. The correction would still only be .1 dB. The correction is important when some analytical profiles are used. Here the receiver or source sound velocity may get very low (admittedly unrealistic), and the correction becomes significant.

Once the normal mode summing program was written and checked out, we did a few straightforward comparisons in order to verify the output of the normal mode program. We compared results from our program to results from two other programs for a shallow water profile (Figure 5.1). DiNapoli (24) had originally used this profile to compare his fast field program (FFP) to Bartberger's normal mode program (23). The FFP uses a completely different approach by first fitting the sound velocity profile with exponential layers. It then solves the wave equation directly in terms of Greens functions and uses a fast fourier technique on the computer.

Figure (5.2) shows the two original results in addition to a calculation for the same profile using our normal mode program. Discrepancies in the original comparison were attributed to FFP's use of exponential layers as opposed to Bartberger's linear layer fit of the velocity profile (Figure 5.1).

We would expect our results to be closer to the other normal mode result, since both use constant gradient segments. However our normal mode calculation includes only "trapped modes" (i.e. modes whose phase velocity is less than the sound velocity in the bottom fluid). This is the discrete portion of the mode spectrum. Bartberger's normal mode program continues calculating modes up into the continuum (phase velocity greater than bottom fluid sound velocity), and so it should yield a different result. But the comparisons in Figure (5.2) show essentially the same propagation loss versus range for all three theories. This comparison gave us confidence in the program as originally written for shallow water cases.

We then proceeded to test the normal mode program for a deep water case. We chose a typical deep water case yielding a well developed convergence zone (Figure 5.3). This ray diagram for a 305 m source depth indicates that to the right of the caustic (Figure 5.3, line AB) bordering the convergence zone, there is a well developed double arrival region. One arrival has passed through the caustic, the other is approaching it. We then ran CONGRATS for a 500 m receiver and 100 Hz source frequency. We chose ranges from 54 km to 62 km, which took the receiver from the shadow zone, over the caustic, and into the double arrival region. In the shadow zone, CONGRATS found no real rays as expected (bottom bounce arrivals were dropped from the calculation as discussed in Section 3). To the right of the caustic, two arrivals were found at each range point. They were then added coherently using the ray

summing program (Appendix I). A $\pi/2$ phase shift was added in CONGRATS to the arrival that had passed through the caustic. This phase shift is a well known but sometimes controversial feature of ray theory. Figure (5.4) shows the propagation loss* versus range curve for a 500 m receiver. The propagation loss is essentially infinite to the left of the caustic - which is indicated by the vertical line at 56.3 km. The propagation loss jumps to zero at the caustic (infinite intensity), then increases to a plateau at about 57 km. From this point on the propagation loss curve oscillates as the two arrivals interfere first destructively, then constructively. Both are very roughly equal in amplitude. That plus the $\pi/2$ phase shift results in this particular curve (Figure 5.4). There have been many supportive papers (45-47) on the use of the $\pi/2$ phase shift at caustics, and later we will add our own example of how this is the phase shift necessary for ray theory to be consistent with modified ray theory and normal mode theory.

In any event, now that we had the ray theory result, we ran the normal mode program for the same profile. We split the profile into the maximum allowable number of layers, 1000, and found from a preliminary run that there were 139 modes. To match the ray calculation geometry we set the bottom density equal to 1 and the bottom fluid velocity equal to the velocity in the water at the bottom (this is a matched impedance with no

*All propagation loss values will be in dB re 1 yd unless otherwise specified.

first order bottom reflections). We then used the normal mode program to calculate all the mode shapes, stored the mode amplitudes for each mode for source (305 m) and receiver (500 m) depths, and found the propagation loss using the mode summing program (Appendix III). Figure (5.5) shows this curve as well as the ray theory curve. They couldn't be more out of phase if we had tried to make them so.

This disagreement was unexpected, to say the least. We proceeded to examine both programs in order to find the problem and eventually found the difficulty to be with the normal mode calculation. We were calculating 139 modes and using 1000 finite difference layers in the water column. This meant that for the higher modes that were oscillating one hundred times or more in the water column, we were allowing 10 finite difference layers or less to fit each oscillation. The scarcity of layers would result in a poor representation of higher modes as we followed the wave function from one layer to the next, and more layers would enable us to more accurately find that mode shape. This inaccuracy in mode shape would affect not only the normalization constant but also the choice of mode wave number, k_n.

Figure (5.6) shows the normal mode calculation for 2000 layers. The comparison is better, but still not satisfying. Figure (5.7) shows the normal mode calculation for 3000 layers. Here there is still closer agreement with ray theory. And the change in the normal mode calculation from 2000 to 3000 layers is small compared to the change from 1000 to 2000 layers. It was felt that calculations for more than 3000 layers were

unnecessary, and a rule of thumb was adopted that at least 20 times the number of modes equaled the number of finite difference layers required for the calculation.

The larger number of layers required necessitated a rewriting of the program. We now calculate one mode at a time, extract the required information, and go on to the next. This is as opposed to the original storage of a group of twelve modes at a time. The program was substantially rewritten to keep its size small while increasing the number of finite difference layers. A listing is shown in Appendix (II). We also made several changes to improve the accuracy and speed of the calculation, using knowledge gained while looking for the flaw in the program. For example, regula falsi (48) is usually faster than simple halving as a root finding technique, and as such it was used exclusively in the original program. But for the lower modes in the deep water case, we found that the first trial values of k_n were yielding values of the unnormalized wave function at the surface on the order of $\pm 10^{100}$. This was instead of the very small value, $\epsilon < 1$, needed to satisfy the pressure release boundary condition. Because of this, regula falsi was taking excessively long to zero in on the proper k_n. So we now use halving of the difference between successive k_n's until the wave function at the surface is less than 10^{50} (Appendix II, Subroutine Half, lines 45-70), and then we use regula falsi until the wave function at the surface is less than ϵ. In general, this cut the number of iterations required by more than half for the lower modes.

Another change in the program involved the method used for zeroing the wave function near the surface. Ideally, for each mode one can find a k_n so that the mode has the proper number of zero crossings (n-1) and reaches an amplitude value of zero at the surface. In practice, using numerical evaluation of the mode shape, the amplitude is never quite zero at the surface. Even for changes in k_n of one part in 10^{12}, the surface wave function value may still be small, but finite. So the program was set up to satisfy the surface boundary condition as follows:

$$Z_n (\eta = 0) \leq \epsilon \qquad (5.14)$$

where ϵ is some small number on the order of .01 or less.

If k_n is changing by less than one part in 10^{+10}, and the amplitude still isn't within ϵ of zero at the surface, the iteration process stops. At this point the wave function will look like Figure (5.8A) or Figure (5.8B). It will approach zero amplitude at the surface, miss reaching zero amplitude at the surface, or cross too early resulting in one too many zero crossings. This information near the surface is incorrect, and essentially useless. Newman and Ingenito (22) decided to zero the mode amplitude at these depths in the following way. They calculated the mode shape, again starting from the bottom. They checked until there were n-1 zero crossings (for the n^{th} mode), Point A, Figure (5.8A). Then they followed the wave function as it first increases (AB) and then decreases beyond B. At this point, beyond B, the wave function should monotonically decrease to zero at the surface. If it does (Figure 5.8A),

it is left alone. But if it doesn't, at some point it may cross the axis or start to increase again (Figure 5.8B). This is the point where the wave function is assumed to misbehave, and it is zeroed from there to the surface. This is done in subroutine (Iterate) when Flag equals 2.

While this apprcach works well for many profiles, it can yield incorrect results for some modes with some profiles. For example, consider an asymmetric, double well profile (Figure 5.9). While most modes present no problem, consider mode 4 (Figure 5.10). This is the unnormalized wave function. The program would follow it to point (A), continue up to (B), and then down to (C). There would be the proper number of zero crossings, so it wouldn't expect the amplitude to increase beyond point (B). It would then incorrectly zero out the mode beyond (C) in the upper well and normalize incorrectly, resulting in an incorrect mode (Figure 5.11). To avoid this, we chose to zero the amplitude starting from the surface. The possibilities are the same as before (Figure 5.8) with the first case being left alone, while the other two require zeroing. So we start from the top and see which shape the first oscillation has. This is, of course, after first generating and storing the entire mode shape by starting at the bottom-water interface, and using the last value of k_n obtained. This mode shape is not correct near the surface, but it is the best we can do within the accuracy limitations of the method and computer. We then zero the mode amplitude

near the surface where necessary. Figure (5.12) shows mode 4 again, but this time after proper zeroing, w' see the correct normalized mode shape. These changes were made in Subroutine Iterate, Appendix (II).

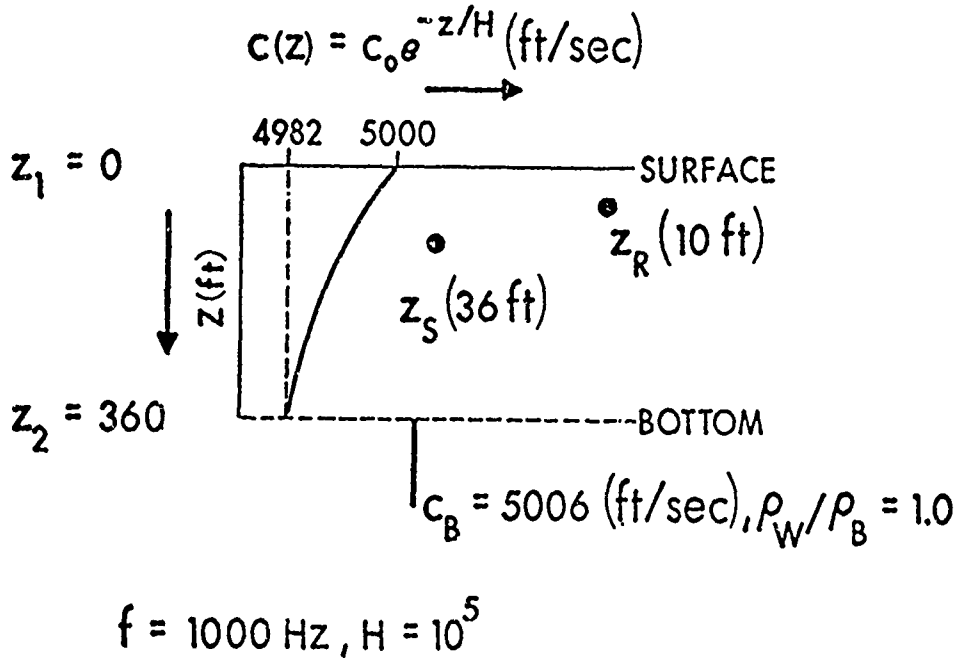

Figure 5.1 Environmental Description for a Single Exponential Layer(From DiNapoli(24))

Figure 5.2 Shallow Water Test Case Comparisons

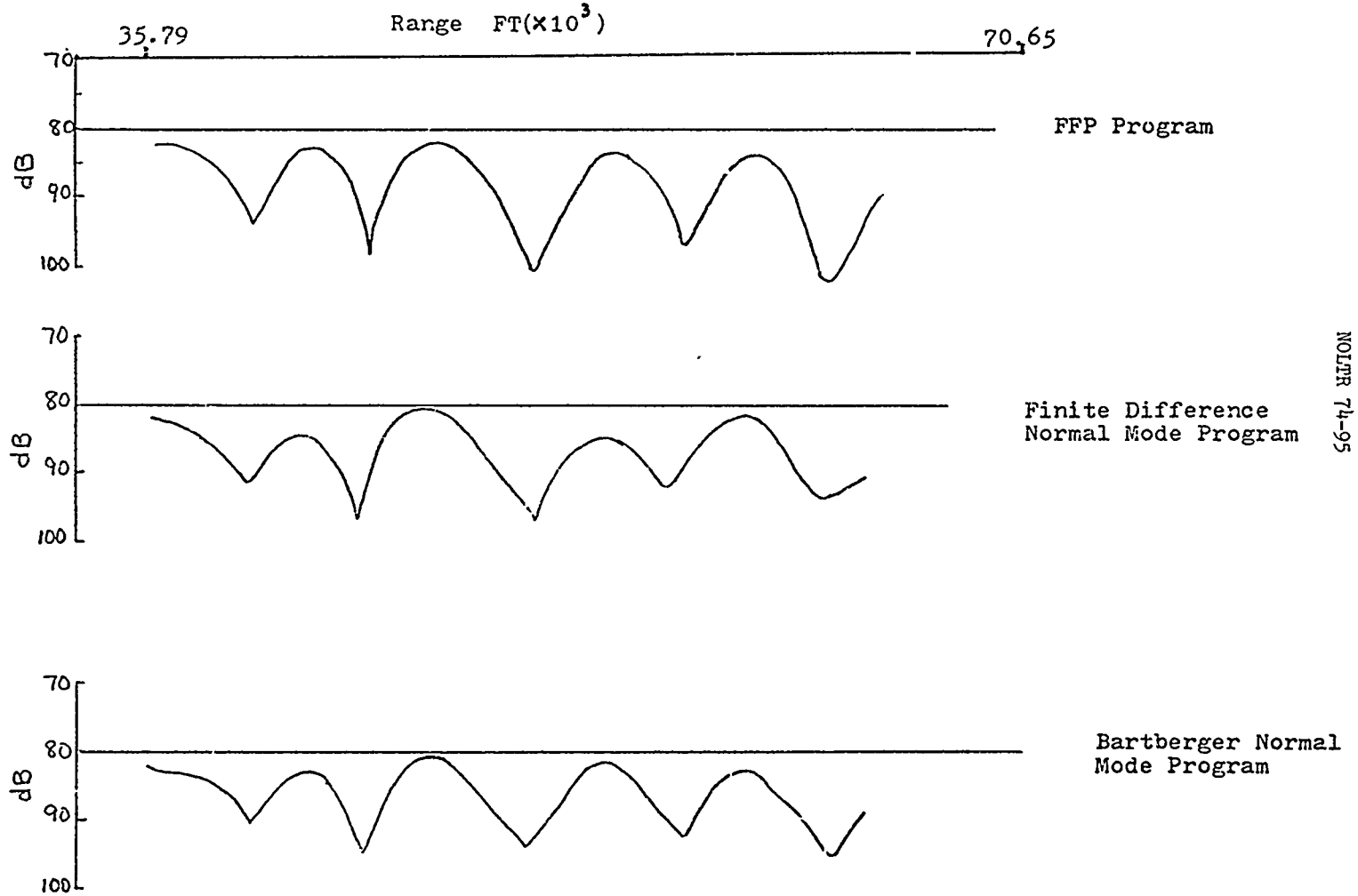

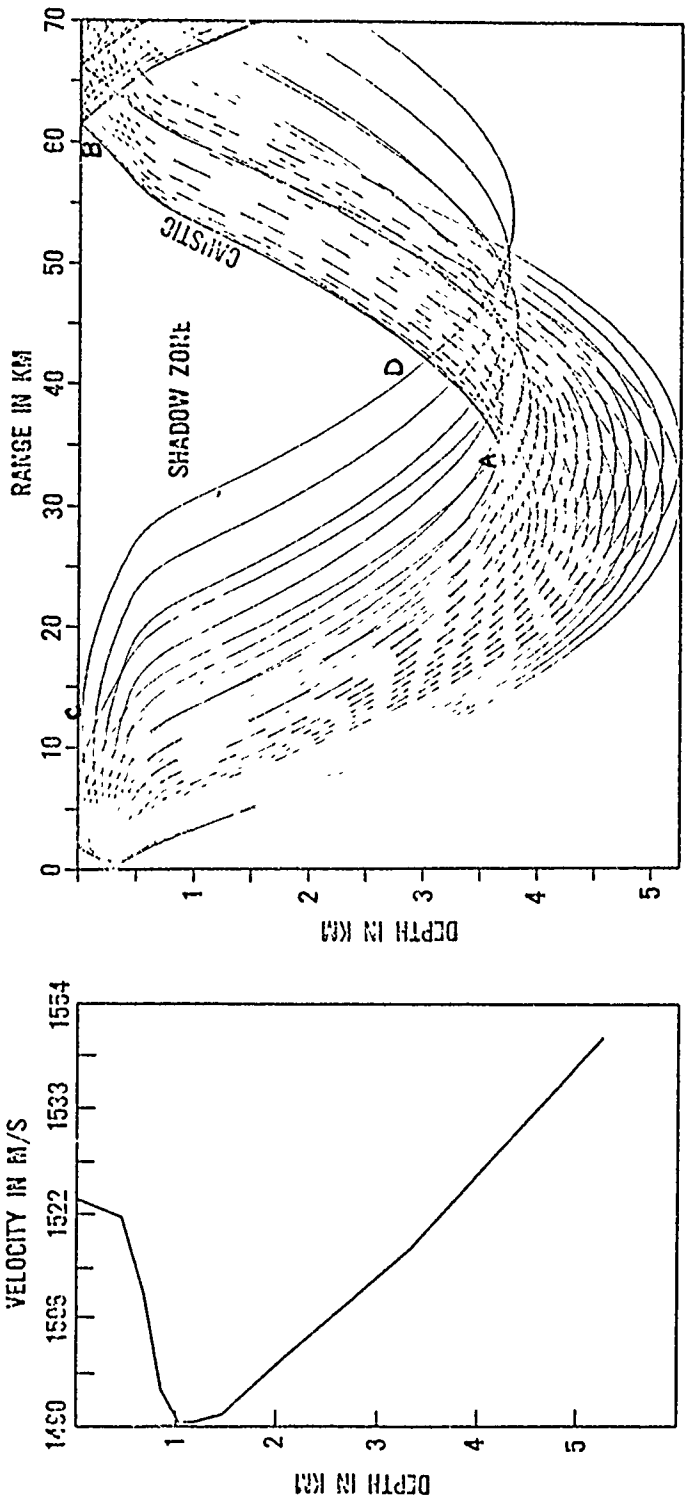

Figure 5.3 Profile I: Sound Velocity Profile and Ray Diagram Showing Convergence Zone

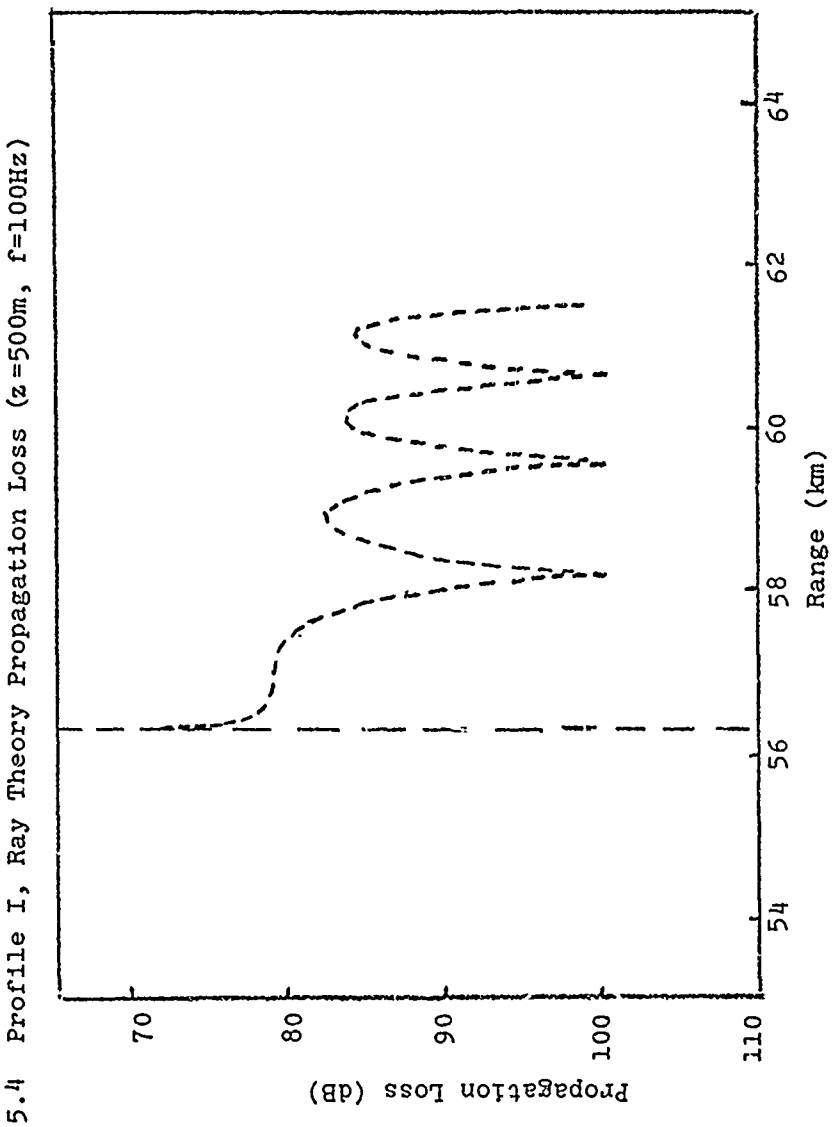

Figure 5.4 Profile I, Ray Theory Propagation Loss (z=500m, f=100Hz)

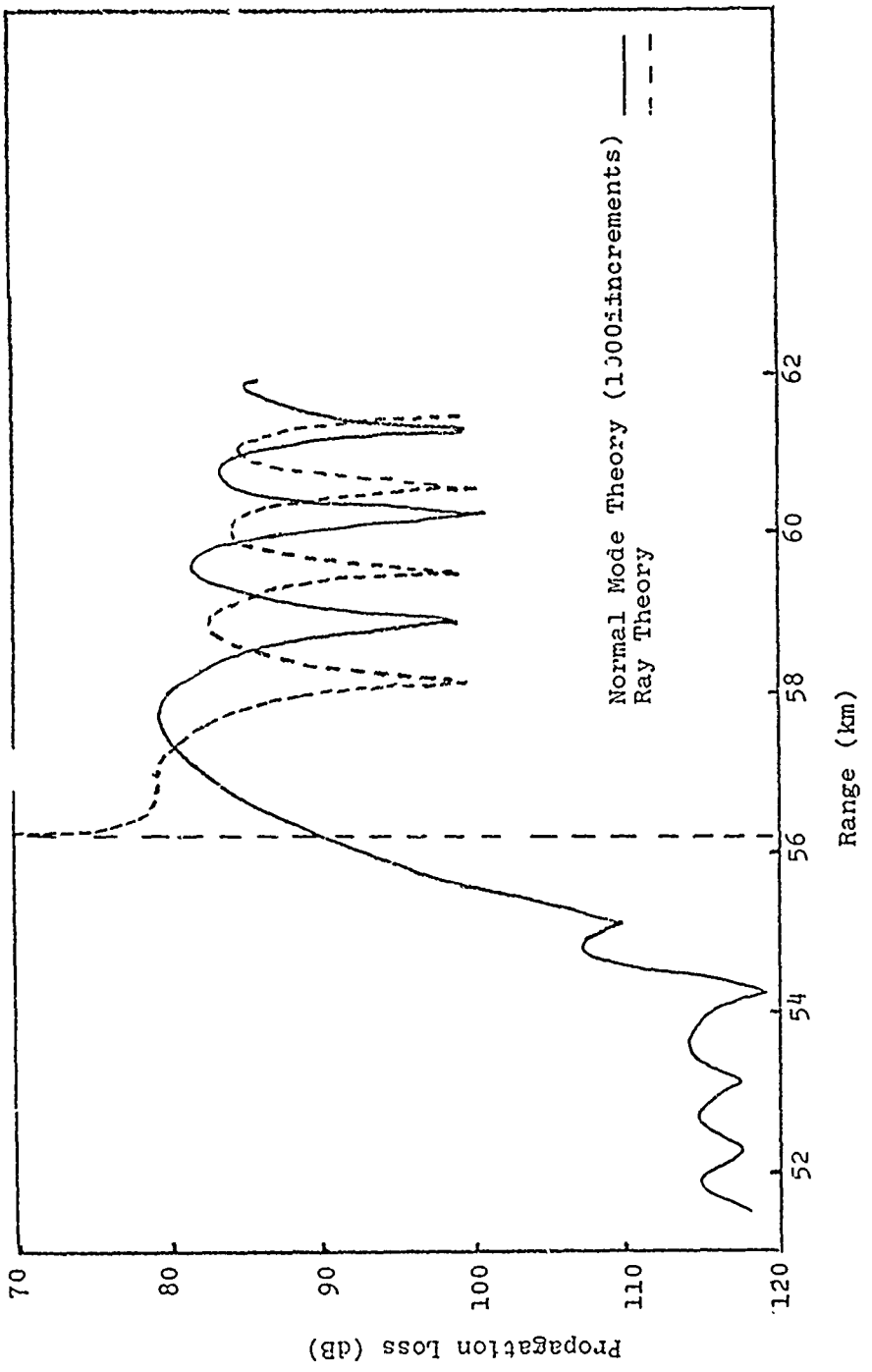

Figure 5.5 Profile I, Normal Mode vs Ray Theory (z=500m, f=100Hz)

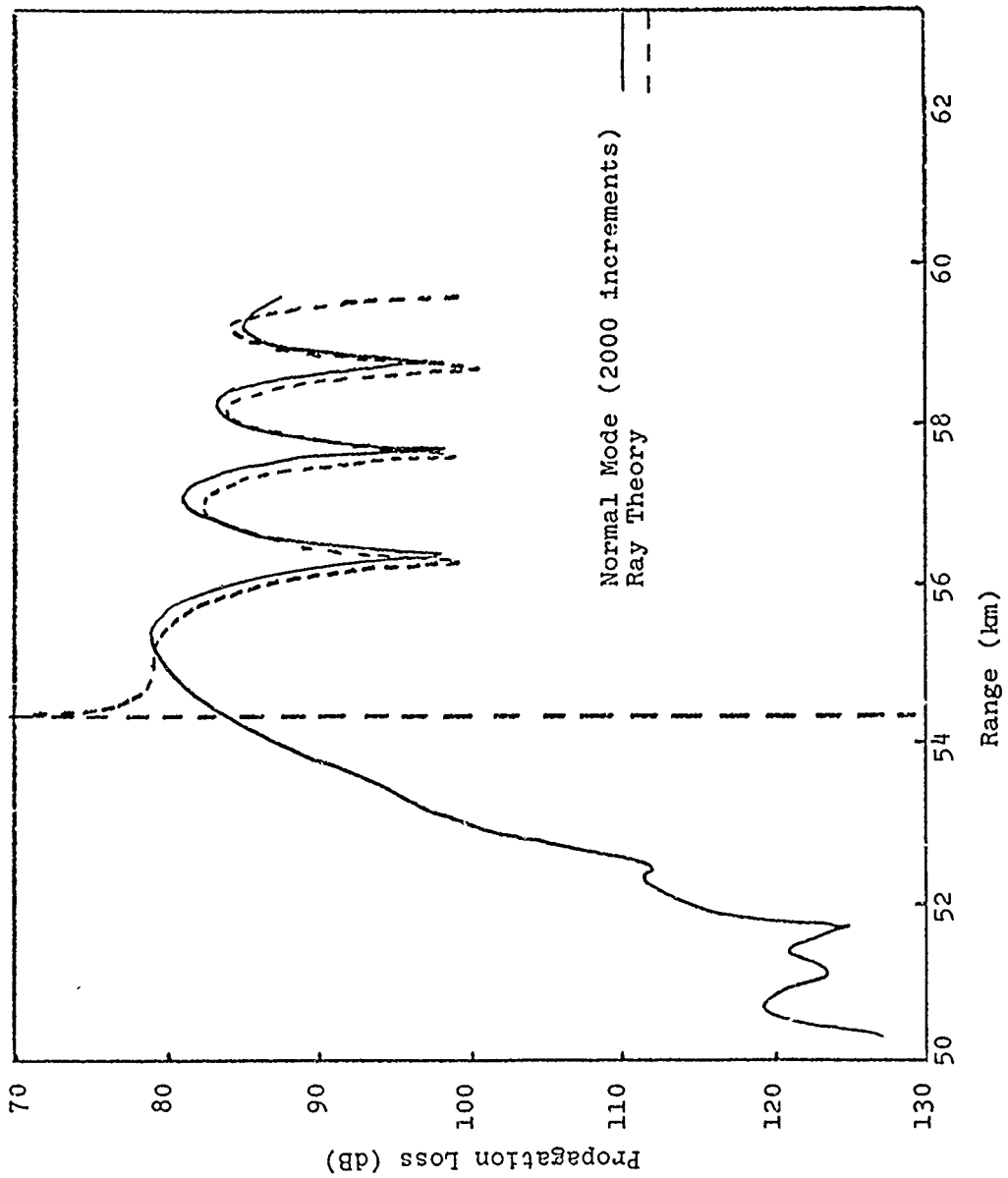

Figure 5.6 Profile I, Normal Mode (2000 inc.) and Ray Theory (z=500m, f=10Hz)

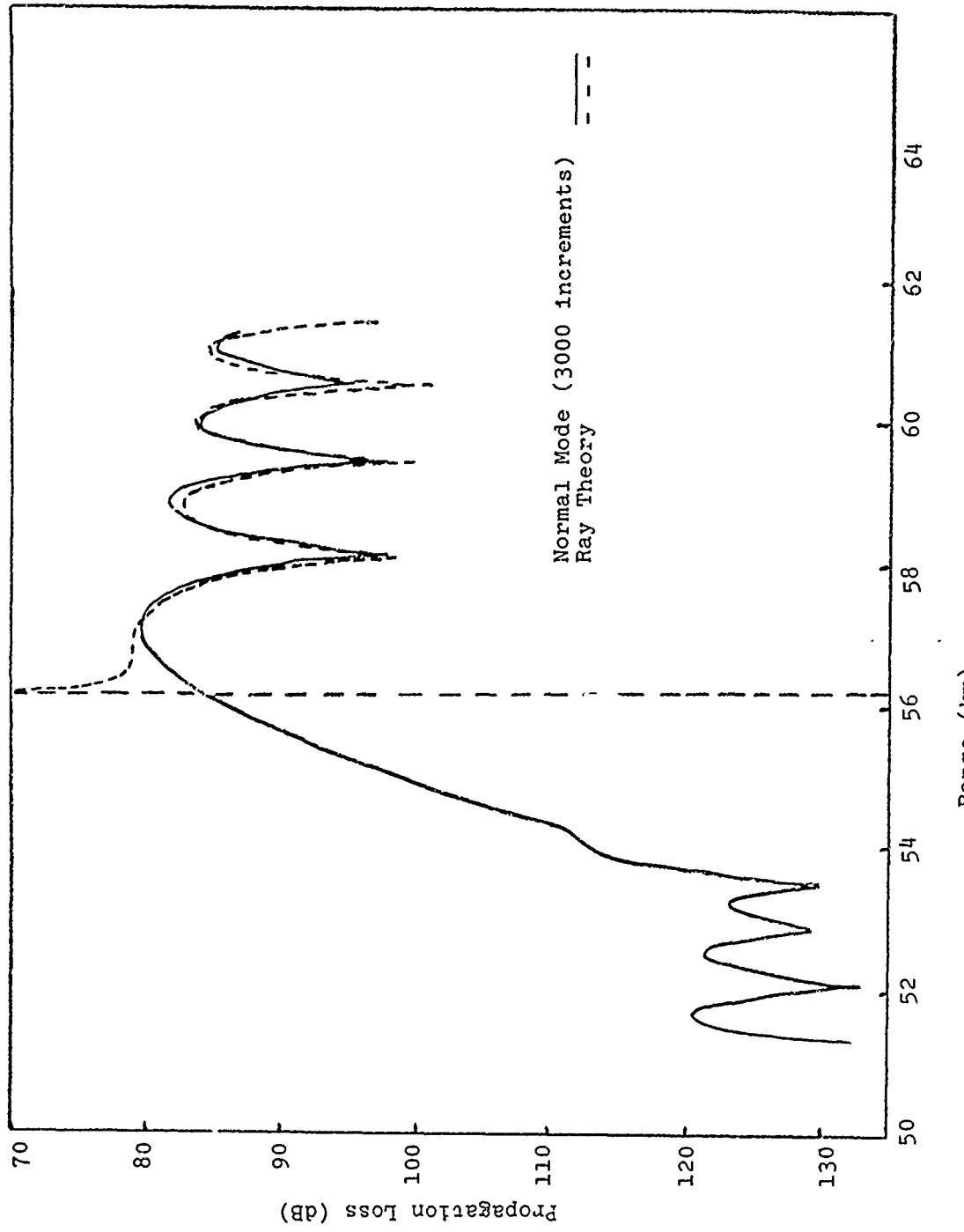

Figure 5.7 Profile I, Normal Mode (3000 inc) and Ray Theory (z=500m, f=100Hz)

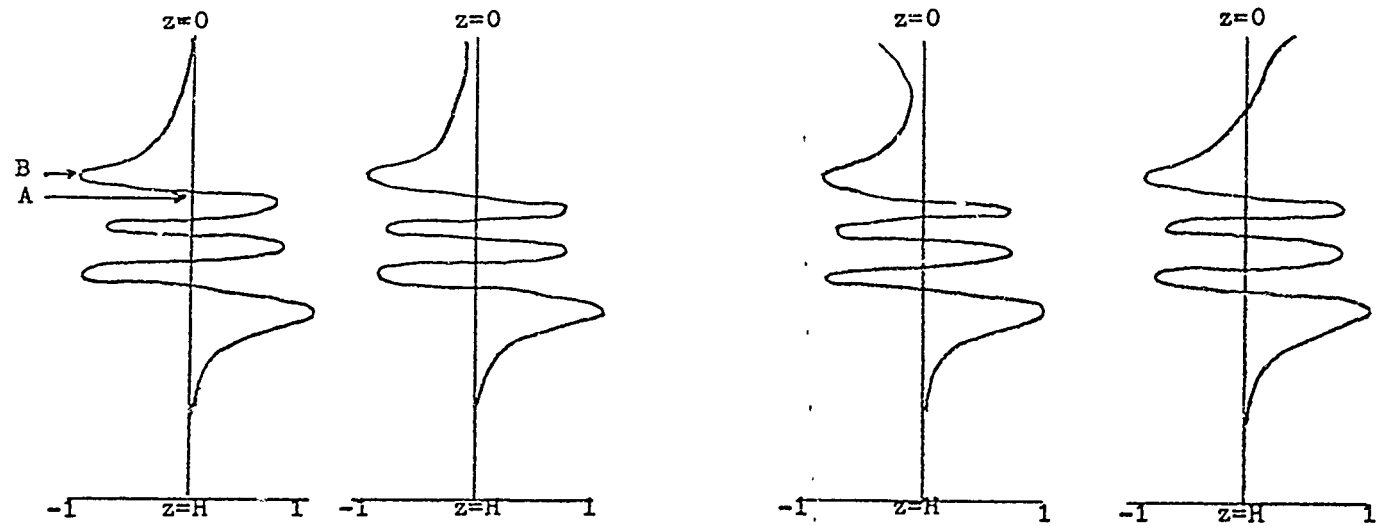

5.8A:Acceptable 5.8B:Not Acceptable

Figure 5.8 Alternative Mode Tails near Surface

Figure 5.9 Double Well Sound Velocity Profile

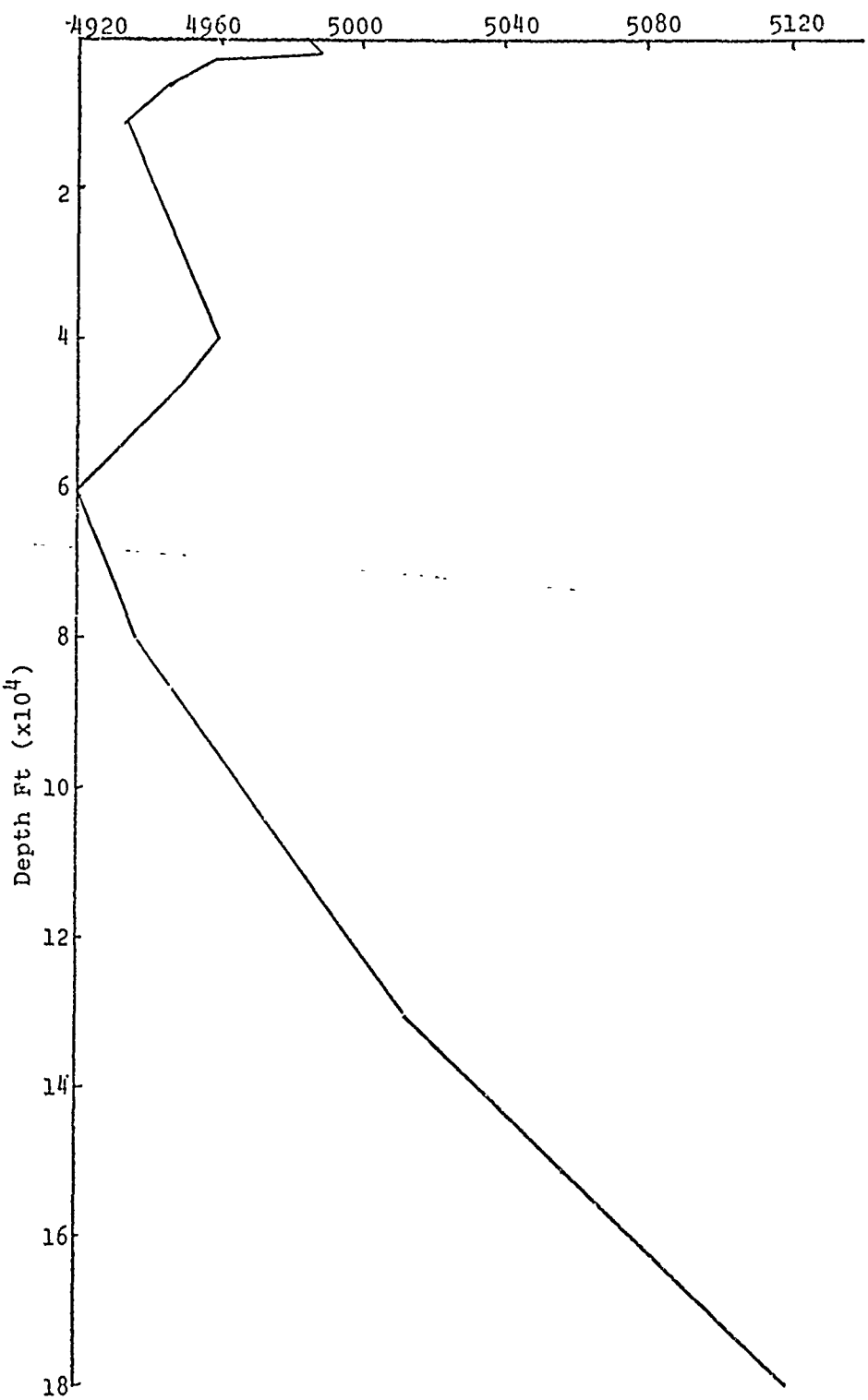

Figure 5.10 Mode 4, Unnormalized

(Amplitude Scale Representative, Actual Amplitude in Top Well Two Orders of Magnitude Greater Than in Bottom Well)

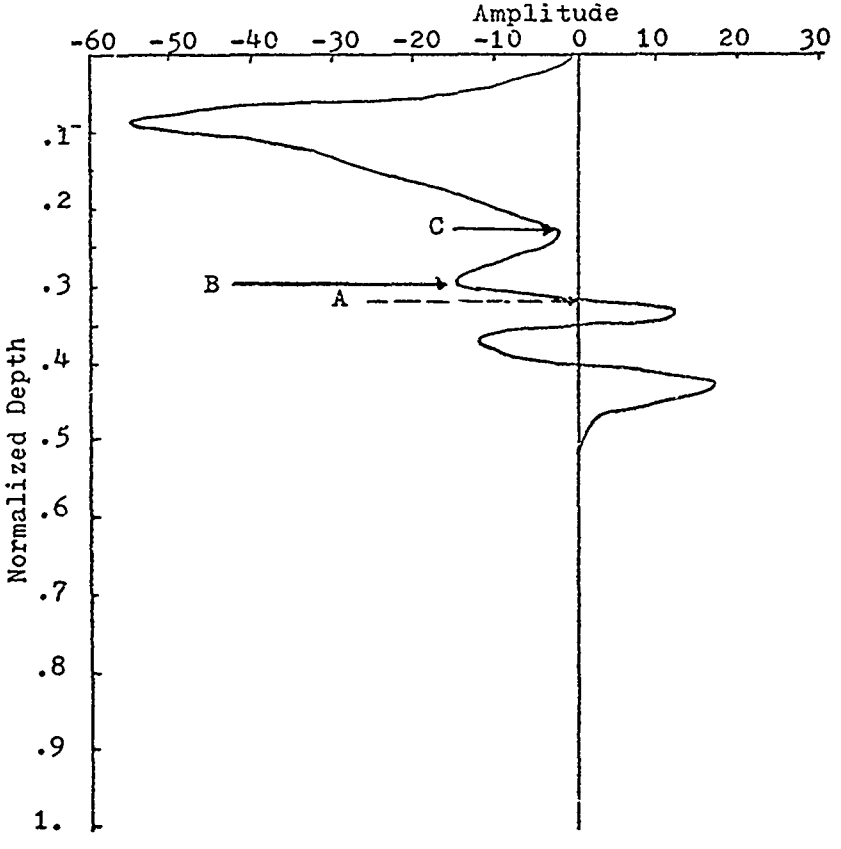

Figure 5.11 Mode 4, Normalized Incorrectly

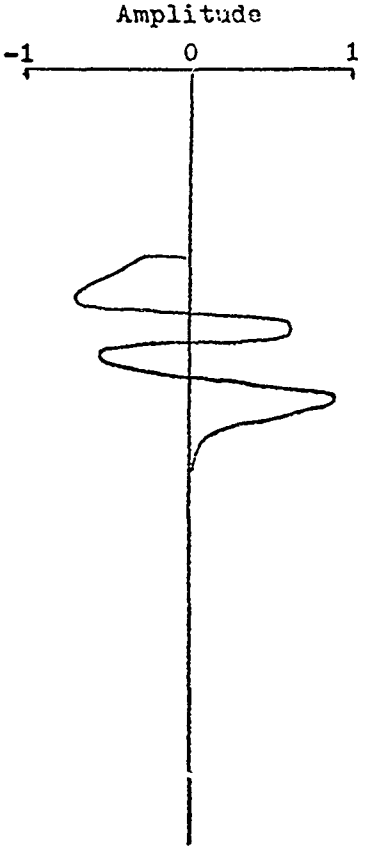

Figure 5.12 Mode 4, Correctly Normalized

(Small Amplitude Oscillation in Bottom Well Roughly One Tenth as Large as Shown Here)

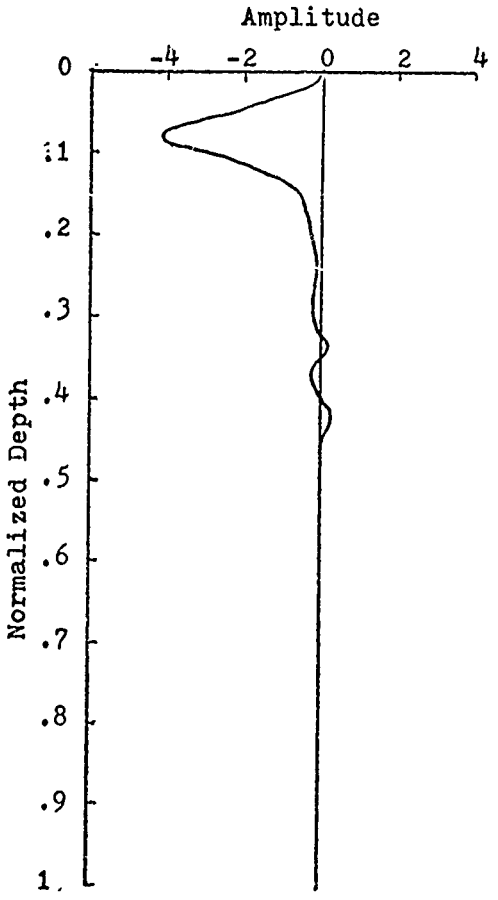

6. Profile I, Comparisons Near a Single Caustic

Our first comparisons of the three theories were done using the deep ocean profile used in our checkout of the normal mode program (Section 5, pages 57-60). Profile I*(Figure 5.3) was specifically chosen so that the caustic bordering the convergence zone (Figure 5.3, line AB) would have a well developed double arrival region to the right of it. While we are also interested in comparisons close in and for more than one caustic, we felt it would first be advisable to compare the theories in the simplest region where all three are valid, near a single caustic. To the left of the caustic (line AB), there is at first a simple caustic-related shadow zone. This region will not turn out to be completely free from effects of the surface reflected shadow zone boundary close in (Figure 5.3, line CD). But the two boundaries are far enough apart so that we can separate out the effects of each. To the right of the caustic, because of the bottom depth of the profile, we have a double arrival region free from other arrivals for an appreciable distance from the caustic. This enables us to compare the three theories not only in the caustic region, but for several oscillations in the double arrival region as well.

Calculations were done for a source depth of 305 m, and receiver depths of 250 m, 500 m, and 1500 m. This way we were treating different situations - a receiver shallower than the source, between the source and sound channel axis depths, and near the sound channel axis. Figure (6.1) shows comparisons between ray theory and modified ray theory at the two deeper

*Input sound velocity profile data in Appendix V.

depths for a source frequency of 100 Hz. As expected, ray theory propagation loss diverges as the caustic is approached from the right, and reaches zero (infinite peak pressure) at the caustic - indicated by the vertical line in each part of the figure. Modified ray theory indicates a finite, non-zero propagation loss at the caustic, and the intensity falls off exponentially from there into the shadow zone. Just to the right of the caustic, for Airy function argument $|\rho| \leq 1.5$, we are in the caustic region - or caustic boundary layer (13). Here we expect modified ray theory to be better than ray theory. This is the region in each part of Figure (6.1) where the modified ray theory propagation loss first decreases and finally reaches a minimum, before again starting to increase. We see that at about this minimum point, ray and modified ray theories merge and reach their best agreement (Figure (6.1A) at 57 km, for example).

Beyond this point we expect ray theory to be valid; modified ray theory may agree with it, but this will depend on the local geometry of the caustic. At 500 m (Figure 6.1A), modified ray theory does do well in this double arrival region and follows the ray theory oscillations adequately. At 1500 m (Figure 6.1B), however, modified ray results fail rapidly in the double arrival region. It is soon almost completely out of phase with the ray theory results. This disagreement is not unexpected (49), and points out that care must be exercised in extending modified ray theory far into the double arrival region.

In Figure (6.2), we now add normal mode theory results at each depth. On the caustic at each depth, modified ray results agree with the normal mode results. Thus, modified ray theory does yield valid predictions on the caustic. Then looking at 500 m, we see that normal mode values duplicate the modified ray results in the caustic region, and then it agrees with both ray and modified ray theories in the double arrival region. To the left of the caustic, the normal mode results agree with modified ray results in predicting an exponential drop off in intensity into the shadow zone. Only when the pressure has fallen 35 to 40 dB and a weaker diffraction pattern from the close in boundary and bottom starts to predominate, does modified ray theory fail. So in this case, it predicts the caustic related shadow zone effect as far as we can see it.

Now we look at 1500 m where ray and modified ray disagree in the double arrival region (Figure 6.1B). Since we are using normal mode theory as the standard of comparison valid everywhere, we expect it to agree with modified ray theory in the caustic region ($0 \leq \rho \leq -1.5$) - where modified ray is valid. Then we expect normal mode results to agree with ray theory results in the double arrival region (beyond 52.5 km) - where ray theory is valid. Figure (6.2B) verifies this behavior. In the shadow zone, modified ray results are still in good agreement with normal mode results. Thus the tendency of modified ray to be valid in some region to the right of the caustic appears to be accompanied by a similar tendency to the left of the caustic. Sachs (49) has explored this problem of the shadow zone validity of modified ray theory using an idealized model

resulting in a circular caustic. He demonstrated that as one proceeds into the shadow zone (large positive arguments ρ of the Airy function), modified ray theory breaks down when compared to an exact solution of his particular problem (Figure 6.3). So if we could follow modified ray farther into the shadow zone - and we will do this later in a multi-caustic case- we would expect it to fail. However, for our realistic profile, modified ray theory is still in good agreement with normal mode theory when the intensity is quite low.

Sachs (49) also considers the use of complex ray theory in the shadow zone. Complex ray theory is the ray type solution valid in shadow zones where regular ray theory is not useful. From Figure (6.3), we can see that complex ray theory does work well in the shadow zone. It is somewhat more difficult to use, since it requires solutions for complex roots of the ray equations for range, time, etc. However, it can be a useful addition to ray solutions for work in the deep shadow zone.

We next did the same comparison for 50 Hz (Figure 6.4).* The agreement among the three theories is about the same as for 100 Hz. There are fewer oscillations over the same range increment because of the lower frequency. Furthermore, the disagreement between ray and modified ray theory at 1500 m (Figure 6.4C) starts to occur at a different range - at about 56 to 57 km - between the first and second nulls. What is roughly constant at the point of disagreement is ρ, the argument of the Airy function - which is a function of the frequency through $k^{2/3}$ and also distance off the caustic, Δr.

*Here we include a 250 m receiver for the first time.

Thus for the same geometry caustic (constant δ), and different frequencies, ρ is the factor that scales the Airy function by spreading or shrinking it over the space coordinate r. Finally, Figure (6.5) shows the results for 50 and 100 Hz in the shadow zone at 500 m depth. Modified ray predicts that intensity will fall off exponentially with $k^{2/3}$ and distance off the caustic, Δr. Figure (6.5) demonstrates that both of these modified ray theory approximations are good estimates of the behavior predicted near the caustic by normal mode theory. Finally, it should also be noted that the consistency of all three theories in the double arrival region depends on the $\pi/2$ phase shift that is inserted in the ray theory result for the ray that has passed through the caustic. This phase shift is also implicit in the modified ray theory result (50). Only this way do they agree with normal mode theory. So this is just one more demonstration of the presence of a $\pi/2$ phase shift at a caustic.

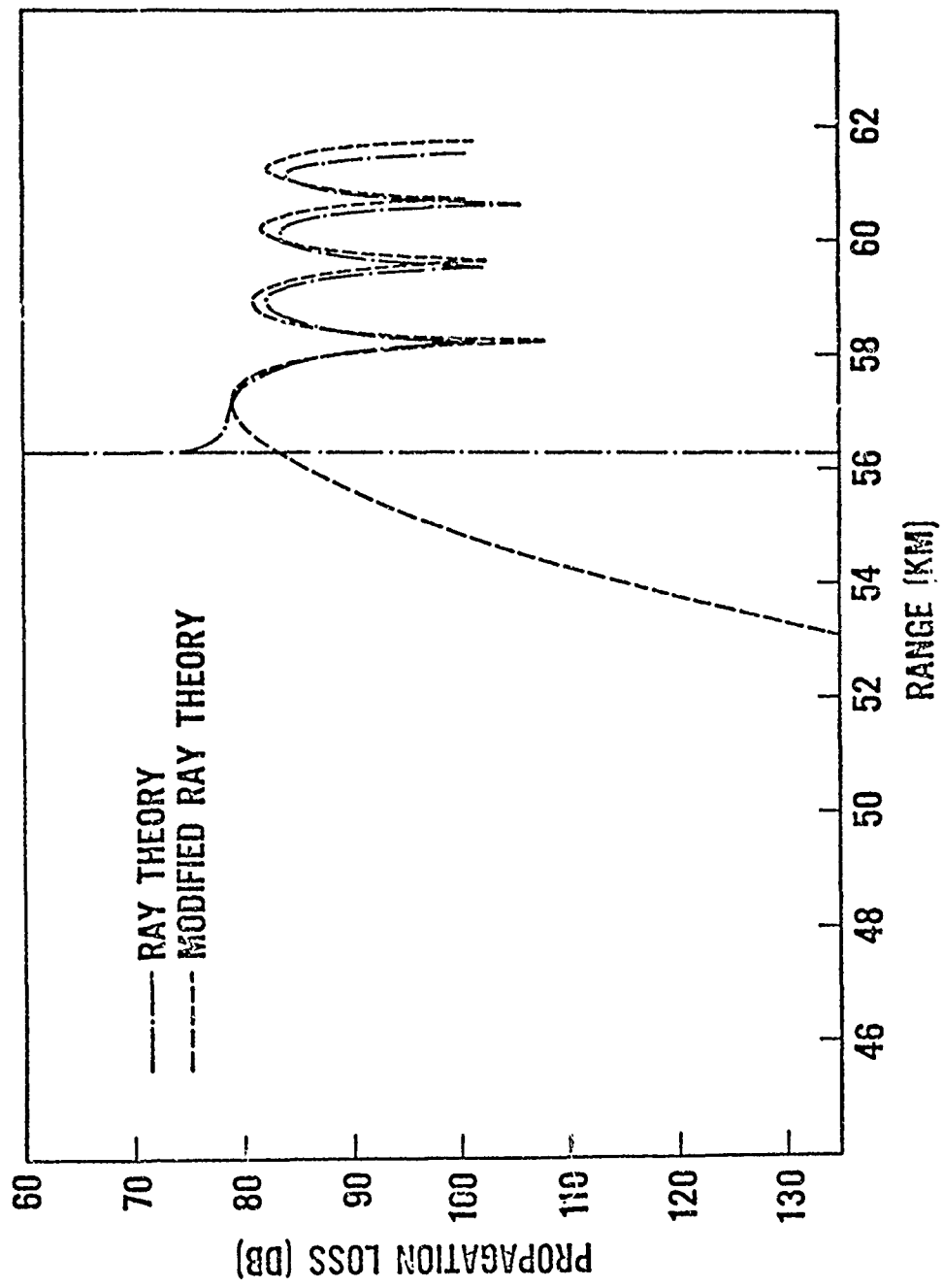

Figure 6.1A Profile I, Ray and Modified Ray Theory
(Δ =500m, f=100Hz)

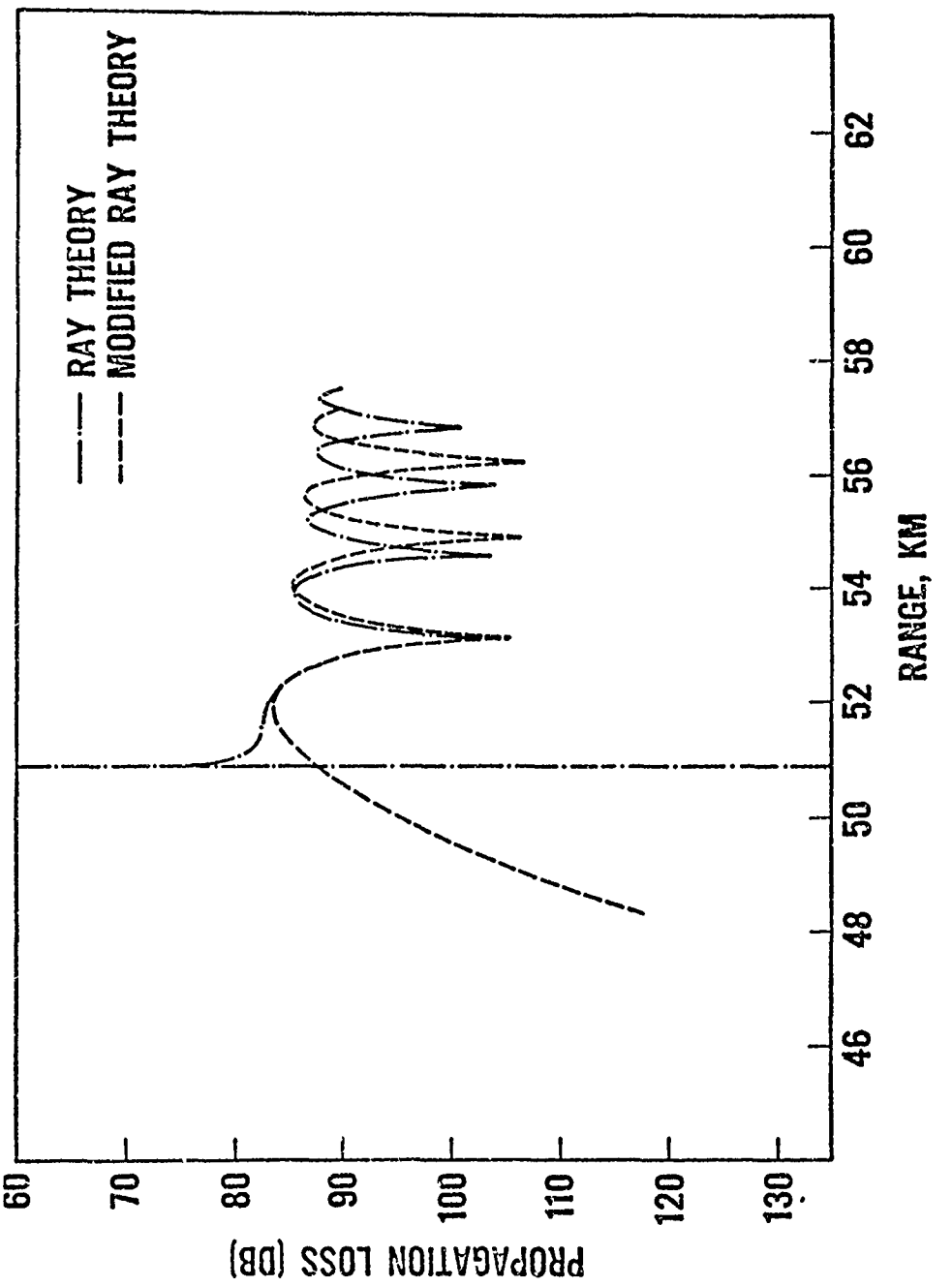

Figure 6.1B Profile I, Ray and Modified Ray Theories (z=1500m, f=100Hz)

Figure 6.2A Profile I, Normal Mode, Ray, and Modified Ray Theories
(z =500m, f=100Hz)

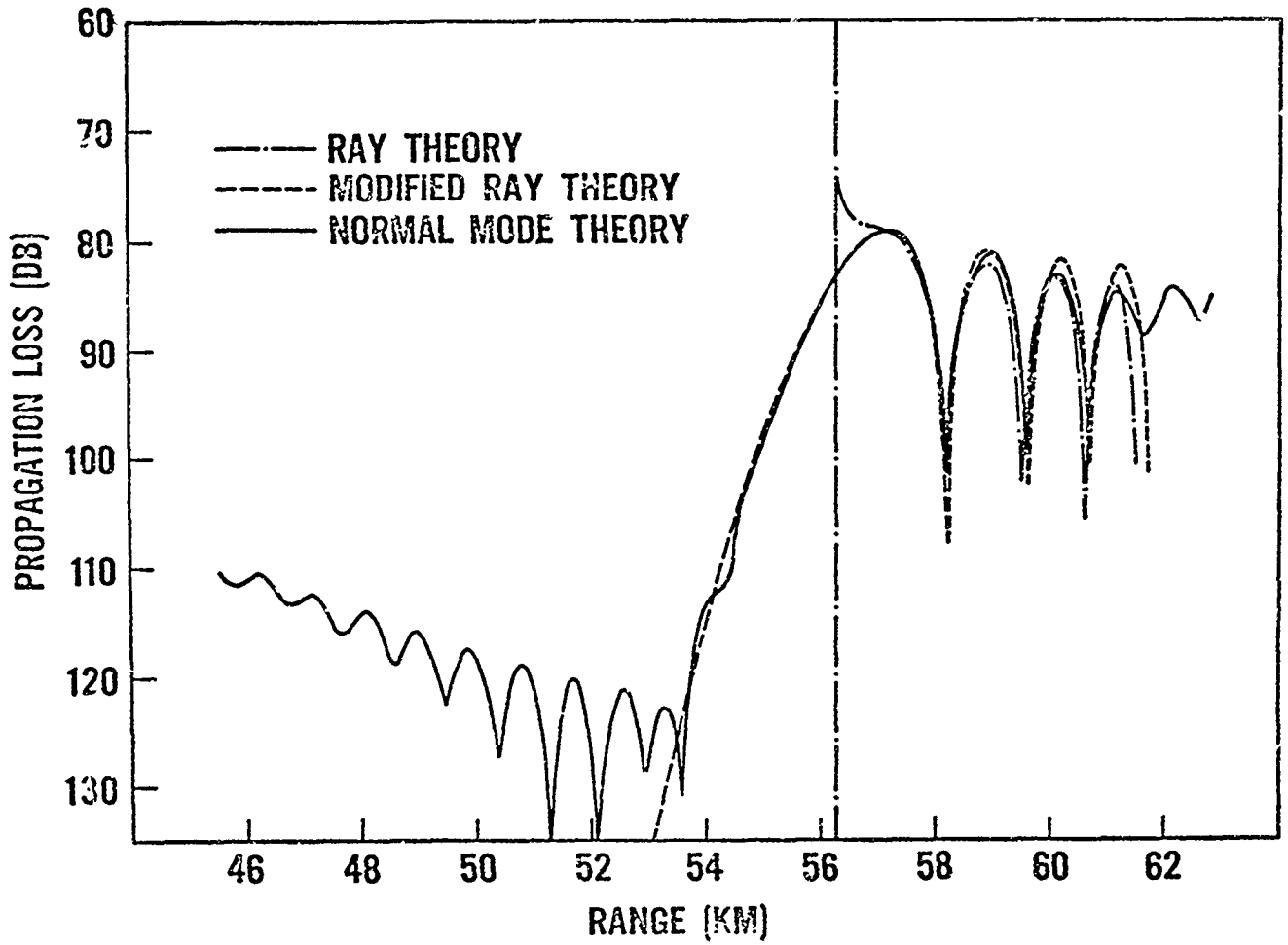

Figure 6.2B Profile I, Normal Mode, Ray, and Modified Ray Theory (z_s=1500m, f=100Hz)

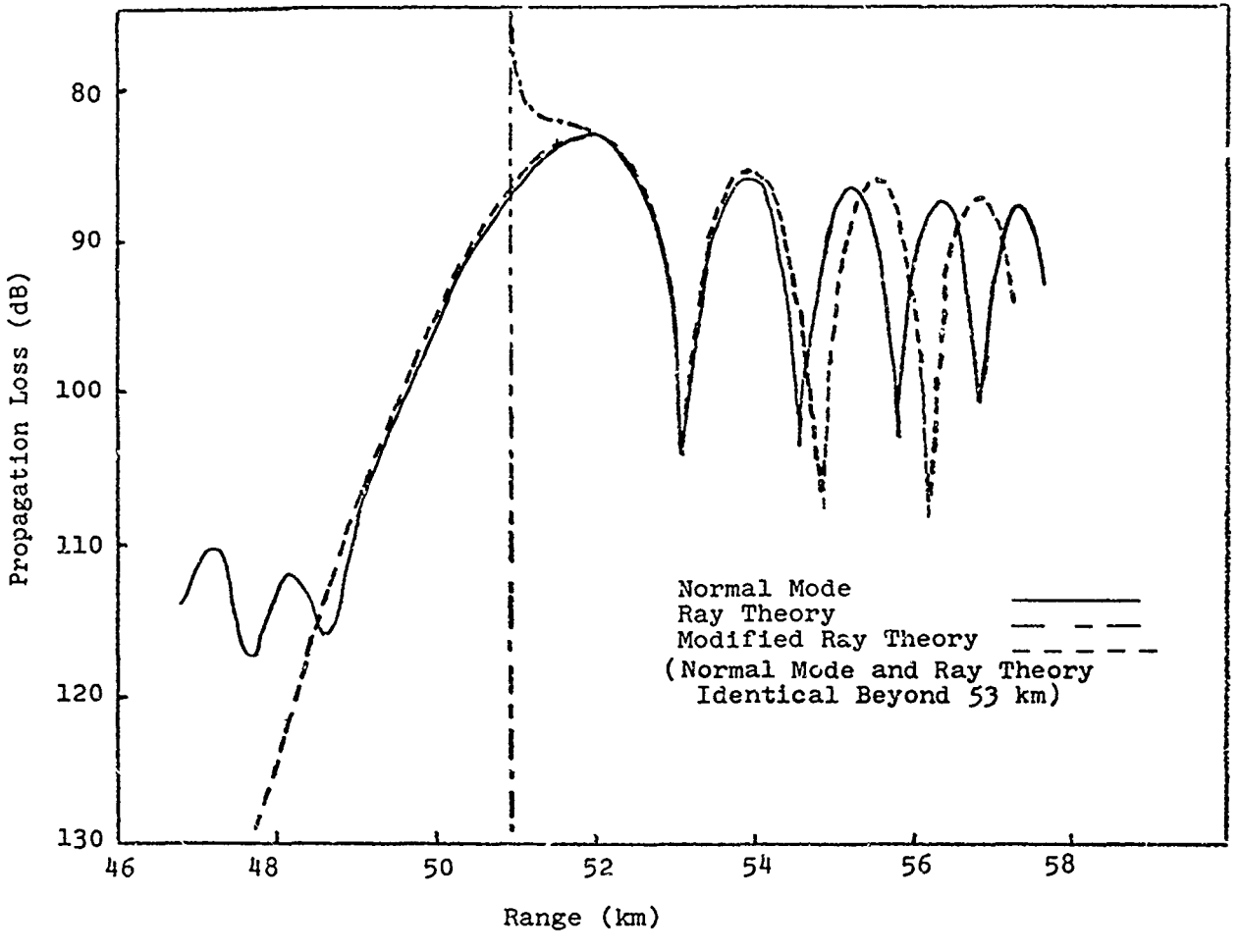

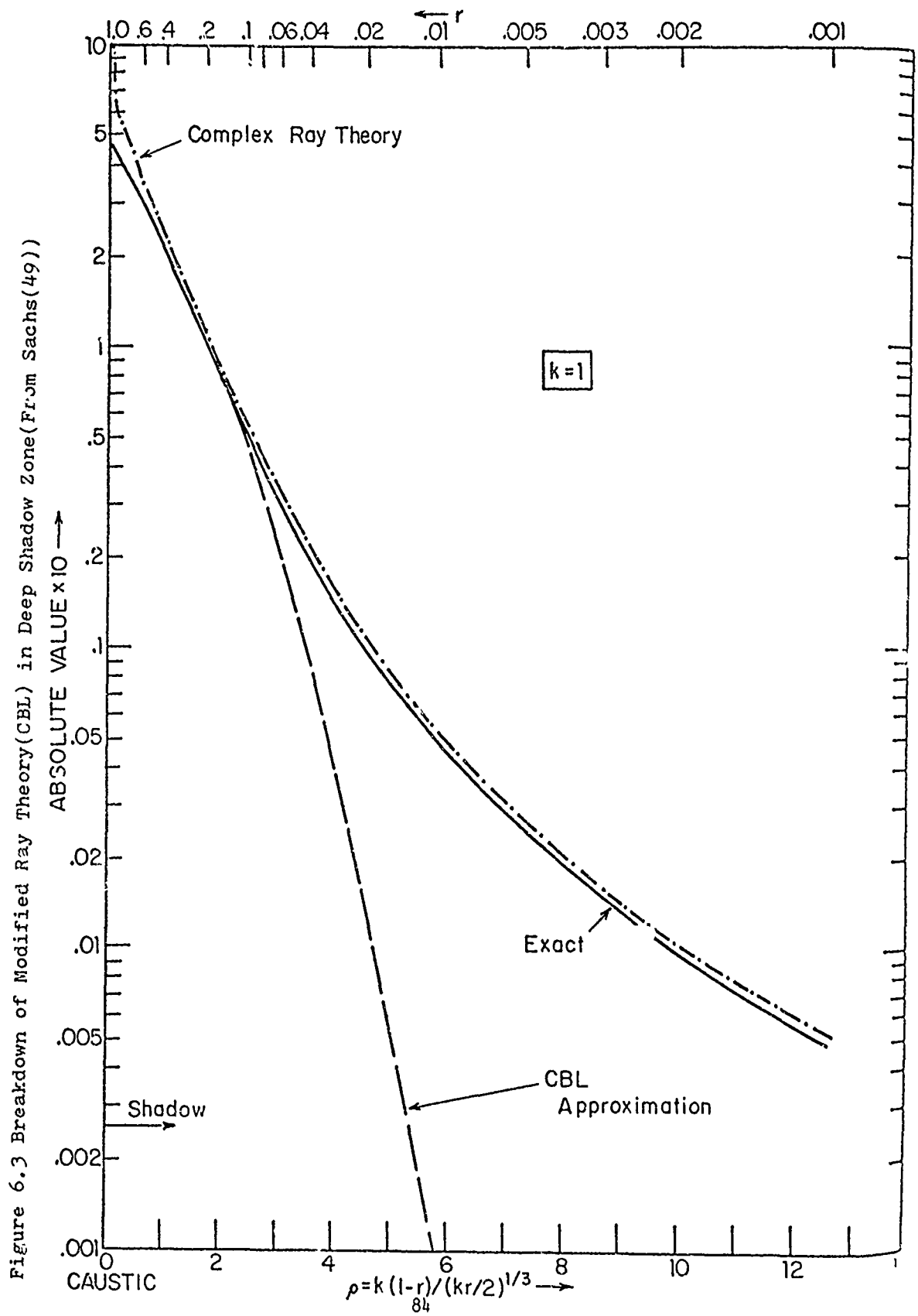

Figure 6.3 Breakdown of Modified Ray Theory(CBL) in Deep Shadow Zone(From Sachs(49))

Figure 6.4A Profile I Normal Mode, Ray, and Modified Ray Theory (z=250m, f=50Hz)

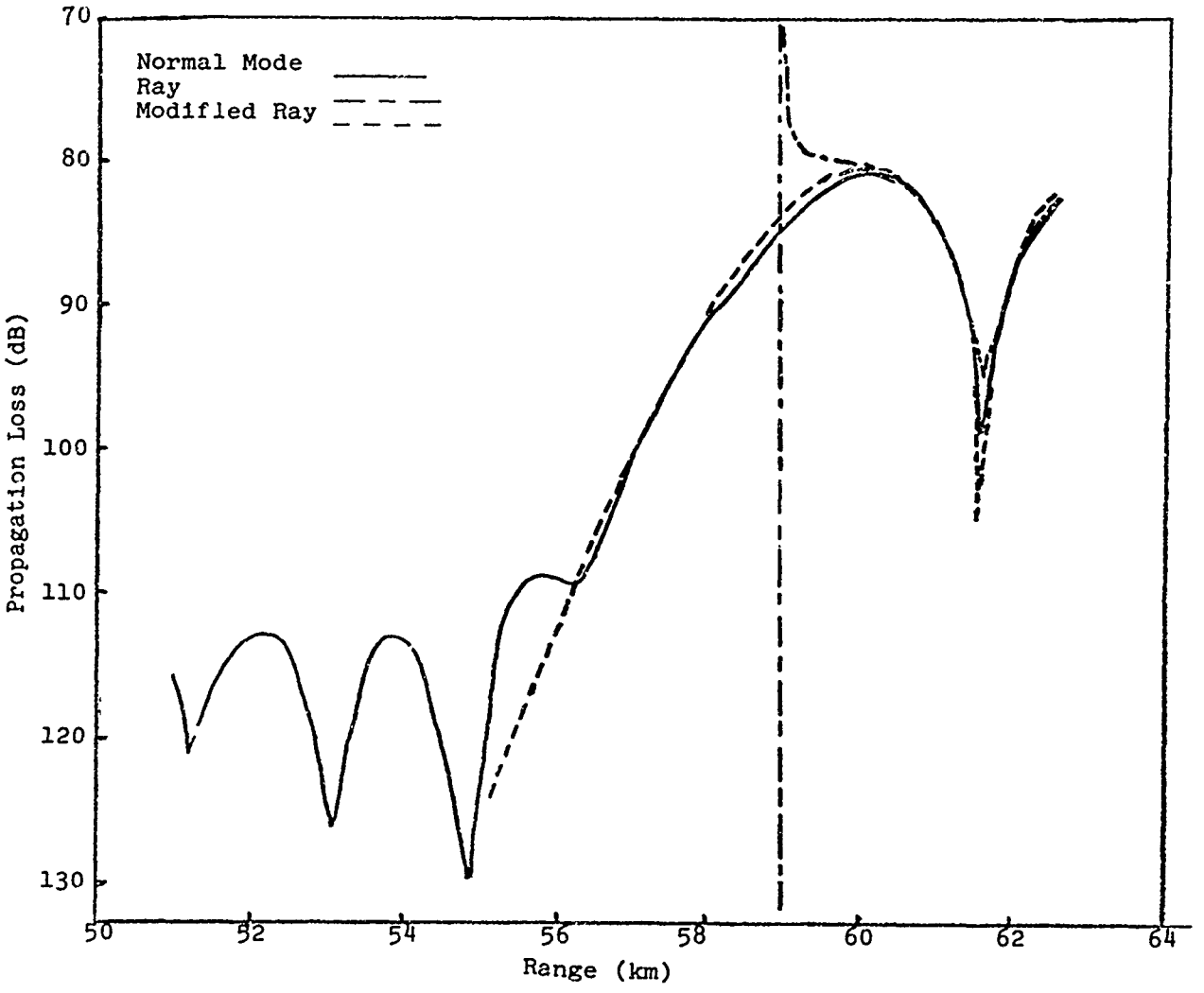

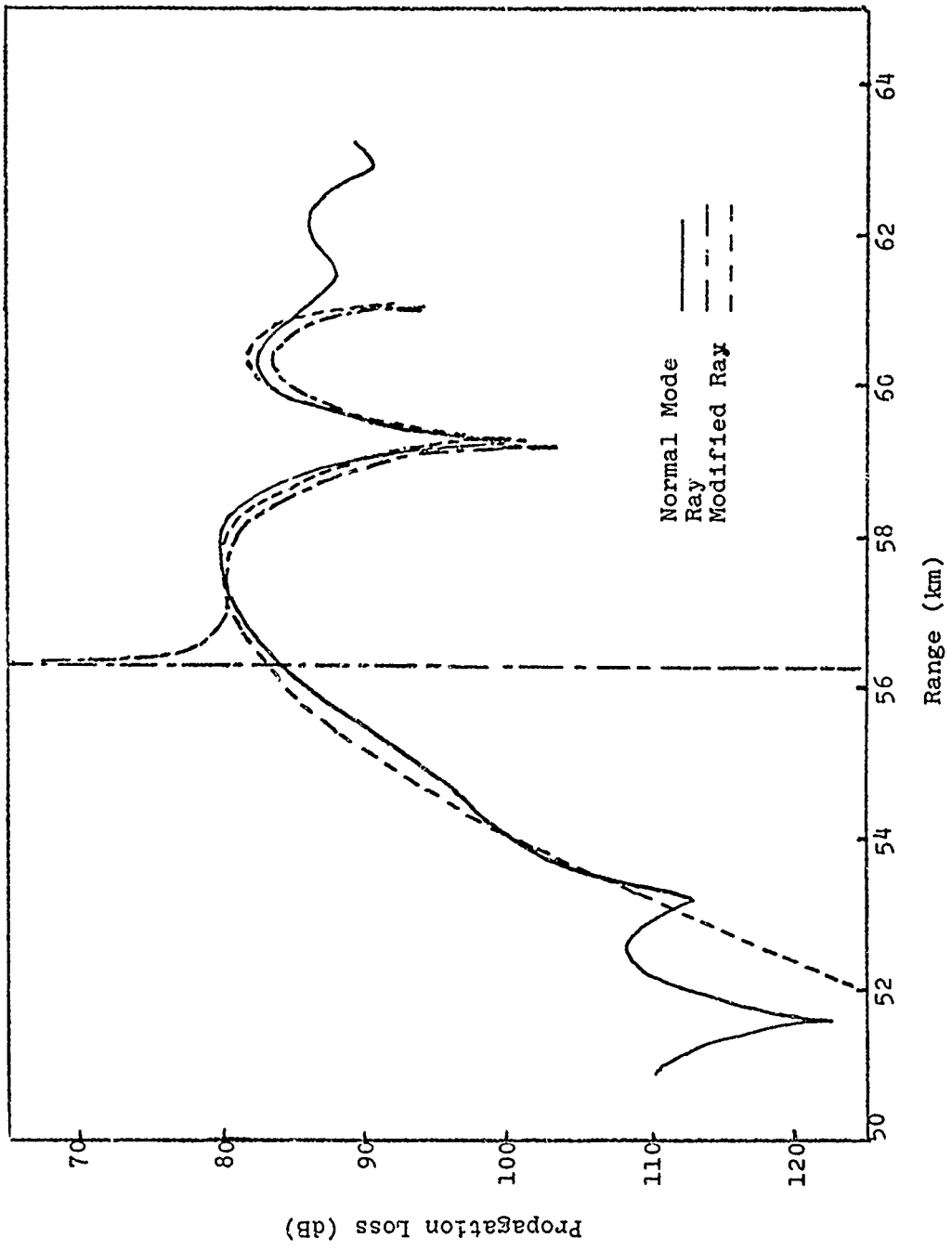

Figure 6.4B Profile I, Normal Mode, Ray, and Modified Ray (z =500m, f=50Hz)

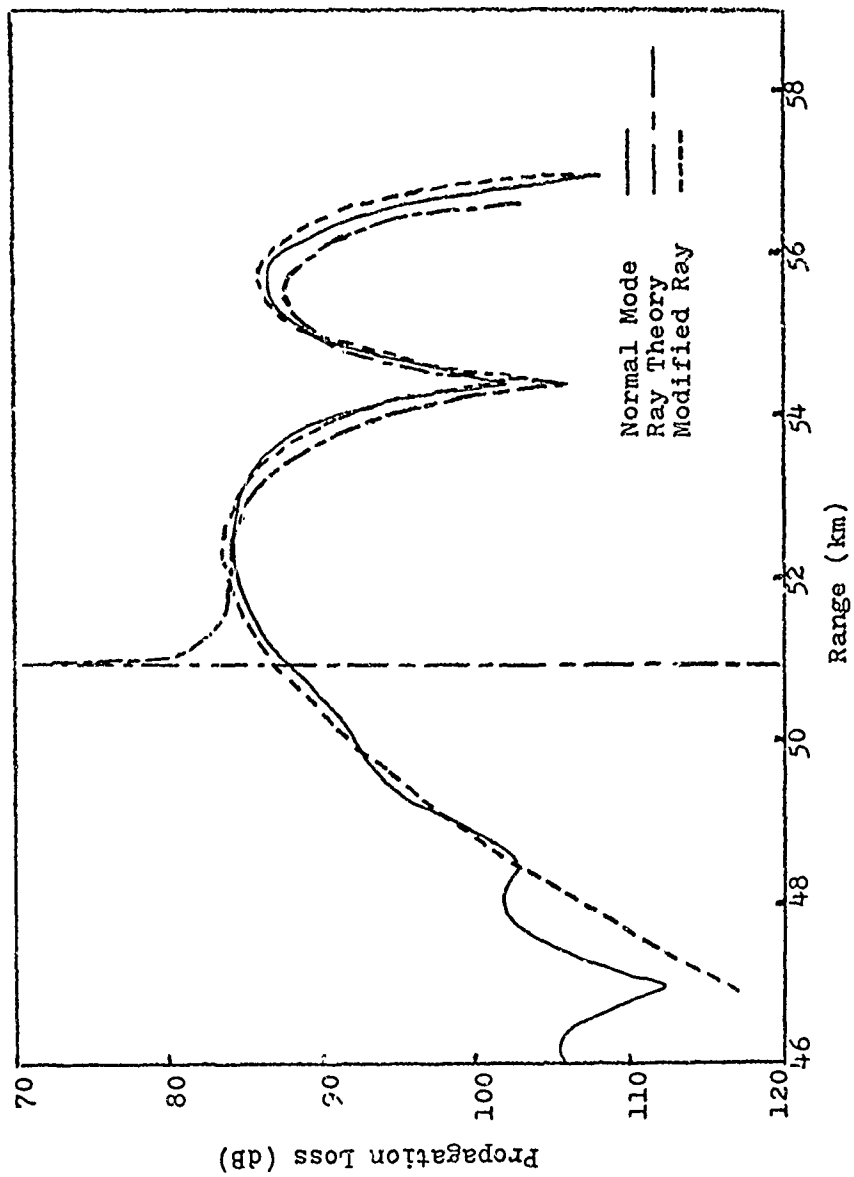

Figure 6.4C Profile I, Normal Mode, Ray, and Modified Ray Theory (z=1500m, f=50Hz)

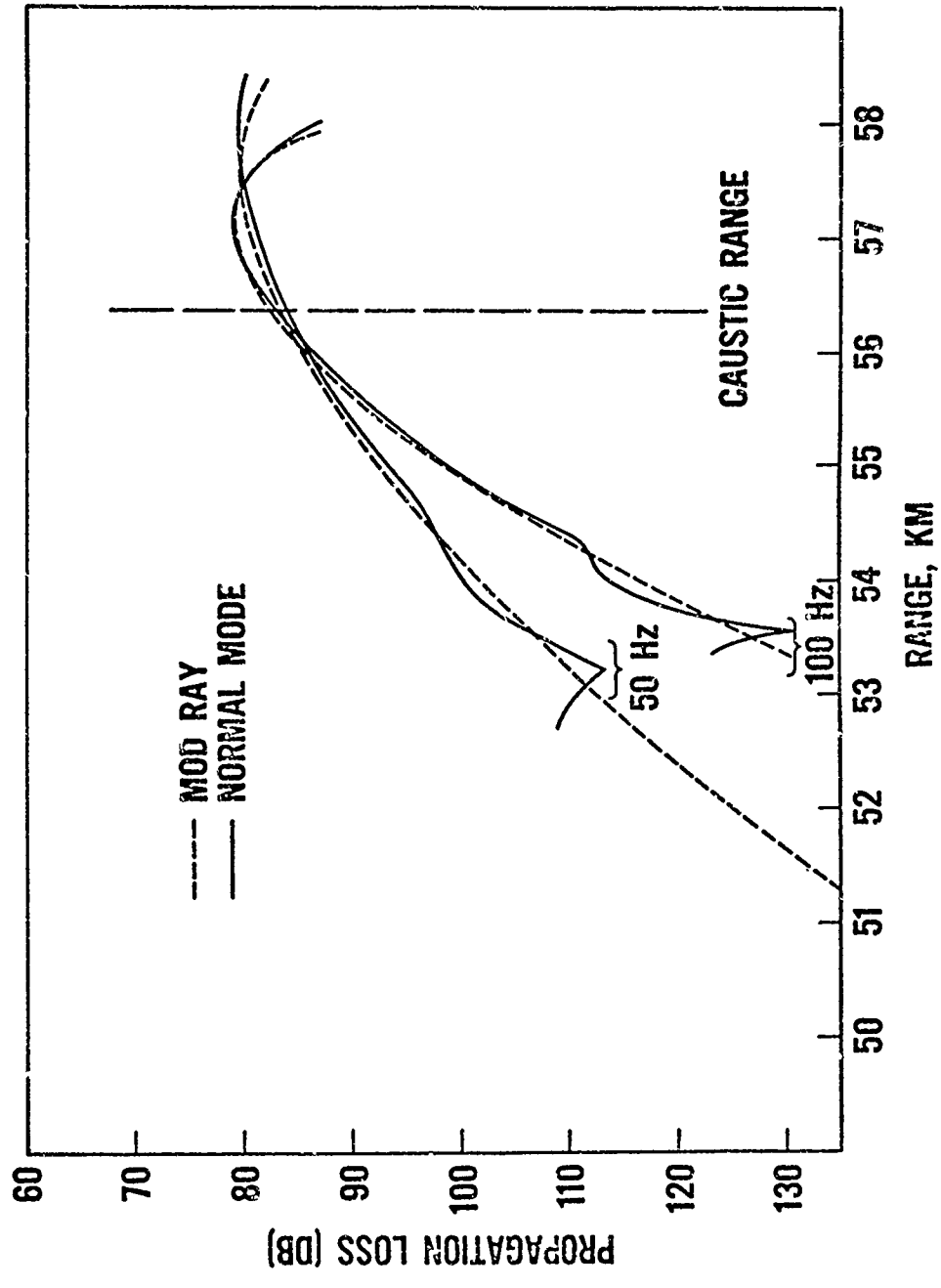

Figure 6.5 Frequency Dependence of Normal Mode and Modified Ray Theory in Shadow Zone Adjacent to the Caustic (z=500m, f=50, 100Hz)

7. Profile II, Comparisons for a Multi-Caustic Convergence Zone

While our main concern is with caustics and the convergence zone, for completeness we compared ray theory to normal mode theory in the near field region to the left of the shadow zone. Figure (7.1) shows the velocity profile* and ray diagram considered. Figure (7.2) shows the near field comparisons for the three depths of interest. Because we are using the asymptotic expression for the Hankel function, good for large arguments, we do not expect the normal mode result to be valid within a range of about one water depth of the source. And this breakdown does show up (for example, at ranges less than 10 km in Figure (7.2C)) where the normal mode result starts to diverge.

In Figure (7.2), the propagation loss curve oscillates several times as the direct and surface reflected rays interfere. Then at a specific range at each depth (29.6 km at 1500 m, for example), the ray theory propagation loss increases to infinity as we enter the shadow zone. Normal mode results continue to indicate a finite amount of energy present in the shadow zone. At 250 m (Figure 7.2A), the general fall off in diffracted energy with increasing range is most obvious. Superimposed on this fall off is an oscillation due to energy that is probably reflected by the matched impedance, discontinuous gradient bottom. As the receiver depth becomes deeper, the distance between the near shadow zone boundary and caustic shadow zone boundary decreases and the bottom grows closer, so that by the time we reach 1500 m, the average propagation loss remains roughly constant throughout the shadow zone.

*Input sound velocity profile data in Appendix V.

We next examined the convergence zone resulting from the same profile (Figure 7.1). The various caustics present in the ray diagram are shown in Figure (7.3). The receiver depths are the same as before, 250 m, 500 m, and 1500 m. However due to the complexity of the ray pattern, we will discuss each receiver depth separately.

Table (7.1) summarizes the rays passing through each range point at a depth of 250 m in the convergence zone. Figure (7.4) shows the ray theory propagation loss calculated by CONCRATS which summed coherently the rays present at each point. It also contains the propagation loss versus range curve as calculated by normal mode theory. In the ray theory curve, we see a caustic at 58.9 km. Two arrivals interfere to the right of this up to point (U), where the bottom cuts off one of them. The single arrival region extends to point (V), where we pass over the next caustic and pick up one more arrival. This caustic is branch B in Figure (7.3). It is the surface reflected branch made up of those single arrivals adjacent to the first caustic that were not cut off by the bottom. At point (W) we pass over another caustic resulting from rays that are reflected off the surface near the source (Figure 7.3, Branch C). Again we pick up another ray. Finally at point (X). and beyond, we pick up another arrival that has reflected off the surface, passed through a caustic (Figure 7.3, Branch H), and reflected off the surface again.

There are two causes for abrupt, discontinuous changes in the propagation loss curve calculated by ray theory. First, the appearance of the caustic usually results in a sharp spike

in the propagation loss curve. This is seen at 58.9 km, at the border of the convergence zone. The modified ray results we add in will smooth these out as shown in the previous comparisons (Figure 6.1). The other cause of abrupt changes is the sudden cut off of a given group of rays by the bottom. This problem, also discussed by Pedersen and Gordon (16), is present in our matched impedance bottom. In any case, a particular series of rays, each of which turns deeper and reaches a different range point in a smooth pattern, suddenly is cut off by the bottom (Figure 7.5). There is not a smooth transition as rays beyond the critical ray are cut off and so do not continue the previously established smooth pattern. Normal mode results do indicate a smooth transition, and this problem of ray theory we have not treated.

We do, however, treat the caustic problem. We add in modified ray results whenever we are in the shadow zone or on the caustic. Furthermore, we add in the modified ray results, and take out the two divergent ray arrivals, whenever we are in the caustic region, $0 > \rho \geq -1.5$ in the Airy function.* Figure (7.6) shows the combination of ray theory and modified ray theory, as compared to normal mode theory. As in other comparisons, the convergence zone boundary is adequately described by modified ray results. At point (Y), we see the start of an oscillation caused by the single "real" ray interfering with a shadow zone arrival from the caustic

*Wherev r we talk of putting in modified ray results in the caustic region, it will be understood that we take out of the sum of all rays those particular rays associated with that caustic.

at point (V). In general, ray plus modified ray goes a long way toward matching the normal mode results. As discussed previously, the worst points of comparison are where the bottom cuts off an arrival, Points (U) and (Z). Normal mode results indicate a smooth transition, but simple ray theory has no way of treating this. Instead an arrival abruptly disappears, resulting in a sudden increase or decrease in propagation loss.

Figure (7.7) shows ray theory versus normal mode theory at a depth of 500 m. Table (7.2) summarizes the rays at each point, a similar pattern to that at 250 m. Here, however, we are out of the caustic region at point (U) where bottom cut off of one arrival occurs. And the caustic at point (V) is more obvious. Figure (7.8) shows the ray theory combined with modified ray results, as well as the normal mode results. We see again the interference of a single ray arrival with a shadow zone arrival, point (W) to point (V). But the normal mode result shows an additional oscillation, point (U) to point (W). This suggests an appreciable shadow zone contribution far to the left of the caustic at point (V), much farther than modified ray theory results indicate. This shows that the modified ray theory intensity probably falls off too quickly, and breaks down beyond some point off the caustic. This verifies the failure of modified ray theory far into shadow zones discussed by Sachs (49). The extra points indicated by asterisks in Figure (7.8) include in the coherent sum of all arrivals the ray double arrivals to the right of the caustic at point (V). But these two arrivals are in the caustic region,

and the modified ray results should be used instead. So as we indicated before, the modified ray results are inserted in place of the two ray arrivals in the dashed curve in Figure (7.8). This result is clearly more appropriate than the result indicated by the asterisks that includes the rays from that caustic within the caustic region.

Figure (7.9) shows the ray results and normal mode results for a depth of 1500 m. Table (7.3) summarizes the ray arrivals at the various range points. Figure (7.9) contains a somewhat simpler ray pattern. The caustic region and partial double arrival region are followed by a single arrival region, another caustic, and finally at point (U), a different double arrival region. Here each arrival has passed through a caustic, and one is further surface reflected. So we have a modified interference pattern. Figure (7.10) shows modified ray plus ray theory and normal mode theory. Again modified ray theory takes care of many of the problems of ray theory. Beyond point (V) in the normal mode solution, we see an oscillation superimposed on the interference pattern shown by ray theory. This oscillation is similar to the oscillation in the first shadow zone from 40 km to 48 km and caused by the matched impedance, discontinuous gradient bottom. We believe that the oscillation beyond point (V) is also due to bottom effects. Again the abrupt changes in propagation loss where bottom cut off occurs (points W and X) are obviously regions where improvement is needed.

We then did the same comparisons for a 50 Hz source frequency. While the ray arrivals at each point are the same (Tables 7.1 - 7.3), the frequency is different. So the oscillation pattern is different. Figures (7.11 - 7.13) show ray theory versus normal mode theory. Figures (7.14 - 7.16) are the ray plus modified ray calculations for 250 m, 500 m, and 1500 m. Also shown are the normal mode results. For 250 m, the general agreement is good. However, the ray plus modified ray result (Figure 7.14A) shows two nulls at points (U) and (V), while the normal mode result shows one null near Point (V). The nulls in the ray result are due to single diverging rays in the caustic regions to the right of caustics near these points. We were reluctant to substitute the modified ray result here, because we didn't have two arrivals to remove as in a normal caustic region. It is not obvious that a caustic region where bottom cut-off of one arrival is occurring is the same as a normal one with two diverging arrivals. It would seem that this region should be somewhat different, even though the two arrivals couldn't be resolved in the caustic region if both were there. But we put in the modified ray result in this region to the right of each caustic - and removed the single arrival from each caustic - to see what it would do (Figure 7.14B). The use of modified ray theory does appear to eliminate most of the first null, or merge the two together. It does not work completely, which is not unexpected. So our feeling that the modified ray result is somewhat like - and somewhat different from - a single arrival caustic region seems to be correct.

At 500 m (Figure 7.15), we again note the general agreement. The asterisks starting at point (U) are another set of points where we have added the modified ray result instead of the single arrival in the caustic region. Here, however, the region of single arrivals from the caustic is quite wide. And the modified ray is actually worse than the use of the single ray associated with the caustic. This just points out that transitions from caustic to caustic at low frequencies are quite complex and take place over a considerable distance. So caution must be used in trying to apply modified ray results in wide, single arrival caustic regions.

Figure (7.16) shows comparisons of the theories for 1500 m. Beyond point (U), results from the two theories start to diverge. Figure (7.17) shows calculations for the convergence zone and adjacent shadow zones, using normal mode theory and two different bottoms. The use of a hard bottom (Figure 7.17B) not only changes the first shadow zone (up to point V) and the convergence zone, but also changes the region beyond point (U) where the direct ray arrivals are getting weak. So we attribute the disagreement beyond point (U) in Figure (7.16) to bottom effects in a region where non-bottom reflected arrivals are contributing comparatively less energy.

Using Profile II, we next tabulated the propagation loss partial sum as a function of the number of modes in the sum. For 50 Hz there are a total of 53 discrete modes. For a 500 m receiver the intensity is highest, or conversely the propagation loss is lowest, in the convergence zone (50-68 km). Intuitively, one would expect most of the modes to contribute here. In

the shadow zone, the intensity is lowest, so intuitively one would expect a fewer number of modes to contribute. So from intuition alone, one would expect the shadow zone propagation loss level to be achieved after perhaps 10 to 30 modes were summed, and the convergence zone level to be achieved only after almost all the modes are summed.

In actual fact, the reverse is true. Figures (7.18) and (7.19) show the propagation loss as a function of the number of modes included in the sum. This was done for two points in the convergence zone (57.8 and 67 km) and two points in the shadow zone (44 and 50.4 km). For both points in the convergence zone, the propagation loss curve levels off after about 32 to 34 modes are included in the sum. From this point up to the point where the last mode contribution is included in the sum, there is very little change in the propagation loss. On the other hand, the points in the shadow zone show considerable oscillation in the propagation loss as more modes are included in the sum. The propagation loss partial sum changes by as much as 15 dB from mode to mode, and only with the addition of the last mode do we reach the correct level. Thus the high intensity levels in the convergence zone are actually closer to being average levels, and the lower intensity levels in the shadow zone are built up (or more appropriately broken down) from the convergence zone levels by the destructive interference of higher modes.

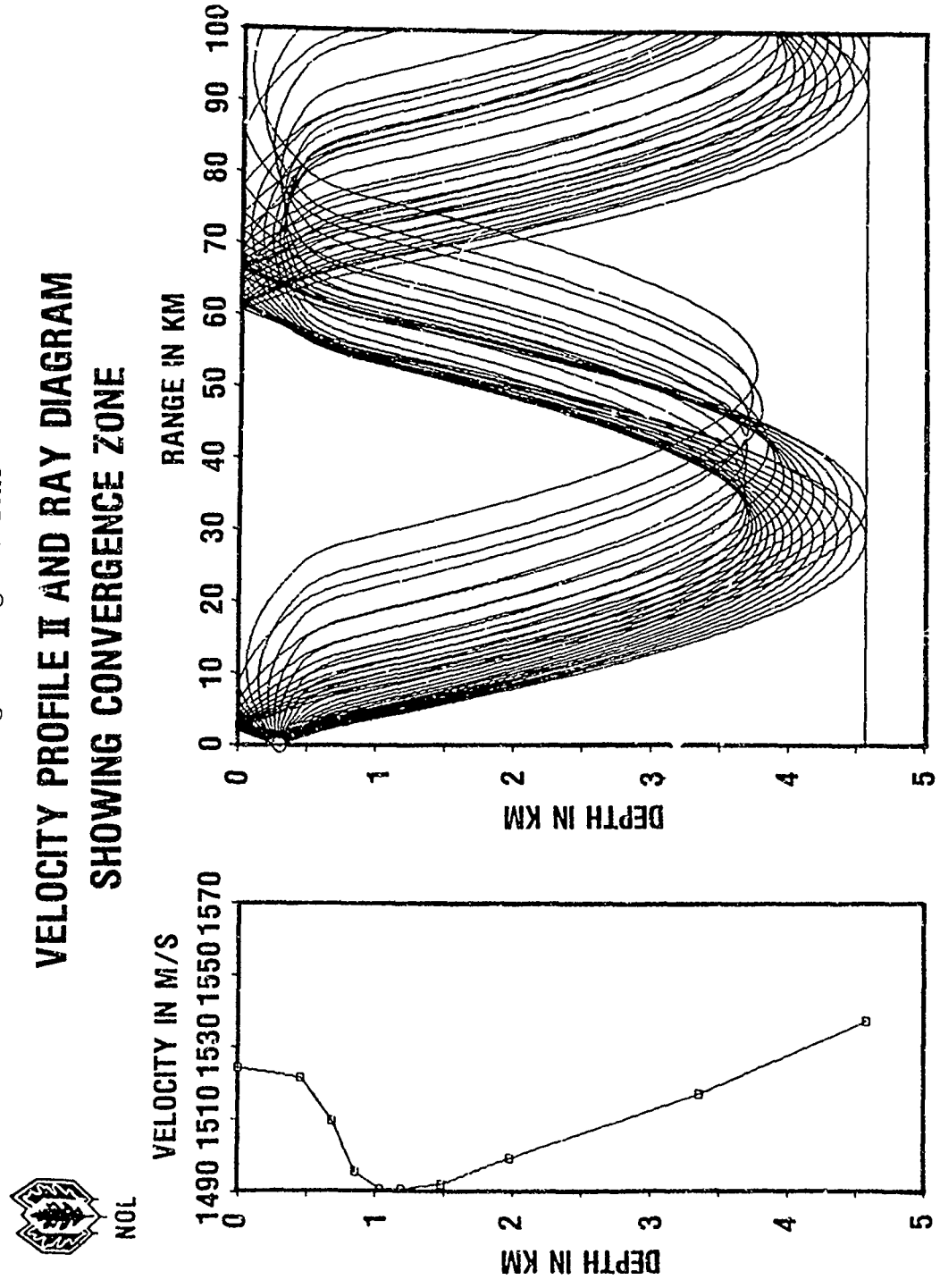

Figure 7.1 Velocity Profile II and Ray Diagram Showing Convergence Zone

Figure 7.2A Profile II, Close-in Comparison (z=250m, f=100Hz)

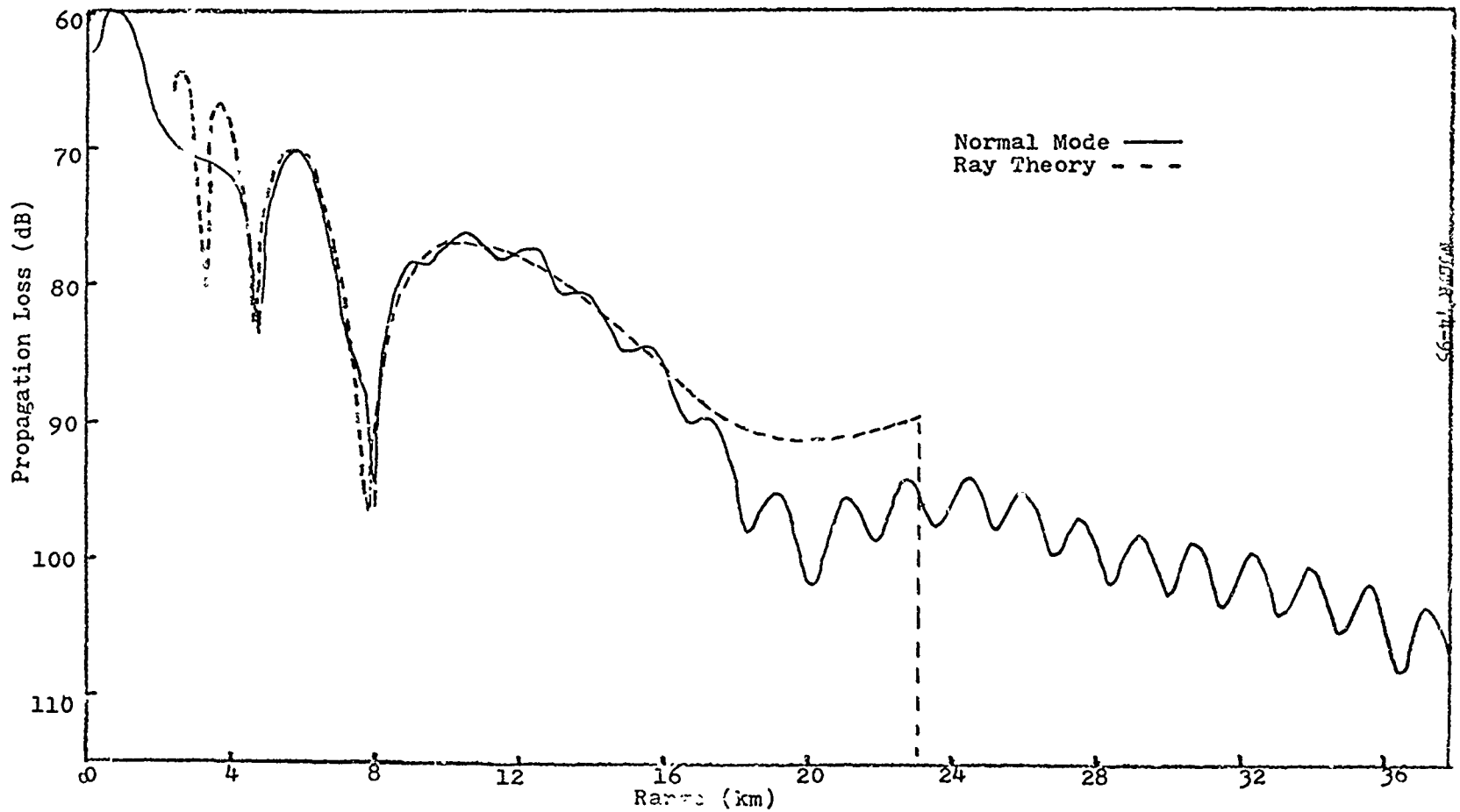

Figure 7.2B Profile II, Close-in Comparisons (z=500m, f=100Hz)

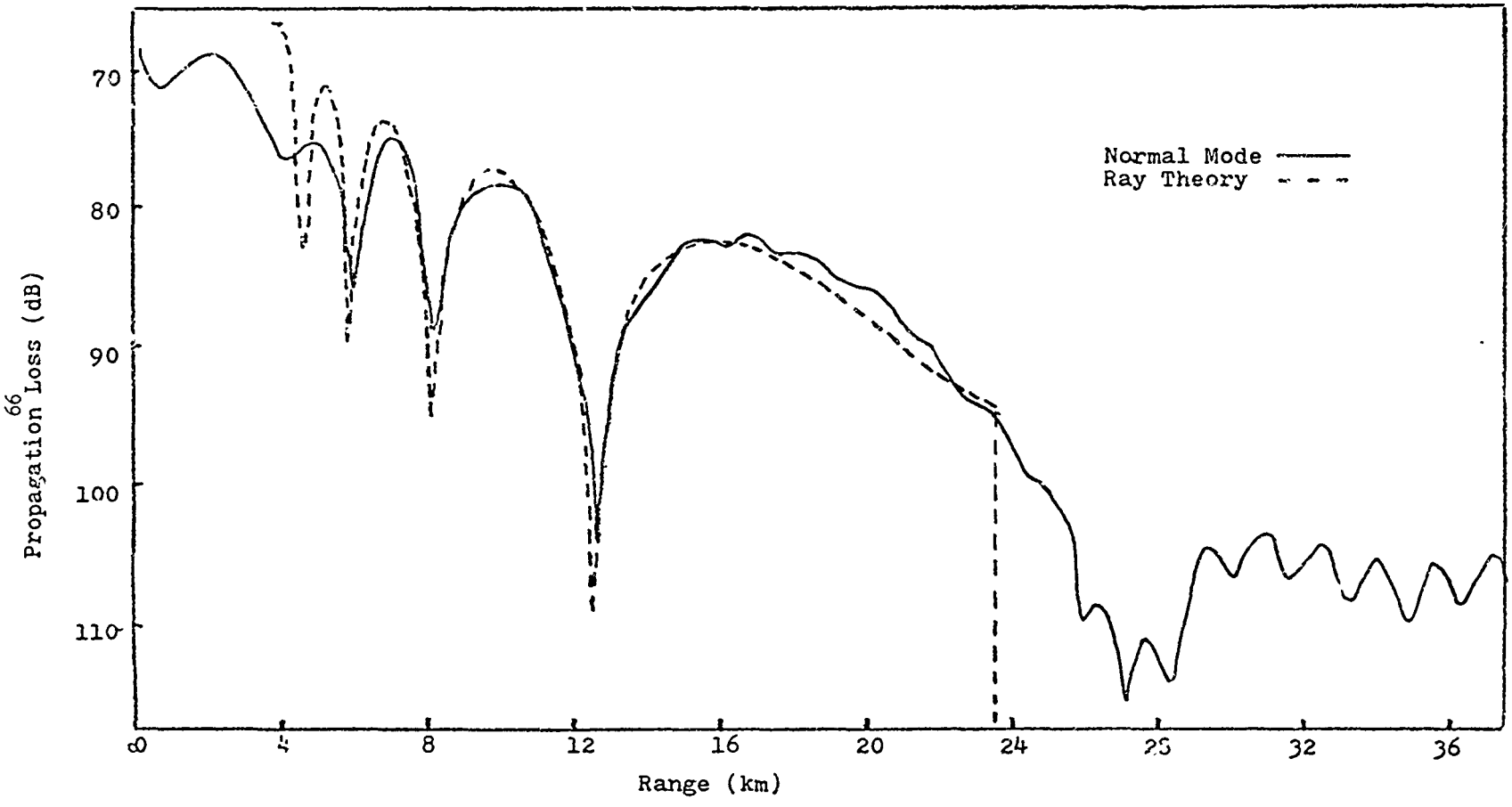

NOLTR 74-95

Figure 7.2C Profile II, Close-in Comparisons (z=1500m, f=100Hz)

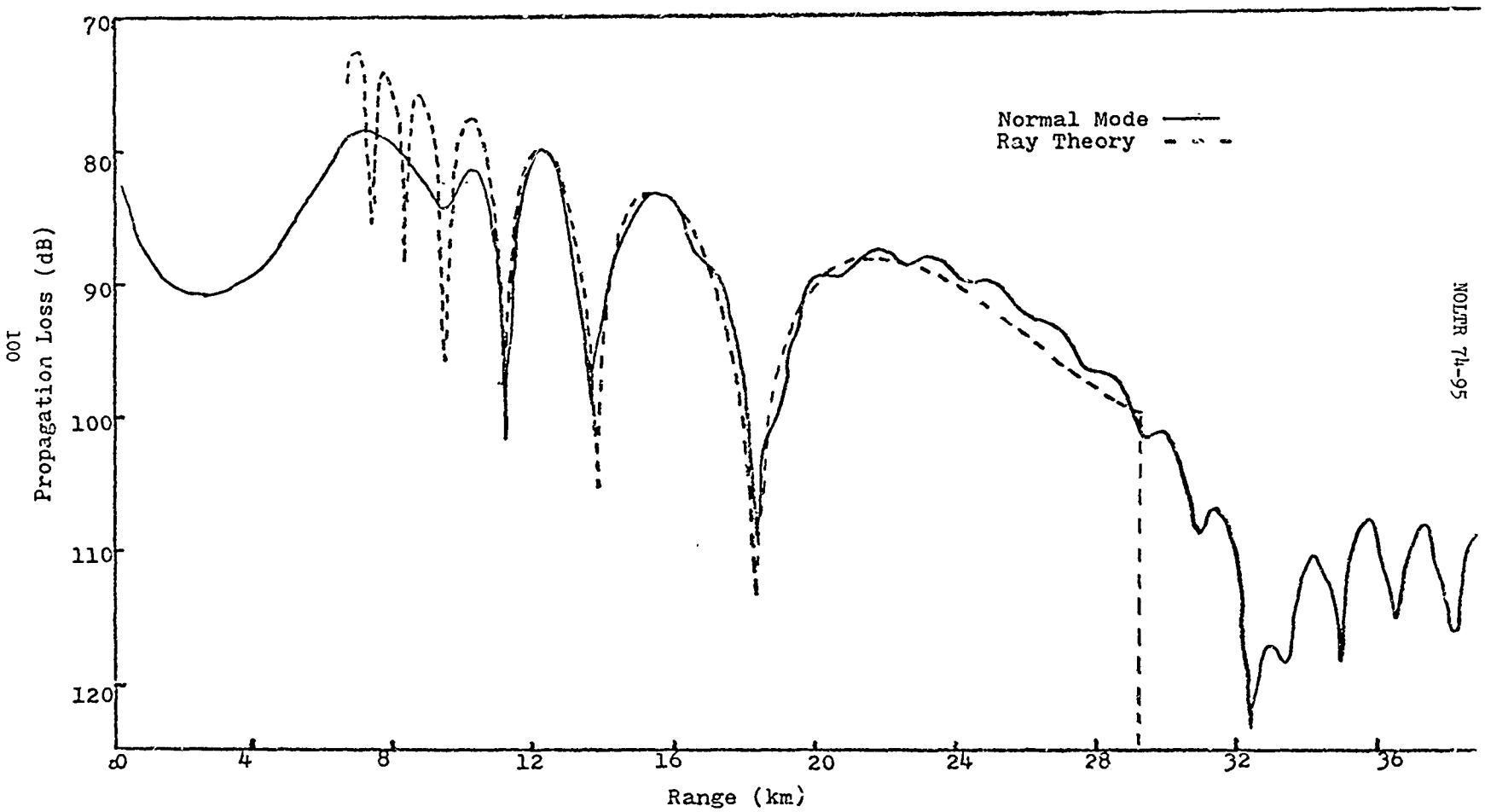

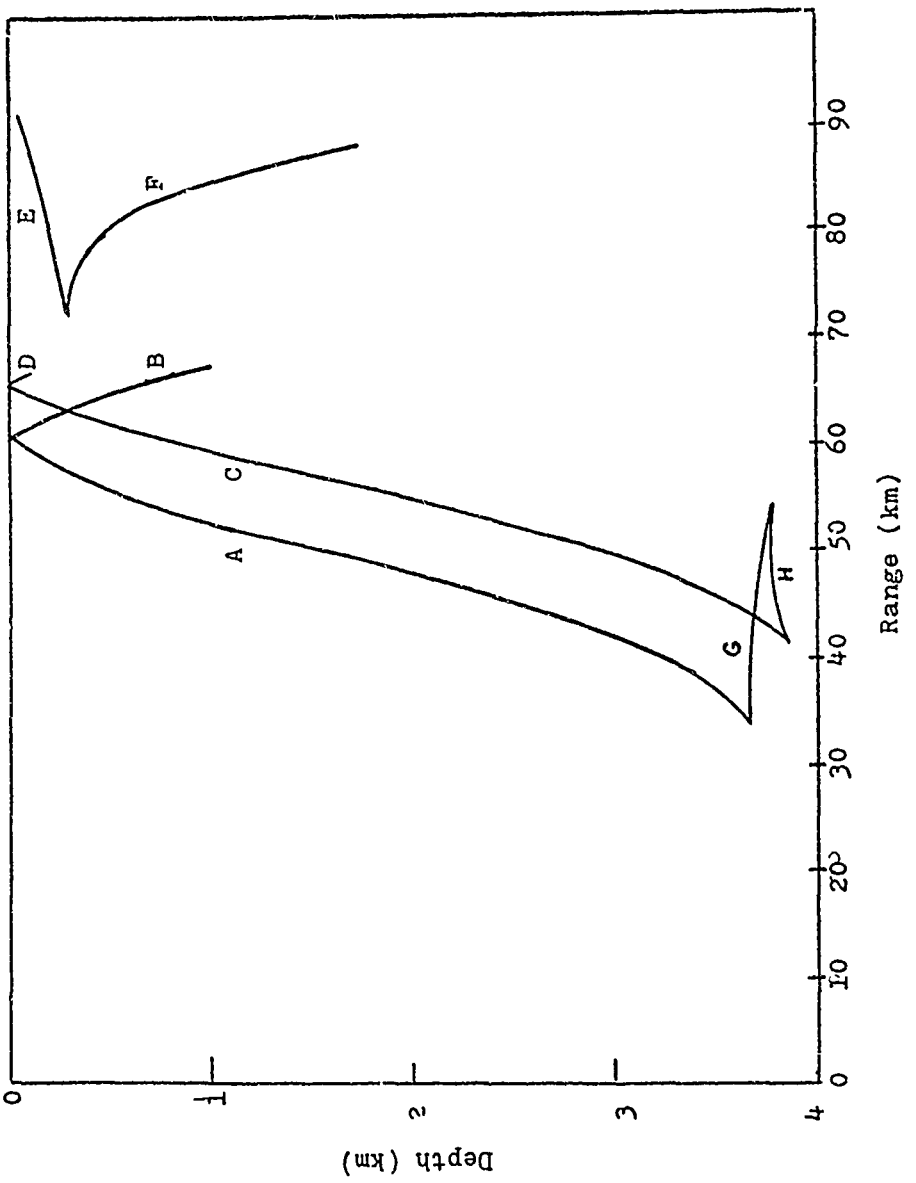

Figure 7.3 Profile II, Caustics in Convergence Zone

Table 7.1: Profile II, Receiver Depth - 250 m

Rays Passing Through Range Points of Interest

Group	Range (km)	Angle Source	Angle Receiver	History
I	59-59.8	Down	Up	Caustic
		Down	Up	
II	59.9-63.4	Down	Up	Caustic
III	63.6-64.2	Down	Up	Caustic
		Down	Down	Far S.R.*, Caustic
IV	64.4-67.8	Up	Up	Near S.R., Caustic
		Down	Up	Caustic
		Down	Down	Far S.R., Caustic
V	68-70	Up	Up	Near S.R., Caustic
		Up	Down	Near S.R.,Caustic,Far S.R.
		Down	Up	Caustic
		Down	Down	Caustic, Far S.R.

* Far S.R. - Surface reflection at convergence zone (60-70 Km)

Near S.R. - Surface reflection near source (0-15 Km)

Caustic Parameters for 100 Hz

Branch/Range (km)	θ_o (Deg)	θ_r	AMPDB (dB)	Time (Sec)	ϑ	ϕ
A/58.93	5.919		82.8	39.34	.0025	0
B/63.44	7.427	7.33	84.2	42.32	.0028	$-\pi$
C/64.27	-7.65	-7.55	84.4	42.87	.0029	$-\pi$
E/79.6	-1.365	-.66	88.7	53	.00024	$-\pi/2$

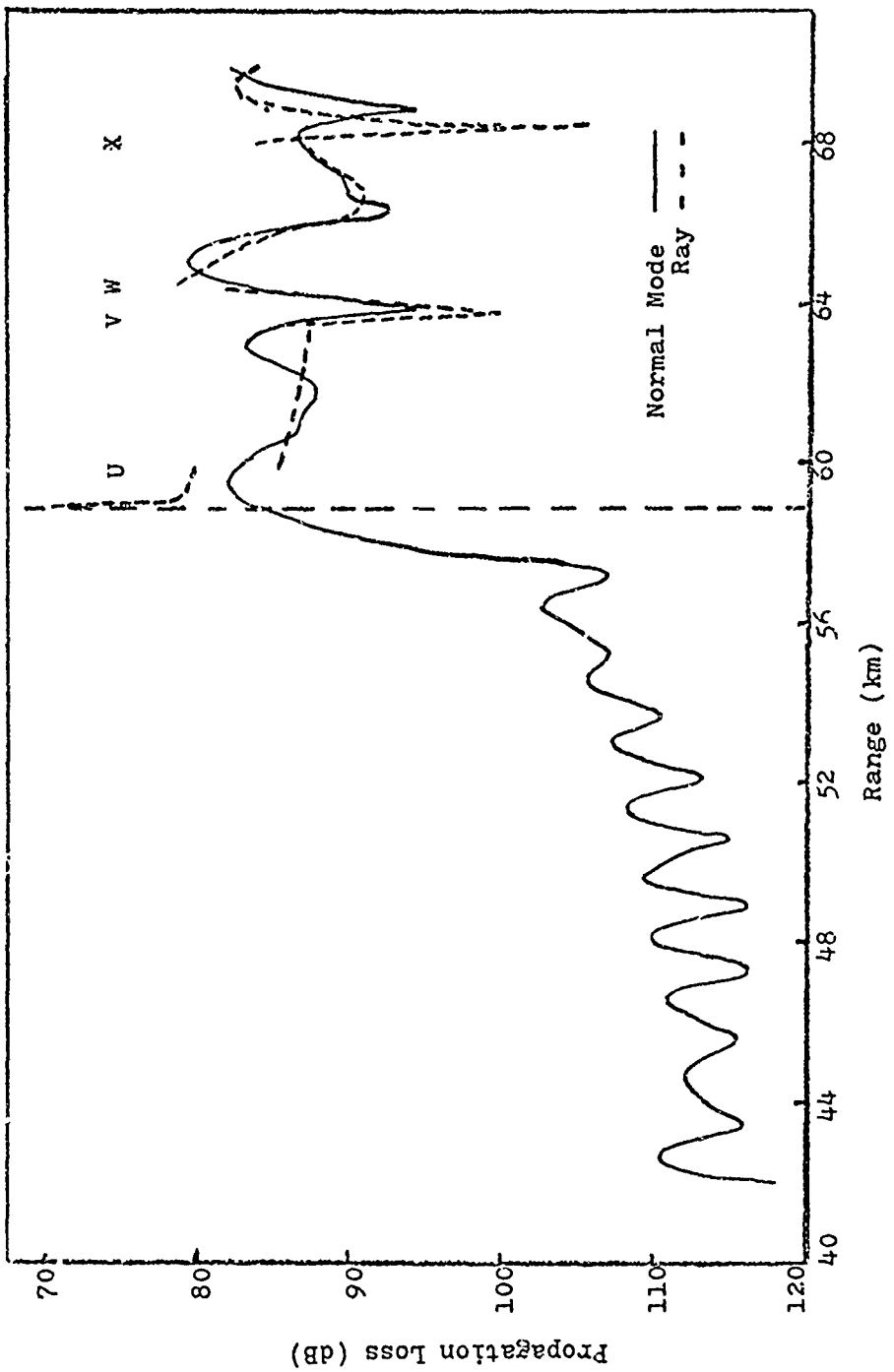

Figure 7.4 Profile II, Normal Mode and Ray Theory (z =250m, f=100Hz)

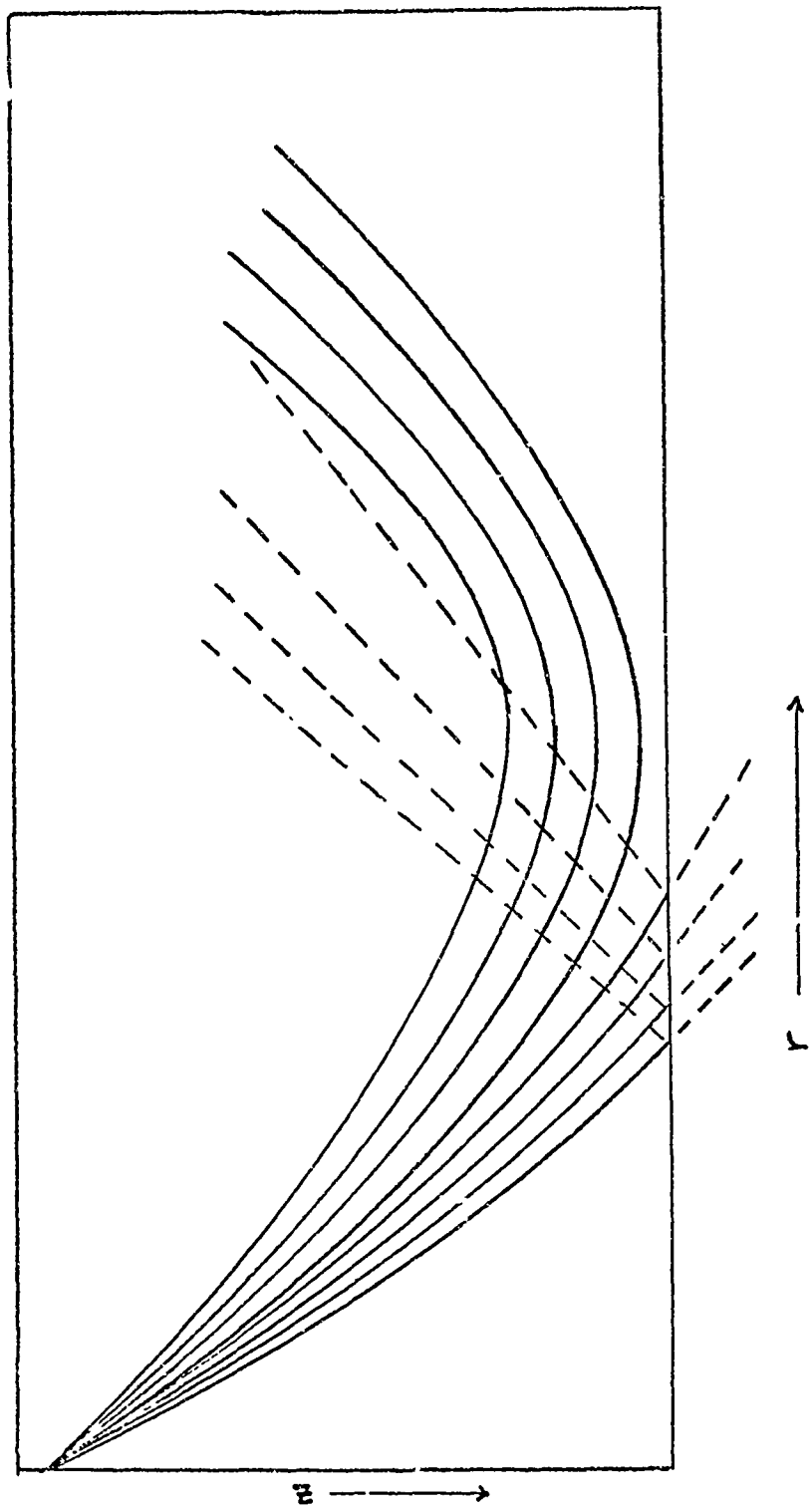

Figure 7.5 Abrupt Cutoff of Ray Group by Bottom

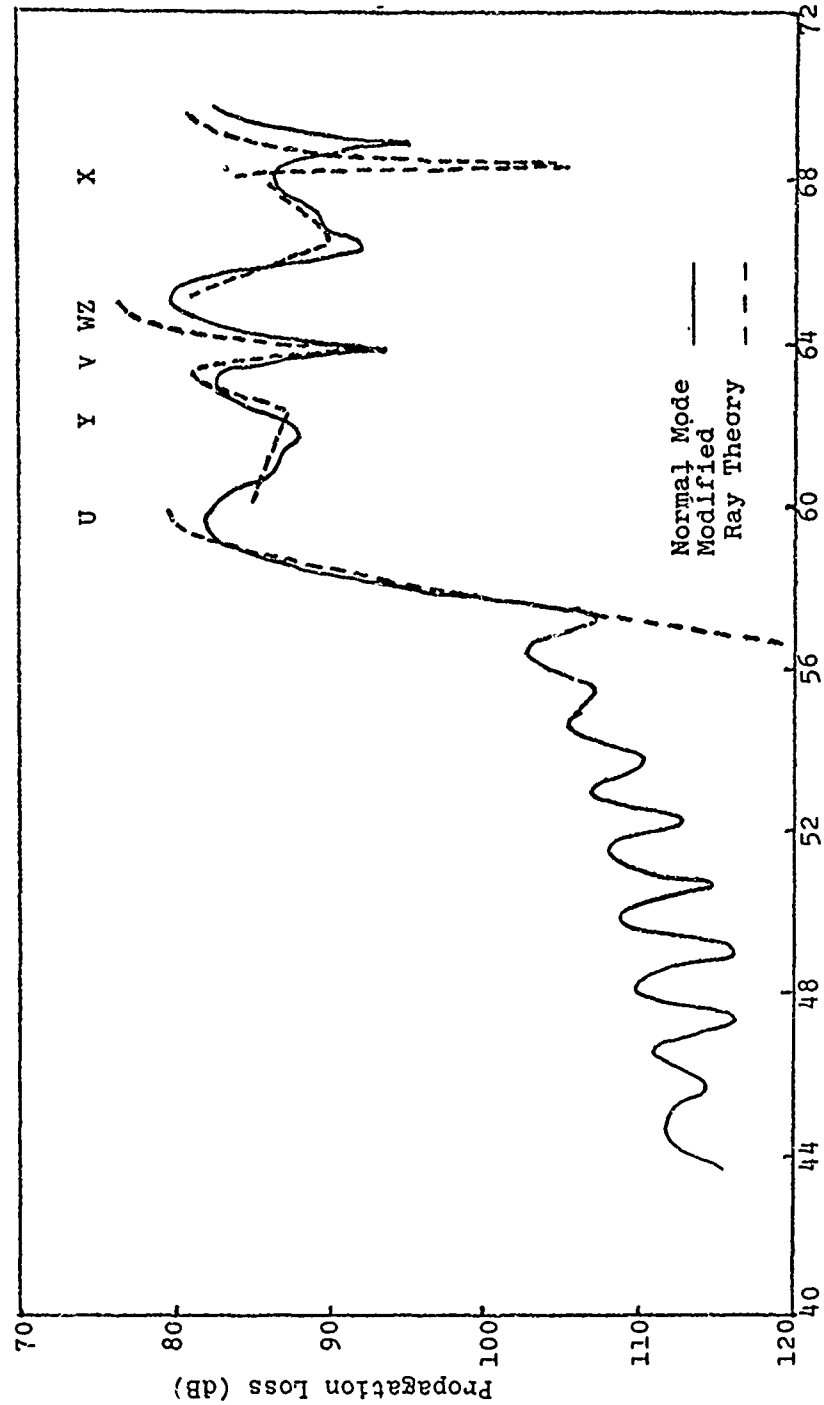

Figure 7.6 Profile II, Normal Mode and Modified Ray Theory (z=250m, f=100Hz)

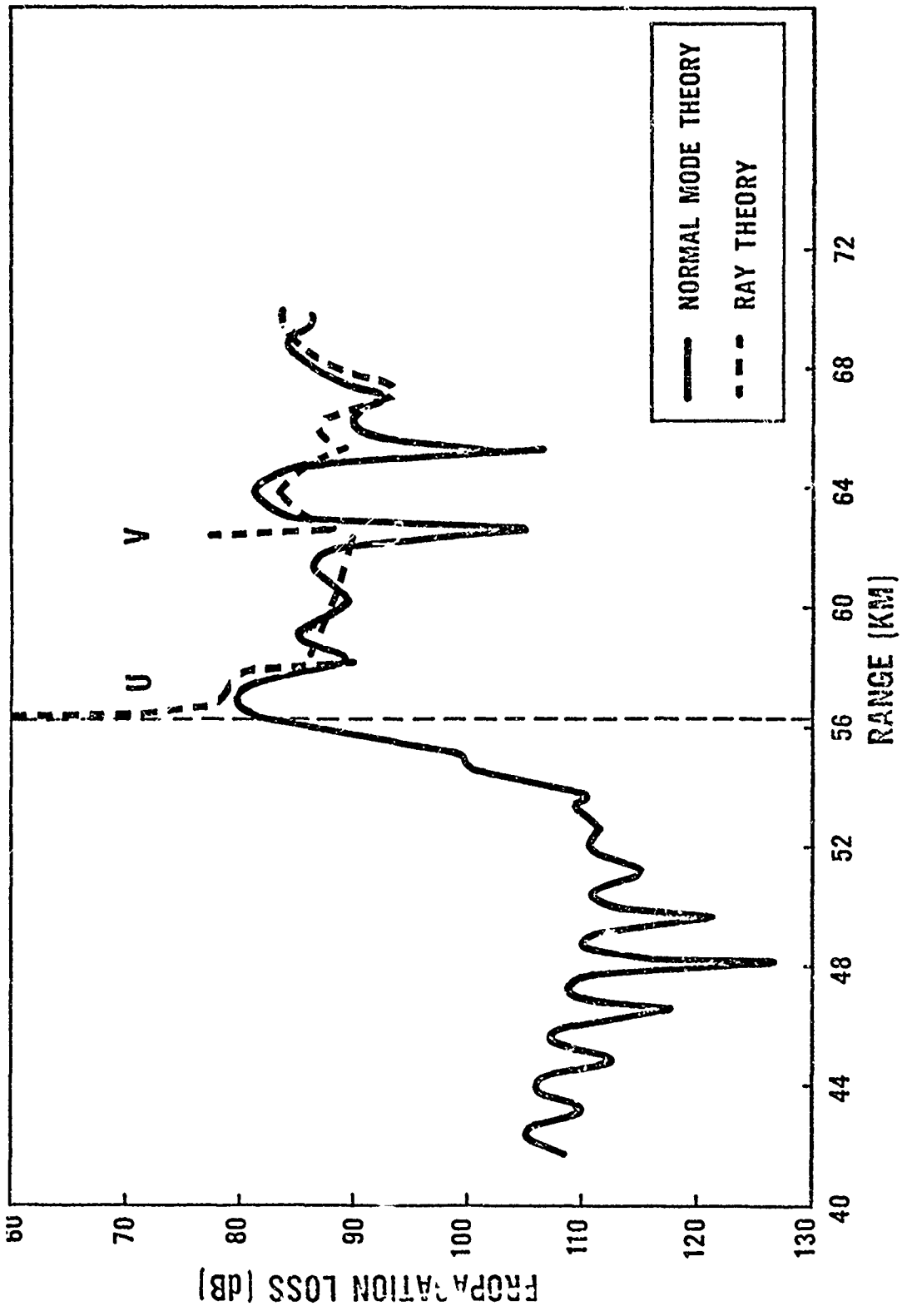

Figure 7.7 Profile II, Normal Mode and Ray Theory (z_s=500m, f=100Hz)

Table 7.2: Profile II, Receiver Depth - 500 m

Rays Passing Through Range Points of Interest

Group	Range (km)	Angle Source	Angle Receiver	History
I	56.4-58	Down	Up	Caustic
		Down	Up	
II	58.2-62.2	Down	Up	Caustic
III	62.6-65.2	Up	Up	Near S.R.*, Caustic
		Down	Up	Caustic
IV	65.4-69.4	Up	Up	Near S.R., Caustic
		Up	Up	Caustic
		Down	Down	Caustic, Far S.R.
V	69.6-70	Up	Up	Near S.R., Caustic
		Up	Down	Near S.R., Caustic, Far S.R.
		Up	Up	Caustic
		Down	Down	Caustic, Far S.R.

* Far S.R. - Surface reflection at convergence zone (60-70 Km)

Near S.R. - Surface reflection near source (0-15 Km)

Caustic Parameters for 100 Hz

Branch/Range (km)	Θ_o (Deg)	Θ_r	AMPDB (dB)	Time (Sec)	γ_n	ϕ_n
A/56.33	4.66		82.6	37.63	.0023	0
B/65.26	7.89	8.7	85	43.53	.0029	$-\pi$
C/62.39	-7.17	-8.0	84.7	41.63	.0027	$-\pi$
F/81.05	.75	3.76	92.7	53.87	.00027	$-\frac{\pi}{2}$

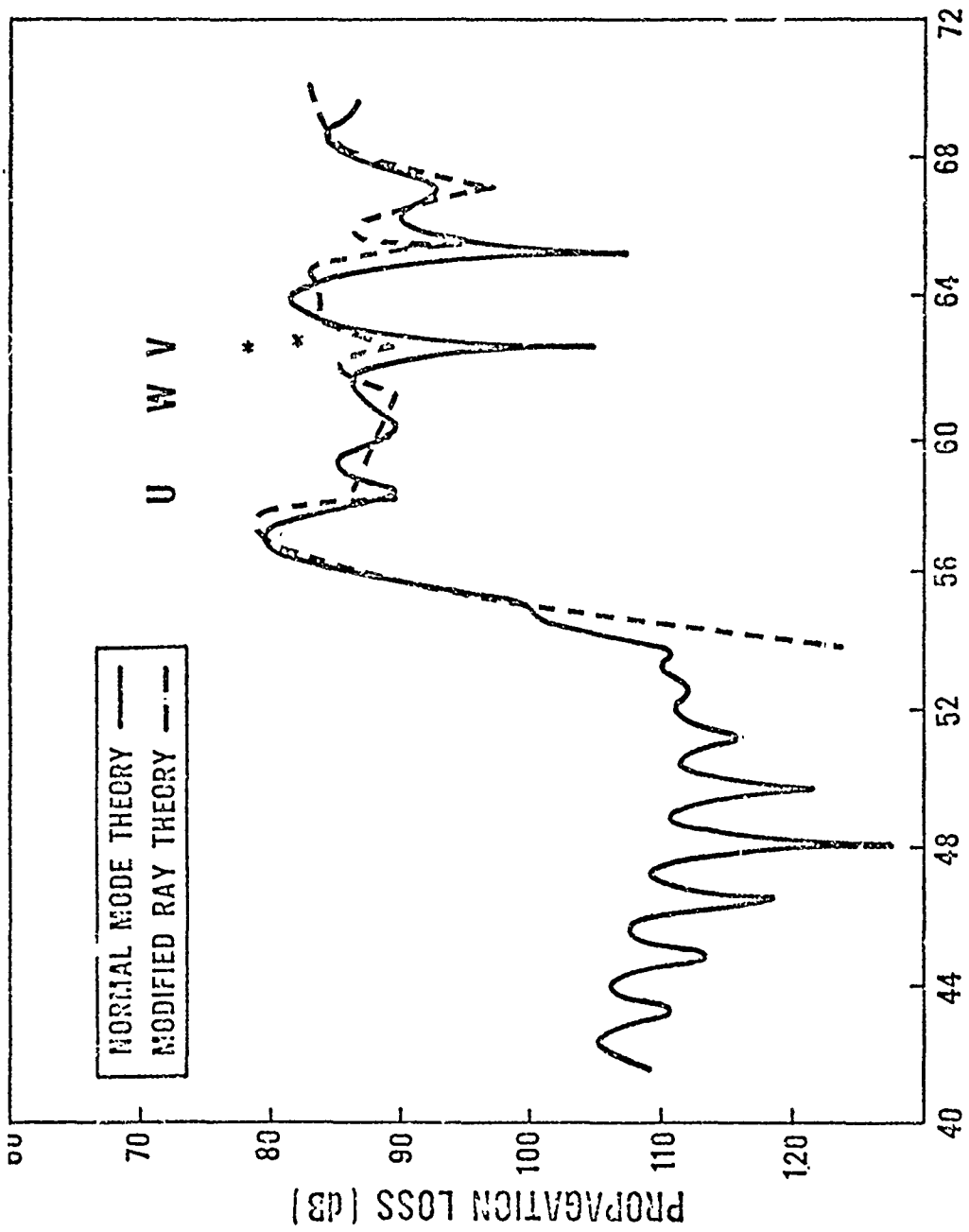

Figure 7.8 Profile II, Normal Mode and Modified Ray Theory (z_s=500m, f=100Hz)

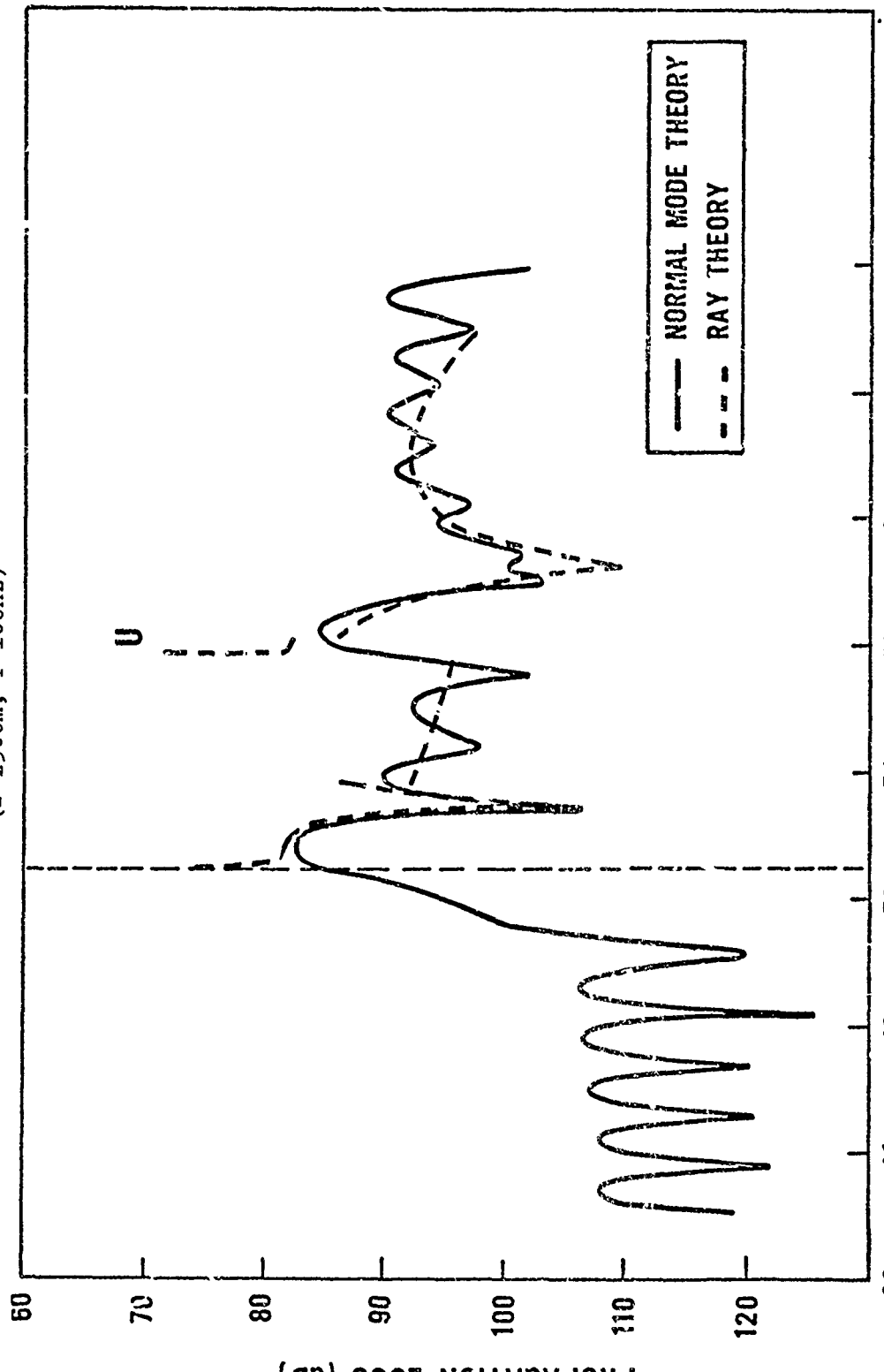

Figure 7.9 Profile II, Normal Mode and Ray Theory (z=1500m, f=100Hz)

Table 7.3: Profile II, Receiver Depth - 1500 m

Rays Passing Through Range Points of Interest

Group	Range (km)	Angle Source	Angle Receiver	History
I	51-53.6	Down	Up	Caustic
		Down	Up	
II	53.8-57.6	Down	Up	Caustic
III	57.8-58	Up	Up	Near S.R.*
		Up	Up	Near S.R., Caustic
		Up	Up	Caustic
IV	58.2-69	Up	Up	Near S.R., Caustic
		Up	Up	Caustic

* Far S.R. - Surface reflection at convergence zone (60-70 Km)

Near S.R. - Surface reflection near source (0-15 Km)

Caustic Parameters (for 100 Hz)

Branch/Range (km)	θ_o (Deg)	θ_r	AMPDB (dB)	Time (Sec)	ζ	ϕ_n
A/50.95	3.99		86	33.98	.0019	0
C/57.69	-6.69	-1[illegible]	87	38.42	.0025	$-\pi$
F/87.13	.76	11.5	98	57.98	.00028	$-\frac{\pi}{2}$

Figure 7.10 Profile II, Normal Mode and Modified Ray Theory
(z =1500m, f=100Hz)

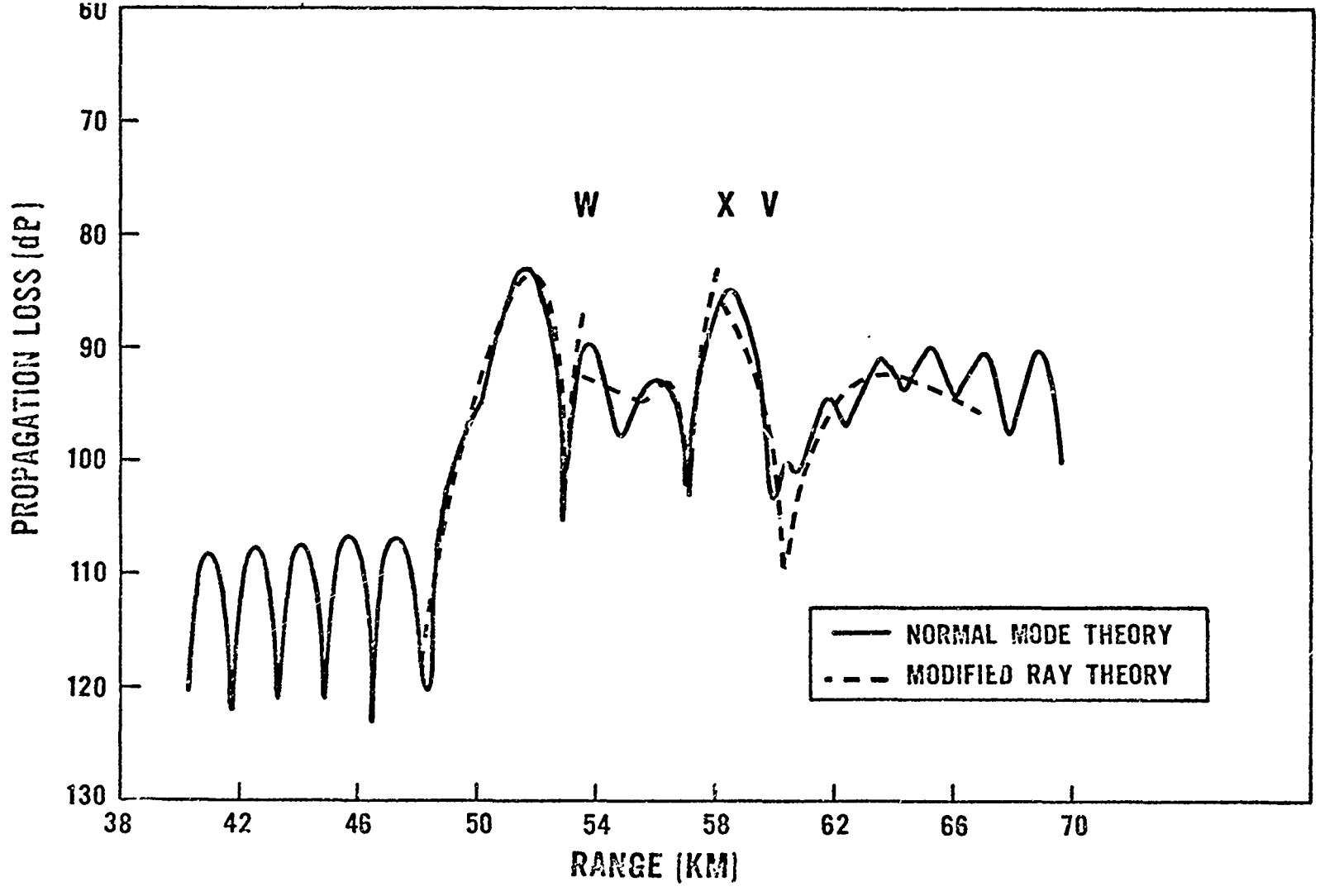

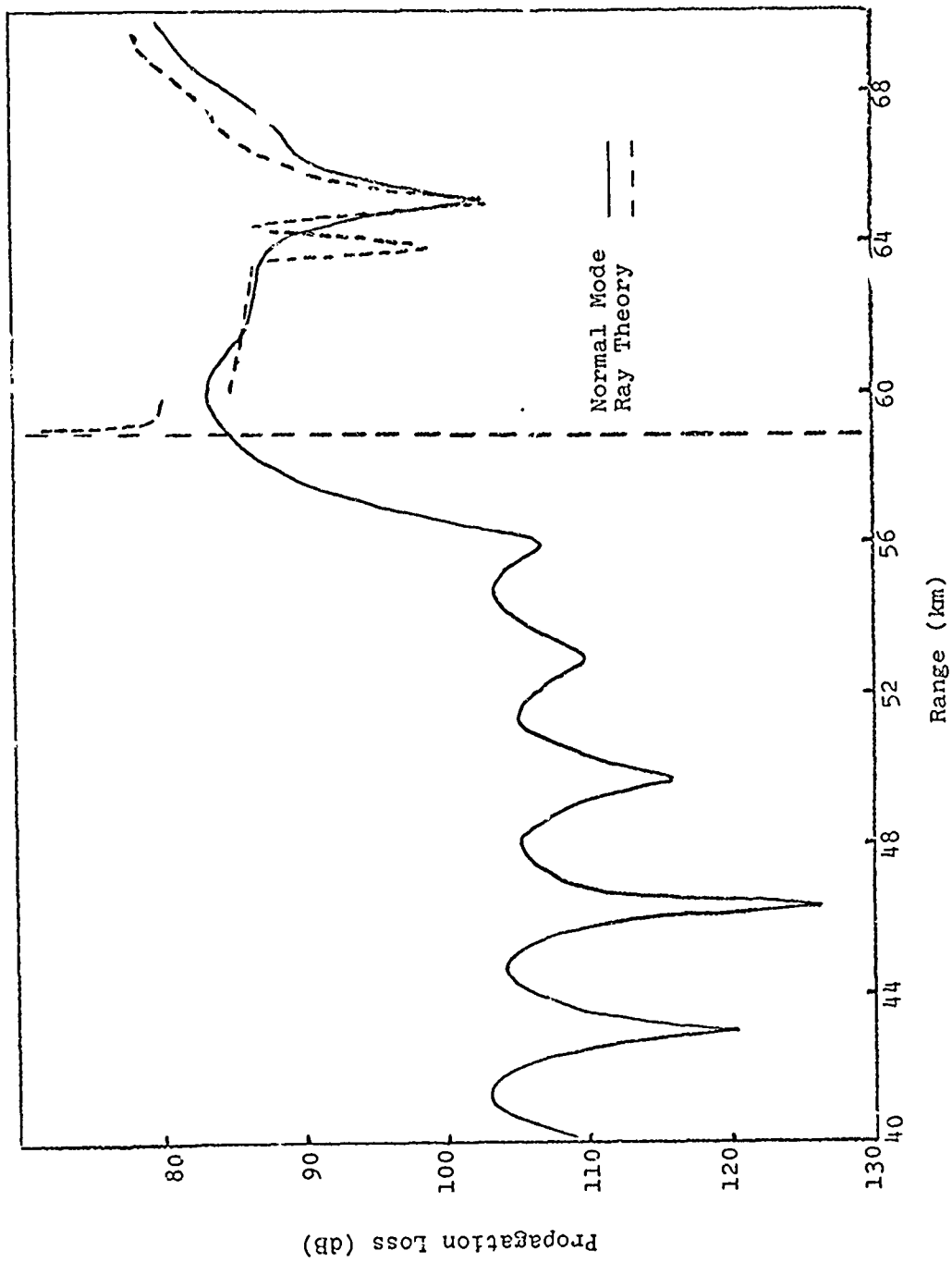

Figure 7.11 Profile II, Normal Mode and Ray Theory (z=250m, f=50Hz)

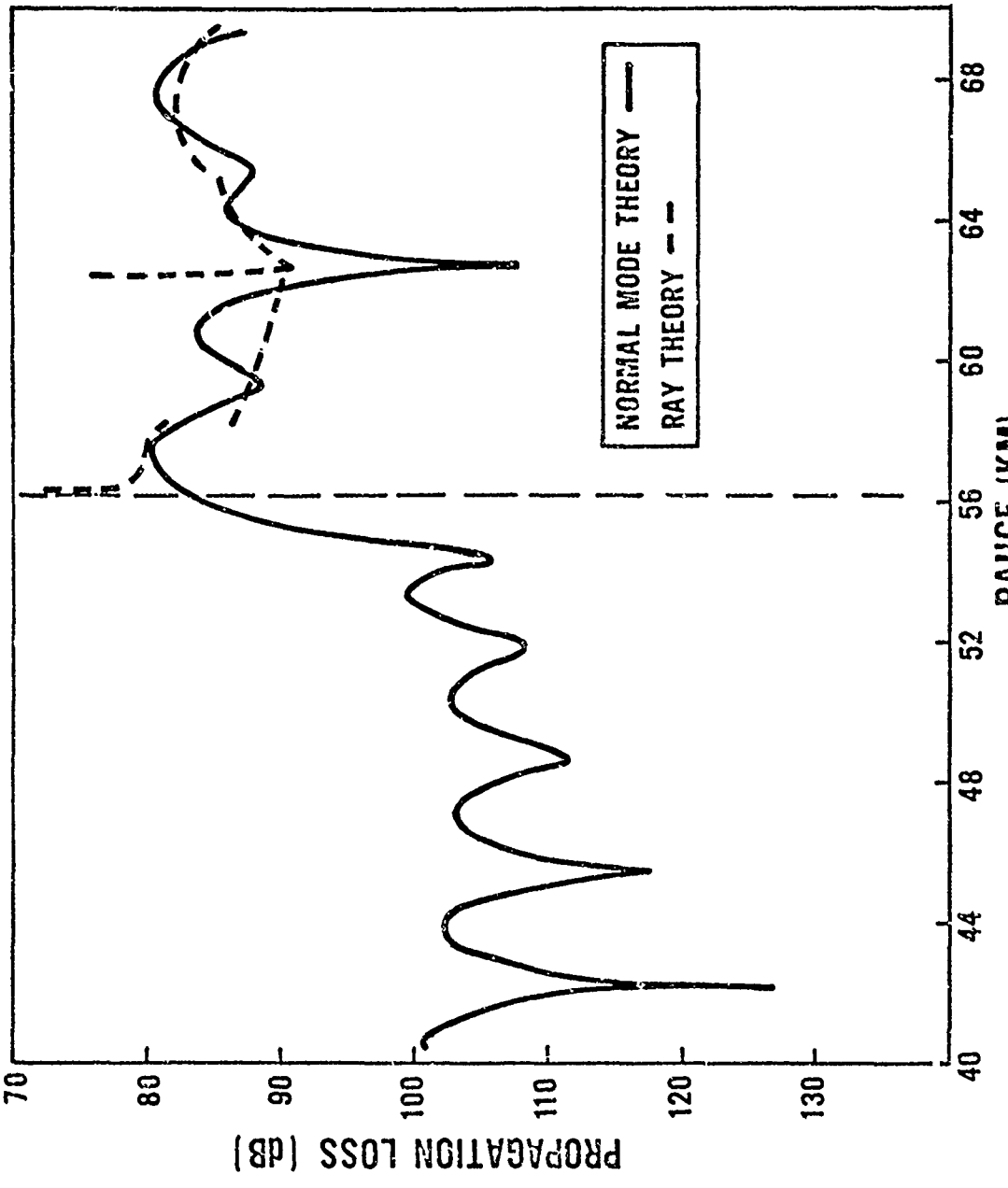

Figure 7.12 Profile II, Normal Mode and Ray Theory
(z_s=500m, f=50Hz)

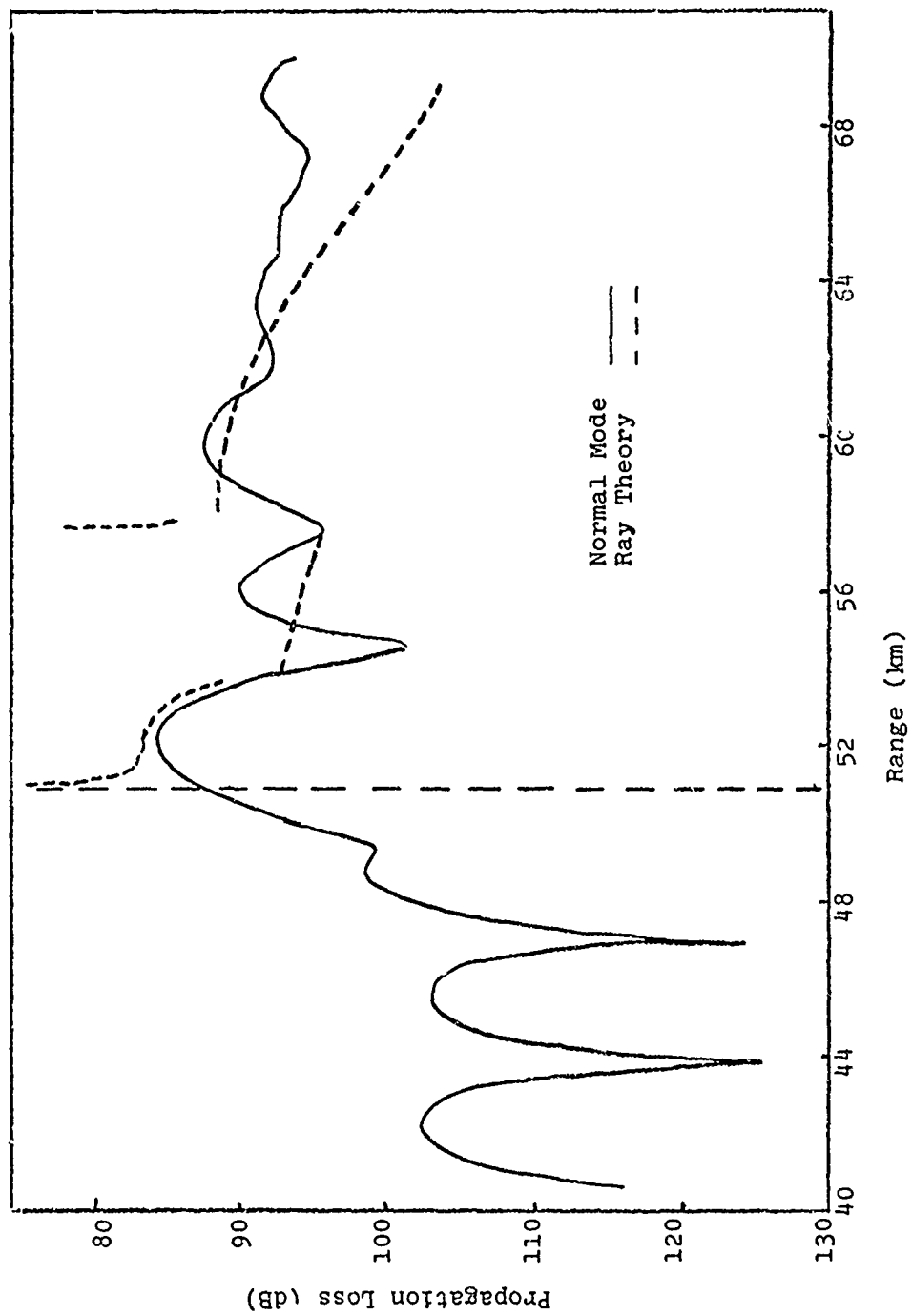

Figure 7.13 Profile II, Normal Mode and Ray Theory (z =1500m, f=50Hz)

Figure 7.14A Profile II, Normal Mode and Modified Ray Theory (z=250m, f=50Hz)

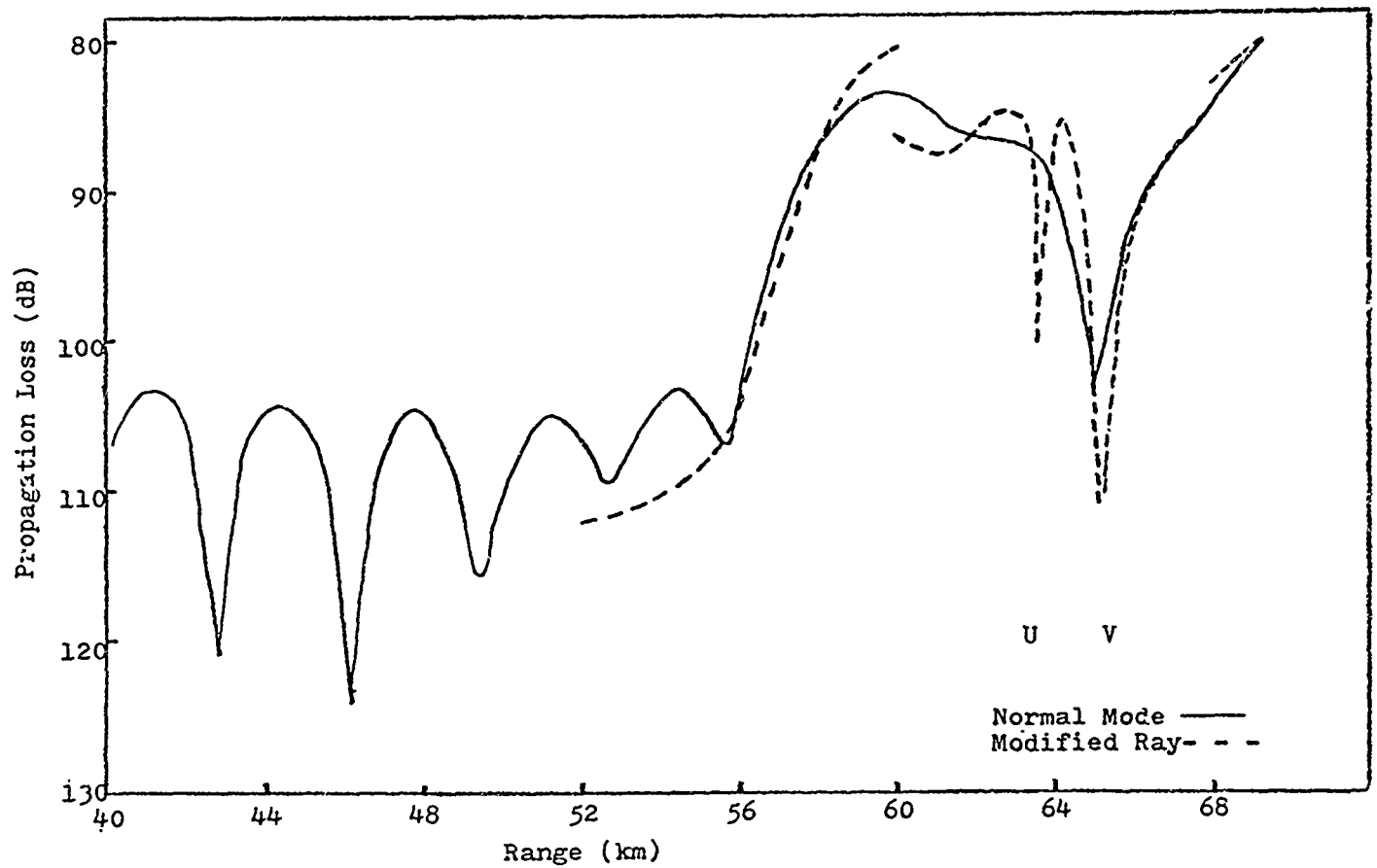

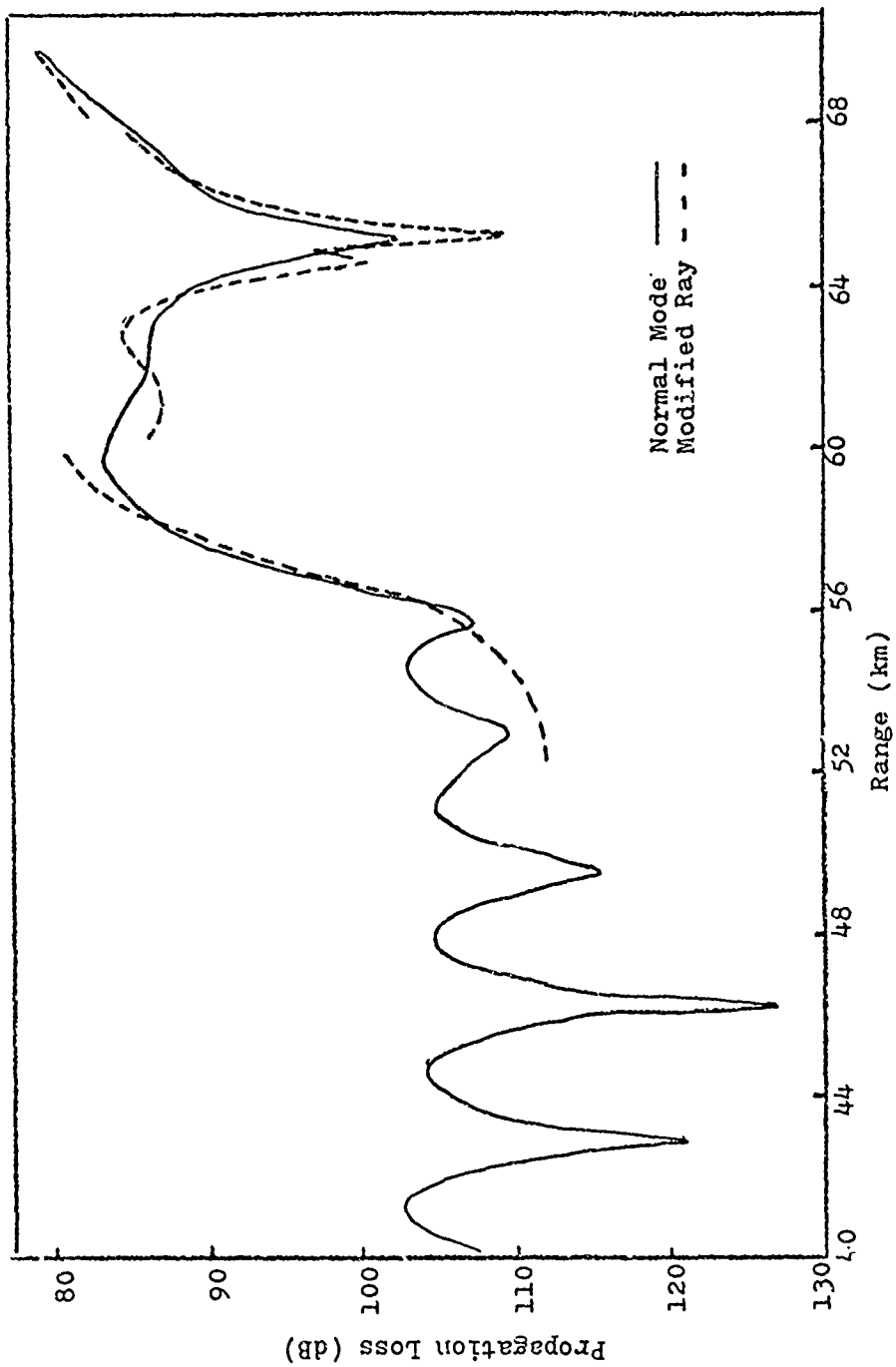

Figure 7.14B Profile II, Normal Mode and Modified Ray Theory (z=250m, f=50Hz)

Figure 7.15 Profile II, Normal Mode and Modified Ray Theory
(ℓ =500m, f=50Hz)

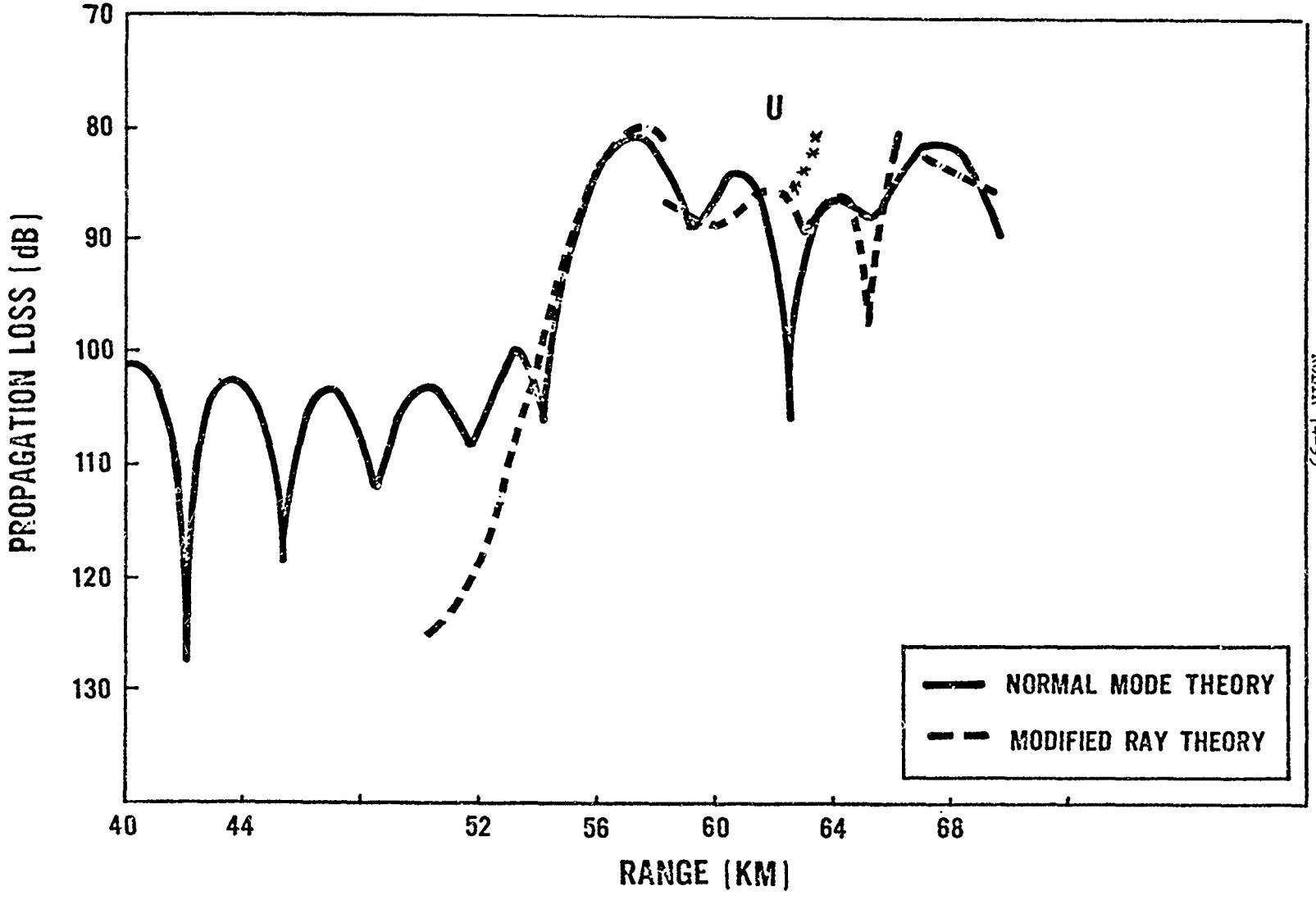

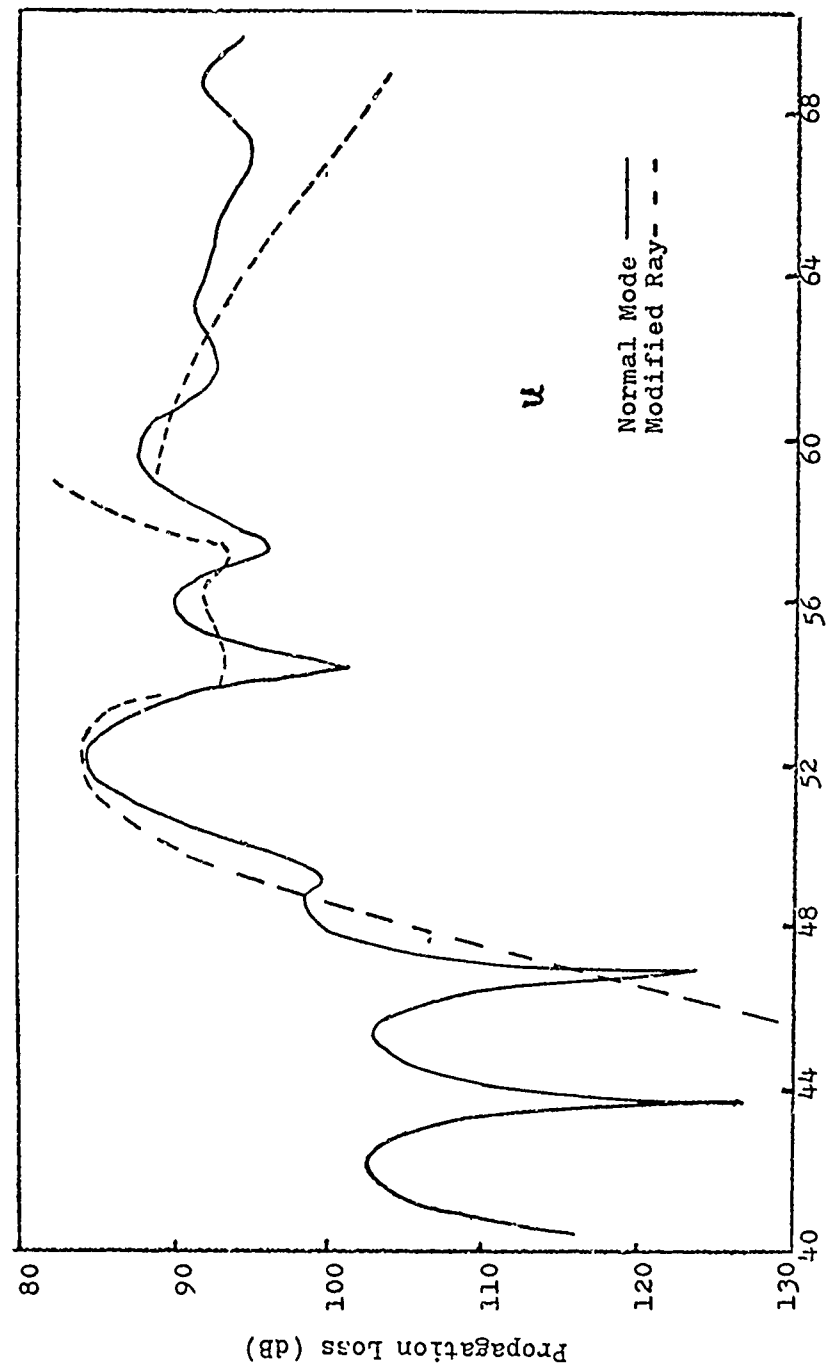

Figure 7.16 Profile II, Normal Mode and Modified Ray Theory (z=1500, f=5GHz)

Figure 7.17A Convergence Zone with Matched Impedance Bottom (z=1500 m, f=50 Hz)

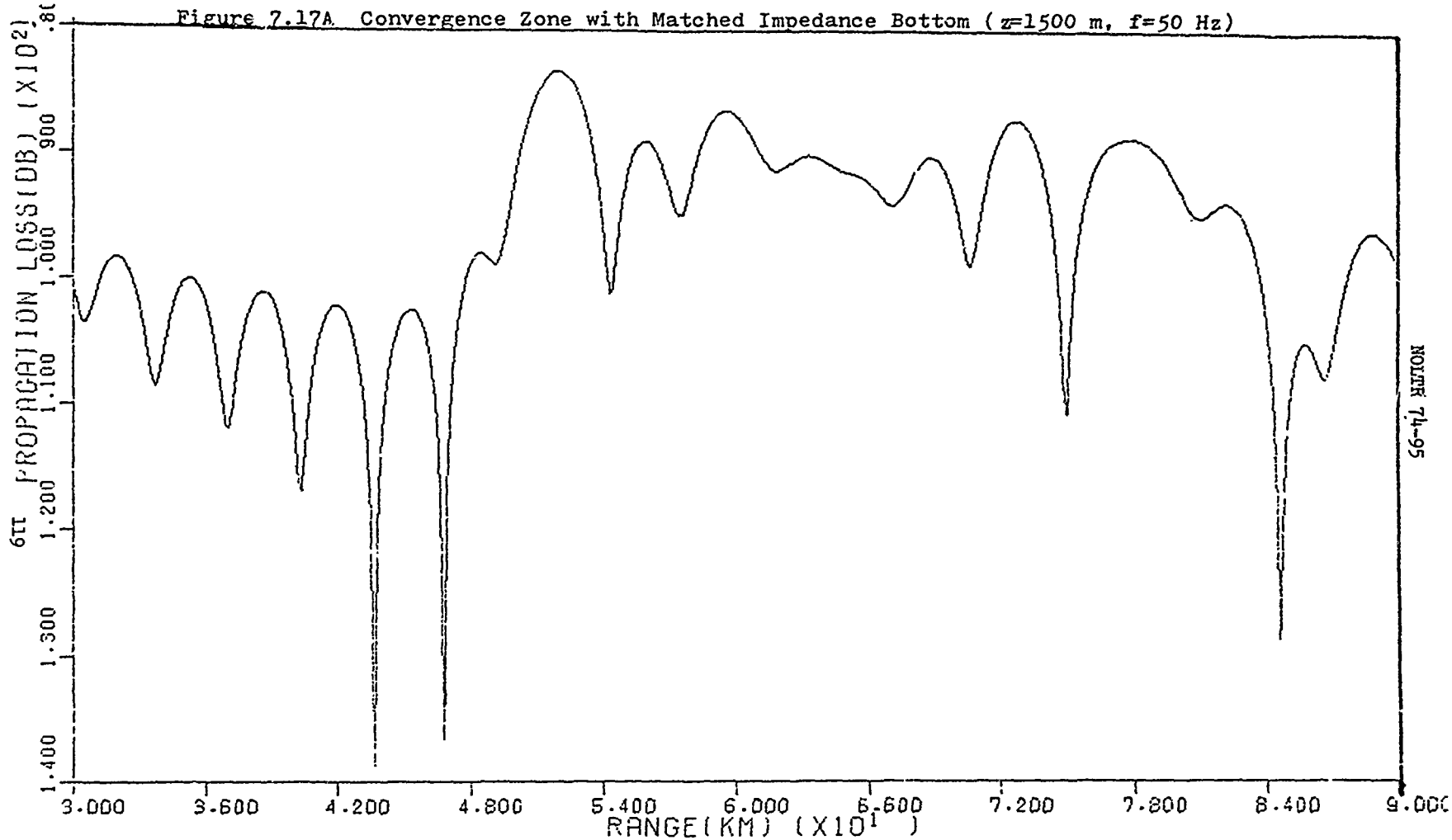

Figure 7.17B Convergence Zone with Hard Bottom ($\rho_2 = 1.38$, $c_2 = 1545$)(z=1500m, f=50Hz)

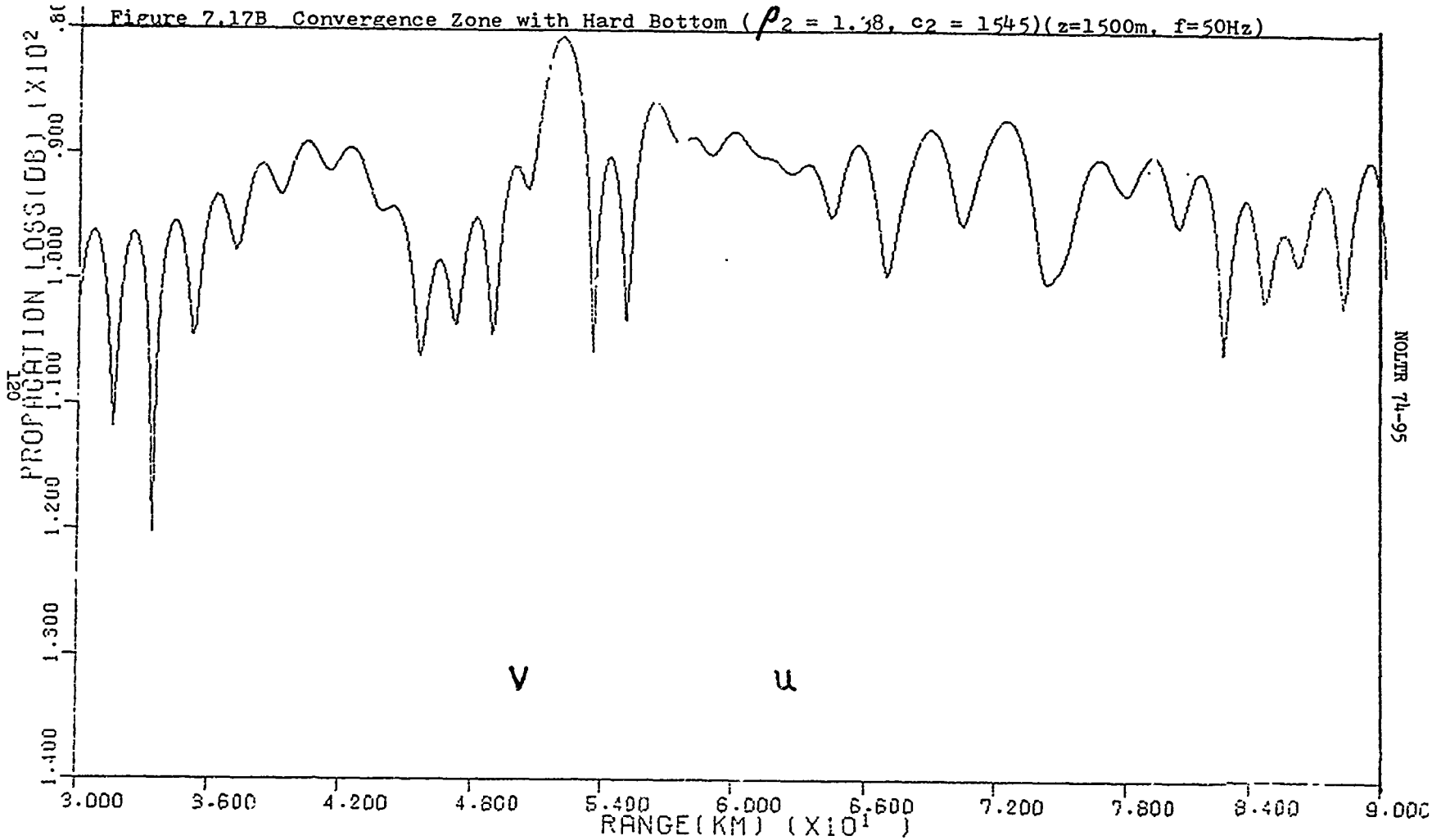

Figure 7.18 Partial Sum of Modes (50.4km and 67km)

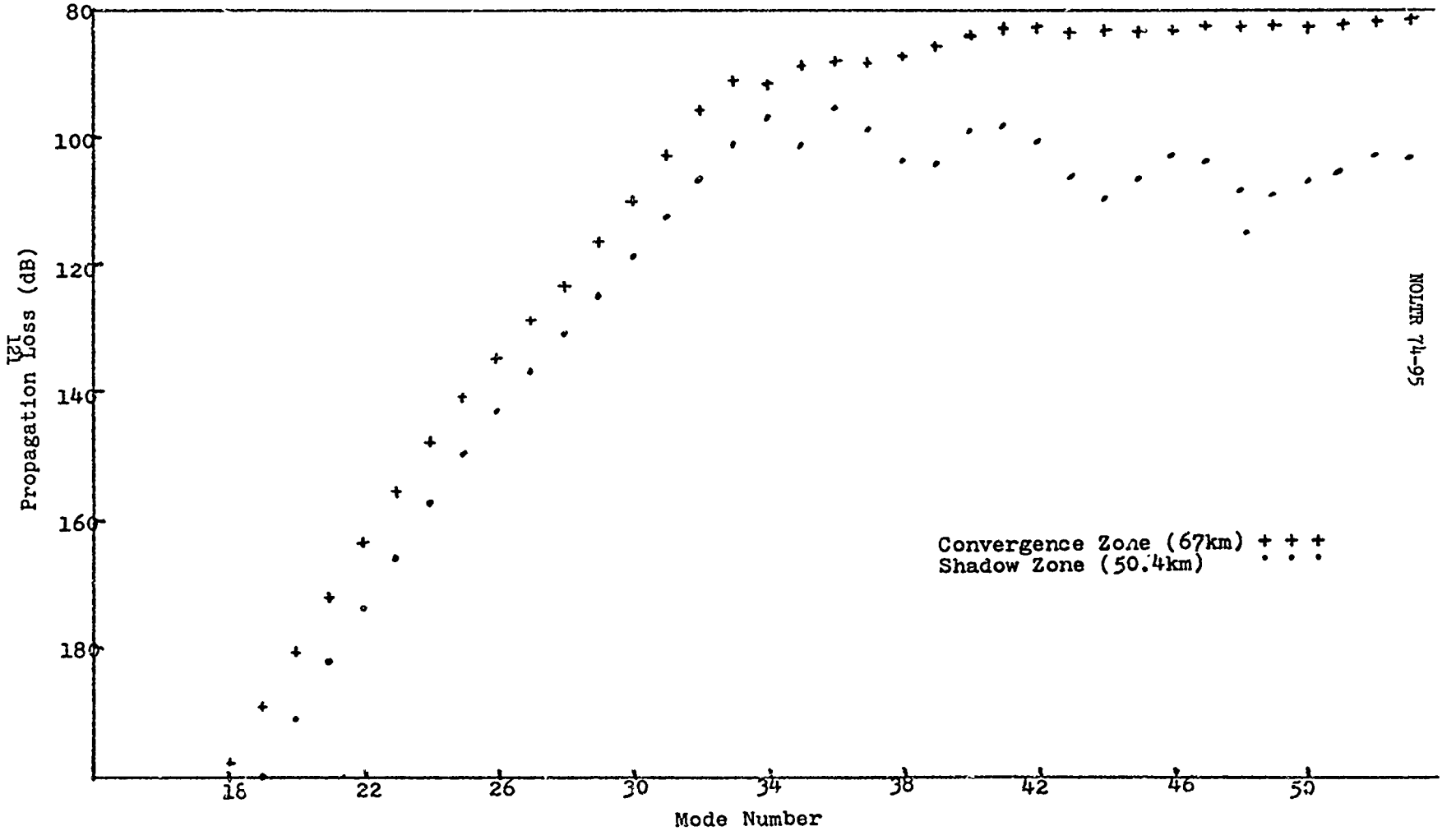

Figure 7.19 Partial Sum of Modes (44km and 57.8km)

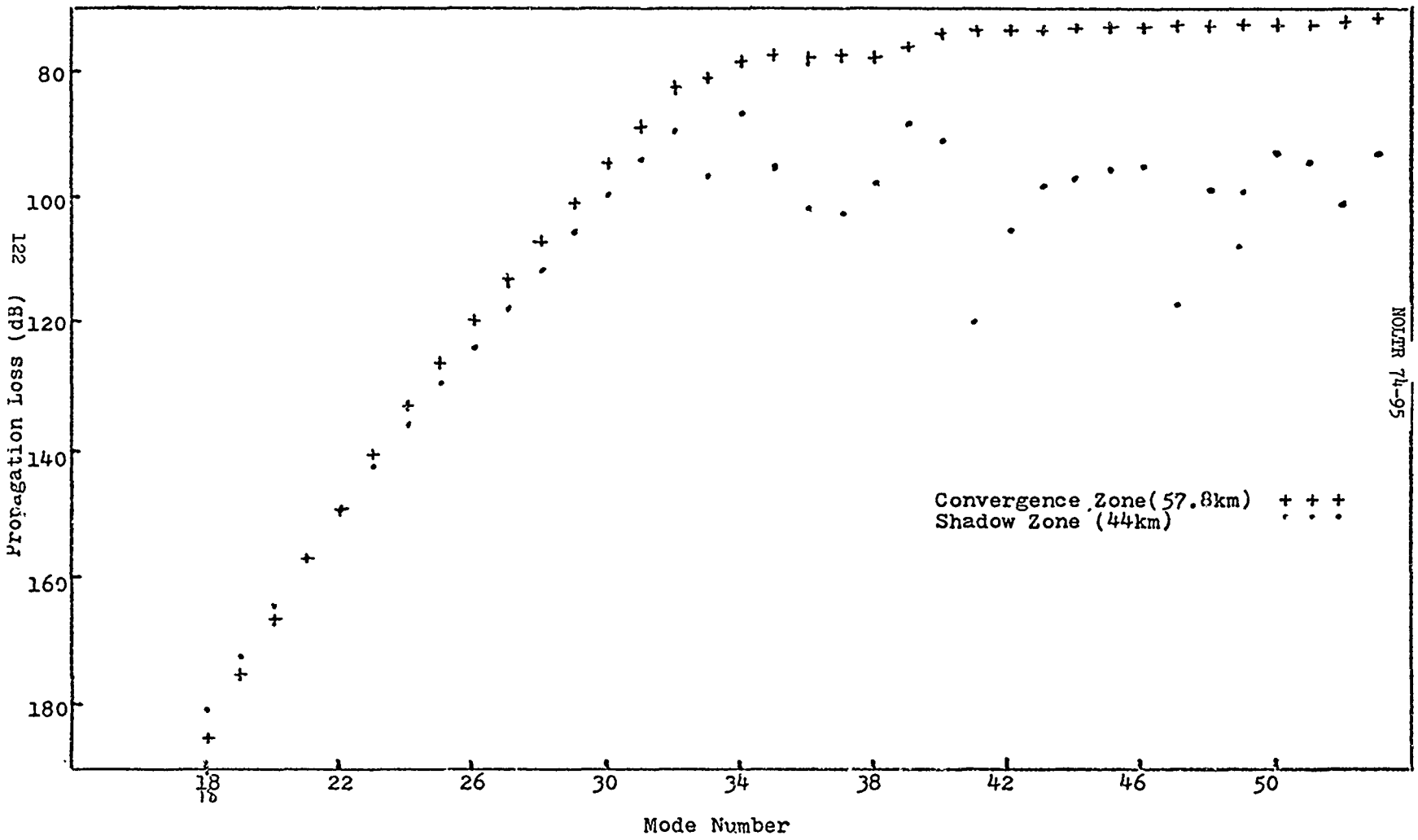

8. Comparisons for Horizontal Caustics

Up to this point we have concerned ourselves with one class of caustics. These we have characterized as vertical (depth to range slope 1:10, $\delta \approx .002$). Now we will examine the caustics we characterize as horizontal (depth to range slope of 1:100, $\delta < .001$). As discussed in Section (4), these are caustics for which a normal expansion off the caustic, such as Ludwig's, would seem more appropriate. However, for some horizontal caustics, a horizontal expansion off the caustic is still possible and convenient. For these, we would like to know how accurate the shadow zone and caustic predictions are.

We originally intended to use an arbitrary velocity profile of 10 to 20 layers in treating this case. However, the complicated ray patterns arising from such profiles tend to interfere with the examination of the horizontal caustics themselves. So we selected a bilinear profile*(Figure 8.1), for which we could separate out the caustic regions more easily. Figure (8.2) shows the ray diagram for this profile and a source depth of 1000 m. The caustics of interest are quite clear. They are summarized in Figure (8.3) for the second convergence zone. There is a cusped caustic (ABC) nested inside the caustic that limits the convergence zone on the left (GH). Table (8.1) sums up the caustic parameters for caustics at two depths, 201 m and 281 m.

*Input sound velocity profile data in Appendix V.

At a depth of 201 m, the caustics are far enough apart so that we can examine the shadow zone for each one individually. Looking at the second convergence zone, Figure (8.4) shows the comparison between normal mode theory and ray theory for a 50 Hz source frequency, and Figure (8.5) shows normal mode and modified ray theory. The first thing we notice in Figure (8.5) is that the intensity falls off more slowly with range into the shadow zone than for the vertical caustics previously considered. For example, for the caustic at 153.5 km in Figure (8.5), the propagation loss has increased 10 dB at a distance of 3500 m into the shadow zone. For a vertical caustic (Figure 6.1), the first 10 dB increase occurs in 1500 m, less than half the distance. This is in line with our description of horizontal caustics as weak caustics, where the energy is spread out over a broader region to either side of it. For both caustics in Figure (8.5), the modified ray calculation in the shadow zone is good for about 2000-4000 m into the shadow zone. For each caustic, the normal mode calculations show a more rapid decrease in intensity with increasing Δr in the shadow zone than does the modified ray prediction. A possible explanation shows the value of a normal caustic expansion. Consider point (M) in Figure (8.3). We have obtained a value for the propagation loss there by horizontal expansion from point (N) to the right. But the caustic point closest to point (M) is point (L), and this is a weaker caustic point than point (N). So a prediction for point (M) based on point (L) would yield a lower intensity, one more in line with the normal mode calculation. We see that one disadvantage of a

horizontal expansion for a horizontal caustic is that we may be fairly close to a much weaker caustic point, and not be taking this into account. But with this caution in mind, we have demonstrated that a smooth, simple caustic, whether horizontal or vertical, can be treated by a horizontal expansion.

Finally, we considered a deeper receiver (281 m), where the shadow zone of one caustic overlaps the single arrival ray region of the previous caustic. Figure (8.6) shows a comparison of ray theory to normal mode theory for this depth. It is typical of the previous cases, with divergent rays near caustics and single arrival regions far enough to the right of each caustic (138 km to 144 km, for example). We then added in modified ray results in each shadow zone and caustic region (Figure 8.7). From 143 km to 147 km, we see an interference pattern resulting from a combination of a real single arrival and the shadow zone contribution from the caustic at 150.5 km. The pattern is similar to that in Figure (7.6), around 64 km, but here the agreement is poor. The oscillation pattern is not quite correct, and the level is too high. This is probably due to an excessively large shadow zone contribution of the type discussed in the previous paragraph. This disagreement demonstrates how modified ray theory results using a horizontal expansion can be incorrect when the point of interest is far enough from the caustic.

Figure 8.1 -Profile III, Bilinear Sound Velocity Profile

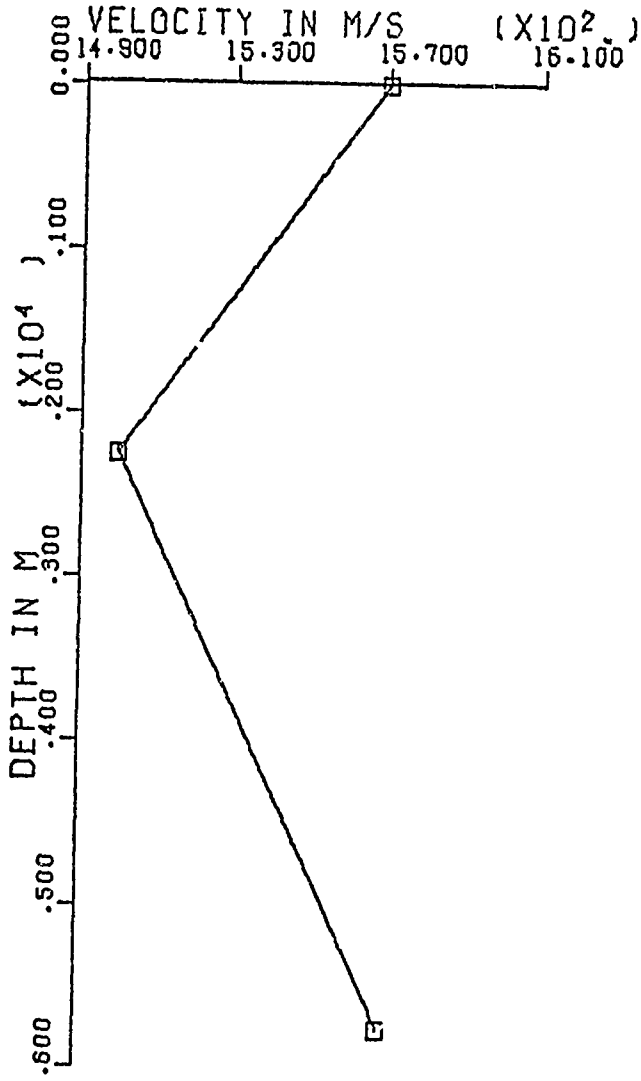

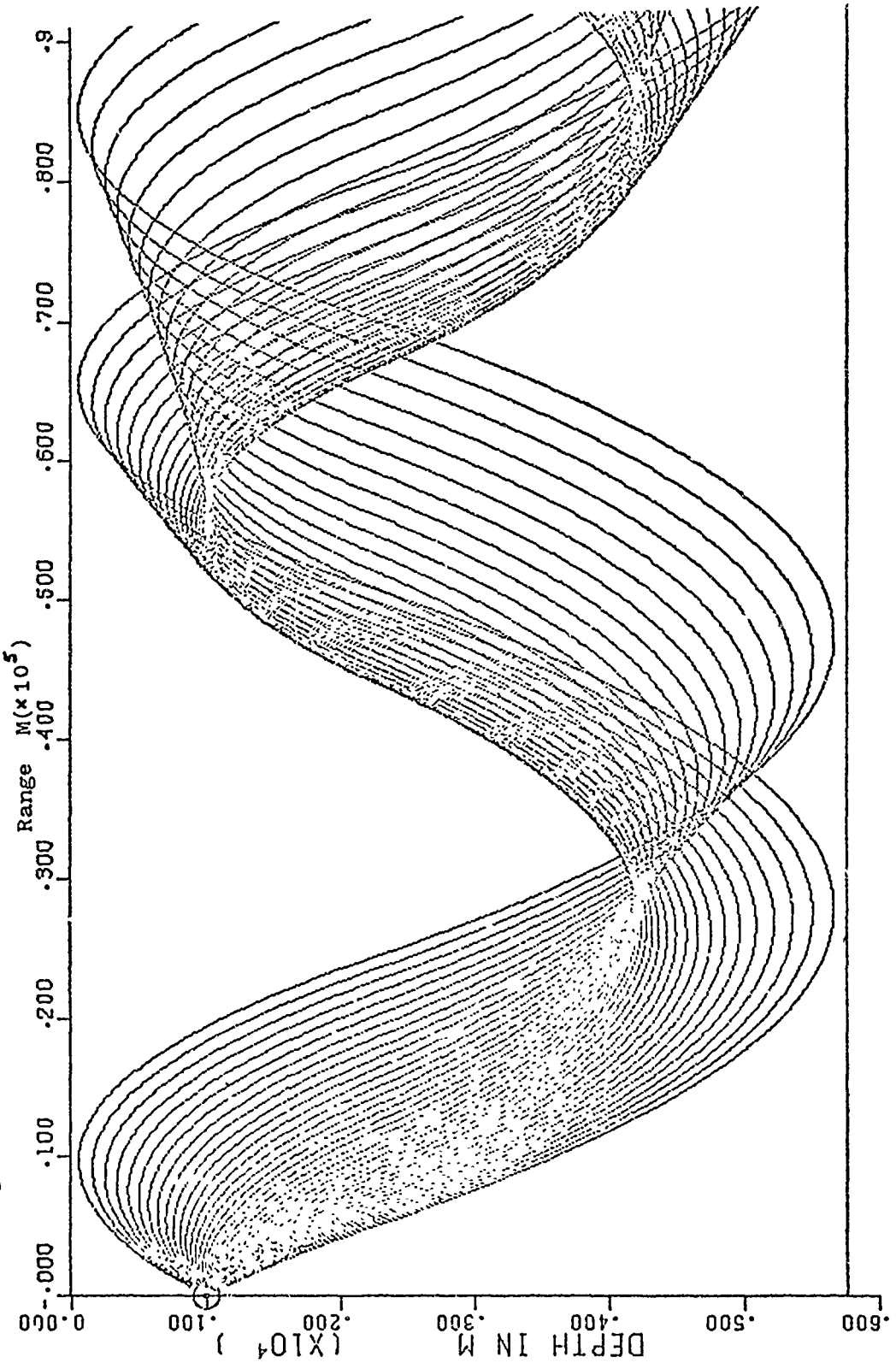

Figure 8.2A Ray Diagram for Profile III, First Convergence Zone

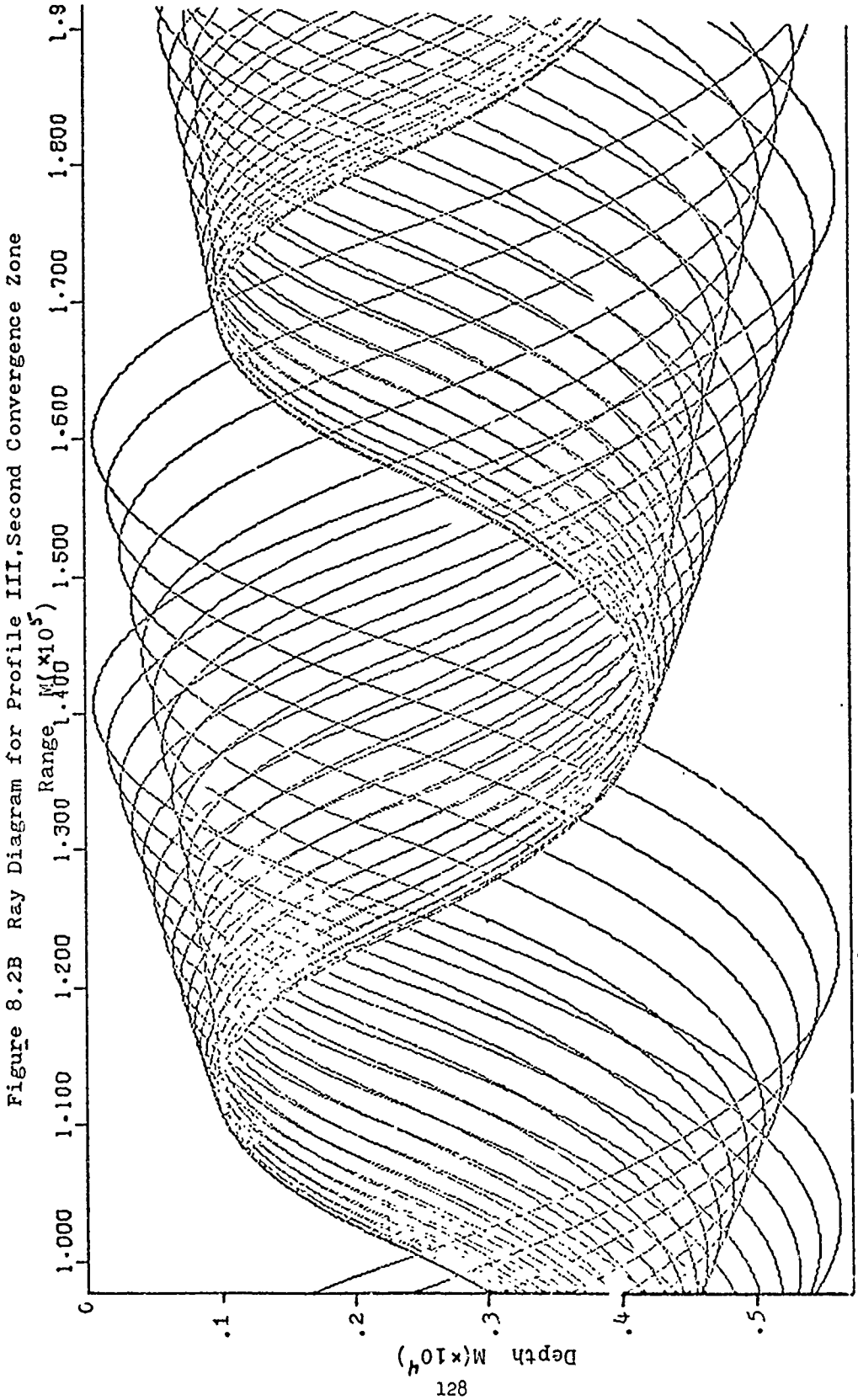

Figure 8.2B Ray Diagram for Profile III, Second Convergence Zone

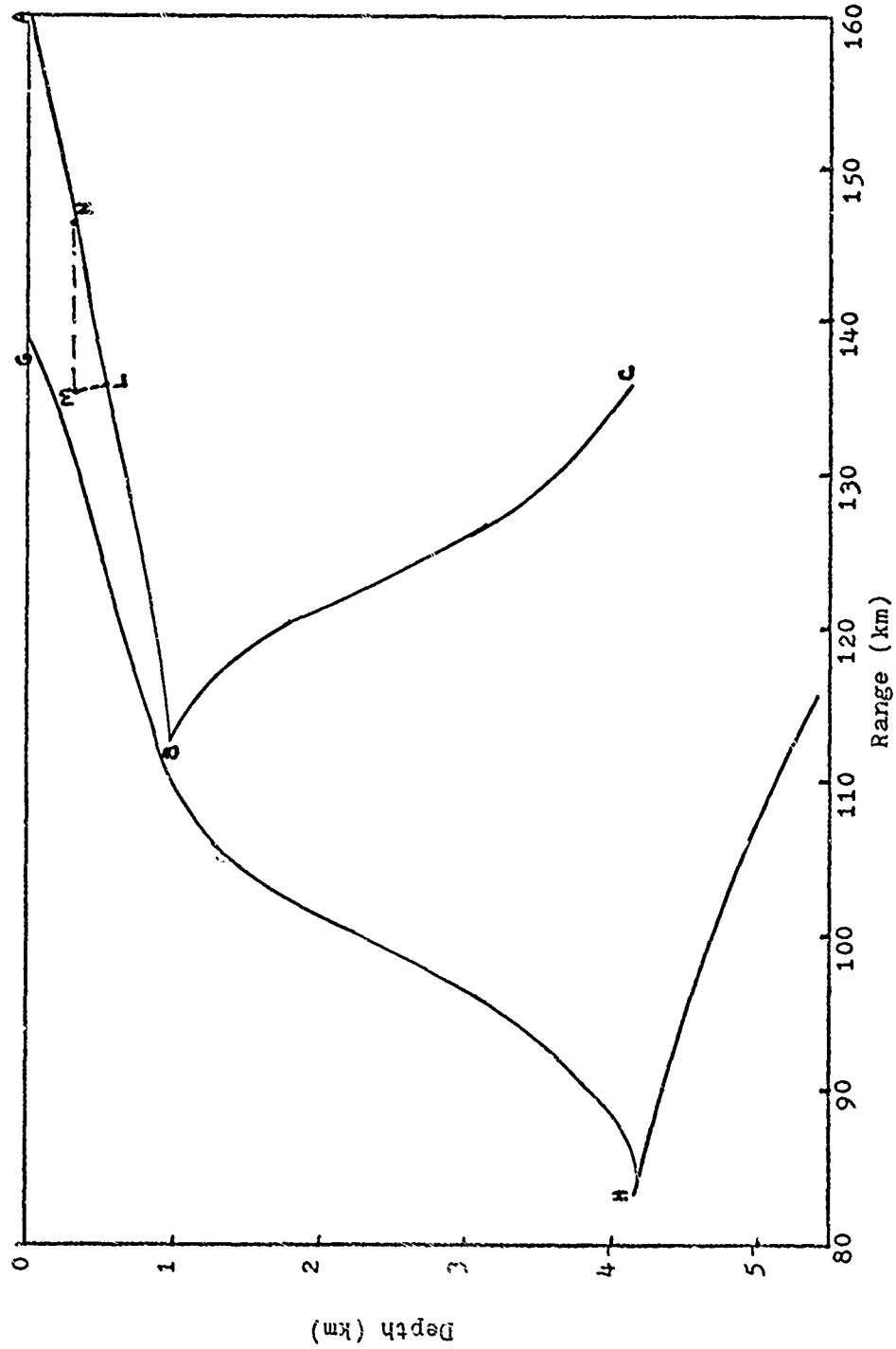

Figure 8.3 Profile III ,Caustics in Second Convergence Zone

Table 8.1: Caustic Summary: Profile III, Second Convergence Zone

Depth=201 m

r_c (m)	θ_o	T_c (sec)	P.L. (dB)	γ	Extra Phase Shift
135455	10.4	89.16	91	.001117	$-\pi$
153540	-10.33	100.85	93	.000815	$-3\pi/2$

Depth=281 m

r_c (m)	θ_o	T_c (sec)	P.L. (dB)	γ	Extra Phase Shift
133075	9.9	87.635	91.8	.001105	$-\pi$
150147	-9.8	98.674	93.7	.000798	$-3\pi/2$

Figure 8.4 Profile III, Normal Mode and Ray Theory (z =201m,f=50Hz)

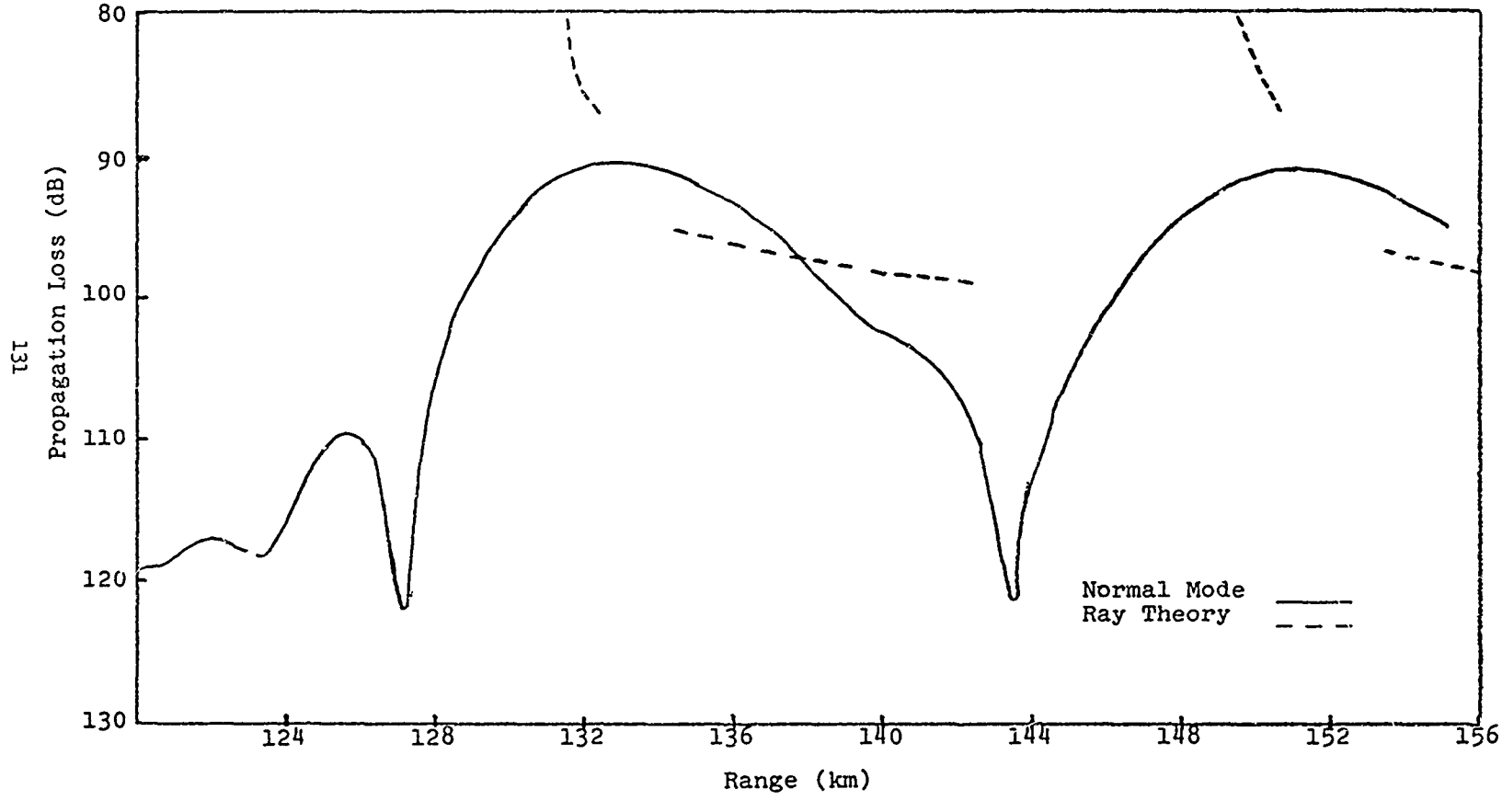

NOLTR 74-95

Figure 8.5 Profile III, Normal Mode and Modified Ray Theory (z =20lm, f=50Hz)

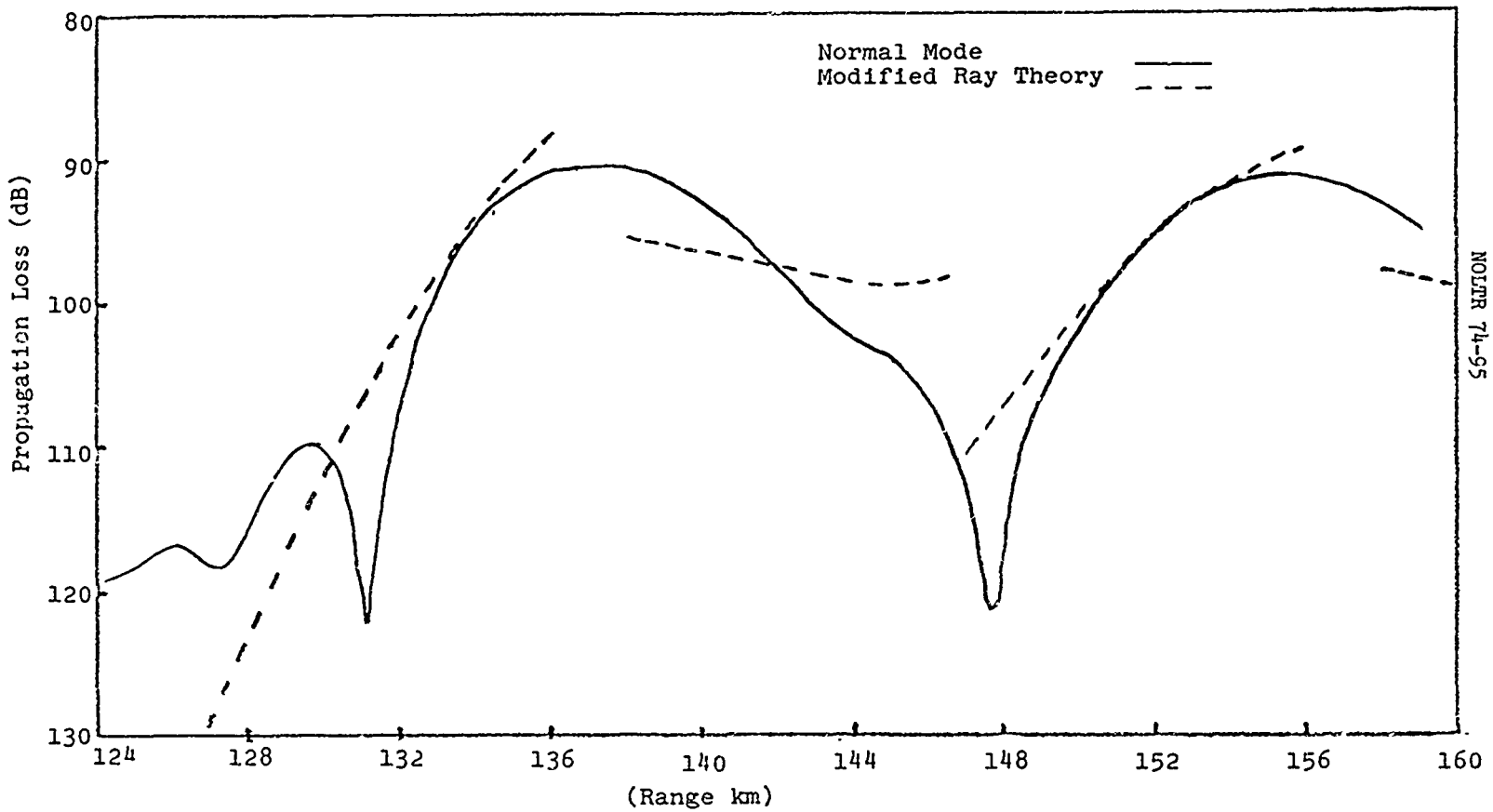

Figure 8.6 Profile III, Normal Mode and Ray Theory (z_s=281m, f=50Hz)

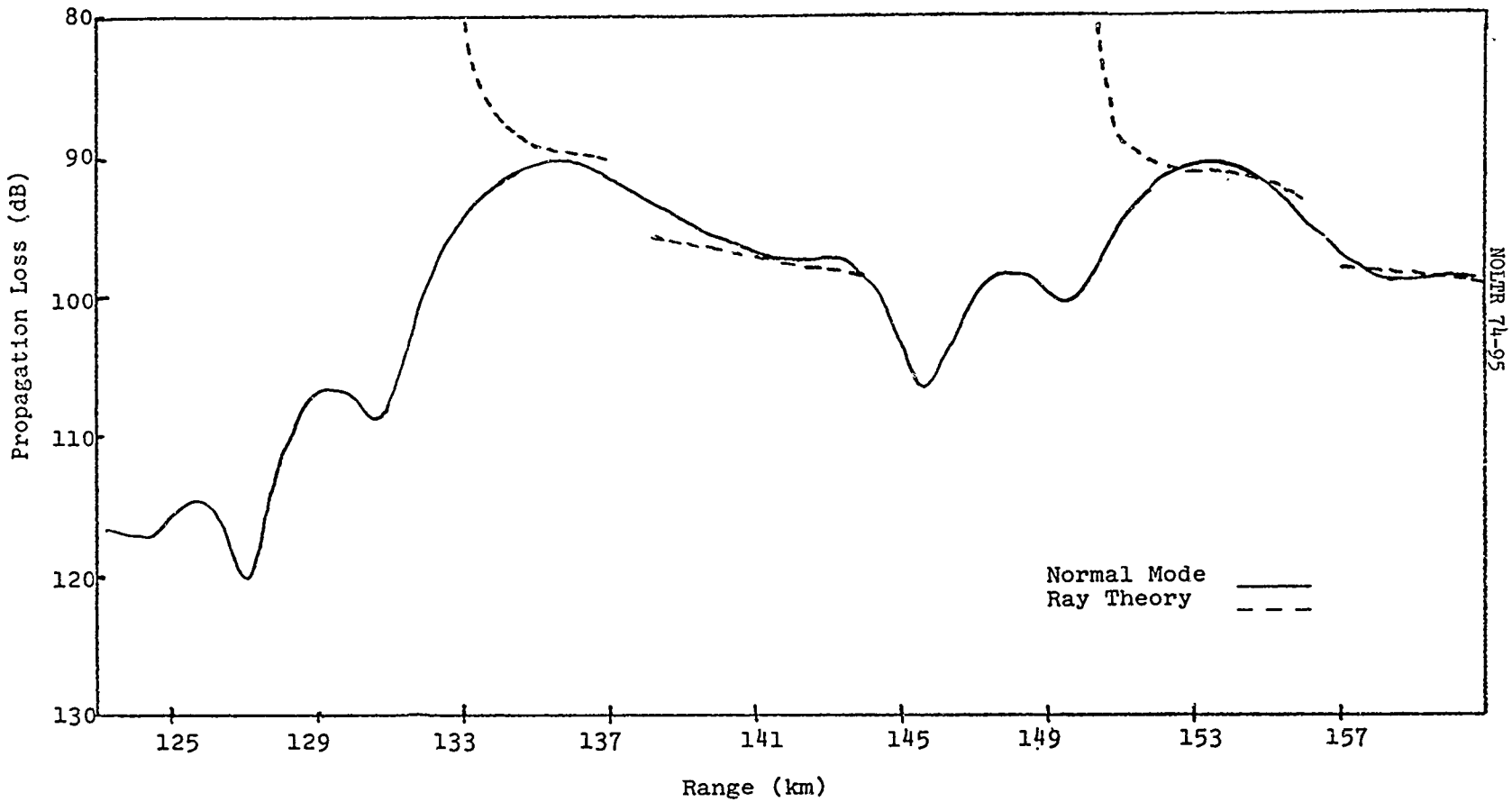

Figure 8.7 Profile III, Normal Mode vs. Modified Ray Theory (z=281m, f=50Hz)

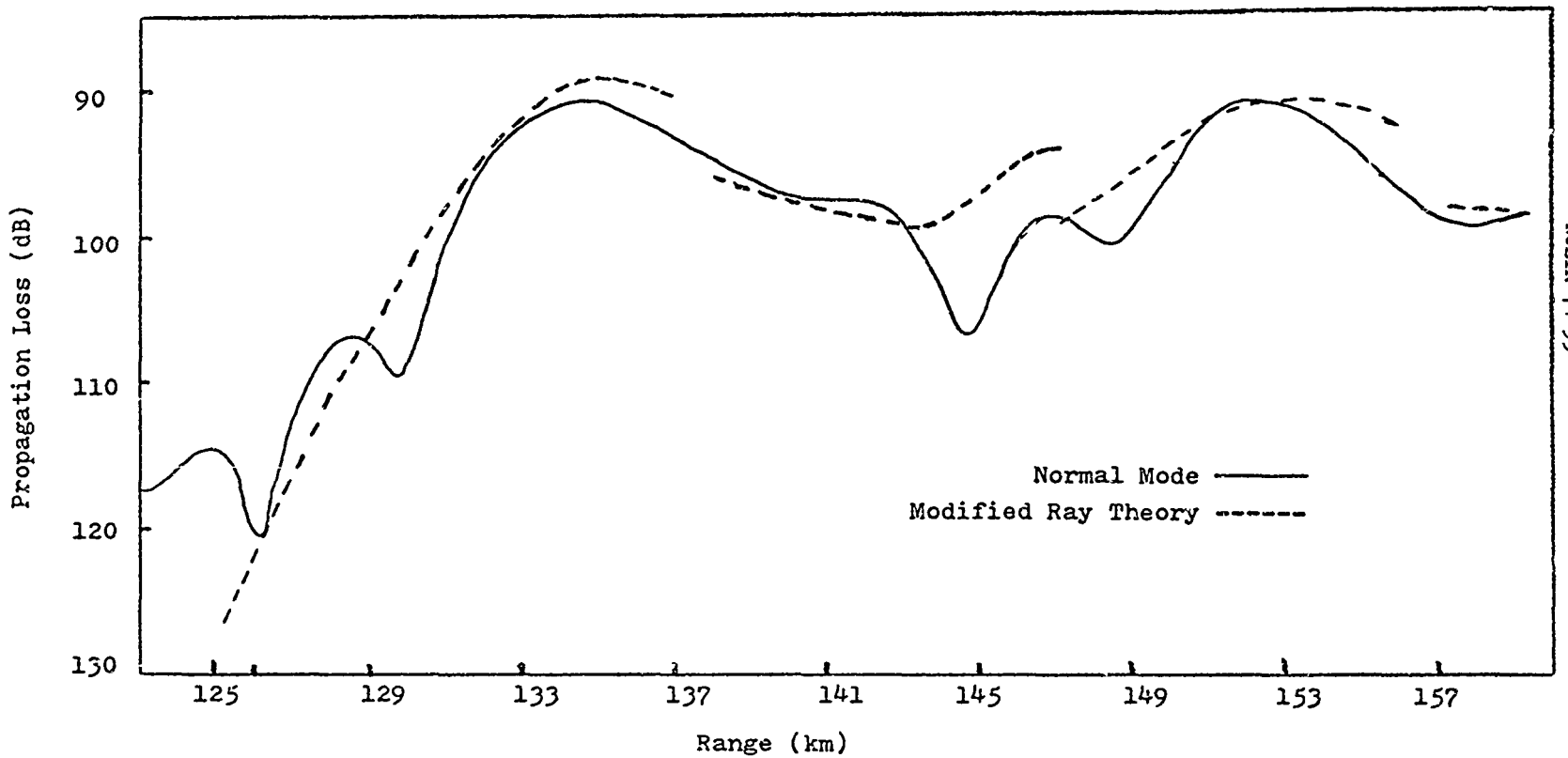

9. Conclusion

The comparisons we have made can be evaluated in several different ways: in terms of the usefulness of the modified ray theory we have applied at caustics, in terms of the validation of a particular normal mode program we have used, or in terms of the general usage of ray theory and normal mode theory. As in every comparison of several theories, this has been an iterative process. Knowledge gained in calculating ray theory curves leads to information about normal mode theory, which in turn leads to information about modified ray theory, and so on. In this way, we feel that knowledge can be gained about each approach that would not become apparent in the consideration of one approach by itself.

It should be noted that what we call modified ray theory (12) has also been termed a caustic boundary layer solution (13), a uniform asymptotic theory (14), and a caustic correction. To further complicate things, there is a completely different derivation termed modified ray theory (51, 52) which is useful when rays turn near boundaries. While this author is comfortable with modified ray theory (it is after all a result of modifying the basic ray equations), perhaps "caustic ray correction" would distinguish derivations intended for use near caustics from more general expressions.

Whatever it is called, we feel that these comparisons have once more demonstrated the usefulness of modified ray theory near caustics. In many cases, the addition of modified ray theory results at caustics to simple ray theory yields a much more satisfying propagation loss vs. range curve when

compared to normal mode theory. The interference between "real" rays and shadow zone contributions from adjacent caustics helps explain many of the oscillations present in normal mode results and absent in simple ray theory results. Thus caustic shadow zone contributions are an important part of the convergence zone intensity picture. For what we characterize as vertical caustics, the horizontal expansion we use works quite well. For horizontal caustics, the expansion can at best be said to give only fair agreement.

For the horizontal caustics, a normal expansion such as Ludwig's (14) or Kratsov's (15) should be better. But in reality, it should take just a coordinate transformation to make Sachs and Silbiger's horizontal expansion equivalent to Ludwig's non-uniform normal expansion. The real value of Ludwig's approach is in its uniform asymptotic theory applications. By uniform asymptotic theory, we mean that for a smooth caustic, one can obtain an expression that is valid everywhere - on the caustic, in the caustic region, and out into the double arrival region. The expression will automatically be identical with ray theory in the double arrival region. Thus, haphazard agreement in the double arrival region can be avoided. While this approach is quite powerful, in practice it is often difficult to take advantage of. In many realistic deep water profiles (as in our Profile II), the bottom cuts off one of the two caustic-related arrivals relatively near the caustic, and the uniform asymptotic theory is equally helpless. In our comparisons at 100 Hz, we barely get one full oscillation in the double arrival region before bottom cutoff of one arrival

occurs. For frequencies of 1 kHz or above (where there are many oscillations over the same range increment), the uniform asymptotic theory would be useful as long as the caustic curvature remained constant (otherwise further modifications would be necessary). However, for frequencies on the order of 100 Hz, and realistic velocity profiles, a non-uniform approach is just as useful. This may be either the horizontal expansion (12, 13) or Ludwig's (14) non-uniform result, since each has its own advantages. In any event, the modified ray theory we have used does work on the caustic. It works well in the caustic region. And for vertical caustics, it accurately predicts the near shadow zone field out to a range where the pressure has dropped some 40 dB from maximum.

As far as normal mode theory is concerned, we feel that Section (5) demonstrates the need for validation of any theory by comparisons. Only this way can apparently accurate calculations be verified. By comparing the normal mode results to ray theory, we verified that the caustics were where they should be, and that the close in direct-surface reflection interference pattern was accurately predicted. So we validated the particular normal mode program being used. Comparisons for idealized profiles with exact solutions (3, 16) are necessary. These standard cases give a good indication of the inherent accuracy of the program or theory under consideration. But comparisons for realistic profiles such as we have dealt with are also necessary to verify a program or theory's behavior for ranges, frequencies, and cases of practical interest.

Thus we feel that an arbitrary profile input - such as allowed in the finite difference normal mode program we use - is desirable for evaluation of realistic cases of interest.

One disadvantage of realistic comparisons is that they often contain a bottom, and we are sometimes interested in minimizing bottom effects to examine other phenomena, such as caustic effects. For this reason, we treated profiles with a matched impedance bottom. This way we eliminated first-order bottom reflections. This did lower the level of bottom reflected energy in the convergence zone, and enabled us to separate out caustic shadow zone effects; but we were still getting abrupt changes in propagation loss where bottom cutoff occurred and also probably getting bottom reflected energy from the gradient mismatch at the bottom. No doubt these effects could be accounted for by a bottom reflection treatment plus a diffraction correction past the critical ray, but we were primarily interested in caustic treatments. In obtaining reality in our comparisons, we sacrificed simplicity. So we were forced to weed out the phenomena of interest from other phenomena equally interesting, but not pertinent to this study.

With all the problems associated with the ray theory results: caustics, bottom reflections, and diffraction corrections for bottom cutoff, the question often arises - why bother at all? Normal mode theory, and other approaches, sum all these effects purely and simply. A cynic might attribute the continuing usage of ray theory to the huge investment in time and energy put into ray tracing programs all over the country. But there are cases and situations where ray theory

is still better than normal mode theory. For shallow water and surface channel calculations, normal mode theory is generally accepted as superior. For deep water profiles, and frequencies on the order of 100 Hz, normal mode and ray theory are roughly equal - even though normal mode theory does include all the effects that must be tacked on in ray theory. At higher frequencies ray effects become more important than wave effects, and ray theory is probably better. Ray theory is far superior as an interpretive tool, indicating in ray diagrams how the energy gets from one place to another. And for some applications, fast ray tracing programs (7) can easily outperform normal mode programs. Ray theory and modified ray theory are especially useful in the treatment of pulses. Because they both have an explicit frequency dependence, one can trace ray paths and caustic locations independent of frequency. Then one can put in the frequency dependence as the arrivals are coherently summed and the total pulse reconstructed by Fourier synthesis (8). This is as opposed to normal mode theory where one has to calculate intensity for each frequency independently. Finally, the need will always remain for well known ray theory calculations with which to compare the new, more complex methods of calculation continually being developed.

References

1. P. G. Frank, P. G. Bergmann, and A. Yaspan, Ray Acoustics, Physics of Sound in the Sea, NRDC Volume 8, Dept. of Navy, Washington, D. C.,1969.

2. C. B. Officer, Introduction to the Theory of Sound Transmission, Chapters 2, 3, McGraw Hill, New York, 1958.

3. I. Tolstoy and C. S. Clay, Ocean Acoustics: Theory and Experiment in Underwater Sound, McGraw Hill, New York, 1966.

4. L. M. Brekhovskikh, Waves in Layered Media, Academic Press, New York, 1960.

5. M. A. Pedersen, Comparison of Experimental and Theoretical Image Interference in Deep Water Acoustics, J. Acoust. Soc. Am., 34, 1197, 1962.

6. H. Weinberg, CONGRATS I, Ray Plotting and Eigenray Generation, Naval Undersea Sound Lab., NUSL Report 1052, 1969.

7. C. Spofford, Fast Asymptotic Coherent Transmission Model, Acoustic Environmental Support Detachment, ONR, Private Communication.

8. I. M. Blatstein, Calculations of Underwater Explosion Pulses at Caustics, J. Acoust. Soc. Am., 49, Number 5 (Part 2), 1568-1579, 1971.

9. R. M. Barash and J. A. Goertner, The Applicability of Underwater Explosion Shock Wave Refraction Data to Oceanic Acoustics Research, Naval Ordnance Lab. NOLTR 71-213, 1971.

10. R. Urick, Observations of the Sound Field in the Deep Sea, Naval Ordnance Lab., NOLTR 67-103, 1967.

11. R. Porter, Dispersion of Axial SOFAR Propagation in the Western Mediterranean, J. Acoust. Soc. Am., 53, 181-190, 1973.

12. L. M. Brekohvskikh, Ref. 4, Chapter VI, Section 38.

13. D. Sachs and A. Silbiger, The Focusing of Harmonic Sound and Transient Pulses in Stratified Media, J. Acoust. Soc. Am., 49, 824-840, 1971.

14. D. Ludwig, Uniform Asymptotic Expansions at a Caustic, Commun. Pure Appl. Math., 19, 215-250, 1966.

15. Yu. A. Kratsov, One Modification of the Geometric Optics Method, Soviet Radiophysics, Vol. 7, No. 4, 104-117, 1964.

16. M. A. Pedersen and D. F. Gordon, Normal Mode and Ray Theory Applied to Underwater Acoustic Condition of Extreme Downward Refraction, J. Acoust. Soc. Am., 51, 323-368, 1972.

17. P. R. Tatro and C. W. Spofford, Underwater Acoustics Models, Proceedings of Ocean '73, IEEE, New York, 1973.

18. M. A. Pedersen and D. F. Gordon, Normal Mode Theory Applied to Short Range Propagation in an Underwater Acoustic Surface Duct, J. Acoust. Soc. Am., 37, 105-118, 1965.

19. Ref. 2, Chapters 2 and 4.

20. Ref. 3, Chapters 3-5.

21. A. O. Williams, Underwater Acoustics, Chapter 2, Edited by R. W. B. Stephens, Wiley Interscience, New York, 1970.

22. A. Newman and F. Ingenito, A Normal Mode Computer Program for Calculating Sound Propagation in Shallow Water with an Arbitrary Velocity Profile, Naval Research Lab., NRL Mem. Report 2381, 1972.

23. C. Bartberger and L. L. Ackler, Normal Mode Solutions and Computer Programs for Underwater Sound Propagation, Naval Air Development Center, NADC Report

24. F. DiNapoli, Acoustic Propagation in a Stratified Medium, Naval Underwater Sound Lab., NUSL Report 1046, 1969.

25. F. DiNapoli, Fast Field Program for Multilayered Media, Naval Underwater Systems Center, NUSC 4103, 1971.

26. I. M. Blatstein, Comparison of Ray Theory and Modified Ray Theory Near a Convergence Zone Caustic, J. Acoust. Soc. Am., 52, 1060-1061, 1972.

27. D. H. Wood, An Example of Uniform Approximation Near a Caustic, Paper 0013, 86th Meeting of the Acoustical Society of America, Los Angeles, California, November 2, 1973.

28. R. M. Barash and J. A. Goertner, Refraction of Underwater Explosion Shock Waves: Pressure Histories Measured at Caustics in a Flooded Quarry, Naval Ordnance Lab., NOLTR 67-9, 1967.

29. I. M. Blatstein, Refraction of Underwater Explosion Shock Waves. A Method for Prediction of Pressures at Caustics, Naval Ordnance Lab., NOLTR 69-181, 1970.

30. I. M. Blatstein, Refraction of Underwater Explosion Shock Waves. Calculations of Pressure Histories in a Convergence Zone, Naval Ordnance Lab., NOLTR 71-93, 1971.

31. H. Weinberg, Continuous-Gradient Curve-Fitting Technique for Acoustic Ray Analysis, J. Acoust. Soc. Am., 51, 975-984, 1971.

32. A. Silbiger, Focusing of Sound and Explosive Pulses in the Ocean, Cambridge Acoustical Assoc., TR U-286-188, June 1968.

33. Ref. 32, Equation 19.

34. Ref. 22, Page 2.

35. M. A. Pedersen, Acoustic Intensity Anomalies Introduced by Constant Velocity Gradients, J. Acoust. Soc. Am., 33, 465-474, 1961.

36. Ref. 2, Page 50.

37. Ref. 1, Page 44.

38. Ref. 8, Appendix A

39. H. Weinberg, A Continuous Gradient Ray Tracing Technique, Naval Underwater Systems Center, Rpt. No. 829, 1967.

40. Ref. 32, Equation 29.

41. Ref. 3, Chapter 4.

42. Ref. 22, Pages 5 and 6.

43. Ref. 22, Equation 15.

44. R. Ferris and F. Ingenito, Experimental Separation and Identification of Acoustic Normal Modes in Shallow Water, Naval Research Lab., NRL Report 7174, 1970.

45. R. M. Barash, Evidence of Phase Shifts at Caustics, J. Acoust. Soc. Am., 43, 378(1), 1968.

46. A. Silbiger, Phase Shifts at Caustics and Turning Points, J. Acoust. Soc. Am., 44, 653(L), 1968.

47. Ref. 16, Pages 333-334, 338-339.

48. Mathews and Walker, Mathematical Methods of Physics, W. A. Benjamin Inc., New York, 1965.

49. D. Sachs, Domain of Validity of High Frequency Methods Used in Wave Propagation Problems, Cambridge Acoustical Assoc., Report U-404-228, 1973.

50. Ref. 32, Page 13.

51. E. L. Murphy, Modified Ray Theory for the Two-Turning Point Problem, J. Acoust. Soc. Am., 47, 899-908, 1970.

52. J. A. Davis and E. L. Murphy, Modified Ray Theory in the Presence of a Boundary, Paper presented at Eighty-First Meeting of the Acoustical Society of America, Washington, D. C., April 1971.

53. Ref. 4, Section 21.

Appendix I: Program RAYTRV Listing
(Coherent Ray Sorting Program)

PROGRAM RAYTRV CDC 6400 FTN V3.0-

```
      PROGRAM RAYTRV(INPUT,OUTPUT,TAPE2)
      COMPLEX SUM(100),DUM
      DIMENSION IRD(100,2)
      DIMENSION TARGET( 110,3),SP(210,2),RP(210,2),VP0(210,
     5
      DIMENSION TEST(8),TEST1(8),BUFFER(9,800),IBFR(9,800)
      EQUIVALENCE(BUFFER,IBFR)


C     TAPE2 IS OUTPUT OF CONGRATS
C     NCASE EQUALS THE NUMBER OF PROCESS CARDS IN CONGRATS
C     NCASE IS THE NUMBER OF CASES TO BE PROCESSED
C        IPRN.GT. 0 MEANS PRINT OUT DATA
C     IPROC.GT. 0 MEANS ADD ARRIVALS COHERENTLY
C     ISHDAR=N.GT. 0 MEANS N SHADOW ZONE ARRIVALS
C          ARE TO BE READ IN
      CARD READ STATEMENTS - LINES 18, 23, 26, 27, 115
      READ 976,NCASE
  976 FORMAT(I5)
        DO 1820 NCA=1,NCASE
      NSTOP=0
      NSTART=-99
      READ 975,IPRN,IPROC,ISHDAR
      NARRIV=0
  975 FORMAT(3I5)
      READ 1000,(TEST(J),J=1,8)
      READ 1000,(TEST1(J),J=1,8)
 1000 FORMAT(8A10)
      READ (2)(TARGET(I),I=1, 330)
      READ (2)(SP(I),I=1,420)
      READ (2)(RP(I),I=1,420)
      READ(2)(VP0(I),I=1,1260)
      READ(2)
      IF(EOF(2).NE.0.) GO TO 100
   90   STOP 5
  100   NSTOP=NSTOP+100
      NSTART=NSTART+100
      READ(2)((BUFFER(I,J),I=2,9),J=NSTART,NSTOP)
      DO 1001 JK=NSTART,NSTOP
      IF(IBFR(2,JK).EQ.0) GO TO 101
 1001 CONTINUE
      IF(NSTOP.NE.800) GO TO 100
      STOP 7
  101 NRT=IFIX(TARGET( 110,1))
      NZT=IFIX(TARGET( 110,2))
      NARRIV=       JK-1
      IF(NARRIV.LE.0) GO TO  1820
      IF(IPRN.LE.0) GO TO 725
      PRINT 200
  200 FORMAT(1H1,40X,16HCONGRATS RESULTS,////,20X,
     1 34HINPUT INFORMATION USED IN FINDING ,//,20X,
     2 37HRAYS PASSING THROUGH SPECIFIED TARGET,//,20X,
     3   17HRANGES AND DEPTHS)
      PRINT 275,TARGET( 109,1),TARGET( 109,2),TARGET( 109,3)
  275 FORMAT(///,5X,21HSOURCE RANGE IN KYDS=,E15.8,5X,
```

```
 PROGRAM      RAYTRV                                  CDC 6400 FTN V3.0-P316 OP

                1  21HSOURCE DEPTH IN KYDS=,E15.8,5X,
                2   26HSOURCE VELOCITY IN KYDS/S=,E15.8)
                  PRINT 300,TARGET(NZT+2,2),TARGET(NZT+2,3)
              300 FORMAT(///,46X,22HSURFACE DEPTH IN KYDS=,E15.8,5X,
60       60     1   27HSURFACE VELOCITY IN KYDS/S=,E20.8)
                  PRINT 350,TARGET(NZT+1,2),TARGET(NZT+1,3)
              350  FORMAT(///,46X,21HBOTTOM DEPTH IN KYDS=,E15.8,5X,
                1   26HBOTTOM VELOCITY IN KYDS/S=,E20.8)
                  IF(TARGET( 108,3).LE.0.) GO TO 3690
65                PRINT 375,TARGET( 108,3),TARGET( 108,1)
              375 FORMAT(///,35X,17HFREQUENCY(RAD/S)=,E20.8,5X,
                1  22HATTENUATION IN DB/KYD=,E20.8)
             3690    NVP0=IFIX(VP0(210,1))
             3700  PRINT 3702
70           3702 FORMAT(///,45X,28HCONGRATS VELOCITY PARAMETERS,
                1    / 45X 26H----------------------------,
                2  //,6H LAYER,7X,6HZ0-KYD,12X,8HV0-KYD/S,14X,2HG0,17X,2HG1,
                417X,   2HG2,14X,7HV-KYD/S//)
                  PRINT 3712,(N,(VP0(N,J),J=1,6),N=1,NVP0)
75           3712  FORMAT(I4,1P6E19.8)
                  PRINT 400
              400  FORMAT(///,50X,21HTARGET DEPTHS IN KYDS)
                  PRINT 500,(TARGET(I,2),I=1,NZT)
              500  FORMAT(1H ,6E20.8)
80       80       PRINT 550
              550   FORMAT(///,50X,21HTARGET RANGES IN KYDS)
                  PRINT 500,(TARGET(I,1),I=1,NRT)
                  PRINT 700
              700 FORMAT(/////, 40X,22HCOLLECTION OF ARRIVALS)
85            725  DO 1350 J=1,NZT
             1350  TARGET(J,2)=TARGET(J,2)/TARGET( 104,2)
                  DO 1360 J=1,NRT
             1360  TARGET(J,1)=TARGET(J,1)/TARGET( 104,1)
                  DO 1370 J=1,NARRIV
90                 BUFFER(3,J)=BUFFER(3,J)/(1.74532925E-2)
             1370   BUFFER(4,J)=BUFFER(4,J)/(1.74532925E-2)
                   IF(ISHOAR.LE.0) GO TO 740


95
                C   ALL QUANTITIES READ IN HERE ARE IN ORIGINAL UNITS
                C          SAME UNITS AS FEED INTO CONGRATS
                C      ZC IS DEPTH OF INTEREST
                C       RC IS CAUSTIC RANGE AT DEPTH ZC
100      100    C  ***********************************
                C    MAKE ZC,RC BOTH SAME UNITS
                C   EITHER METERS,FEET,YDS,ETC

                C  ***********************************
105             C      THETA0 IS INITIAL ANGLE(IN DEG) OF RAY GOING THROUGH CAUSTIC
                C      TC IS TRAVEL TIME TO CAUSTIC
                C      AMPRD IS PROP. LOSS TO CAUSTIC IN DB
                C     PS IS ANY ADDITIONAL PHASE SHIFT-DUE TO SURFACE,ETC.
                C       W1 IS THIRD DERIVATIVE OF W NEEDED IN AIRY FUNCTION
110             C      ISIGN IS SIGN OF THIRD DERIVATIVE--+1 OR -1
```

```
   PROGRAM      RAYTRV                                  CDC 6400 FTN V3.0-P316 OP

                      C2=TARGET(109,3)/TARGET(104,1)
                      AK=TARGET(108,3)/C2
                      AIO=AI(0.)
                      DO 2990 IF=1,ISHOAR
 110        115       READ 2010,THEAT0,ZC,RC,TC,AMPDB,W1,PS,ISIGN
           2010 FORMAT(7E10.3,I2)
                      XIC=COS(THEAT0*1.74532925E-2)
                     DO 2900 IF2=1,NZT
                      IF(ABS(TARGET(IF2,2)-ZC).GE..00001) GO TO 2900
 120                  DO 2899 IF1=1,NRT
                      DELR=TARGET(IF1,1)-RC
                      RHO=(AK**(.6667))*W1*DELR*ISIGN
                      IF(RHO.LE. 0. ) GO TO 2899
                      NARRIV=NARRIV+1
 125                  IF(NARRIV.LE.800) GO TO 2200
                     STOP 4
           2200       BUFFER(6,NARRIV)=AMPDB-20.*ALOG10(ABS(AI(RHO))/AIO)
                      BUFFER(5,NARRIV)=TC+XIC*DELR/C2
                      BUFFER(7,NARRIV)=TARGET(108,3)*BUFFER(5,NARRIV)-.78539816+P
 130                  IBFR(8,NARRIV)=IF1
                      IBFR(2,NARRIV)=IF2
                      BUFFER(3,NARRIV)=0.
                      BUFFER(4,NARRIV)=0.
                      IBFR(9,NARRIV)=99999
 135        2899      CONTINUE
            2900     CONTINUE
            2990     CONTINUE


 140        140
             740      DO 750 I=1,NARRIV
             750     IBFR(1,I)=100*IBFR(2,I)+IBFR(8,I)
                       J=9*NARRIV
                     CALL COMSOT(IBFR,J,9,0,1,1)
 145                 IF(IPRN.LE.0) GO TO 1400
                     PRINT 1200
            1200 FORMAT(1H-,3X,12HTARGET DEPTH,15H TARGET RANGE  ,
                1 15H INITIAL ANGLE ,15H  FINAL ANGLE  ,15H  TRAVEL TIME  ,
                2  15H   PROP. LOSS   ,15H     PHASE
 150            3  15H  PHASE SHIFT ,10HNO. OF REV)
                  PRINT 1250,(TEST(J),J=1,4),(TEST1(L),L=1,4)
            1250  FORMAT(1H ,12A10)
                   DO 1390 J=1,NARRIV
                    PS=BUFFER(7,J)-TARGET(108,3)*BUFFER(5,J)
 155           1390  PRINT 1395,TARGET(IBFR(2,J),2),TARGET(IBFR(8,J),1),
                1  (BUFFER(I,J),I=3,7),PS,IBFR(9,J)
            1395  FORMAT(8E15.8,I10)
            1400   IF(IPROC.LE.0) GO TO 1820
                  DO 1420 J=1,100
 160           1420  SUM(J)=CMPLX(0.,0.)
                  J=0
                  IC=0
                    IZT=0
                1455  IZT=IZT+1
 165        165 1460   IRT=1
```

```
   PROGRAM      RAYTRV                                   CDC 6400 FTN V3.0-P316 OPT:

              1465  IC=IC+1
              1475     J=J+1
                    IF(J.GT.NARRIV) GO TO 1700
                    IF(IRFR(2,J).NE.I7T) GO TO 1600
170       170       IF(IRFR(8,J).NE.IRT) GO TO 1590


              C------THIS  FLAGS BOTTOM( OR SURFACE) BOUNCES WHEN LOSS
              C----------IN CONGRATS IS SET TO 9.E+03 OR SO ONE
175           C--------CAN DELETE THEM FROM THE SUM OF ARRIVALS
                 ---  - -  - - -    - -  - -- -- -  -    --
                 - - -    - -  - - -  - -      -- ------   -
                 -    - -  ----- - --  -          - - - -
                 --- - -  ---------  -- - -            ----
180                -- --- ------  ---   --          R  -  --
                                                      - --  ---

              1477    CONTINUE
                       IF(BUFFER(6,J).GE.9.E+03) GO TO 1485
185


                    AMP=10.**(-(BUFFER(6,J)/20.))
                    PH=                BUFFER(7,J)
                    RE=AMP*COS(PH)
190                 AIG=AMP*SIN(PH)
                      DUM=CMPLX(RE,AIG)
                      GO TO 1490
              1485    DUM=CMPLX(0.,0.)
              1490    SUM(IC)=SUM(IC)+DUM
195       195       IRD(IC,1)=I7T
                    IRD(IC,2)=IRT
                    GO TO 1475
              1590   IF(IRT.EQ.NRT) GO TO 1455
                    IRT=IRT+1
200                 J=J-1
                    GO TO 1465
              1600   J=J-1
                    GO TO 1455
              1700     PRINT 1750
205                 PRINT 1760 ,TEST(1),TEST(2),TEST(3)
                    DO 1800 IJ=1,IC
                   IF((REAL(SUM(IJ)).EQ.0.).AND.(AIMAG(SUM(IJ)).EQ.0.)) GO TO 180
              2100  FORMAT(I10,4E15.7)
                    Y=CABS(SUM(IJ))
210                 Y1=REAL(SUM(IJ))
                    Y2=AIMAG(SUM(IJ))
                    P1=ATAN2(Y2,Y1)
                     DB=-20.*ALOG10(Y)
                    GO TO 1799
215           1750 FORMAT(////,30X,27HRESULTANT AT TARGET POINTS,//,
                  1   3X,12HTARGET DEPTH,4X,15HTARGET RANGE    ,6X,
                  2    19HRESULTANT AMPLITUDE,10X,5HPHASE)
              1760 FORMAT(/,3A10,7X,3HPSI,12X,2HDB,12X,3HRAD)
              1770   Y=99999.
220       220       DB=99999.
```

```
PROGRAM      RAYTRV                                    CDC 6400 FTN V3.0-P316

                    P1=0.
                1799  PRINT 1810,TARGET(IRD(IJ,1),2),TARGET(IRD(IJ,2),1),Y,DB,P
                1800    CONTINUE
                 1810  FORMAT(/,5E15.7)
225       225    1820   CONTINUE
                       END
```

CONGRATS RESULTS

INPUT INFORMATION USED IN FINDING
RAYS PASSING THROUGH SPECIFIED TARGET
RANGES AND DEPTHS

SOURCE RANGE IN KYDS= 0. SOURCE DEPTH IN KYDS= .33333267E+00 SOURCE VELOCITY IN KYDS/S= .16650010E+01

SURFACE DEPTH IN KYDS= 0. SURFACE VELOCITY IN KYDS/S= .16669914E+01

BOTTOM DEPTH IN KYDS= .49999900E+01 BOTTOM VELOCITY IN KYDS/S= .16813396E+01

FREQUENCY(RAD/S)= .31415927E+03 ATTENUATION IN DB/KYD= 0.

CONGRATS VELOCITY PARAMETERS

LAYER	Z0-KYD	V0-KYD/S	G0	G1	G2	V-KYD/S
1	0.	3.59159758E-01	2.57812022E-03	-4.61720756E-06	-3.58197922E-09	1.66699141E+00
2	4.99994999E-01	3.61154224E-01	2.25772516E-02	-3.52851408E-04	-3.12572508E-02	1.66400586E+00
3	7.49998499E-01	3.66053396E-01	3.79887574E-02	-9.83435351E-04	-5.17750734E-02	1.65100282E+00
4	9.33331466E-01	3.73729419E-01	1.21793170E-02	-9.91739657E-05	-1.42856248E-02	1.63533137E+00
5	1.13331919E+00	3.76379552E-01	6.06049120E-05	-2.43968521E-09	-8.65111375E-05	1.63000549E+00
6	1.29999755E+00	3.76389053E-01	-1.97757499E-03	-2.59766605E-06	2.42705934E-03	1.62998362E+00
7	1.41466343E+00	3.75766559E-01	-6.67599970E-03	-2.98304172E-05	8.09992538E-03	1.63133969E+00
8	2.16666233E+00	3.72104663E-01	-5.95099898E-03	-2.37932987E-05	7.09640473E-03	1.63933399E+00
9	3.46665933E+00	3.63332656E-01	-7.33983865E-03	-3.70684391E-05	1.01006142E-02	1.65899712E+00
10	4.99998999E+00	3.53749031E-01	-7.33983865E-03	-3.70684391E-05	1.01006142E-02	1.68133959E+00

TARGET DEPTHS IN KYDS

.16404167E+01

TARGET RANGES IN KYDS

.65514667E+02	.65885389E+02	.66054111E+02	.66272833E+02	.66491555E+02	.66710278E+02
.67147722E+02	.67366444E+02	.67585167E+02	.67803889E+02	.68022611E+02	
.68241333E+02	.68460055E+02	.68678778E+02	.68897500E+02	.69116222E+02	.69334944E+02
.69553667E+02	.69772389E+02	.69991111E+02	.70209833E+02	.70428555E+02	.70647278E+02
.70865000E+02	.71014722E+02	.71303444E+02	.71522167E+02	.71740889E+02	.71959611E+02
.72178333E+02	.72397055E+02	.72615778E+02	.72834500E+02	.73053222E+02	.73271944E+02
.73490667E+02	.73709389E+02	.73928111E+02	.74146833E+02	.74365555E+02	.74584278E+02
.74803000E+02	.75021722E+02	.75240444E+02	.75459167E+02	.75677889E+02	.75896611E+02
.76115333E+02	.76334055E+02	.76552778E+02			

COLLECTION OF ARRIVALS

Arrivals with 99999 in Last Column Are Shadow Zone Arrivals from Appropriate Caustics

TARGET DEPTH M	TARGET RANGE KM	INITIAL ANGLE DEG	FINAL ANGLE DEG	TRAVEL TIME SEC	PROP. LOSS DB	PHASE RAD	PHASE SHIFT RAD	NO. OF REV
.150000C0JE+04	.6?0000000E+05	-.9?533?41E+01	.14583452E+02	.40322702E+04	.90986720E+04	.12661467E+05	-.62831853E+01	3
.1500010C0E+04	.6?0000000E+05	-.437?6148E+11	-.12274442E+02	.39932399E+02	.93487428E+02	.12540?21E+05	-.47123890E+01	2
.1500000?0E+04	.6?0000000E+05	-.557283?7E+00	-.11494456E+02	.39921313E+02	.96688946E+02	.12540080E+05	-.157?7963E+01	2
.1500?C0J?+04	.6?0000000E+05	.8540?863E+01	.14274944E+02	.40263116E+02	.90997223E+04	.12645840E+05	-.31415927E+01	2
.1500?0?0?+04	.6?0?00000E+05	0.	0.	.4016?883E+02	.12564617E+03	.12617385E+05	-.78539816E+00	99999
.1500?0?00?+04	.6?2?0?0?0E+05	-.902530?6E+01	.14566?05E+02	.40452?35E+02	.90987787E+04	.12702?24E+05	-.62831853E+01	3
.1500?0?0?+04	.6?2?0?0?0E+05	-.4?945??0E+01	-.1224791?E+02	.40063?89E+02	.93870?15E+02	.12581?72E+05	-.47123890E+01	2
.1500?0?0?+04	.6?2?0?0?0E+05	-.5?255?56E+00	-.11496196E+02	.40052671E+02	.96709134E+02	.12581?47E+05	-.157?7963E+01	2
.1500?C0?0+ 4	.6?2?0?0?0E+05	.8?165?8?E+01	.14262086E+02	.40393028E+02	.90998?08E+04	.12686?02E+05	-.31415927E+01	2
.1500?0?0?+04	.6?2?0?0?0E+05	0.	0.	.40294236E+02	.12536173E+03	.12658651E+05	-.78539816E+00	99999
.1500?0?0?+04	.6?4?0?0?0E+05	-.89974144E+01	.14549274E+02	.40582179E+02	.90988897E+04	.12742?84E+05	-.62831853E+01	3
.1500?0?0?+04	.6?4?0?0?0E+05	-.442?5271E+01	-.12223535E+02	.40196391E+02	.94076592E+02	.12622?85E+05	-.47123890E+01	2
.1500?0?0?+04	.6?4?0?0?0E+05	-.6473?142E+00	-.11498018E+02	.40184029E+02	.96793679E+02	.12622514E+05	-.157?7963E+01	2
.1500?0?0?+04	.6?4?0?0?0E+05	.8?9719?4E+01	.14249491E+02	.40522947E+02	.90999443E+04	.12727?18E+05	-.31415927E+01	2
.1500?0?0?+04	.6?4?0?0?0E+05	0.	0.	.40427589E+02	.12507820E+03	.12699?16E+05	-.78539816E+00	99999
.1500?0?0?+04	.6?6?0?0?0E+05	-.8?701120E+01	.14532633E+02	.40711932E+02	.90988990E+04	.12783?47E+05	-.62831853E+01	3
.1500?0?0?+04	.6?6?0?0?0E+05	-.4156?111E+01	-.12200851E+02	.40325404E+02	.94279?30E+02	.12663087E+05	-.47123890E+01	2
.1500?0?0?+04	.6?6?0?0?0E+05	-.6?1?42?1E+00	-.11499924E+02	.40316365E+02	.96880596E+02	.12663?81E+05	-.157?7963E+01	2
.1500?0?0?+04	.6?6?0?0?0E+05	.8?7?2343E+01	.14237173E+02	.40652873E+02	.90999548E+04	.12768335E+05	-.31415927E+01	2
.1500?0?0?+04	.6?6?0?0?0E+05	0.	0.	.40553942E+02	.12479550E+03	.12741182E+05	-.78539816E+00	99999
.1500?0?0?+04	.6?8?0?0?0E+05	-.8?429845E+01	.14516130E+02	.40641695E+02	.90990150E+04	.12?24514E+ 5	-.62831853E+01	3
.1500?0?0?+04	.6?8?0?0?0E+05	-.41?35?66E+01	-.12179?1?E+02	.40454429E+02	.94086?86E+02	.12705049E+05	-.47123890E+01	2
.1500?0?0?+04	.6?8?0?0?0E+05	-.6?592?45E+00	-.11501910E+02	.40447?40E+02	.96895736E+02	.12705147E+05	-.157?7963E+01	2
.1500?0?0?+04	.6?8?0?0?0E+05	.84557?00E+01	.14225159E+02	.40782807E+02	.91000736E+04	.12809155E+05	-.31415927E+01	2
.1500?0?0?+04	.6?8?0?0?0E+05	0.	0.	.4069?295E+02	.12451388E+03	.12782448E+05	-.78539816E+00	99999
.1500?0?0?+04	.6?0?0?0?0E+05	-.8?163457E+01	.14499956E+02	.40971467E+02	.90990243E+04	.12865?43E+05	-.62831853E+01	3
.1500?0?0?+04	.6?0?0?0?0E+05	-.4?3411?6E+01	-.12169?5?E+02	.40587463E+02	.94098?21E+02	.12746?15E+05	-.47123890E+01	2
.1500?0?0?+04	.6?0?0?0?0E+05	-.7?955833E+00	-.11503966E+02	.40578095E+02	.96980056E+02	.12746414E+05	-.157?7963E+01	2
.1500?0?0?+04	.6?0?0?0?0E+05	.8?357072E+01	.14213405E+02	.40912747E+02	.91001?85E+04	.12849?77E+05	-.31415927E+01	2
.1500?0?0?+04	.6?0?0?0?0E+05	0.	0.	.4082164?E+02	.12423310E+03	.12823?14E+05	-.78539816E+00	99999
.1500?0?0?+04	.6?2?0?0?0E+05	-.8?8?9?98E+01	.14483940E+02	.41101249E+02	.90991459E+04	.12900?55E+05	-.62831853E+01	3
.1500?0?0?+04	.6?2?0?0?0E+05	-.3??7d?78E+01	-.12141934E+02	.40718507E+02	.95113992E+02	.12787384E+05	-.47123890E+01	2
.1500?0?0?+04	.6?2?0?0?0E+05	-.7?2922?8E+00	-.11506101E+02	.40709448E+02	.97061?57E+02	.12787?9?E+05	-.157?7963E+01	2
.1500?0?0?+04	.6?2?0?0?0E+05	.8?1665?8E+01	.14201905E+02	.41042693E+02	.91003300E+04	.12890?01E+05	-.31415927E+01	2
.1500?0?0?+04	.6?2?0?0?0E+05	0.	0.	.40953001E+02	.12395324E+03	.12864979E+05	-.78539816E+00	99999
.1500?0?0?+04	.6?4?0?0?0E+05	-.6?646114E+01	.14463245E+02	.41231040E+02	.90991592E+04	.12946?30E+05	-.62831853E+01	3
.1500?0?0?+04	.6?4?0?0?0E+05	-.3?243?50E+01	-.12124775E+02	.40849559E+02	.95334134E+02	.12828555E+05	-.47123890E+01	2
.1500?0?0?+04	.6?4?0?0?0E+05	-.7?597550E+00	-.11508310E+02	.40844?01E+02	.97076943E+02	.12828?45E+05	-.157?7963E+01	2
.1500?0?0?+04	.6?4?0?0?0E+05	.83967d50E+01	.14194?653E+02	.41172647E+02	.91004491E+04	.12931627E+05	-.31415927E+01	2
.1500?0?0?+04	.6?6?0?0?0E+05	0.	0.	.41084354E+02	.12367431E+03	.12906?45E+05	-.78539816E+00	99999
.1500?0?0?+04	.6?8?0?0?0E+05	-.80383746E+01	.14452744E+02	.41364840E+02	.90992831E+04	.12987?08E+05	-.62831853E+01	3
.1500?0?0?+04	.6?8?0?0?0E+05	-.3?736376E+01	-.12108664E+02	.4098?.620E+02	.95559135E+02	.12869?29E+05	-.47123890E+01	2
.1500?0?0?+04	.6?8?0?0?0E+05	-.84?60197E+00	-.11510?81E+02	.40972152E+02	.97156?65E+02	.12870?10E+05	-.157?7963E+01	2
.1500?0?0?+04	.6?8?0?0?0E+05	.83?798?0E+01	.14179685E+02	.41304606E+02	.9100479?E+04	.12972?55E+05	-.31415927E+01	2
.1500?0?0?+04	.6?8?0?0?0E+05	0.	0.	.41215?07E+02	.12359430E+03	.12947511E+05	-.78539816E+00	99999
.1500?0?0?+04	.6?0?0?0?0E+05	-.8?13115?E+01	.14437550E+02	.41496650E+02	.90992925E+04	.13028349E+05	-.62831853E+01	3
.1500?0?0?+04	.6?0?0?0?0E+05	-.3?2536?6E+01	-.12093516E+02	.41116?8?E+02	.95789546E+02	.12910?05E+05	-.47123890E+01	2
.1500?0?0?+04	.6?0?0?0?0E+05	-.8?10113?E+00	-.11512?8?E+02	.41109502E+02	.97?3?197E+02	.12911475E+05	-.157?7963E+01	2
.1500?0?0?+04	.6?0?0?0?0E+05	.83596?0?E+01	.14169021E+02	.41432572E+02	.91006?75E+04	.13013?85E+05	-.31415927E+01	2
.1500?0?0?+04	.6?0?0?0?0E+05	0.	0.	.?.347060E+02	.12311?22E+03	.12988?77E+05	-.78539816E+00	99999

.1500[illegible] 4	.6200000E+05	-.8931178 9E+00	-.11515341E+02	.4 4852E+02	.97248224E+02	.12952740E+05	-.157 7963E+	2
.1500[illegible]E+04	.6200000E+05	.8341748E+01	.14158592E+02	.41562544E+02	.91007849E+04	.13054117E+05	-.31415927E+01	2
.1500[illegible]E+04	.6200000E+05	0.	0.	.4147 413E+02	.12284909E+03	.13030042E+05	-.78539816E+00	99999
.1500[illegible]E+04	.6220000E+05	-.87636618E+01	.1440783 E+02	.4175 295E+02	.9099436 E+04	.13109959E+05	-.52831853E+01	3
.1500[illegible]E+04	.6220000E+05	-.3735502 5E+01	-.12 65749E+02	.41378846E+02	.96269211E+02	.12993665E+05	-.4712389 E+01	2
.1500[illegible]E+04	.6220000E+05	-.9446807 6E+00	-.11517814E+02	.41364200E+02	.97322A09E+02	.12994004E+05	-.157 7963E+01	2
.1500[illegible]E+04	.6220000E+05	.8324170 E+01	.14148382E+02	.41692522E+02	.91009537E+04	.1309495 E+05	-.31415927E+01	2
.1500[illegible]E+04	.6220000E+05	0.	0.	.41600766E+02	.12256787E+03	.13071308E+05	-.78539816E+00	99999
.1500[illegible]E+04	.6240000E+05	-.8739451 E+01	.1439331 E+02	.41886130E+02	.90795797E+04	.13150748E+ 5	-.62831853E+01	3
.1500[illegible]E+04	.6240000E+05	-.3093531 E+01	-.12 53014E+02	.41594935E+02	.9552001 E+02	.13034447E+ 5	-.4712389 E+01	2
.1500[illegible]E+04	.6240000E+05	-.9564639 E+00	-.11523 59E+02	.41497547E+02	.97395143E+02	.13035268E+05	-.157 7963E+01	2
.1500[illegible]E+04	.6240000E+05	.8307189 E+01	.14138532E+02	.41822505E+02	.91009645E+04	.13135786E+05	-.31415927E+01	2
.1500[illegible]E+04	.6240000E+05	0.	0.	.41741119E+02	.12229360E+03	.13112574E+05	-.78539816E+00	99999
.1500[illegible]E+04	.6260000E+05	-.8715654 E+01	.1437907 E+02	.42000973E+02	.90995892E+04	.13191539E+05	-.62831853E+01	3
.1500[illegible]E+04	.6260000E+05	-.3053480 E+01	-.12 4 966E+02	.41634029E+02	.96529501E+02	.13075632E+05	-.4712389 E+01	2
.1500[illegible]E+04	.6260000E+05	-.9077174 E+00	-.11 229 E+02	.41628892E+02	.9741010 E+02	.13076531E+05	-.157 7963E+01	2
.1500[illegible]E+04	.6260000E+05	.8296588 E+01	.14128915E+02	.41952494E+02	.91011464E+04	.13176023E+05	-.31415927E+01	2
.1500[illegible]E+04	.6280000E+05	0.	0.	.41873472E+02	.12202027E+03	.13153840E+05	-.78539816E+00	99999
.1500[illegible]E+04	.6280000E+05	-.8092121 E+01	.1436501 E+02	.42136825E+02	.90997413E+04	.13232433E+05	-.62831853E+01	3
.1500[illegible]E+04	.6280000E+05	-.3015474 E+01	-.12 29643E+02	.41767130E+02	.96789116E+02	.13116818E+05	-.4712389 E+01	2
.1500[illegible]E+04	.6280000E+05	-.1018731 E+01	-.11525624E+02	.4176 237E+02	.97480239E+02	.13117795E+05	-.157 7963E+01	2
.1500[illegible]E+04	.6280000E+05	.8474292 E+01	.14119489E+02	.42082489E+02	.91013439E+04	.13217462E+05	-.31415927E+01	2
.1500[illegible]E+04	.6280000E+05	0.	0.	.42003825E+02	.12174788E+03	.13195106E+05	-.78539816E+00	99999
.1500[illegible]E+04	.6300000E+05	-.8069091 E+01	.1435127 E+02	.42266665E+02	.90997508E+04	.13273130E+05	-.62831853E+01	3
.1500[illegible]E+04	.6300000E+05	-.3078459 E+01	-.12 18865E+02	.41899236E+02	.97058430E+02	.13158007E+05	-.4712389 E+01	2
.1500[illegible]E+04	.6300000E+05	-.1 49 E+01	-.11528355E+02	.41891580E+02	.97495165E+02	.13159057E+05	-.157 7963E+01	2
.1500[illegible]E+04	.6320000E+05	.8458654 E+01	.1411 453E+02	.42212489E+02	.91013548E+04	.13256038E+05	-.31415927E+01	2
.1500[illegible]E+04	.6320000E+05	0.	0.	.42136178E+02	.12147645E+03	.13236371E+05	-.78539816E+00	99999
.1500[illegible]E+04	.6320000E+05	-.8046199 E+01	.1433764 E+02	.42396553E+02	.90999135E+04	.13313929E+05	-.62831853E+01	3
.1500[illegible]E+04	.6320000E+05	-.3043742 E+01	-.12 08566E+02	.42029347E+02	.97338A04E+02	.13199196E+05	-.4712389 E+01	2
.1500[illegible]E+04	.6320000E+05	-.1 6000 E+01	-.11531133E+02	.42022922E+02	.97563164E+02	.13200319E+05	-.157 7963E+01	2
.1500[illegible]E+04	.6320000E+05	.8443337 E+01	.1410161 E+02	.42342494E+02	.91015709E+04	.13299145E+05	-.31415927E+01	2
.1500[illegible]E+04	.6320000E+05	0.	0.	.42267531E+02	.12120596E+03	.13277037E+05	-.78539816E+00	99999
.1500[illegible]E+04	.6340000E+05	-.8023968 E+01	.1432443 E+02	.42924429E+02	.90999231E+04	.13354731E+05	-.62831853E+01	3
.1500[illegible]E+04	.6340000E+05	-.3010274 E+01	-.11796864E+02	.42164463E+02	.97348971E+02	.13240389E+05	-.4712389 E+01	2
.1500[illegible]E+04	.6340000E+05	-.1116445 E+01	-.11533978E+02	.42154262E+02	.97629133E+02	.13241581E+05	-.157 7963E+01	2
.1500[illegible]E+04	.6340000E+05	.8422462 E+01	.1409317 E+02	.42475503E+02	.91015819E+04	.13339789E+05	-.31415927E+01	2
.1500[illegible]E+04	.6340000E+05	0.	0.	.42397885E+02	.12093642E+03	.13318903E+05	-.78539816E+00	99999
.1500[illegible]E+04	.6360000E+05	-.8081736 E+01	.1431124 E+02	.42656312E+02	.90999327E+04	.13395535E+05	-.62831853E+01	3
.1500[illegible]E+04	.6360000E+05	-.3047258 E+01	-.11980665E+02	.42291583E+02	.97642255E+02	.13281580E+05	-.4712389 E+01	2
.1500[illegible]E+04	.6360000E+05	-.1144564 E+01	-.11534878E+02	.422A8602E+02	.97643994E+02	.13282843E+05	-.157 7963E+01	2
.1500[illegible]E+04	.6360000E+05	.8414097 E+01	.1408478 E+02	.42609518E+02	.91018207E+04	.13380834E+05	-.31415927E+01	2
.1500[illegible]E+04	.6360000E+05	0.	0.	.42520238E+02	.12066784E+03	.13360169E+05	-.78539816E+00	99999
.1500[illegible]E+04	.6380000E+05	-.8058 2745E+01	.1429852 E+02	.42780203E+02	.91001089E+04	.13436941E+05	-.62831853E+01	3
.1500[illegible]E+04	.6380000E+05	-.3047115 E+01	-.1198 785E+02	.42422706E+02	.97950231E+02	.13322774E+ 5	-.4712389 E+01	2
.1500[illegible]E+04	.6380000E+05	-.1175462 E+01	-.11539825E+02	.42416940E+02	.97707980E+02	.13324104E+05	-.157 7963E+01	2
.1500[illegible]E+04	.6380000E+05	.8399391 E+01	.1407663 E+02	.42736537E+02	.91020879E+04	.13426181E+05	-.31415927E+01	2
.1500[illegible]E+04	.6380000E+05	0.	0.	.42664591E+02	.1 940022E+ 3	.13401434E+05	-.78539816E+00	99999
.1500[illegible]E+04	.6400000E+05	-.8055870 E+01	.1428586 E+02	.42916101E+02	.91001177E+04	.13477150E+05	-.62831853E+01	3
.1500[illegible]E+04	.6400000E+05	-.3017036 E+01	-.11972 6 E+02	.42553837E+02	.97960792E+02	.13363970E+05	-.4712389 E+01	2
.1500[illegible]E+04	.6400000E+05	-.1400246 E+01	-.1154285 E+02	.42548276E+02	.9777008 E+02	.13365364E+05	-.157 7963E+01	2
.1500[illegible]E+04	.6400000E+05	.8185594 E+01	.14 68965E+02	.42866561E+02	.91020990E+04	.13462529E+05	-.31415927E+01	2
.1500[illegible]E+04	.6400000E+05	0.	0.	.42791944E+02	.12013357E+03	.13442700E+05	-.78539816E+00	99999
.1500[illegible]E+04	.6420000E+05	-.8037994 E+01	.1427352 E+02	.43044006E+02	.91003078E+04	.13517961E+ 5	-.62831853E+01	3
.1500[illegible]E+04	.6420000E+05	-.3008355 E+01	-.11764514E+02	.42684970E+02	.96286139E+02	.13405155E+ 5	-.4712389 E+01	2
.1500[illegible]E+04	.6420000E+05	-.1429714 E+01	-.11545919E+02	.42670611E+02	.97784978E+02	.13406025E+05	-.157 7963E+01	2
.1500[illegible]E+04	.6420000E+05	.8173953 E+01	.1426137 E+02	.42992589E+02	.91024025E+04	.13503379E+05	-.31415927E+01	2
.1500[illegible]E+04	.6420000E+05	0.	0.	.42923297E+02	.11986787E+03	.13483966E+05	-.78539816E+00	99999
.1500[illegible]E+04	.6440000E+05	-.8017461 E+01	.1426142 E+02	.43178918E+02	.91001175E+04	.13558774E+05	-.62831853E+01	3
.1500[illegible]E+04	.6440000E+05	-.3002121 E+01	-.11956933E+02	.42814107E+02	.96296A72E+02	.13446364E+05	-.4712389 E+01	2
.1500[illegible]E+04	.6440000E+05	-.1459 8 E+01	-.11549032E+02	.42811945E+02	.97845148E+02	.13447884E+05	-.157 7963E+01	2
.1500[illegible]E+04	.6440000E+05	.8160 871E+01	.1425422 E+02	.43[illegible]22E+02	.91024137E+04	.13544270E+05	-.31415927E+01	2

.1500[illegible]	.67[illegible]E+05	-.3[illegible]E+01	-.11[illegible]E+02	.[illegible]E+02	.10[illegible]E+03	.13982022E+05	-.47123890E	2
.1500[illegible]	.67[illegible]E+05	-.19[illegible]E+01	-.11[illegible]E+02	.[illegible]E+02	.98[illegible]E+02	.13984615E+05	-.15707963E+01	2
.1500[illegible]	.67[illegible]E+05	.80[illegible]E+01	.13984565E+02	.44[illegible]E+02	.91054924E+04	.14075[illegible]E+05	-.31415927E+01	2
.1500[illegible]	.670[illegible]E+05	0.	0.	.44762[illegible]E+02	.11[illegible]E+03	.14061[illegible]E+05	-.78539816E+00	99999
.1500[illegible]	.672[illegible]E+05	-.82[illegible]E+01	.14116252E+02	.44998[illegible]E+02	.91[illegible]E+04	.14130367E+05	-.62831853E+01	3
.1500[illegible]	.672[illegible]E+05	-.39761778E+01	-.11[illegible]E+02	.44652[illegible]E+02	.10097[illegible]E+03	.14023631E+05	-.47123890E+01	2
.1500[illegible]	.672[illegible]E+05	-.19536311E+01	-.11598013E+02	.44644[illegible]E+02	.9635[illegible]E+02	.14025468E+05	-.15707963E+01	2
.1500[illegible]	.672[illegible]E+05	.80[illegible]E+01	.13980961E+02	.44943[illegible]E+02	.91055[illegible]E+04	.14116253E+05	-.31415927E+01	2
.1500[illegible]	.672[illegible]E+05	0.	0.	.44893[illegible]E+02	.11000041E+03	.14102752E+05	-.78539816E+00	99999
.1500[illegible]	.674[illegible]E+05	-.82534040E+01	.14107423E+02	.45129[illegible]E+02	.91017468E+04	.14171408E+05	-.62831853E+01	3
.1500[illegible]	.674[illegible]E+05	-.39[illegible]365E+01	-.11[illegible]856E+02	.44783508E+02	.10098432E+03	.14064442E+05	-.47123890E+01	2
.1500[illegible]	.674[illegible]E+05	-.19[illegible]941E+01	-.11601[illegible]5E+02	.4478 759E+02	.98372[illegible]99E+02	.14066720E+05	-.15707963E+01	2
.1500[illegible]	.674[illegible]E+05	.80255820E+01	.13977359E+02	.45[illegible]507E+02	.91055161E+04	.14157118F+05	-.31415927E+01	2
.1500[illegible]	.674[illegible]E+05	0.	0.	.45[illegible]945F+02	.11575[illegible]60E+03	.14144218E+05	-.78539816E+00	99999
.1500[illegible]	.676[illegible]E+05	-.82391574E+01	.14099204E+02	.45251363E+02	.91021552E+04	.14212051E+05	-.62831853E+01	3
.1500[illegible]	.676[illegible]E+05	-.3[illegible]E+01	-.11873135E+02	.44914687E+02	.10162318E+03	.14105053E+05	-.47123890E+01	2
.1500[illegible]	.676[illegible]E+05	-.17[illegible]E+01	-.11605769E+02	.44912066E+02	.98418997E+02	.14107971E+05	-.15707963E+01	2
.1500[illegible]	.676[illegible]E+05	.80[illegible]E+01	.13974933E+02	.45[illegible]586E+02	.91076150E+04	.14197944E+05	-.31415927E+01	2
.1500[illegible]	.676[illegible]E+05	0.	0.	.45156[illegible]98F+02	.11590180E+03	.14185484E+05	-.78539816E+00	99999
.1500[illegible]	.678[illegible]E+05	-.82[illegible]83E+01	.14091167E+02	.45380374E+02	.91021655E+04	.14252895E+05	-.62831853E+01	3
.1500[illegible]	.678[illegible]E+05	-.3[illegible]751E+01	-.11[illegible]E+02	.45[illegible]866E+02	.10163481E+03	.14146844E+05	-.47123890E+01	2
.1500[illegible]	.678[illegible]E+05	-.17[illegible]E+01	-.11609714E+02	.45[illegible]371E+02	.98433404E+02	.14149422E+05	-.15707963E+01	2
.1500[illegible]	.678[illegible]E+05	.80177654E+01	.13972718E+02	.45333666F+02	.91070472E+04	.14238859E+05	-.31415927E+01	2
.1500[illegible]	.678[illegible]E+05	0.	0.	.45287651E+02	.11529403E+03	.14226750E+05	-.78539816E+00	99999
.1500[illegible]	.680[illegible]E+05	-.82112591E+01	.14083139E+02	.4551[illegible]90E+02	.91021757E+04	.14293741E+05	-.62831853E+01	3
.1500[illegible]	.680[illegible]E+05	-.3[illegible]778E+01	-.11866481E+02	.4517704[illegible]E+02	.10164441E+03	.14188076E+05	-.47123890E+01	2
.1500[illegible]	.680[illegible]E+05	-.17617343E+01	-.11613706E+02	.45174675E+02	.98479120E+02	.14190972E+05	-.15707963E+01	2
.1500[illegible]	.680[illegible]E+05	.80138520E+01	.13976503E+02	.45463748E+02	.91076593E+04	.14279716E+05	-.31415927E+01	2
.1500[illegible]	.680[illegible]E+05	0.	0.	.4541[illegible]004E+02	.11500728E+03	.14268016E+05	-.78539816E+00	99999
.1500[illegible]	.682[illegible]E+05	-.81976023E+01	.14075287E+02	.4564[illegible]410E+02	.91026857E+04	.14334588E+05	-.62831853E+01	3
.1500[illegible]	.682[illegible]E+05	-.3[illegible]E+01	-.11863174E+02	.4530[illegible]231E+02	.10106579E+03	.14229288E+05	-.47123890E+01	2
.1500[illegible]	.682[illegible]E+05	-.17[illegible]012E+01	-.11617742E+02	.45[illegible]976E+02	.98493486E+02	.14231721E+05	-.15707963E+01	2
.1500[illegible]	.682[illegible]E+05	.80[illegible]96E+01	.13968286E+02	.45593[illegible]31E+02	.91076714E+04	.14320583E+05	-.31415927E+01	2
.1500[illegible]	.682[illegible]E+05	0.	0.	.4555[illegible]357E+02	.11479157E+03	.14309281E+05	-.78539816E+00	99999
.1500[illegible]	.684[illegible]E+05	-.81851691E+01	.14068147E+02	.4577[illegible]435E+02	.91026962E+04	.14375436E+05	-.62831853E+01	3
.1500[illegible]	.684[illegible]E+05	-.2[illegible]E+01	-.11861141E+02	.45439416E+02	.10242712E+03	.14270501E+05	-.47123890E+01	2
.1500[illegible]	.684[illegible]E+05	-.19151621E+01	-.11621826E+02	.45437276[illegible]+02	.98538[illegible]73E+02	.14272970F+05	-.15707963E+01	2
.1500[illegible]	.684[illegible]E+05	.80060252E+01	.13966075E+02	.45723916E+02	.91076835E+04	.14361450E+05	-.31415927F+01	2
.1500[illegible]	.684[illegible]E+05	0.	0.	.4564[illegible]710E+02	.11451[illegible]90E+03	.14350947E+05	-.78539816E+00	99999
.1500[illegible]	.686[illegible]E+05	-.81727359E+01	.14061014E+02	.4590[illegible]464E+02	.91027[illegible]66E+04	.14416[illegible]86E+05	-.62831853E+01	3
.1500[illegible]	.686[illegible]E+05	-.2[illegible]E+01	-.11857384E+02	.4557[illegible]602E+02	.10243[illegible]82E+03	.14311[illegible]4E+05	-.47123890E+01	2
.1500[illegible]	.686[illegible]E+05	-.19417433E+01	-.11625944E+02	.45568574E+02	.98552397E+02	.14314[illegible]9E+05	-.15707963F+01	2
.1500[illegible]	.686[illegible]E+05	.80021118E+01	.13963862E+02	.45954001E+02	.91076955E+04	.14402[illegible]9E+05	-.31415927E+01	2
.1500[illegible]	.686[illegible]E+05	0.	0.	.45[illegible]063E+02	.11427326E+03	.14391813E+05	-.78539816E+00	99999
.1500[illegible]	.688[illegible]E+05	-.816[illegible]026E+01	.14053889E+02	.46[illegible]96E+02	.91027170E+04	.14457137E+05	-.62831853E+01	3
.1500[illegible]	.688[illegible]E+05	-.2[illegible]E+01	-.11854637E+02	.457[illegible]789E+02	.10245[illegible]49E+03	.14352[illegible]8E+05	-.47123890E+01	2
.1500[illegible]	.688[illegible]E+05	-.19[illegible]E+01	-.11630[illegible]E+02	.4562[illegible]E+02	.9859[illegible]E+02	.14355[illegible]E+05	-.15707963E+01	2
.1500[illegible]	.688[illegible]E+05	.79[illegible]E+01	.13962076E+02	.4598[illegible]087E+02	.91103707E+04	.14443[illegible]E+05	-.31415927E+01	2
.1500[illegible]	.688[illegible]E+05	0.	0.	.45944416E+02	.11403[illegible]E+03	.14433079E+05	-.78539816E+00	99999
.1500[illegible]	.690[illegible]E+05	-.81481746E+01	.14046945E+02	.46163533F+02	.91033988E+04	.14497989E+05	-.62831853E+01	3
.1500[illegible]	.690[illegible]E+05	-.2[illegible]E+01	-.11851900E+02	.45833978E+02	.10240212E+03	.14394142E+05	-.47123890E+01	2
.1500[illegible]	.690[illegible]E+05	-.19[illegible]E+01	-.11634323E+02	.45831163E+02	.98610191E+02	.14396714E+05	-.15707963E+01	2
.1500[illegible]	.692[illegible]E+05	.79[illegible]E+01	.13960988E+02	.46114174E+02	.91112260E+04	.14484053E+05	-.31415927E+01	2
.1500[illegible]	.692[illegible]E+05	0.	0.	.46[illegible]769E+02	.11378912E+03	.14474344E+05	-.78539816E+00	99999
.1500[illegible]	.692[illegible]E+05	-.81375222E+01	.14043851E+02	.46294573F+02	.91034095E+04	.14538843E+05	-.62831853E+01	3
.1500[illegible]	.692[illegible]E+05	-.2[illegible]E+01	-.11849173E+02	.45964168E+02	.10247372E+03	.14435357E+05	-.47123890E+01	2
.1500[illegible]	.692[illegible]E+05	-.19[illegible]E+01	-.11638571E+02	.45962455E+02	.98652474E+02	.14437950E+05	-.15707963E+01	2
.1500[illegible]	.692[illegible]E+05	.79955892E+01	.13960175E+02	.46244261E+02	.91120421E+04	.14524922E+05	-.31415927E+01	2
.1500[illegible]	.692[illegible]E+05	0.	0.	.46207122E+02	.11354A63E+03	.14515810E+05	-.78539816E+00	99999
.1500[illegible]	.694[illegible]E+05	-.81268698E+01	.14034763E+02	.46428617E+02	.91034201E+04	.14579697E+05	-.62831853E+01	3
.1500[illegible]	.694[illegible]E+05	-.2[illegible]E+01	-.11846993E+02	.4609[illegible]359E+02	.10346507E+03	.14476572E+05	-.47123890E+01	2
.1500[illegible]	.694[illegible]E+05	-.19471034E+01	-.11642871E+02	.46093[illegible]745E+02	.98666917E+02	.14479206E+05	-.15707963E+01	2.

.1500[illegible]E+04	.6960[illegible]E+05	.79946431E+01	.13959641E+02	.[illegible]349E+02	.91147230E+04	.14565790E+05	-.31415927E	2
.1500[illegible]E+04	.6960[illegible]E+05	0.	0.	.46330475E+02	.11330919E+03	.14556876E+05	-.78539816E+00	99999
.1500[illegible]E+04	.6960[illegible]E+05	-.81162174E+01	.14328681E+02	.46554665E+02	.91034307E+04	.14620553E+05	-.62831853E+01	3
.1500[illegible]E+04	.6960[illegible]E+05	-.29324550E+01	-.11844829E+02	.46224551E+02	.11347681E+03	.14517787E+05	-.47123890E+01	2
.1500[illegible]E+04	.6960[illegible]E+05	-.19731892E+01	-.11647203E+02	.46225033E+02	.98708421E+02	.14520452E+05	-.15707963E+01	2
.1500[illegible]E+04	.6960[illegible]E+05	.79942573E+01	.13959423E+02	.46504437E+02	.34693318E+04	.14605672E+05	-.41276344E+01	2
.1500[illegible]E+04	.6960[illegible]E+05	0.	0.	.46466828E+02	.11307081E+03	.14598142E+05	-.78539816E+00	99999
.1500[illegible]E+04	.6960[illegible]E+05	-.81055650E+01	.14328604E+02	.46688716E+02	.91034413E+04	.14661409E+05	-.62831853E+01	3
.1500[illegible]E+04	.6960[illegible]E+05	-.19992549E+01	-.11651588E+02	.46354318E+02	.98722623E+02	.14561996E+05	-.15707963E+01	2
.1500[illegible]E+04	.6960[illegible]E+05	.76304229E+01	.13757077E+02	.46434558E+02	.86370575E+02	.14645966E+05	-.47123890E+01	2
.1500[illegible]E+04	.6960[illegible]E+05	0.	0.	.46601181E+02	.11283349E+03	.14639407E+05	-.78539816E+00	99999
.1500[illegible]E+04	.7000[illegible]E+05	-.80959844E+01	.14017142E+02	.46818770E+02	.91044795E+04	.14702267E+05	-.62831853E+01	3
.1500[illegible]E+04	.7000[illegible]E+05	-.20251711E+01	-.11656002E+02	.46487602E+02	.98763192E+02	.14602940E+05	-.15707963E+01	2
.1500[illegible]E+04	.7000[illegible]E+05	.76261112E+01	.13539989E+02	.46764824E+02	.86391366E+02	.14686890E+05	-.47123890E+01	2
.1500[illegible]E+04	.7000[illegible]E+05	0.	0.	.46732534E+02	.11259723E+03	.14680673E+05	-.78539816E+00	99999

RESULTANT AT TARGET POINTS.

TARGET DEPTH	TARGET RANGE	RESULTANT AMPLITUDE		PHASE
M	KM	PSI	DB	RAD
.1500[illegible]E+04	.6000000E+05	.3523765E-04	.8905986E+02	-.9416432E+00
.1500[illegible]E+04	.6020000E+05	.3453292E-04	.8923533E+02	.2556255E+01
.1500[illegible]E+04	.6040000E+05	.3404529E-04	.8935866E+02	-.2237012E+00
.1500[illegible]E+04	.6060000E+05	.3346070E-04	.8950930E+02	-.3006916E+01
.1500[illegible]E+04	.6080000E+05	.3247438E-04	.8976918E+02	.5986177E+00
.1500[illegible]E+04	.6100000E+05	.3173676E-04	.8996886E+02	-.2262979E+01
.1500[illegible]E+04	.6120000E+05	.3093920E-04	.9018982E+02	.1254954E+01
.1500[illegible]E+04	.6140000E+05	.3019388E-04	.9040162E+02	-.1516483E+01
.1500[illegible]E+04	.6160000E+05	.2930162E-04	.9066234E+02	.2002820E+01
.1500[illegible]E+04	.6180000E+05	.2837530E-04	.9094119E+02	-.7602454E+00
.1500[illegible]E+04	.6200000E+05	.2751228E-04	.9120947E+02	.2763382E+01
.1500[illegible]E+04	.6220000E+05	.2653531E-04	.9152352E+02	.4626849E-02
.1500[illegible]E+04	.6240000E+05	.2554406E-04	.9185420E+02	-.2752133E+01
.1500[illegible]E+04	.6260000E+05	.2500101E-04	.9204085E+02	.7704290E+00
.1500[illegible]E+04	.6280000E+05	.2398473E-04	.9240130E+02	-.1983082E+01
.1500[illegible]E+04	.6300000E+05	.2303819E-04	.9275103E+02	.1555469E+01
.1500[illegible]E+04	.6320000E+05	.2201920E-04	.9314397E+02	-.1198569E+01
.1500[illegible]E+04	.6340000E+05	.2136120E-04	.9340749E+02	.2326142E+01
.1500[illegible]E+04	.6360000E+05	.2041173E-04	.9380240E+02	-.4172237E+00

.150[illegible]E+04	.6340[illegible]E+05	.1940951E-04	.9423971E+02	.3123098E+01
.150[illegible]E+04	.6[illegible]E+05	.1875385E-04	.9453819E+02	.3674134E+00
.150[illegible]E+04	.6420[illegible]E+05	.1782831E-04	.9497779E+02	-.2369180E+01
.150[illegible]E+04	.6440[illegible]E+05	.1718008E-04	.9529950E+02	.1150227E+01
.150[illegible]E+04	.6460[illegible]E+05	.1627996E-04	.9576693E+02	-.1571856E+01
.150[illegible]E+04	.6480[illegible]E+05	.1564546E-04	.9611223E+02	.1957921E+01
.150[illegible]E+04	.6500[illegible]E+05	.1477946E-04	.9666671E+02	-.7671720E+00
.150[illegible]E+04	.6520[illegible]E+05	.1416409E-04	.9697623E+02	.2764127E+01
.150[illegible]E+04	.6540[illegible]E+05	.1329942E-04	.9752335E+02	.4316759E-01
.150[illegible]E+04	.6560[illegible]E+05	.1274925E-04	.9789031E+02	-.2703830E+01
.150[illegible]E+04	.6540[illegible]E+05	.1193993E-04	.9845994E+02	.8671381E+00
.150[illegible]E+04	.6660[illegible]E+05	.1141471E-04	.9885076E+02	-.1877431E+01
.150[illegible]E+04	.6680[illegible]E+05	.1045856E-04	.9928456E+02	.1657869E+01
.150[illegible]E+04	.6640[illegible]E+05	.1017635E-04	.9984816E+02	-.1033856E+01
.150[illegible]E+04	.6660[illegible]E+05	.9516666E-05	.1003079E+03	.2501461E+01
.150[illegible]E+04	.6680[illegible]E+05	.9170553E-05	.1007521E+03	-.2394601E+00
.150[illegible]E+04	.6720[illegible]E+05	.8565382E-05	.1013451E+03	-.2918848E+01
.150[illegible]E+04	.6720[illegible]E+05	.8084613E-05	.1018449E+03	.6234053E+00
.150[illegible]E+04	.6740[illegible]E+05	.7649832E-05	.1023270E+03	-.2112287E+01
.150[illegible]E+04	.6760[illegible]E+05	.7191585E-05	.1028636E+03	.1517203E+01
.150[illegible]E+04	.6780[illegible]E+05	.6796920E-05	.1033538E+03	-.1212809E+01
.150[illegible]E+04	.6800[illegible]E+05	.6376996E-05	.1039050E+03	.2337097E+01
.150[illegible]E+04	.6820[illegible]E+05	.6003778E-05	.1044315E+03	-.3902294E+00
.150[illegible]E+04	.6840[illegible]E+05	.5745223E-05	.1047536E+03	-.3005454E+01
.150[illegible]E+04	.6860[illegible]E+05	.5460609E-05	.1052552E+03	.5574609E+00
.150[illegible]E+04	.6880[illegible]E+05	.5112903E-05	.1058265E+03	-.2164824E+01
.150[illegible]E+04	.6900[illegible]E+05	.4839692E-05	.1063577E+03	.1401539E+01
.150[illegible]E+04	.6920[illegible]E+05	.4484415E-05	.1069659E+03	-.1317573E+01
.150[illegible]E+04	.6940[illegible]E+05	.4083740E-05	.1065801E+03	.2397203E+01
.150[illegible]E+04	.6960[illegible]E+05	.4414490E-05	.1071024E+03	-.3144991E+00
.150[illegible]E+04	.6980[illegible]E+05	.4091792E-04	.8776173E+02	-.3026838E+00

Appendix II: Normal Mode Program Listing

The following is a card by card listing of the data deck. This precedes the program listing. While the program has undergone extensive revision, the main logic and substance of the program follows Newman and Ingenito (22).

Card 1 READ 500, KKK, INC
500 FORMAT (2I4)
KKK - number of sound speed profiles for which calculations are to be made
INC-If MODSHAPE=1, prints amplitude at layers: 1, 1 + INC, 1 + 2 · INC, etc.

Card 2 READ 4500, PROPLT, MODSHAPE, MODEPLT, GRUVEL, GRUPLT, GRUVELS
4500 FORMAT (F5.1, 2I5, 3F5.1)
PROPLT = 1 - plots sound speed profile otherwise - no plot
MODSHAPE = 1 - prints mod amplitude values otherwise - no print
MODEPLT = 1 - plots mode amplitudes - otherwise - no plot
GRUVEL = 1 - indicates group velocities are to be calculated otherwise - program terminates
GRUPLT = 1 - plots group velocity curves otherwise - no plot
GRUVELS = 1 - prints group velocities over frequency range specified otherwise - no print

Card 3 READ 1000, TITLE
1000 FORMAT (10A8)
TITLE - word and/or number description of problem

Card 4 READ 2000, VELNO
2000 FORMAT (I10)
VELNO - number identification of sound speed profile

Card 5 READ 4000, F, CT, R1, R2, H, LI, ND, NM, NF, EPSILON
4000 FORMAT (5F10.3, 4I4, F10.4)
F - Frequency of source
CT - second layer sound speed
R1 - density of first layer
R2 - density of second layer
H - first layer depth (water layer)
L1 - number of increments into which first layer is to be divided for finite difference equations
ND - number of sound speed depths
NM - number of normal modes or eigenfunctions wanted
NF - number of additional frequencies
EPSILON - criterion for acceptable solutions

Card 6 READ 6000, (Z1(I), C1(I), I=1, ND)
6000 FORMAT (2F10.3)
Z1(I), C1(I) - profile depth and sound speed

Card ND+6 READ 7500, SD, (RD(I), I=1,5)
7500 FORMAT 6F10.3
SD - Source Depth
RD(I) - Receiver Depth

Card ND+7 READ 14000 (LB1(I), LB2(I), I=1,10)
14000 FORMAT (10(2I4))
LB1, LB2 Specific modes to be calculated
i.e. 1 5 100 110 0 0
Means calculate modes 1 through 5, and 100 through 110

Card ND+8 READ 1300 F
1300 FORMAT (F10.3)
F - New source frequency

Card ND+NF+8 READ 14000, FMIN, FMAX, FDELF
FMIN Lowest frequency for group velocity calculation
FMAX Largest frequency for group velocity calculation
DELF Frequency increment for group velocity calculation

```
PROGRAM     NORMOD3                                    CDC 6400 FTN V3.0-P316 OPT=1

                 PROGRAM NORMOD3(INPUT,OUTPUT,TAPE1,TAPE7,PUNCH=TAPE7,TAPE9)
                COMMON/1/ XT(   3100)
                COMMON/2/Z2N(3100),          C2D(3100)
                COMMON/AA/CP(20,20),V(20,20),GV(20,20),C(20,20),DKN(20,20)
          5     COMMON/AB/Z1(50),C1(50),Z1N(50),LLB(10),LUB(10),MNU(30),LB1(10),
               *LB2(10)
                COMMON/AC/AKN( 12),BB( 12),PV( 12),AN( 12),ZF(12)
                COMMON/AD/EPSILON,H,HD,HD3,DL,DLS,R,IT,CT,CTD,MODSHAP ,MODEPLT,
               *GRUVEL,GRUPLT,IZERO,IGV
                COMMON/AE/LDEPTH   ,LAMP   ,LGRU   ,LFRE
                DIMENSION INDEX(6),AMPMOD(6,12)
                 DIMENSION BD(5)
                 DIMENSION ZT(3100),ZZ(3100)
                DIMENSION PLTMODE(254),TITLE(10)
                EQUIVALENCE(Z2N,ZT),(XT,ZZ)
                 DATA LAMP/9HAMPLITUDE/
                 DATA LDEPTH/8H DEPTH  /
                DATA LFRE/9HFREQUENCY/
                 DATA LGRU/9HGROUP VEL/
           11111 FORMAT(2I4)
             800 FORMAT(F5.1,2I5,3F5.1)
            1000 FORMAT(10A8)
            2000 FORMAT(1H1,10A8)
            3000 FORMAT(I10)
            4000 FORMAT(///)
            5000 FORMAT(* FREQUENCY/BOTTOM V./H2O DEN./BOTTOM DEN/H2O DEPTH/ LI/
                */ NM/ NF/  EPSILON *)
            6000 FORMAT(5F10.3,4I4,F10.4)
            7000 FORMAT(2F10.3)
      30    8000 FORMAT(* SOUND SPEED PROFILE *)
            9000 FORMAT(*   DEPTH    VELOCITY *)
           10000 FORMAT(1H1,* SOURCE FREQUENCY = *,F8.3)
           11000 FORMAT(/)
           12000 FORMAT(* MAXIMUM NO. OF ZERO CROSSINGS = *,I4)
           13000 FORMAT(*  MODE CUTOFF AT THIS SOURCE FREQUENCY *)
           14000 FORMAT(10(2I4))
           15000 FORMAT(* MODE = *,I3)
           16000 FORMAT(*     WAVE NUMBER         PHASE VELOCITY          *    R  *)
           17000 FORMAT(3E20.13)
           18000 FORMAT(1H1)
           19000 FORMAT(* MODE AMPLITUDES FOR SOURCE FREQUENCY(HZ) = *,F8.2)
           20000 FORMAT(10X,12(3X,*MODE*,I3))
           21000 FORMAT(4X,A.  ,12(X,A9))
           22000 FORMAT(13F10.3)
           23000 FORMAT(F10.3)
           24000 FORMAT(3F10.3)
           25000 FORMAT(* GROUP VELOCITIES *)
           26000 FORMAT(X,A8,A1,12(X,A8,A1))
           27000  FORMAT(10F11.4)
           27001  FORMAT(2F11.4)
                 CALL PLOTS(PLTMODE,254,1)
           C  FIVE READ STATEMENTS STORE CONSTANTS AND FLAG INFORMATION
                 READ11111,KKK,INC
                 DO 9997 M=1,KKK
      55    55         READ  800,PROPLT,MODSHAP ,MODEPLT,GRUVEL,GRUPLT,GRUVELS
```

```
PROGRAM     NORMOD3                                   CDC 6400 FTN V3.0-P316 OPT=1

            READ 1000,TITLE
            PRINT  2000,TITLE
            READ 3000,VELNO
            IF(PROPLT.EQ.0.0)  GO TO 5
   60        CALL PLOT(0.,9.,3,1)
            CALL SYMBL4(0.0,-6.0,0.14,10HPROFILE ID,90.0,10)
             CALL NUMBR(0.0,-4.0,0.14,VELNO,90.0,-1  )
             CALL PLOT(2.5,0.,3,1)
          5 PRINT  4000
            READ 6000,F,CT,R1,R2,H,LI,ND,NM,NF,EPSILON
            PRINT 5000
            PRINT 6000,F,CT,R1,R2,H,LI,ND,NM,NF,EPSILON
            PRINT  4000
      C  SIXTH READ STATEMENT STORES SOUND SPEED PROFILE
            READ 7000,(Z1(I),C1(I),I=1,ND)
            PRINT 8000
            PRINT 9000
            PRINT 7000,(Z1(I),C1(I),I=1,ND)
             READ 7500,SD,(RD(IL),IL=1,5)
     7500  FORMAT(6F10.3)
             ISTEP=6*INC
             JSTEP=5*INC
             SDEP=SD/H
             DO 7 I=1,5
        7     RD(I)=RD(I)/H
             PUNCH 7600,SDEP,(RD(IL),IL=1,5),LI
            WETEST=.5/FLOAT(LI)
     7600  FORMAT(6F10.6,I5)
   85 C NORMALIZATION OF SOUND VELOCITY PROFILE DEPTHS
            DO 10 I=1,ND
       10    Z1N(I)=Z1(I)/H
            N=LI+1
            DL=1.0/LI
      C NORMALIZATION OF INCREMENTAL DEPTHS
            DO 20 I=1,N
       20  Z2N(I)=DL*(I-1)
      C CALL TO SUBROUTINE WHICH LINEAR INTERPOLATES BETWEEN THE ABOVE TWO SI
      C     NORMALIZED WATER DEPTHS TO YIELD A SET OF SOUND VELOCITIES FOR TI
      C     NORMALIZED INCREMENTAL WATER DEPTHS
            CALL ZCINTER (ND,N,F,C2MIN,PROPLT)
            I=0
            DLS=DL*DL
            CTD=CT*CT
            HD=H*H
            R=R2/R1
            IT=N
            HD3=HD*H
      C CALCULATION OF LARGEST KN (AK2) AND SMALLEST KN (AK1)
       30    AK1=(6.283185307179*F)/CT
             AK2=(6.283185307179*F)/C2MIN
            FD=(39.47841760436*F*F)
            AK3=AK1
            IF(MODEPLT.EQ.0)  GO TO 40
             CALL PLOT(5.,0.,3,1)
  110       CALL SYMBL4(0.0,-6.0,0.14,20HSOURCE FREQUENCY(HZ),90.0,20)
```

```
PROGRAM     NORMOD3                                   CDC 6400 FTN V3.0-P316 OPT=1

                CALL NUMBR(0.0,-2.0,0.14,F,90.0,1.     )
            C CALCULATION OF MAXIMUM MODE AVAILABLE USING A SUBROUTINE WHICH ITERA
            C     FROM BOTTOM TO SURFACE USING A FALSE POSITION TECHNIQUE
            C  SUBROUTINE ITERATE CALCULATES A MODE SHAPE FOR A GIVEN EIGENVALUE
      115   C     BY THE METHOD OF FALSE POSITION(REGULA FALSI)
               40 IZERO=0
                  CALL ITERATE(AK1,FD,H,C2D,DLS,HD,HD3,CTD,IT,NCR,R,Z,A,ZZ,DL,IZER(
                 *I)
                   DO 41  IL=1,6
               41  INDEX(IL)=0
                  PRINT 10000,F
                  PRINT 11000
                  PRINT  12000,NCR
                  PUNCH 11500,F,R1,H,NCR
           11500 FORMAT(3F10.3,I4)
                  PRINT 11000
                  IF(NCR.EQ.0)  50,60
               50 PRINT 13000
                  READ 14000,(LB1(I),LB2(I),I=1,10)
                  GO TO 250
               60 ICOUNT=JPAGE=0
                  READ 14000,(LB1(I),LB2(I),I=1,10)
                  PRINT 14000,(LB1(I),LB2(I),I=1,10)
                  DO 70 I=1,10
                  LLB(I)=LB1(I)
               70 LUB(I)=LB2(I)
                  FLAG=0.0
                  SKIP=IC=1
                   DO 120 J=1,10
                  JJ=LLB(J)
               80 IF(JJ.LE.NCR)   110,90
               90 LUB(J)=NCR
                  GO TO 120
              110 IF(JJ.EQ.LUB(J))   120,115
      145     115 JJ=JJ+1
                  GO TO 80
              120 CONTINUE
              130 ICOUNT=ICOUNT+1
                  AK1=AK3
                  I=LLB(ICOUNT)
                  IUR=LUB(ICOUNT)
                  IF( I .EQ.0)  240,140
              140 PRINT 15000,I
            C  SUBROUTINE HALF DETERMINES EIGENVALUE FOR EACH MODE SHAPE BY THE
            C     HALF INTERVAL SEARCH TECHNIQUE
                  CALL HALF(AK1,AK2,FD,NCR,A,I,IC)
                  RA=SQRT(A)
                  LJ=LI-1
                  ODD=EVEN=0.0
            C CALCULATION OF NORMALIZATION CONSTANT USING SIMPSONS RULE
                  DO 160 J=2,LI,2
              160 EVEN=EVEN+ZZ(J)*ZZ(J)
                  DO 170 J=3,LJ,2
              170 ODD=ODD+ZZ(J)*ZZ(J)
      165     C SIMPSONS EQUATION  PARABOLIC RULE VERSION HILDEBRAND
```

```
PROGRAM     NORMOD3                                   CDC 6400 FTN V3.0-P314 OPT=1

                AI1=R1*(DL/3.)*(ZZ(1)*ZZ(1)+4.*EVEN+2.*ODD+ZZ(N)*ZZ(N))
                AI2=P2*(1.0/(2.0*RA))
                AND=(1.0/(AI1+AI2))
                AN(IC)=SQRT(AND).
     170    C  SUBROUTINE PLOTS MODE SHAPES
                 CALL SHAPE(N,IC,I)
                RR(IC)=(6.28318530*F*P2*AND)/(CT*AKN(IC)*2.0*RA)
                PV(IC)=(6.28318530*F)/AKN(IC)
                PRINT 16000
                PRINT 17000,AKN(IC),PV(IC),RR(IC)
                PUNCH 17000,AKN(IC),PV(IC),RR(IC)
                PRINT 4000
                JPAGE=JPAGE+1
                IF(JPAGE.EQ.7)  180,185
              180 PRINT 18000
                JPAGE=0
            C TEST TO DETERMINE WETHER ADDITIONAL MODES ARE REQUIRED
              185 AK2=AKN(IC)
                AK1=AK3
                MNU(IC)=I
                IC=IC+1
                I=I+1
                 GO TO 230
              190 PRINT 18000
                IF((AFLAG.EQ.1.).AND.(FLAG.EQ.2.)) GO TO 250
                 AFLAG=1.
                ENDFILE 7
                JPAGE=0
                IK=IC-1
     195        IC=1
               222   JPUN=0
                PUNCH 21400,ZT(INDEX(1)),(AMPMOD(1,K2),K2=1,12),JPUN
               226   JPUN=1
                DO 1190 III=2,INDEN
              1190  PUNCH 21400,ZT(INDEX(III)),(AMPMOD(III,K3),K3=1,12),JPUN
             21400 FORMAT(F10.6,3F20.13/4E20.13/4E20.13/E20.13,I2)
                ENDFILE 7
                PRINT 18000
                IF(FLAG.EQ.2)   GO TO 250
                 GO TO 236
               230   IF(I.LE.(LLP(1)+1))1230,1300
               1230   DO 1235 J=1,N
                IF((ZT(J)-WETEST).LT.SDEP.AND.(ZT(J)+WETEST).GE.SDEP) INDEX(1)=J
                 DO 1232 ILK=1,5
                IF((ZT(J)-WETEST).LT.RD(ILK).AND. (ZT(J)+WETEST).GE.RD(ILK).AND.P
               *(ILK).NE.0.) INDEX(ILK+1)=J
              1232  CONTINUE
              1235  CONTINUE
                INDEN=1
                DO 1236 ILK1=2,6
                IF(INDEX(ILK1).NE.0)INDEN=INDEN+1
               1236  CONTINUE
               1300  AMPMOD(1,(IC-1))=XT(INDEX(1))
                DO 1303 JJ=1,N,ISTEP
     220        IEND=JJ+JSTEP
```

```
PROGRAM      NORMOD3                                    CDC 6400 FTN V3.0-P316 OPT=1

                    IEND=MIN0(IEND,N)
                    PRINT 27000,(ZT(LL),XT(LL),LL=JJ,IEND,INC)
                1303 CONTINUE
                    AFLAG=0.
225             1305 DO 1305 III=2,INDEN
                1305 AMPMOD(III,(IC-1))=XT(INDEX(III))
                    IF(IC.EQ.13) GO TO 190
                 236 IF(I.EQ.IUB+1)   130,140
                 240 FLAG=2
                    GO TO 190
                 250 NF=NF-1
                    ENDFILE 7
                    IF( NF .GE.0)  260,270
                 260 READ 23000  ,F
                    GO TO 30
                 270 IF(GROUVEL.EQ.1.0)  280,9997
                 280 READ 24000  ,FMIN,FMAX,DELF
                    IC=1
                    K=(((FMAX-FMIN)/DELF)+0.5)+5.0
                    ICOUNT=J=0
                 290 ICOUNT=ICOUNT+1
                    I=LB1(ICOUNT)
                    IUB=LB2(ICOUNT)
                    IF(I.EQ.0)   370,300
245              300 IF(I.EQ.IUB+1)   290,310
                 310 F=(FMIN-(2.0*DELF))
                 320 J=J+1
                    AK1=(6.2831853*F)/CT
                    AK2=(6.2831853*F)/C2MIN
                    FD=(39.4784176*F*F)
                    IGV=IZERO=0
                    CALL ITERATE(AK),FD,H,C2D,DLS,HD,HD3,CTD,IT,NCR,R,Z,A,ZZ,DL,IZERO
                   *I)
                    IF(NCR.GE.I)  330,340
                 330 CALL HALF(AK1,AK2,FD,NCR,A,I,IC)
                    DKN(IC,J)=AKN(IC)
                    C(IC,J)=(6.2831853*F)/DKN(IC,J)
                    GO TO 350
                 340 C(IC,J)=0.0
                 350 F=F+DELF
                    IF(J.EQ.K)   360,320
               C    CALL ORDERROR(0.0)
                 360 I=I+1
                    IC=IC+1
                    J=0.
                    GO TO 300
                 370 L=K-2
                    ICOUNT=0
                    IC=1
                    J=2
                    BFLAG=0.0
                 380 ICOUNT=ICOUNT+1
                    I=LB1(ICOUNT)
                    IUB=LB2(ICOUNT)
275                 IF(I.EQ.0)  520,390
```

```
PROGRAM     NOPMOD3                                   CDC 6400 FTN V3.0-P316 OPT=1

            390 J=J+1
                IF(C(IC,J-2).EQ.0.0)  400,450
            400 IF(C(IC,J-1).EQ.0.0)  410,430
            410 IF(C(IC,J).EQ.0.0)    420,440
    280     420 GV(IC,J-2)=10.0E10
                GO TO 470
            430 CP(IC,J-2)=(C(IC,J+1)-C(IC,J-1))/(12.5663707*DELF)
                GO TO 460
            440 CP(IC,J-2)=(-C(IC,J+2)+4.0*C(IC,J+1)-3.0*C(IC,J))/(12.5663707*DEL
               *)
                GO TO 460
            450 CP(IC,J-2)=(-C(IC,J+2)+8.0*C(IC,J+1)-8.0*C(IC,J-1)+C(IC,J-2))/
               *           (75.3982235*DELF)
            460 V(IC,J-2)=(1.0/C(IC,J))-(DKN(IC,J)/C(IC,J))*CP(IC,J-2)
                GV(IC,J-2)=(1.0/V(IC,J-2))
            470 IF(J.EQ.L)    480,390
            480 MNU(IC)=I
                IC=IC+1
                I=I+1
                J=2
                IF(IC.EQ.13)    490,510
            490 PRINT 18000
                IK=IC-1
                PRINT 25000
    300         PRINT 11000
                PRINT 20000,(MNU(J),J=1,IK)
                PRINT 26000,LFRF,(LGRU, J2=1,IK)
                F=FMIN
                DO 500 N=3,L
                PRINT 22000,F,(GV(J,N-2),J=1,IK)
            500 F=F+DELF
                IF(BFLAG.EQ.2.0)    GO TO 530
            510 IF(I.EQ.IUB+1)    380,390
            520 BFLAG=2.0
                GO TO 490
          C  SUBROUTINE PLOTS GROUP VELOCITIES
            530 IF(GRUPLT.EQ.1.0)  540,9997
            540 CALL GROUP(     IC,K,FMIN,FMAX,DELF)
           9997 CONTINUE
    415    9998   CALL PLOT(20.,0.,3,1)
           9999  CONTINUE
                 END
```

CDC 6400 FTN V3.0-P316 OPT=1

```
      SUBROUTINE GROUP(IC,K,FMIN,FMAX,DELF)
      COMMON/AA/CP(20,20),V(20,20),GV(20,20),C(20,20),DKN(20,20)
      KK=K-4
    5 C  CALCULATION TO FIND MAX. AND MIN. GROUP VELOCITIES
      GVMAX=0.0
      DO 20 I=1,IC
      DO 10 J=1,KK
   10 IF(GV(I,J).GE.GVMAX.AND.GV(I,J).NE.10.0**10)  GVMAX=GV(I,J)
   20 CONTINUE
      GVMIN=GVMAX
      DO 40 I=1,IC
      DO 30 J=1,KK
   30 IF(GV(I,J).LE.GVMIN)  GVMIN=GV(I,J)
   40 CONTINUE
    C SCALING OF GROUP VELOCITIES
      IGVMIN=GVMIN/10.0
      GVMIN=IGVMIN*10.0
      GVDIFF=GVMAX-GVMIN
      IF(GVDIFF.LE.10.0)  50,60
   50 GVMI=1.0
      SCALE=1.0
      GO TO 120
   60 IF(GVDIFF.LE.20.0)  70,80
   70 GVMI=2.0
      SCALE=2.0
      GO TO 120
      ) IF(GVDIFF.LE.40.0)  90,100
   90 GVMI=4.0
      SCALE=4.0
      GO TO 120
  100 IF(GVDIFF.LE.60.0)  110,115
  110 GVMI=6.0
      SCALE=6.0
      GO TO 120
  115 IF(GVDIFF.LE.80.0)  116,120
  116 GVMI=8.0
      SCALE=8.0
    C SCALING OF FREQUENCIES
  120 FDIFF=FMAX-FMIN
      IF(FDIFF.LE.10.0)  130,140
  130 FNI=1.0
      FSCALE=1.0
      GO TO 260
  140 IF(FDIFF.LE.50.0)  150,160
  150 FNI=5.0
      FSCALE=5.0
      GO TO 260
  160 IF(FDIFF.LE.100.0)  170,180
  170 FNI=10.0
      FSCALE=10.0
      GO TO 260
  180 IF(FDIFF.LE.250.0)  190,200
  190 FNI=25.0
   55 FSCALE=25.0
```

```
  SUBROUTINE  GROUP                                   CDC 6400 FTN V3.0-P316 OPT=1

                    GO TO 260
                200 IF(FDIFF.LE.500.0)  210,220
                210 FNI=50.0
                    FSCALE=50.0
                    GO TO 260
                220 IF(FDIFF.LE.1000.0)  230,240
                230 FNI=100.0
                    FSCALE=100.0
                    GO TO 260
                240 IF(FDIFF.LE.1500.0)  250,260
                250 FNI=150.0
                    FSCALE=150.0
               C PLOT PACKAGE FOR GROUP VELOCITIES
                260  CALL PLOT(5.5,-10.,3,1)
                    CALL AXIS(0.0,0.0,21HGROUP VELOCITY(M/SEC),21,10.0,90.0,GVMIN,
                   *GVMI)
                    CALL AXIS(0.0,0.0,13HFREQUENCY(HZ),-13,10.0,0.0,    FMIN,FNI)
                    DO 350 I=1,IC
                    DUMF=FMIN
                    DO 340 J=1,KK
                    X=(DUMF-FMIN)/FSCALE
                    IF(GV(I,J).EQ.10.0**10)  280,290
                280 DUMF=DUMF+DELF
                    CALL PLOT(X,Y,3,-1)
                    GO TO 340
                290 Y=(GV(I,J)-GVMIN)/SCALE
                    IF(GV(I,J-1).EQ.10.0**10)  294,295
                294 CALL PLOT(X,Y,0,-1)
                295 IF(J.EQ.1)  300,310
                300 CALL PLOT(X,Y,3,-1)
                    GO TO 320
                310 CALL PLOT(X,Y,2,-1)
                320 DUMF=DUMF+DELF
                    IF(J.EQ.KK)  330,340
                330 X=X+0.1
                    Y=Y-0.03
                    CALL SYMBL4(X,Y,0.07,4HMODE,0.0,4)
                    X=X+0.5
                     XIM=FLOAT(I)
                    CALL NUMBR(X,Y,0.07,XIM,0.0,-1)
                340 CONTINUE
                350 CONTINUE
                    CALL PLOT(15.0,0.0,3,1)
                360 RETURN
                    END
```

```
 SUBROUTINE  HALF                                  CDC 6400 FTN V3.0-P316 OPT=1

                SUBROUTINE HALF(AK1,AK2,FD,NCR,A,I,IC)

                COMMON/1/ XT(   3100)
                COMMON/2/Z2N(3100),          C2D(3100)
 5          5   COMMON/AA/CP(20,20),V(20,20),GV(20,20),C(20,20),DKN(20,20)
                COMMON/AB/Z1(50),C1(50),Z1N(50),LLB(10),LUB(10),MMU(30),LB1(10),
               *LB2(10)
                COMMON/AC/AKN( 12),BB( 12),BV( 12),AN( 12),ZF(12)
                COMMON/AD/EPSILON,H,HD,HD3,DL,DLS,R,IT,CT,CTD,MODSHAP ,MODEPLT,
10             *GROVEL,GRUPLT,IZERO,IGV
                EQUIVALENCE(XT,ZZ)
             1000 FORMAT(*   UPPER AMPLITUDES ARE ZEROED FOR THIS MODE *)
               C HALF INTERVAL SEARCH FOR THE KNS ASSOCIATED WITH THE MODES DESIRED
                JUMP=0
15            10 AK1=AK2-AK1
                DIVIDE=2.0
               11 BKN=AK1+(AK1/DIVIDE)
                IZERO=0
                CALL ITERATE(BKN,FD,H,C2D,DLS,HD,HD3,CTD,IT,NCR,R,Z,A,ZZ,DL,IZER
20             *I)
                IF(JUMP.EQ.1)  40,20
               20 IF(NCR.EQ.I-1)  50,30
               30 IF(NCR.LT.I-1)  35,36
               35 DIVIDE=DIVIDE+1.0
25              GO TO 11
               36 AK1=BKN
                GO TO 10
               40 IF(NCR.EQ.I)  70,45
               45 IF(NCR.LT.I)  35,36
30         30  50 JUMP=JUMP+1
               60 AK2=BKN
                 ZT1=Z
                GO TO 10
               70 IF(Z)  80,160,90
35             80 AKNL=BKN
                ZL=Z
                AKNR=AK2
                ZR=ZT1
                 GO TO 98
40             90 AKNR=BKN
                ZR=Z
                AKNL=AK2
                ZL=ZT1
               98    CONTINUE
45            C---------------------------------------
              C---ADDED 3/2   HALVING  APPROACH
                IF(ABS(ZL).LT.1.E50.OR.ZR.LT.1.E50) GO TO 100
                DIFF2=(AKNR-AKNL)/2.
                 AKA=AKNL+DIFF2
50            101    IZERO=0
                CALL ITERATE(AKA,FD,H,C2D,DLS,HD,HD3,CTD,IT,NCR,R,Z,A,ZZ,DL,IZERO
               *I)
                 IF(ABS(Z).LE.EPSILON) 170,91
               91  IF(ZR*Z)92,94,94
55         55  92   DIFF=(AKNR-AKA)/2.
```

```
 SUBROUTINE  HALF                                        CDC 6400 FTN V3.0-P316 OPT=1

                    IF(ABS(DIFF).LE.1.E-12) 160,93
                93   AKNL=AKA
                     ZL=Z
                     AKA=AKA+DIFF
60          60       GO TO 101
                94   DIFF=(AKA-AKNL)/2.
                    IF(ABS(DIFF).LE.1.E-12) 160,95
                95   AKNR=AKA
                     AKA=AKA-DIFF
65                   ZR=Z
                       GO TO 101
               C-------------------------------------
               C LOCATING THE KN ASSOCIATED WITH THE MODE DESIRED USING THE KNL AND K
               C      FOUND ABOVE BY THE METHOD OF FALSE POSITION
70               100 AKA=AKNL+(ZL*(AKNR-AKNL))/(ZL-ZR)
                1001  FORMAT(I5,8F18.10)
                     IZERO=0
                     CALL ITERATE(AKA,FD,H,C2D,DLS,HD,HD3,CTD,IT,NCR,R,Z,A,ZZ,DL,IZER
                    *I)
75                   IF(ABS (Z).LE.EPSILON)  170,110
                 110 IF(ZR*Z)  120,140,140
                 120 IF(ABS (AKNL-AKA).LE.1.0E-12)  160,130
                 130 ZL=Z
                     AKNL=AKA
80          80       GO TO 100
                 140 IF(ABS (AKNR-AKA).LE.1.0E-12)  160,150
                 150 ZR=Z
                     AKNR=AKA
                     GO TO 100
95               160 IZERO=1
                     PRINT 1000
                 165 CALL ITERATE(AKA,FD,H,C2D,DLS,HD,HD3,CTD,IT,NCR,R,Z,A,ZZ,DL,IZER(
                    *I)
                 170 AKN(IC)=AKA
100                  ZF(IC)=Z
                     IGV=0
                     RETURN
                100  END
```

CDC 6400 FTN V3.0-P316 OPT=1

```
      SUBROUTINE ITERATE(AKN,FD,H,C2D,DLS,HD,HD3,CTD,IT,NCR,R,Z,A,ZZ,
     *IZERO,I)
      DIMENSION ZZ(IT),C2D(IT)
5     C SUBROUTINE USES A FINITE DIFFERENCE TECHNIQUE TO NUMERICALLY FIND TH
      C     SHAPE ASSOCIATED WITH A GIVEN KN
      C CONSTANT IN FRONT OF FUNCTION ASSUMED TO BE ONE INITIALLY
      MAXFLAG=0
      N=IT
10    A=HD*ABS (AKN*AKN-(FD/CTD))
      ZM1=R
      XND=HD*((FD/C2D(IT))-(AKN*AKN))
      XNW=HD*((FD/C2D(IT-1))-(AKN*AKN))
      C----NEXT CARD ADDED AS TEST NOL 3/6/73
15    XNW=HD*(((FD*(SQRT(C2D(IT-1))))/(C2D(IT)**1.5))-(AKN*AKN))
      C TAYLOR SERIES EXPANSION TO OBTAIN NEXT Z
      Z=ZM1*(1.+((DL/R)*SQRT(A))-(5.*DLS*XND/6.)+(DLS*XNW/3.)-
     *(((DL*DLS)/6.0)*SQRT(A)*XND*(1./R)))
      NCR=0
20    IF(ZM1*Z.LE.0.0) 10,20
   10 NCR=NCR+1
   20 PS=(2.0-(HD*DLS)*((FD/C2D(IT-1))-(AKN*AKN)))
      ZP1=(PS*Z)-ZM1
      IF(Z*ZP1.LE.0.0) 30,40
2'    30 NCR=NCR+1
   40 ZZ(IT)=ZM1
      ZM1=Z
      Z=ZP1
      C****CHANGE  NOL  4/6  REMOVE    DOWN TO 77
30    80 IT=IT-1
      IF(IT-2.LT.0)  90,20
   90 IT=N
      ZZ(2)=ZM1
      ZZ(1)=Z
35    GO TO 130
  100 IT=IT-1
      IF(IT-2.LT.0)  120,110
  110 ZZ(IT)=0.0
      GO TO 100
40    120 IT=N
      ZZ(1)=Z=0.0
      ZZ(2)=ZM1=0.0
  130 CONTINUE
      C*****CHANGE NOL  4/6   ADD TO 140
45    IF(IZERO.NE.1) GO TO 140
      IF(NCR.GT.(I-1)) 131,136
  131 DO 134  IT=1,N
      IF((ZZ(IT)*ZZ(IT+1)).LE.0.) GO TO 135
      ZZ(IT)=0.
50    134 CONTINUE
  135 ZZ(IT)=0.
      GO TO 1139
  136 DO 139  IT=1,N
      IF(ABS(ZZ(IT+1)).GT.ABS(ZZ(IT))) GO TO 1139
55    55    ZZ(IT)=0.
```

```
      SUBROUTINE  ITERATE                                  CDC 6400 FTN V3.0-P316 OPT=1

                   139     CONTINUE
                  1139    IT=N
                   140     CONTINUE
                          RETURN
60          60            END
```

CDC 6400 FTN V3.0-P316 OPT=1

```
      SUBROUTINE SHAPE(N,I,IMODE)
      COMMON/1/ XT(   3100)
      COMMON/2/Z2N(3100),          C2D(3100)
5     COMMON/AA/CP(20,20),V(20,20),GV(20,20),C(20,20),DKN(20,20)
      COMMON/AB/Z1(50),C1(50),Z1N(50),LLB(10),LUB(10),MNU(30),LB1(10),
     *LB2(10)
      COMMON/AC/AKN( 12),PR( 12),PV( 12),AN( 12),ZF(12)
      COMMON/AD/EPSILON,H,HD,HD3,DL,DLS,R,IT,CT,CTD,MODSHAP ,MODEPLT,
10   *GRUVFL,GRUPLT,IZERO,IGV
      COMMON/AE/LDEPTH   ,LAMP   ,LGRU   ,LFRE
      DIMENSION ZT(3100),ZZ(3100)
      EQUIVALENCE(Z2N,ZT),(XT,ZZ)
C  I PERTAINS TO IC IN MAIN PROGRAM
15    DO 10 JT=1,N
      XT(  JT)=ZZ(JT)*AN(I)
   10 ZT(JT)=Z2N(JT)
      WRITE(9,12)IMODE
      WRITE(9,14)(ZT(LL),XT(LL),LL=1,N)
20    12  FORMAT(I10)
      14  FORMAT(4E20.10)
      IF(MODEPLT.EQ.1)  20,40
C PLOT PACKAGE FOR MODE SHAPES
   20 IF(IZERO.EQ.1)  24,25
25    24 XB=6.5
      XD=-2.0
      XL=4.0
      XI=-4.0
      GO TO 26
30  30  25 XB=4.5
      XD=-1.0
      XL=2.0
      XI=-2.0
   26 CALL PLOT( XB,0.0 ,3,1)
35    CALL AXIS(  XD,0.0,20HNORMALIZED AMPLITUDE,20, XL,0.0,XI,2.0)
      CALL AXIS(0.0,-5.0,16HNORMALIZED DEPTH,1.,5.0,90.0,  ,  1.0,-0.2)
      CALL SYMBL4(-0.5,-6.0,0.095,4HMODE,0.0,4)
      XIB=FLOAT(IMODE)
      CALL NUMBR(0.25,-6.0,0.095,XIB,0.0,-1)
40    NN=3
      DO 30 JT=1,N
      X=XT(  JT)/2.0
      Y=-ZT(JT)*5.0
      CALL PLOT(X,Y,NN,-1)
45  45  30 NN=2
   40 RETURN
      END
```

CDC 6400 FTN V3.0-P316 OPT=1

```
      SUBROUTINE ZCINTER (ND,N,F,C2MIN,PROPLT)
      COMMON/1/ XT(   3100)
      COMMON/2/Z2N(3100),          C2D(3100)
      COMMON/AA/CP(20,20),V(20,20),GV(20,20),C(20,20),DKN(20,20)
      COMMON/AB/Z1(50),C1(50),Z1N(50),LLB(10),LUB(10),MMU(30),LR1(10),
     *LR2(10)
      COMMON/AC/AKN( 12),PR( 12),PV( 12),AN( 12),ZF(12)
      COMMON/AD/EPSILON,H,HD,HD3,DL,DLS,P,IT,CT,CTD,MODSHAP ,MODEPLT,
     *GRUVEL,GRUPLT,IZERO,IGV
      COMMON/AE/LDEPTH   ,LAMP   ,LGRU   ,LFRE
C LINEAR INTERPOLATION
      DO 50 J=1,N
      DO 40 I=1,ND
      IF(Z1N(I).EQ.Z2N(J)) 10,20
   10  C2D(J)=C1(I)
      GO TO 50
   20 IF(Z1N(I).GT.Z2N(J)) 30,40
   30 ZGT=Z1N(I)
      ZLT=Z1N(I-1)
      CGT=C1(I)
      CLT=C1(I-1)
C EQUATION USED FOR LINEAR INTERPOLATING
      C2D(J)=((Z2N(J)-ZLT)/(ZGT-ZLT))*(CGT-CLT) + CLT
      GO TO 50
   40 CONTINUE
   50 CONTINUE
C SEARCH FOR MINIMUM SOUND VELOCITY ON SOUND VELOCITY PROFILE (ALSO FI
C     MAXIMUM SOUND VELOCITY)
      C2MAX=0.0
      DO 60 I=1,N
   60 IF(C2D(I).GE.C2MAX)  C2MAX=C2D(I)
      C2MIN=C2MAX
      DO 70 I=1,N
   70 IF(C2D(I).LE.C2MIN)  C2MIN=C2D(I)
C PLOT PACKAGE FOR SOUND SPEED PROFILE
      IF(PROPLT.EQ.1.0)  75,200
   75 CDIFF=C2MAX-C2MIN
      IC2M=C2MIN/10.0
      C2M=IC2M*10.0
      IF(CDIFF.LE.5.0)  80,90
   80 PL=2.5
      PI=0.5
      C2MI=1.0
      SCALE=0.5
      GO TO 170
   90 IF(CDIFF.LE.10.0)  100,110
  100 PL=2.5
      PI=0.5
      C2MI=2.0
      SCALE=0.25
      GO TO 170
  110 IF(CDIFF.LE.25.0)  120,130
  120 PL=2.5
      PI=0.5
```

```
      SUBROUTINE  ZCINTER                                   CDC 6400 FTN V3.0-P316 OPT=1

                      C2MI=5.0
                      SCALE=0.1
                      GO TO 170
                  130 IF(CDIFF.LE.50.0)  140,150
60          60      140 PL=5.0
                      PI=0.5
                      C2MI=5.0
                      SCALE=0.1
                      GO TO 170
65                150 IF(CDIFF.LE.100.0)  160,170
                  160 PL=5.0
                      PI=0.5
                      C2MI=10.0
                      SCALE=0.05
70                170   CALL PLOT(0.,0.,3,1)
                      PL=PL+PI
                      CALL AXIS(0.0,-5.0,16HNORMALIZED DEPTH,16,5.0,90.0,     1.0,-0.2)
                      CALL AXIS(0.0,0.0,18HSOUND SPEED(M/SEC),18,PL ,0.0,     C2M,C2MI)
                      NN=3
75                    DO 180 I=1,N
                      X=(C2D(I)-C2M)*SCALE
                      Y=-Z2N(I)*5.0
                      CALL PLOT(X,Y,NN,-1)
                  180 NN=2
80                     CALL PLOT(2.5,0.,3,1)
                  200 CONTINUE
                       DO 210 J=1,N
                  210   C2D(J)=C2D(J)*C2D(J)
                       RETURN
85          85       END
```

SUBROUTINE LINE CDC 6400 FTN V3.0-P316 OPT=1

```
      SUBROUTINE LINE (X,Y,N,K)
      DIMENSION X(1),Y(1)
      I3=3
      NP=N*K
5     5 DO 10 I=1,NP,K
      CALL PLOT (X(I),Y(I),I3,-1)
   10 I3=2
      RETURN
       END
```

PROGRAM NORMSUM CDC 6400 FTN V3.0-P

```
      PROGRAM NORMSUM(INPUT,OUTPUT,TAPE7       ,TAPE1)

C     TAPE7 IS OUTPUT FILE OR TAPE FROM NORMAL MODE PROG.
5     5
C     SR- STARTING RANGE FOR CALC.
C     RINC-RANGE INCREMENT
C     NR-NUMBER OF INCREMENTS

10    C     PRD(1,2,...,5) ARE UP TO 5 RECEIVER DEPTHS
C     SOURCE IS SOURCE DEPTH
C     ABOVE MUST BE ONE OF DEPTHS USED IN NORMAL MODE PROG.

C     NPRIN .GT. 0--PRINT RESULTS
15    C     NPLOT .GT. 0.--PLOT RESULTS
C     PRINTR-INITIAL RANGE ON PLOT
C     PRINC-RANGE INCREMENT/INCH ON PLOT
C     PDBINT-INITIAL PROP LOSS AT BOTTOM OF PLOT
C     PDBIN- PROP LOSS INCREMENT/INCH
20    C     CARD READ STATEMENTS-LINES 28, 31, 33,35

        COMPLEX TEST
       COMPLEX SUM1,PS,FS,   Z,CSI4
      DIMENSIONAKN(1000),                    XTS(1000),XTR(1000,
25    DIMENSIONPRD(5),TS(1000),FS(500),TL(500),RD(5),AXT(12)
       DIMENSION IP(5),IREND(5)
      CALL PLOTS(0.,0.,1)
       READ 1000,SP,RINC,NR
 1000  FORMAT(2F10.3,I5)
30    30      IF(NR.GT.500) STOP 5
       READ 1020,(PRD(IL),IL=1,5)
 1020  FORMAT(5F10.3)
       READ 1021,SOURCE
 1021  FORMAT(F10.3)
35     READ 1010,NPRIN,NPLOT,PRINTR,PRINC,PDBINT,PDBIN
 1010  FORMAT(2I5,4F10.3)
      READ(7,7600)SDEP,(PD(IL),IL=1,5),LI
 7600   FORMAT(6F10.6,I5)
       WETEST=.5/FLOAT(LI)
40     READ(7,11500)F,P1,H,NCR
        NCR1=NCR
11500  FORMAT(3F10.3,I4)

       DO 7 I=1,5
45     IR(I)=1
    7   PRD(I)=PRD(I)/H
       SOURCE=SOURCE/H
       PI=3.14159265359
       CSI4= CMPLX(0.,-PI/4.,
50     SUM1=(P1/H)*SQRT(2.0*3.141592)*CEXP(CSI4)
       J=0
       IS=1
   10  J=J+1
      READ(7,2000)AKN(J),PV,RR
55    55 2000  FORMAT(3E20.13)
```

```
PROGRAM     NORMSUM                                   CDC 6400 FTN V3.0-P316 OPT=1   C

                IF(EOF(7))20,10
             20 J=J-1
             25   READ(7,3000)ADFP,(AXT(III),III=1,12),IF1
           3000 FORMAT(F10.6,3F20.13/4E20.13/4E20.13/E20.13,I2)
          60    IF(EOF(7))30,35
             30 J=J+1
                READ(7,2000)AKN(J),PV,RR
                 IF(EOF(7))60,10
             35  IF(IF1.EQ.0) GO TO 45
                DO 37  IJK=1,5
                IF((IF1.EQ.1).AND.(ABS(RD(IJK)-ADEP).LT.WETEST).AND.(RD(IJK).NE.0
               *)) GO TO 38
             37 CONTINUE
                STOP 6
             38 IREND(IJK)=IR(IJK)+11
                ITP=IREND(IJK)
                ITR=IR(IJK)
                ICO=0
                DO  39  IP=ITR,ITP
                ICO=ICO+1
             39 XTR(IP,IJK)=AXT(ICO)
                IR(IJK)=IR(IJK)+12
                GO TO 25
             45   IEND=IS+11
                ICO=0
                DO 47  IJS=IS,IEND
                ICO=ICO+1
             47 XTS(IJS)=AXT(ICO)
                IS=IS+12
          85    GO TO 25
             60 IF(ABS(SOURCE-SDEP).LT.WETEST) GO TO 64
                DO 62 IC11=1,5
                IF(ABS(SOURCE-RD(IC11)).LT.WETEST) GO TO 63
             62  CONTINUE
                STOP 3
             63  DO 1061 IJJ1=1,1000
                XTS(IJJ1)=XTR(IJJ1,IC11)
           1061 CONTINUE
             64 DO 800 IC=1,5
                IF(PRD(IC).EQ.0.) STOP 2
                R=SR
                DO 65 I0=1,1000
             65 TS(I0)=0.
                DO 66 I01=1,500
             66  FS(I01)=CMPLX(0.,0.)
                 DO 90  IJ=1,5
                IF(ABS(PRD(IC)-RD(IJ)).LT.WETEST) GO TO 95
             90  CONTINUE
           C---IJ IS INDICATOR FOR XTR(1000,IJ) ARRAY
             95  DO 100 IM=1,NCR1
            100  TS(IM)=XTS(IM)*XTR(IM,IJ)/SQRT(AKN(IM))
                DO 200 JJ=1,NR
                 PS= CMPLX(0.,0.)
                DO 180  IJJ=1,NCR1
          110   Z=AKN(IJJ)*R* CMPLX(0.,1.)
```

```
PROGRAM     NORMSUM                                   CDC 6400 FTN V3.0-P316 OPT=1   0

            180    PS=PS+TS(IJJ)*CEXP(Z)
                   FS(JJ)=FS(JJ)+(SUM)/SORT(R))*PS
                   TL(JJ)=-20.*ALOG10(CABS(FS(JJ)))

        115        TL(JJ)=TL(JJ)+20.*ALOG10(1./.9154)
                C-----CONVERTS FROM  RE 1 METER TO RE 1 YARD
                 200  R=R+RINC
                      RA=PRD(IC)*H
                      SA=SOURCE*H
                      PRINT 2500  ,SA,RA
                     IF(NPLOT.EQ.0 ) GO TO 400
                     CALL PLOT(2.,0.,3)
                     CALL SYMBL4(0.,3.,.14,13HSOURCE DEPTH=,90.,13)
                     CALL NUMBR(0.,5.2,.14,SA,90.,1)
                     CALL PLOT(1.,0.,3)
                     CALL SYMBL4(0.,3.,.14,15HRECEIVER DEPTH=,90.,15)
                     CALL NUMBR(0.,5.5,.14,RA,90.,1)
                     CALL PLOT(1.,0.,3)
                     CALL SYMBL4(0.,3.,.14,14HFREQUENCY(HZ)=,90.,14)
                     CALL NUMBR(0.,5.5,.14,F,90.,-1)
                     CALL PLOT(2.,0.,3)

                     CALL AXIS(0.,0.,9HRANGE(KM),-9,10.,0.,PRINTR,PRINC)

                     CALL AXIS(0.,0.,20HPROPAGATION LOSS(DB),20,8.,90.,PDBINT,PDBIN)
                     CALL PLOT(0.,0.,3,-1)
                 400  CONTINUE
                2500 FORMAT(28X,*NORMAL MODE PROPAGATION LOSS RE 1 YD*//25X,*SOURCE DE
                    *TH=*,F10.3,10X,*RECFIVER DEPTH=*,F10.3//30X,*  RANGE    *,*TRANSMI
        140         *SION LOSS(DB)*)
                       R=SR
                     NN=3
                      DO 600 IMP=1,NR
                     IF(NPRIN.EQ.0) GO TO  500
                      PRINT 3500,R,TL(IMP)
                 500 IF(NPLOT.EQ.0) GO TO 600
                     X=((R/(1.E+3))-PRINTR)/PRINC
                      Y=(PDBINT-TL(IMP))/ABS(PDBIN)
                     Y=AMAX1(0.,Y)
                     CALL PLOT(X,Y,NN,-1)
                     NN=2
                 600  R=R+RINC
                3500  FORMAT(25X,F10.3, 5X,F10.3)
                     CALL PLOT(11.,0.,3,1)
        155      800  CONTINUE
                     END
```

Appendix IV: Evaluation of Second Range Derivative

In order to evaluate pressure on the caustic (Equation 4.1), we need to evaluate $\partial^2 R/\partial C_v^2$ and obtain $\partial^3 W_c/\partial \xi^3$ (Equation 4.15). $\partial^3 W_c/\partial \xi^3$ is defined in terms of the derivative of an integral:

$$\frac{\partial^3 W_c}{\partial \xi^3} = \left[\frac{\partial^3}{\partial \xi^3}\int_{z_T}^{z_0}\left[n^2(z)-\xi^2\right]^{1/2}dz\right]_{\xi=\xi_a} + \left[\frac{\partial^3}{\partial \xi^3}\int_{z_T}^{z_c}\left[n^2(z)-\xi^2\right]^{1/2}dz\right]_{\xi=\xi_a} \quad \text{(IV.1)}$$

But the integral can be split up into several integrals, each evaluated in a different sound velocity profile layer:

$$\frac{\partial^3 W_c}{\partial \xi^3} = \left[\frac{\partial^3}{\partial \xi^3}\left\{\int_{z_1}^{z_0}A(z)dz + \int_{z_2}^{z_1}A(z)dz + \cdots + \int_{z_T}^{z_{T-1}}A(z)dz + \int_{z_1}^{z_c}A(z)dz + \cdots + \int_{z_T}^{z_{T-1}}A(z)dz\right\}\right]_{\xi=\xi_a} \quad \text{(IV.2)}$$

where $A(z) = \left[n^2(z)-\xi^2\right]^{1/2}$

Thus we can evaluate $\partial^3 W_c/\partial \xi^3$, or $\partial^2 R/\partial C_v^2$, in each layer and then sum to obtain $\partial^3 W_c/\partial \xi^3$.

In CONGRATS, ΔR in a layer from z_1 to z_2 is defined as (39):

$$R = |\widetilde{\Delta R}| = \frac{2D}{C_v}\left\{\left(1+g_2\overline{\Delta z}\right) + p\left[\frac{1}{c}\left(\frac{H}{2D}-1\right)\right]\right\} \quad \text{(IV.3)}$$

where

$$\overline{\Delta z} = \frac{\Delta z_1 + \Delta z_2}{2}, \qquad \Delta z_a = z - z_a \quad \text{(IV.3A)}$$

$$D = \frac{z_2 - z_1}{Y_1 Y_2 + Y_2^{1/2}} \qquad Y_a = \frac{1}{c}\left(X_a^2 + q\right) \quad \text{(IV.3B)}$$

$$X_a = c\,\Delta z_a + b$$

$$q = ac - b^2$$

$$a = v_0 - C_v^{-2}$$

$$b = a g_2 + \tfrac{1}{2} g_0$$

$$c = a g_2^2 + g_1$$

$$p = c - g_2 b = g_1 - \tfrac{1}{2} g_0 g_2$$

H is one of several results depending on the sign of c and q.

g_0, g_1, g_2 and v_0 are the four parameters (Equation 3.1) in the particular layer being considered.

Weinberg then obtains $\partial R/\partial C_v$, the derivative necessary for amplitude calculation along a ray:

$$\frac{\partial R}{\partial C_v} = \left(\frac{1}{D}\frac{\partial D}{\partial C_v} - \frac{1}{C_v}\right)R + \frac{2D}{C}\left\{g_2 \frac{\partial \bar{\Delta z}}{\partial C_v} + p \frac{\partial}{\partial C_v}\left[\frac{1}{c}\left(\frac{H}{2D} - 1\right)\right]\right\} \quad \text{(IV.4)}$$

He then evaluates the necessary derivatives:

$$\frac{\partial D}{\partial C_v}, \quad \frac{\partial \bar{\Delta z}}{\partial C_v}, \text{ and } \frac{\partial}{\partial C_v}\left[\left(\frac{H}{2D} - 1\right)\frac{1}{c}\right] \quad \text{(IV.5)}$$

for the possible values of c and q, i.e. positive, negative, or zero. For calculation on a caustic, we need one more derivative, $\partial^2 R/\partial C_v^2$. Taking the derivative of Equation (IV.4) yields:

$$\frac{\partial^2 R}{\partial C_v^2} = \frac{-1}{D^2}\left[\frac{\partial D}{\partial C_v}\right]^2 R + \frac{R}{D}\frac{\partial^2 D}{\partial C_v^2} + \frac{R}{C_v^2} + \frac{1}{D}\frac{\partial D}{\partial C_v}\frac{\partial R}{\partial C_v}$$

$$- \frac{1}{C_v}\frac{\partial R}{\partial C_v} + \left\{\frac{2}{C_v}\frac{\partial D}{\partial C_v} - \frac{2D}{C_v^2}\right\}\left\{g_2 \frac{\partial \bar{\Delta z}}{\partial C_v} + p \frac{\partial}{\partial C_v}\left[\frac{1}{c}\left(\frac{H}{2D} - 1\right)\right]\right\}$$

$$+ \frac{2Dg_2}{C_v}\frac{\partial^2 \bar{\Delta z}}{\partial C_v^2} + \frac{2Dp}{C_v}\frac{\partial^2}{\partial C_v^2}\left[\frac{1}{c}\left(\frac{H}{2D} - 1\right)\right] \quad \text{(IV.6)}$$

New derivatives required are:

$$\frac{\partial^2 D}{\partial C_v^2} \; , \; \frac{\partial^2 \Delta\bar{z}}{\partial C_v^2} \; , \; \frac{\partial^2}{\partial C_v^2}\left[\frac{1}{c}\left(\frac{H}{zD}-1\right)\right] \tag{IV.7}$$

B: $\dfrac{\partial^2 D}{\partial C_v^2}$

For $c \neq 0$

$$\frac{\partial D}{\partial C_v} = \frac{-D}{2\left[Y_1^{1/2}+Y_2^{1/2}\right]}\left\{\frac{\partial Y_1/\partial C_v}{Y_1^{1/2}} + \frac{\partial Y_2/\partial C_v}{Y_2^{1/2}}\right\} \tag{IV.8}$$

Then

$$\frac{\partial^2 D}{\partial C_v^2} = \frac{D}{2\left[Y_1^{1/2}+Y_2^{1/2}\right]^2}\left\{\frac{\partial Y_1/\partial C_v}{Y_1^{1/2}} + \frac{\partial Y_2/\partial C_v}{Y_2^{1/2}}\right\}^2 \tag{IV.9}$$

$$\frac{-D}{2\left[Y_1^{1/2}+Y_2^{1/2}\right]}\left\{\frac{\partial^2 Y_1/\partial C_v^2}{Y_1^{1/2}} + \frac{\partial^2 Y_2/\partial C_v^2}{Y_2^{1/2}} - \frac{1}{2}Y_1^{3/2}\left[\frac{\partial Y_1}{\partial C_v}\right]^2 - \frac{1}{2}Y_2^{3/2}\left[\frac{\partial Y_2}{\partial C_v}\right]^2\right\}$$

So we also need $\partial^2 Y_2/\partial C_v^2$.

For c = 0 (Ray vertexes):

$$\frac{\partial Y_2}{\partial C_v} = 0 \quad , \quad Y_2 = 0 \tag{IV.10}$$

Therefore terms multiplied by $\dfrac{\partial Y_2}{\partial C_v}$, or by Y_2 , are zero.

C: $\dfrac{\partial^2 \Delta\bar{z}}{\partial C_v^2}$

From Equation (IV.3A)

$$\frac{\partial \Delta\bar{z}}{\partial C_v} = \frac{1}{2}\frac{\partial z}{\partial C_v} \tag{IV.11}$$

So $$\frac{\partial^2 \Delta\bar{z}}{\partial C_v^2} = \frac{1}{2}\frac{\partial^2 z}{\partial C_v} \tag{IV.12}$$

The quantity $\frac{\partial^2 \overline{\Delta z}}{\partial c_v^2}$ is non-zero only in the layer in which the ray turns. Only here will z_2 be a function of c_v.

D: $\frac{\partial^2 Y}{\partial c_v^2}$

From Equation (IV.3B)

$$\frac{\partial Y_a}{\partial c_v} = (1 + g_2 \Delta z_a)^2 \frac{\partial a}{\partial c_v} \tag{IV.13}$$

except for turning point layer where

$$\frac{\partial Y_2}{\partial c_v} = 0 \tag{IV.14}$$

Then for a non vertex layer $\left(\frac{\partial \overline{\Delta z}_a}{\partial c_v} = 0\right)$

$$\frac{\partial^2 Y_a}{\partial c_v^2} = (1 + g_2 \Delta z_a)^2 \frac{\partial^2 a}{\partial c_v^2} \tag{IV.15}$$

For a vertex layer

$$\frac{\partial z_2}{\partial c_v} = -\frac{(1 + g_2 \Delta z_2)^2}{2 X_2} \frac{\partial a}{\partial c_v} \tag{IV.16}$$

Then

$$\frac{\partial^2 Y_2}{\partial c_v^2} = -g_2 \left(\frac{1 + g_2 \Delta z_2}{X_2}\right)^3 \left[\frac{\partial a}{\partial c_v}\right]^2 + (1 + g_2 \Delta z_2)^2 \frac{\partial^2 a}{\partial c_v^2} \tag{IV.17}$$

Since

$$\frac{\partial a}{\partial c_v} = 2 c_v^{-3} \quad , \quad \frac{\partial^2 a}{\partial c_v^2} = -6 c_v^{-4} \tag{IV.18}$$

E: $\frac{\partial^2}{\partial c_v^2}\left[\frac{1}{c}\left(\frac{H}{2D} - 1\right)\right]$

Starting with $\left[\frac{1}{c}\left(\frac{H}{2D} - 1\right)\right]$, taking two derivatives and recombining several terms, it can be shown that

$$\frac{\partial^2}{\partial c_v^2}\left[\frac{1}{c}\left(\frac{H}{2D} - 1\right)\right] = -\frac{2}{c}\frac{\partial c}{\partial c_v}\left\{\frac{\partial}{\partial c_v}\left[\frac{1}{c}\left(\frac{H}{2D} - 1\right)\right]\right\} + \left[\frac{\partial D}{\partial c_v}\frac{\partial H}{\partial c_v}\right]\left\{-\frac{1}{cD^2}\right\} - \frac{1}{c^2}\left[\frac{H}{2D} - 1\right]\frac{\partial^2 c}{\partial c_v^2} \tag{IV.19}$$

(Equation (IV.19) continued on next page)

$$-\frac{H}{2cD^2}\frac{\partial^2 D}{\partial C_v^2} + \frac{H}{cD^3}\left[\frac{\partial D}{\partial C_v}\right]^2 + \frac{1}{2Dc}\frac{\partial^2 H}{\partial C_v^2}$$

Everything here has been previously obtained except for $\frac{\partial^2 H}{\partial C_v^2}$. This is found to be

$$\frac{\partial^2 H}{\partial C_v^2} = \frac{-1}{4c^{3/2}}\left[D\left(\frac{\partial c}{\partial C_v}\right)^2\right] + \frac{1}{\sqrt{c}}\frac{\partial D}{\partial C_v}\frac{\partial c}{\partial C_v} + \frac{1}{2\sqrt{c}}\left[D\frac{\partial^2 c}{\partial C_v^2}\right] + \sqrt{c}\frac{\partial^2 D}{\partial C_v^2} \qquad \text{(IV.20)}$$

In this Appendix, we have obtained the extra derivatives necessary for calculating $\frac{\partial^2 R}{\partial C_v^2}$. In general they can mostly be expressed in terms of quantities already evaluated in CONGRATS for $\frac{\partial R}{\partial C_v}$. So the proper combinations of the appropriate quantities were programmed into CONGRATS, along with the necessary new terms, in order to evaluate $\frac{\partial^2 R}{\partial C_v^2}$. This was done by Jean Goertner of NOL. Once this was accomplished, the main part of the program was modified to calculate the pressure on the caustic according to Equation (4.1).

Appendix V. Input Sound Velocity Data

Profile I (Source Depth for All Calculations: z_o = 305 m)

Depth m	Velocity m/s
0	1524.3
457.2	1521.57
685.8	1509.68
853.44	1495.35
1036.3	1490.48
1188.7	1490.46
1478.28	1491.7
1981.2	1499.01
3352.8	1516.99
5250	1548.78

Profile II (Source Depth for All Calculations: z_o = 305 m)

Depth m	Velocity m/s
0	1524.3
457.2	1521.57
685.8	1509.68
853.44	1495.35
1036.3	1490.48
1188.7	1490.46
1478.28	1491.7
1981.2	1499.01
3352.8	1516.99
4572	1537.42

Profile III (Source Depth for All Calculations: z_o = 1000 m)

Depth m	Velocity m/s
0	1570
2250	1500
5750	1570

For all profiles, $\rho_1 = \rho_2 = 1$. Unit consistency is not necessary as long as Equation (5.12) is used since density units cancel. However, for evaluation of pressure using Equation (5.9), densities should be in MKS units in order that pressure be in nm^2.